2021-06

Mathematical models of trypanosoma brucei rhodesiense disease transmission and control strategies

Mlyashimbi, Helikumi

NM-AIST

https://doi.org/10.58694/20.500.12479/1370

MATHEMATICAL MODELS OF *TRYPANOSOMA BRUCEI RHODESIENSE* DISEASE TRANSMISSION AND CONTROL STRATEGIES

Mlyashimbi Helikumi

A Dissertation Submitted in Partial Fulfilment of the Requirements for the Degree of Doctor of Philosophy in Mathematical and Computer Sciences and Engineering of the Nelson Mandela African Institution of Science and Technology

Arusha, Tanzania

June, 2021

ABSTRACT

Human African Trypanosomiasis (HAT), also known as sleeping sickness is a neglected disease that impacts 70 million people living in 1.55 million km^2 in sub-Saharan Africa. The disease strikes predominantly poor populations in sub-Saharan Africa and has been targeted for elimination as a public health problem by 2030. Despite decades of control operations, the disease remains enigmatic and persists in populations at low levels of prevalence. Hence several research approaches must be utilized to infer on the feasibility of attaining the set target. Among them, mathematical modeling is a very successful tool and has been extensively used for different diseases.

In this study four mathematical models were proposed to evaluate the effects of educational campaigns, seasonality, memory effects, time delay and heterogeneity in the human population on *Trypanosoma brucei rhodesiense* transmission and control dynamics. In the formulated models the basic reproduction number $\mathscr{R}_0$ was computed and qualitatively used to establish the condition for disease eradication and persistence. In the first model, effects of human awareness through educational campaigns and use of insecticides on short-and long-term dynamics of the disease were evaluated. Analytical results of the study showed that the model undergoes a backward bifurcation.

Further, upon extending the model to incorporate time-dependent educational campaigns and the use of insecticides, it was noted that when the aforementioned strategies were intensified the associated costs were also high, and the reverse was true. Moreover, it was also noted that reducing the upper bound of educational campaign control (u_1) from 1 to 0.5 and insecticide control (u_2) from 1 to 0.3 could lead to a 17.6% reduction in costs.

Next, the model system was extended to include temperature and case detection followed by treatment of infected humans. With the aid of suitable Lyapunov functionals, the global stability of the model's steady states was carried out. Upon simulating the model with temperature fixed at 20 and 25$^\circ C$, it was noted that the value of vector control be greater than 30 and 50% respectively for $\mathscr{R}_0$ to be less than unity. Lastly, the time delay factor was included in the model system to assess the effects of incubation period on the dynamics of *T. brucei rhodesiense* disease in the population. The numerical results demonstrated that the inclusion of the time delay factor in the model system destabilized the endemic equilibrium point leading to Hopf bifurcation.

AUTHOR'S DECLARATION

I, Mlyashimbi Helikumi, do hereby declare to the Senate of Nelson Mandela African Institution of Science and Technology that this dissertation titled: Mathematical Models of *Trypanosoma brucei rhodesiense* Disease Transmission and Control Strategies is my own original work and that it has neither been submitted nor presented for degree award in any other institution.

Mlyashimbi Helikumi
(Candidate)

21/06/2021
Date

The above declaration is confirmed

Prof. Moatlhodi Kgosimore
(Supervisor 1)

21/06/2021
Date

Prof. Steady Mushayabasa
(Supervisor 2)

21/06/2021
Date

Prof. Dimitry Kuznetsov
(Supervisor 3)

03/06/2021
Date

COPYRIGHT

CERTIFICATION

The undersigned certify that they have read and hereby recommend for acceptance by the Nelson Mandela African Institution of Science and Technology the dissertation entitled: Mathematical Models of *Trypanosoma brucei rhodesiense* Disease Transmission and Control Strategies, in fulfillment of the requirements for the degree of Doctor of Philosophy in Mathematical and Computer Sciences and Engineering of the Nelson Mandela African Institution of Science and Technology.

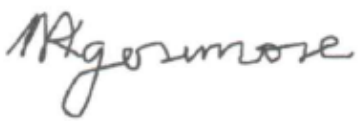

Prof. Moatlhodi Kgosimore
(Supervisor 1)

Date: 21/06/2021

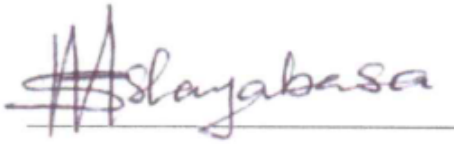

Prof. Steady Mushayabasa
(Supervisor 2)

Date: 21/06/2021

Prof. Dimitry Kuznetsov
(Supervisor 3)

Date: 21/06/2021

ACKNOWLEDGEMENTS

I wish to express my deepest gratitude to my supervisors: Prof. Dimitry Kuznetson, Prof. Moatlhodi Kgosimore and Prof. Steady Mushayabasa for their guidance and motivation during my study. I wholeheartedly appreciate their great advice that was a milestone to-wards my success and I could not have had better mentors in this study. I would like to thank all staff and management of the Nelson Mandela African Institution of Science and Technology (NM-AIST) for the support rendered to me during the time of my study. My special regards should also go to all staff of the Mathematics department at the University of Zimbabwe (UZ) and Faculty of Sciences at the Botswana University of Agriculture and Natural Resources(BUAN) for their warm welcome and amazing hospitality when the time I visited my supervisors. I wish to express my thanks to my employer, Mbeya University of Science and Technology (MUST) for offering me a study leave and financial support towards my study. I would like to acknowledge the Simons Foundation from Botswana International University of Science and Technology (BIUST) for partially funding my study. I also wish to thank all my fellow students at NM-AIST whose support was the milestone on ward the success of this study. Finally, I would like to thank my wife Monica Anderson Mwang'amba and children Johnson, Justine and Jackson for their encouragement and prayers throughout of my study.

DEDICATION

This thesis is dedicated to my mother Mpelwa Lubinza, my wife Monica A. Mwang'amba, my wonderful children Johnson, Justine, Jackson and my late father, Helikumi Budeba(may his soul rest in peace, Amen)

TABLE OF CONTENTS

LIST OF ABBREVIATIONS

ABM	Adam-Bashforth Moulton
BUAN	Botswana University of Agriculture and Natural Resources
BIUST	Botswana International University of Science and Technology
DFE	Disease-Free equilibrium
EE	Endemic equilibrium
HAT	Human African Trypanosomiasis
NM-AIST	Nelson Mandela African Institution of Science and Technology
NTD	Neglected Tropical Diseases
ODEs	Ordinary Differential Equations
PDEs	Partial Differential Equations
UZ	University of Zimbabwe
WHO	World Health Organization
NRMSE	Normalized root-mean square error
T	Trypanosoma
C	Centigrade
VSGs	Variable surface glycoprotein
G	*Glossina*
m	*morsitan*

LIST OF TABLES

LIST OF FIGURES

LIST OF APPENDICES

CHAPTER ONE

INTRODUCTION

1.1 Background of the study

Human African trypanosomiasis (HAT), also known as sleeping sickness, is a neglected tropical disease (NTD) caused by parasites of the genus *Trypanosoma*, which are transmitted by tsetse flies (Kennedy, 2013). The disease has two forms, *T. brucei gambiense* in West and Central Africa and *T. brucei rhodesiense* in East Africa (Moore *et al.*, 2012*a*). However, it is worth noting that Uganda has both forms of the parasite, but in separate zones (Franco *et al.*, 2014*b*). Although these two parasites cause distinct pathologic entities, both of which are included under the general term HAT, they are considered as two separate diseases with different epidemiological and clinical patterns and different patient management (Franco *et al.*, 2014*b*). The HAT can be transmitted to humans and animals (both livestock and wildlife) by over 20 species of *Glossina* tsetse flies (Moore *et al.*, 2012*a*). According to the World Health Organization (WHO, 2013), HAT threatens millions of people in 36 in sub-Saharan African countries. The disease particularly affects people who reside in remote; rural areas with limited access to adequate health services (WHO, 2013;WHO, 2020a).

In the last decade of the 20^{th} century, the number of reported HAT cases reached alarming levels of up to 70 000 new cases reported annually (Lutumba *et al.*, 2007). Therefore such surveillance and control activities against disease were reinforced at the beginning of the 21^{st} century. Through these concerted efforts, the annual number of HAT cases reported annually decreased remarkably and in 2009, only 9878 HAT cases were reported, the least in 50 years (Gilbert *et al.*, 2016). Overall, between 2000 and 2012, the number of HAT cases reduced by almost 73%. The WHO road map set the target of eliminating disease as a public health problem by 2020 and interruption of its transmission (zero cases) by 2030 (Franco *et al.*, 2020). Despite these efforts, WHO estimates that approximately 65 million people are still at risk of HAT infection (Franco *et al.*, 2020).

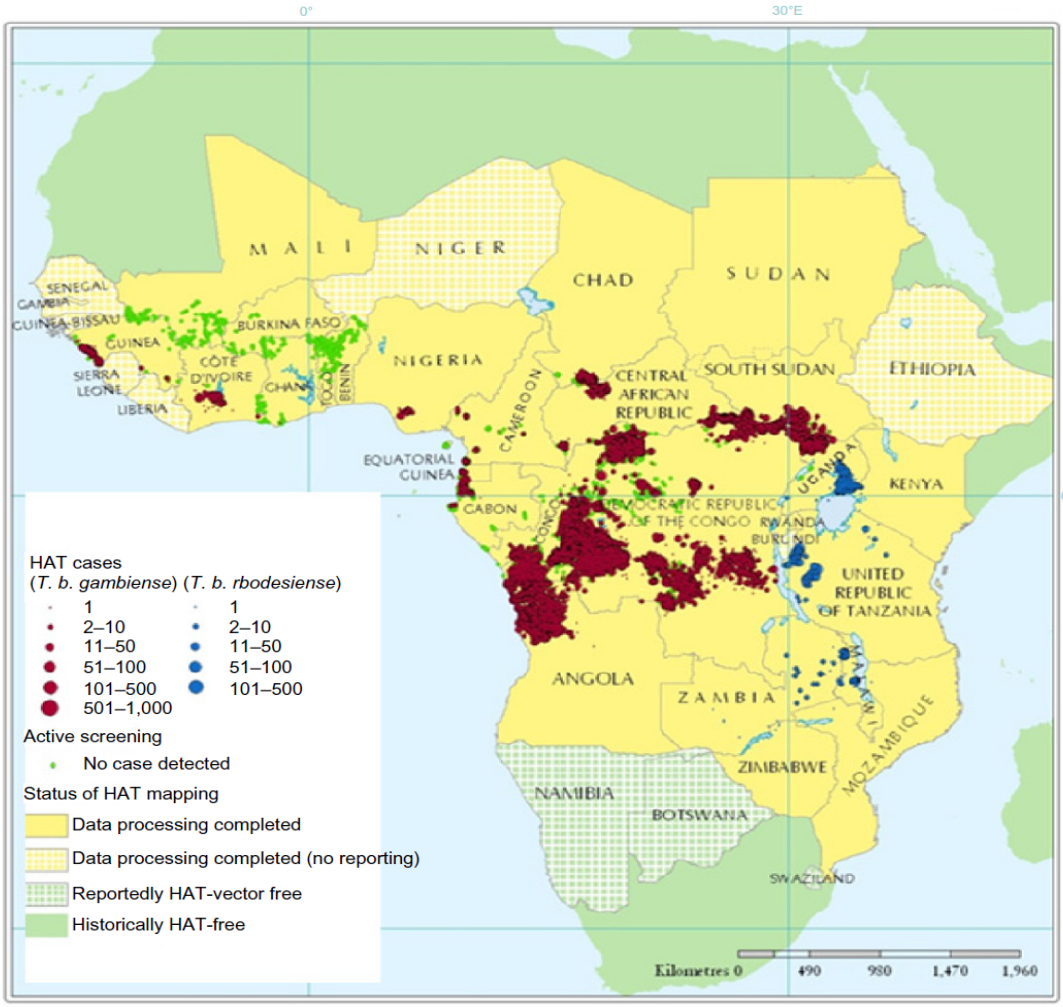

Figure 1: Distribution of HAT cases for the period 2000-2009 (Franco *et al.*, 2014*a*)

Figure 1 depicts the geographical distribution of HAT cases across Africa between 2000 and 2009 and evidently *T. brucei gambiense* is prevalent in West and Central Africa while *T. brucei rhodesiense* is prevalent in the Eastern Africa region. Further, Uganda is the only country with both forms of the parasite. It is, however, worth noting that the map is a dynamic tool, and it is regularly improved and updated in terms of accuracy and completeness (Franco *et al.*, 2014*a*), however, the one presented in Fig. 1 is the most recent.

1.1.1 Epidemiology of the HAT disease in Africa

The HAT disease passes through two clinical stages. The first stage is the haemolymphatic stage, where the parasites are in the blood and lymphatic systems. The patient at this stage exhibits symptoms such as fever, enlarged lymph nodes, fatigue, and headache (Steverding, 2008). The second stage, occurs when the parasites cross the blood-brain barrier and invade the central nervous system, and is called the late or meningo-encephalitic stage. The patient

experiences symptoms like sleeping sickness disorder, severe headache, behaviour change and endocrine disorders (Eperon *et al.*, 2014).

The clinical manifestation of the two forms of the HAT disease differ in management, presentation, and prognosis. Patients with *T. brucei gambiense* disease take several months to years to progress from the early to the late stages of infection, while patients with *T. brucei rhodesiense* disease take only 1-3 weeks to progress from the early to the late stage of infections. Without treatment, both infections may cause death to humans and animals (Aksoy *et al.*, 2017).

1.1.2 Transmission route of HAT disease

Both *T. brucei gambiense* and *T. brucei rhodesiense* diseases are transmitted by tsetse fly vectors belonging to the genus *Glossina* (Ndondo *et al.*, 2016). The tsetse fly acquires or transmits the *trypanosome* parasites to humans or animals by bites during blood meals (Aksoy *et al.*, 2017). There are thirty-one sub-species of tsetse flies, but those that transmit the HAT disease are grouped into three subgenera-; *morsitans*, *palpalis* and *fuscipes* (Shereni *et al.*, 2016). The tsetse flies are found in 38 sub-Saharan African countries, especially in Western, Central, Eastern, and Southern Africa where the high density of woodland, wood savannah forest, rivers, lakes, and other vegetation encourage their growth and reproduction (Glover, 1967).

The transmission of *T. brucei gambiense* in Western and Central African countries occurs through the human-vector-human by tsetse flies of the *Glossina palpalis* group which are mostly found in lake shores, rivers, and wetlands. The transmission route of *T. brucei rhodesiense* in Eastern and Southern African countries on the other hand occurs through the animal-vector-human route by tsetse flies of the *Glossina morsitans* group which are found in forests and Savannah woodlands, specifically in East Africa countries (Ndondo *et al.*, 2016).

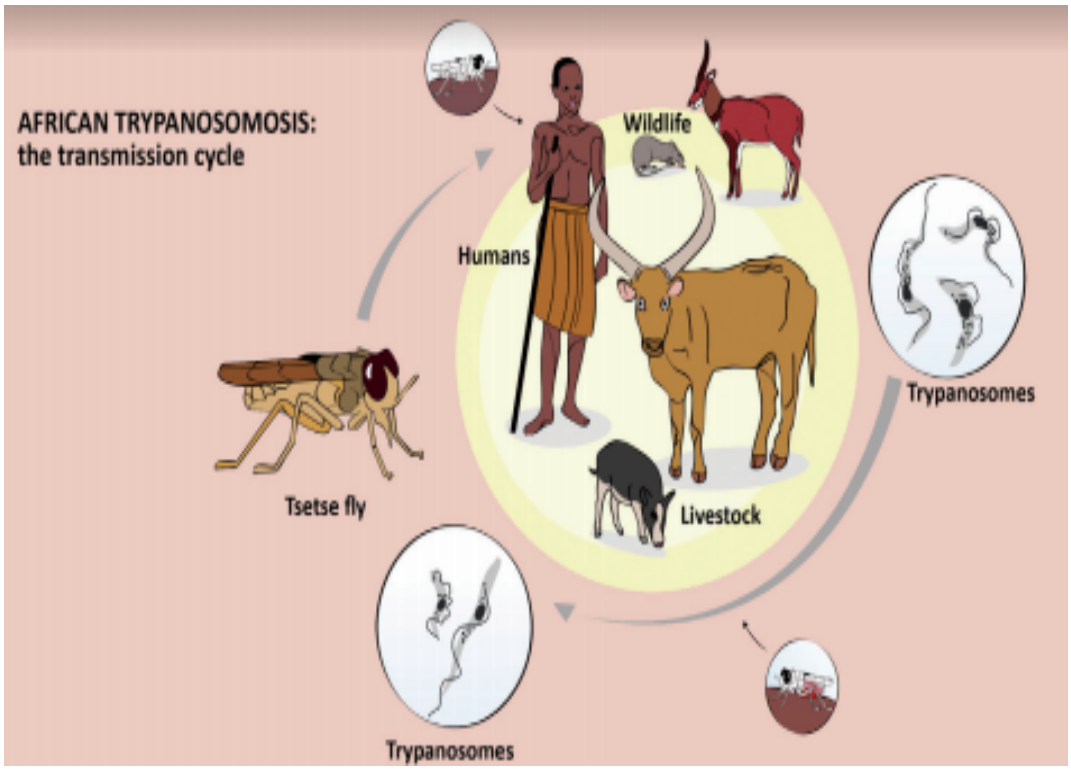

Figure 2: Transmission dynamics of the HAT disease in Africa (Büscher *et al.*, 2017*a*)

Figure 2 shows the transmission dynamics of the HAT disease in Africa. Wild animals especially in game reserves and national parks in countries like Tanzania, Kenya, Uganda, Zimbabwe, Malawi, and Zambia are reservoirs of the *T. brucei rhodesiense* parasites which maintain the dynamics of the disease between humans and animals (Hide, 1999). Most people especially in rural areas become exposed to tsetse flies while farming, hunting, fishing, collecting water, or visiting game reserves, and national parks (Büscher *et al.*, 2017*a*).

The unique feature that differentiate tsetse flies from other insects like mosquitoes is their life cycle. The adult female tsetse fly mates once in a lifetime where by the male deposits a large ball of sperm which moves into spermathecae (Madsen *et al.*, 2013*a*). The female produces a single egg which passes into the uterus wall where it is fertilized for 4 days and hatches into larva which undergoes three stages called instar larva. The development of the larva in the uterus wall takes 5 days and is nourished by milk glands generated by the female tsetse fly (Rogers *et al.*, 1994). Once deposited, the fully developed larva burrow in the ground and pupate after a few minutes (Büscher *et al.*, 2017*a*). The emergence of the pupal to adult fly depends on the surrounding temperature, whereby the lower the temperature, the longer the pupal period and vice versa (Leak, 1999). This life cycle is summarized in Fig. 3

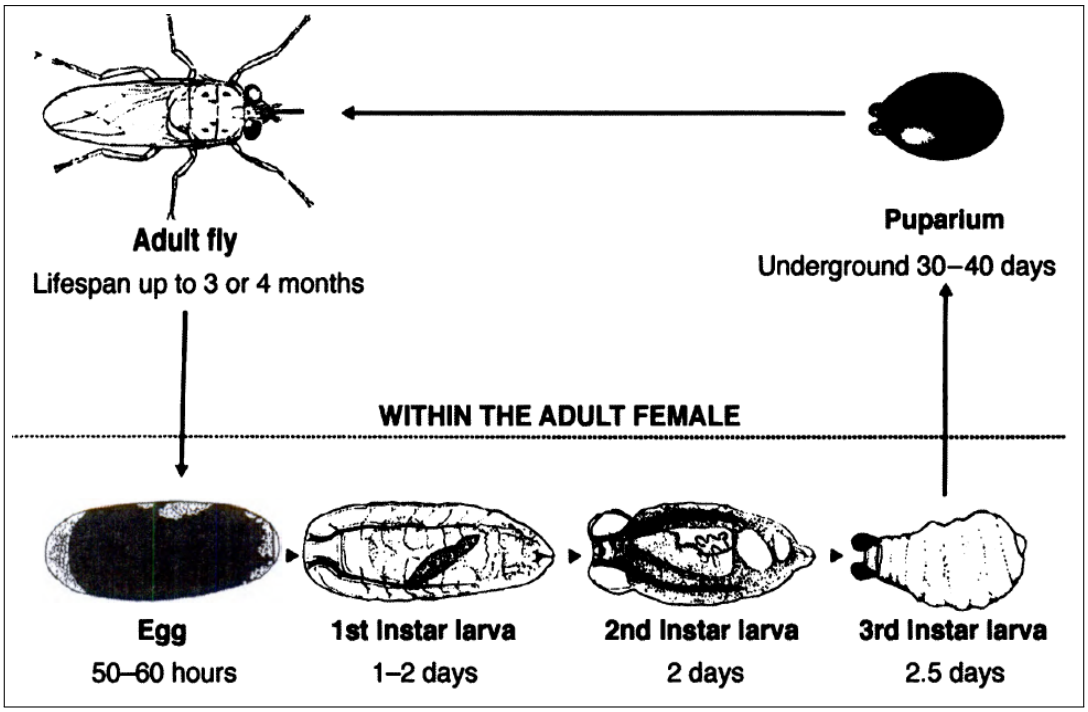

Figure 3: The life cycle of tsetse fly (Leak, 1999)

1.1.3 Effects of climatic changes on the dynamics of HAT diseases

Temperature is one of the environmental factors that plays an integral role in the dynamic of HAT. Previous studies have revealed that the metabolic processes in tsetse flies strongly depend on temperature. The interlaval period, pupal period, adult lifespan, and the period between successive feeds are particularly reduced as temperature increases (Phelps, 1973). A study by Thomson (1994) established that temperature does not only change the different developmental periods of the vector but is also important in the fly's flight activity. While temperatures below 17°C make tsetse flies rest in direct sunlight, and those above 32°C make them inactive forcing them to seek artificial refuge which in most cases are cool shaded places (Vale, 1971).

1.1.4 Control measures of trypanosomiasis

Although there is no vaccine or drug for prophylaxis against the, they are other preventive and treatment options. The preventative strategies are mainly designed to minimize contact between the hosts and vectors. Humans can minimize contact with the tsetse vectors by avoiding bushy areas, wearing long-sleeved garments of medium-weight material in neutral colors that blend with the background environment. Spraying domesticated animals with insecticides also minimizes contact between the vector and the animals. Drugs can also be used to treat infected host species.

Like other NTDs such as the Guinea worm, the development of a HAT vaccine that can be successfully used for hosts remains a formidable challenge. One of the challenges behind this failure has been attributed to the existence of variable surface glycoproteins (VSGs) that cover the body surface of the parasite (Magez *et al.*, 2010). Even though the HAT parasite contains more than 1000 VSGs, only one of these is expressed during infection (Büscher *et al.*, 2017*b*). Although the host's immune system normally develop antibodies to fight the expressed VSG, it is the ability of the parasites to produce new VSGs that remains the greatest challenge the enables their continued survival in the reservoir hosts for long a time (Ranjbarian, 2017). Hence, efforts to eliminate the disease are currently based on the treatment of infected hosts, use of insecticides and other non-pharmaceutical intervention strategies such as avoiding bushy areas and wearing long-sleeved garments of medium-weight material in neutral colors that blend with the background environment.

1.2 Statement of the research problem

Although tremendous progress has been made in controlling the HAT disease, there are still several countries/regions in sub-Saharan Africa where the infection persists in both humans and animals. WHO (2020a) estimates that approximately 65 million people remain at risk of the infection. The WHO's target of elimination the disease as a public health problem by 2030 is fast approaching, it is therefore imperative that various tools and techniques are developed to improve the existing knowledge to effectively manage the disease and attain the set target.

Tools and techniques for the prediction of disease dynamics and evaluation of the strengths and limitations of control strategies have been developed. Mathematical modeling pioneered by Daniel Bernoulli, Sir Ronald Ross, Kermack and McKendrick (Ross, 1916; Macdonald *et al.*, 1950) is one such tool used to predict the course of the epidemic and facilitate the development of control strategies. Following these early works in mathematical modeling, a number of researchers (Chitnis *et al.*, 2008) have extensively engaged in design of models in an attempt to describe and understand several biological phenomena. A few mathematical models have been published in recent years to investigate HAT dynamics (Rogers, 1988; Moore *et al.*, 2012*b*,*a*; Kajunguri, 2013; Funk *et al.*, 2013; Kajunguri *et al.*, 2014; Pandey *et al.*, 2015; Alderton *et al.*, 2016; Gilbert *et al.*, 2016; Ndondo *et al.*, 2016; Lord *et al.*, 2018; Alderton *et al.*, 2018; Meisner *et al.*, 2019; Ndeffo-Mbah *et al.*, 2019). A comprehensive review of these studies is provided in Chapter 2. Despite these efforts, several challenges and gaps remain in the mathematical modeling of HAT:

(i) Studies on other infectious diseases such as malaria, HIV/AIDS, tuberculosis have suggested that coupling pharmaceutical and non-pharmaceutical control interventions has

a significant impact on disease management (Kumar *et al.*, 2017). Among the non-pharmaceutical control interventions, educational campaigns are very successful intervention strategy (Kumar *et al.*, 2017). In particular, prior studies suggest individual behavioural changes whenever they receive information about the disease. Therefore, there is growing interest among researchers to study the impact of such behaviour-influencing factors on the spread of infectious diseases (Greenhalgh *et al.*, 2015; Kumar *et al.*, 2017; Agaba *et al.*, 2017; Musa *et al.*, 2021). To the best of the researcher's knowledge, a mathematical model for HAT that incorporates educational campaigns is yet to be proposed. Hence, a mathematical model for HAT that incorporates educational campaigns has been proposed and analyzed to shed light on how awareness influences HAT dynamics.

(ii) Seasonal variations in climatic factors such as rainfall and temperature have a strong influence on the life cycle of tsetse flies, thereby affecting the seasonal distribution and abundance of vectors (Nnko *et al.*, 2017). For example, tsetse fly-vectors responsible for the transmission of trypanosomiasis in humans and animals need between 16-38°C and 50-80% of temperature and humidity respectively to survive (Franco *et al.*, 2014*b*). To the best of the researcher's knowledge, this aspect is yet to be investigated. As such, a non-autonomous model that incorporates seasonal variations has been proposed and analyzed in this dissertation.

(iii) Memory effects are inherent in many biological process (Kheiri, 2019), and play a critical role in shaping their short-and long-term dynamics. To the best of the author's knowledge, the effects of memory on HAT dynamics is yet to be studied. Existing models for HAT dynamics are based on ordinary differential equations (ODEs) in which the order of the derivative is an integer. Since integer differentiation is a local operator, this does not satisfactorily capture the memory influences in biological systems (Gashirai *et al.*, 2021). Therefore, non-local fractional differentiation needs to be utilized to capture the effects of memory in biological systems. In this dissertation, a mathematical mode for HAT that is based on fractional differentiation has been proposed and analyzed.

(iv) Biological processes have intrinsic delays that can represent gestation periods, immune activation, and incubation periods in infectious diseases (Mushayabasa, 2015, 2016; Ding *et al.*, 2016). There is growing interest among researchers to understand the implications of time delays on the dynamics of infectious and non-infectious diseases. Although existing models have certainly produced many useful results and improved the existing knowledge on HAT dynamics, the effects of time delays on HAT are yet to be investigated. Therefore, a HAT model that incorporates time delay has been proposed and analyzed in this dissertation .

A recent report by WHO (2020b) suggests that there is a slight increase of *T. brucei rhodesiense* cases and based on this assertion, the mathematical models proposed in this study are meant to monitor these dynamics.

1.3 Rationale of the study

The *T. brucei rhodesiense* as a zoonotic disease affects most of the areas such as National Parks, game reserves and other protected areas in East Africa countries. People working on, living close to and visiting these areas are at high risk of contacting tsetse flies. Therefore, understanding the dynamics of sleeping sickness disease and its control will help the people specifically in rural areas to be aware of the disease and be able to identify activities that expose them to tsetse flies and take prevention measures. The study will also help veterinary officers, policy makers and other stakeholders to select the best control strategies and be able to implement them to minimize the transmission of the disease to both humans and animals. Besides, knowing the effects of seasonal (specific temperature) variations on the dynamics of sleeping sickness diseases will help the stake holders to allocate and implement resources at the right place and time. In addition to that, the selected topic of study will add knowledge in the literature review for further studies.

1.4 Research objectives

1.4.1 Main objective

The overall goal of this study was to contribute to the existing knowledge on *T. brucei rhodesiense* dynamics through the development and analysis of new comprehensive models (which extend many of the published models in literature) to gain insights into the qualitative features of the disease (to find effective ways to control its spread both human and animal host).

1.4.2 Specific objectives

The specific objectives of the study were:

(i) To investigate the role of educational campaigns on *T. brucei rhodesiense* dynamics.

(ii) To investigate the effects of seasonal variations on *T. brucei rhodesiense* dynamics.

(iii) To investigate the influence of memory effects on *T. brucei rhodesiense* dynamics.

(iv) To investigate the effects of time delays on *T. brucei rhodesiense*. dynamics

1.5 Research questions

In contrast to the large number and widespread use of models to guide efforts against diseases as diverse as onchocerciasis (Habbema *et al.*, 1996), malaria (Monitoring, 2011) and influenza (Nsoesie *et al.*, 2014), models of HAT are few and their impact on practice and policy limited. Hence, in this study the following research questions were considered:

(i) What is the role of educational campaigns play on *T. brucei rhodesiense* dynamics?

(ii) What are the effects of seasonal variations on *T. brucei rhodesiense* dynamics? dynamics.

(iii) What are the implications of memory effects on *T. brucei rhodesiense* dynamics?

(iii) What are the qualitative and quantitative effects of time delays on *T. brucei rhodesiense* dynamics?

1.6 Significant of the study

The significant of the proposed study includes the following:

(i) The proposed study is envisaged to provide a framework for design of control strategies in Tanzania.

(ii) Inform policy formulation for disease control.

(iii) Provide plat form for further studies in the transmission dynamics of the disease.

1.7 Delineation of the study

Infectious disease continue to pose a formidable challenges to economies and health systems of many nations world over, hence, understanding ways of effectively managing these disease is a subject that requires constant research and update. African trypanosomiasis, in particular, remains endemic to Sub-Saharan Africa and continues to threaten human health and food security (Nnko *et al.*, 2017). Further, the total annual losses in agricultural gross domestic product in all the countries where the disease is endemic is estimated to be USD 4.7 billion (Mulenga *et al.*, 2020). The models and results presented in this dissertation are new and make a significant contribution to the existing body of knowledge on *T. brucei rhodesiense* dynamics.

CHAPTER TWO

LITERATURE REVIEW

2.1 Introduction

Mathematical modelling is commonly regarded as the art of applying mathematics to a real-world problem to better understand the problem (Cheng, 2009). Yanagimoto (2005) argues that mathematical modelling is not just a process of solving a real-life problem using mathematics, but the process that involves applying mathematics in situations where the results are useful in society. McKenzie (2000) defines a mathematical model as an abstraction or simplification of nature by separating important aspects from minor and irrelevant. Models are used to approach questions which are too complex, inaccessible, numerous, diverse, mutable, unique, dangerous, expensive, big, small, slow or fast to approach by other means (McKenzie, 2000). However, it is worth noting that a mathematical model cannot encompass every feature of a problem. The hope is that the missing features are not crucial and that the model will help to distinguish the decisive from the incidental features in the given context (McKenzie, 2000).

Since the pioneering works of Daniel Bernoulli, Sir Ronald Ross, Kermack and McKendrick (Ross, 1916; Macdonald *et al.*, 1950), mathematical modeling has extensively used to understand several biological phenomena (Chitnis *et al.*, 2008; Mushayabasa, 2013). In recent years, mathematical models have been guiding tools to and shedding light on transmission and control of infectious and non-infectious diseases. Models enable researchers to create frameworks that can be accurately utilized to conceptualize and communicate ideas regarding the behavior of a particular system (Keeling, 2005). Through these frameworks, solutions to phenomena that are difficult to measure in the field can be found. Mathematical models have been important tools in controlling the spread of infectious diseases.

The use of mathematical models to understand ways of effectively managing diseases does not only have a long history but has some notable success too. The success of the Onchocerciasis Control Program in West Africa at the turn of the millennium shows that models can make great pragmatic contributions to intervention programs if the modeling is integrated into the overall program, and if the participants are clear about what models can and cannot do (Macdonald *et al.*, 1950).

2.2 Mathematical models of HAT dynamics

Following the long history of malaria modelling, mathematical modelling of HAT began with Rogers (1988) and since then, multiple models of human and animal African trypanosomi-

asis have been built and analysed to investigate various aspects of trypanosome biology and epidemiology (Chitnis *et al.*, 2008). Rogers (1988) proposed a three-dimensional model for the transmission dynamics of *T. brucei gambiense* in West Africa. The three-model included humans, animals and vectors (tsetse flies). The model was quantitatively and qualitatively analyzed to determine the disease threshold parameter and equilibrium points and validated with the aid of *T. brucei gambinese* data from a West African village. Among several outcomes of the work of Rogers, it was demonstrated that peak disease incidence lagged behind peak fly numbers, and the less favoured hosts behind the more favoured hosts.

Milligan (1988) published their first model of animal trypanosomiases in the same year as Rogers (1998). They included enhanced vector susceptibility in teneral flies, multiple host types (cattle and wild animals), and disease-induced mortality in both hosts and vectors. They derived the $\mathscr{R}_0$ and modelled the effects of chemoprophylaxis on cattle. They showed that the effectiveness of chemoprophylaxis depends on the frequency of application and duration of protective efficacy and that the effectiveness of vector control is reduced by the immigration of flies.

Artzrouni (1996*a*) proposed a five-variable compartmental for the dynamics of HAT. Their framework included a single host (humans) and vectors (tsetse flies). Their framework had the following epidemiological classes for the human population: susceptible, incubating, asymptomatic, and removed humans. They validated their work using HAT data from the Democratic Republic of Congo. In a subsequent paper, these authors (Artzrouni, 1996*b*) used their model to compare control strategies.

To assess the impact of host and vector migration on HAT dynamics, Chalvet-Monfray *et al.* (1998) extended the model proposed by Artzrouni (1996*b*). Hargrove *et al.* (2012) modeled the control of trypanosomiasis caused by *T. brucei rhodesiense* in multiple hosts. Their model predicted that treating cattle with insecticides would generally be more effective than treating them with drugs. In addition, Moore *et al.* (2012*a*) utilized a system of ordinary differential equations to explore the impact of climate change on *T. brucei rhodesiense* dynamics. Results from their framework suggested that climate change could lead to 46–77 million additional people being at risk of exposure to HAT infection by 2090. These studies and those cited therein have undeniably produced many useful results and improved the existing knowledge on HAT dynamics.

Funk *et al.* (2013) proposed and analyzed a multiple host model for gambiense HAT and provided field data estimates of the $\mathscr{R}_0$ in Bipindi, Cameroon. Madsen *et al.* (2013*b*) developed a mathematical model for gambiense disease with the aim of evaluating the effects of intervention

strategies that could be utilized to eliminate HAT in the Democratic Republic of Congo. Their work revealed that additional strategies such as vector control and/or improved screening of the human population are required to accelerate progress against Gambian HAT in the Democratic Republic of Congo.

Kajunguri *et al.* (2014) also formulated a multi-host model for HAT caused by *T. brucei rhodesiense*, and in particular found that the restricted application of insecticides to cattle on their legs and belly only (favoured tsetse feeding sites) provided a cost-effective method of control. Ndondo *et al.* (2016) proposed a mathematical model of HAT that takes into account the growth of tsetse fly, from its larval to adult stage. Qualitative and quantitative results from their study showed that model has two equilibrium points, the disease-free and the endemic equilibrium point which exists whenever the $\mathscr{R}_0$ is less and greater than unity respectively.

Ackley (2017) developed a dynamic model to estimate tsetse fly mortality from ovarian dissection data in populations where age distribution is not essentially stable. One of the important results from their study was that mortality increases with temperature concurs with existing field and laboratory findings. Lord *et al.* (2018) utilized a mathematical model to explore the effects of temperature on mortality, larviposition and emergence rates in tsetse vectors. They suggested that an increase in temperature maybe associated with the decline in tsetse abundance in Zimbabwe's Zambezi Valley. They also hypothesized that rising temperatures may have made some higher, cooler, parts of Zimbabwe more suitable for tsetse leading to the emergence of new disease foci.

Alderton *et al.* (2018) proposed an agent-based model to assess the impact of seasonal climatic drivers on trypanosomiasis transmission rates. Simulation results from their demonstrated a perfect fit with the observed HAT datasets thereby demonstrating that seasonality is a key component on trypanosomiasis transmission rates. Stone (2015) employed a system of ODEs to model the implications of heterogeneous biting exposure and animal hosts on *T. brucei gambiense* transmission and control. Their had several outcomes, but overall, their study demonstrated that the effective control of HAT hinges on understanding the its ecological and environmental context particularly for moderate and low transmission intensity settings.

Madsen *et al.* (2013*b*) formulated a mathematical framework to study the effects of seasonality on tsetse fly abundance and trypanosomiasis transmission. Ndeffo-Mbah *et al.* (2019) formulated a dynamical model to characterize the impact of vector migration on the effectiveness of gambiense HAT control strategies. Their study suggested that the WHO 2030 goal of eliminating the disease is at least in theory, achievable. These studies and several others cited therein improved our understanding of sleeping sickness transmission and control.

CHAPTER THREE

MATERIALS AND METHODS

3.1 Introduction

In this Chapter, mathematical models for *T. brucei rhodesiense* dynamics that seek to provide solutions to the set objectives are presented and analyzed. In particular, new comprehensive models (which extend many of the published models in the literature) have been designed and rigorously analyzed. The models incorporate relevant biological and ecological factors, as well the interplay between vectors and the two hosts (humans and animals). The first model seeks to evaluate the role of educational campaigns on *T. brucei rhodesiense* dynamics, the second model evaluates the effects of seasonal variations on *T. brucei rhodesiense* transmission and control, the third model assess the implications of memory effects on *T. brucei rhodesiense* dynamics and the last model investigates qualitative and quantitative effects of time delays on *T. brucei rhodesiense* dynamics. The notation for state variable and model parameters used in the dissertation is described in Table 1 and 2, respectively.

Table 1: Description of state variables of models presented in this dissertation

Variable	Description
S_h	Number of susceptible human population.
E_h	Number of exposed human population.
I_h	Number of infectious human population.
R_h	Number of removed humans who may not get infected.
N_h	Total number of humans, that is., $N_h = S_h + E_h + I_h + R_h$.
S_a	Number of susceptible animal population.
E_a	Number of exposed animal population.
I_a	Number of infectious animal population.
R_a	Number of removed or recovered animal population.
N_a	Total number of animal population.
S_v	Number of susceptible tsetse flies.
E_v	Number of exposed tsetse flies.
I_v	Number of infectious tsetse flies.
N_v	Total number of tsetse flies.

Table 2: Description of state variables of models presented in this dissertation

Variable	Description
β_{hv}	Transmission rate of HAT disease from an infected human to a susceptible vector
β_{av}	Transmission rate of HAT disease from an infected animal to a susceptible vector
β_{vh}	Transmission rate of HAT disease from an infected vector to a susceptible human
β_{va}	Transmission rate of HAT disease from an infected vector to a susceptible animal
γ_h	Progression rate of human population from recovered to susceptible class
γ_a	Progression rate of animal population from recovered to susceptible class
θ_h	Rate at which humans become aware of the disease
d_h	Per capita disease-induced death rate for humans
d_a	Per capita disease-induced death rate for animals
d_a	Per capita disease-induced death rate for animals
p	Proportion of tsetse fly bite on animal
μ_v	Natural mortality rate of tsetse flies
μ_h	Natural mortality rate for humans
μ_a	Natural mortality rate for animals
α_h	Recovery rate of infected humans
α_a	Recovery rate of infected animals
b_v	Per capita birth rate of tsetse flies
b_h	Per capita birth rate of humans
b_a	Per capita birth rate of animals
κ_v	Incubation rate for tsetse flies
κ_a	Incubation rate for animals
κ_h	Incubation rate for humans
W	Proportion of female flies
ξ	Tsetse fly biting rate

3.2 Rhodesiense model with educational campaigns

To assess the role of educational campaigns on *T. brucei rhodesiense* dynamics, a mechanistic, compartment model which describes the infection dynamics in human, animal and tsetse fly population were developed. This model and its variant are based on a Ross-Macdonald-type formulation (Macdonald *et al.*, 1950) with infection stages in humans, animals and tsetse flies. In particular, the host population was partitioned into three distinct classes: susceptible $S_i(t)$, infectious $I_i(t)$ and recovered $R_i(t)$. Thus, the total host population at time t is $N_i = S_i + I_i + R_i$, for $i = a, h$. Furthermore, the tsetse fly population was subdivided into two classes namely: susceptible $S_v(t)$ and infectious $I_v(t)$, such that the total tsetse population considered was equivalent to $N_v(t) = S_v(t) + I_v(t)$. The proposed model was governed by the following assumptions:

(i) Through mass media campaigns, humans were assumed to become aware of the disease at a constant rate θ_h and those that became aware of the disease were assumed to have negligible chances of being infected. Hence, in the proposed framework, these individuals

were removed from the susceptible compartment.

(ii) Recruitment rate was assumed to occur in humans, animals and vectors through birth a constant rate b_h, b_a and b_v, respectively. The new recruits were assumed to be susceptible to infection. Further, humans, animals and vectors were assumed to suffer natural mortality at rates μ_h, μ_a and μ_a, respectively. Without loss in generality, the per capita birth rate was assumed to be equivalent to the natural mortality rate. Thus, the recruitment rate was remodeled to $\mu_h N_h$, $\mu_a N_a$, and $\mu_v N_v$, for humans, animals and vectors. Infected humans and animals were assumed to suffer disease-related death at rate d_h and d_a, respectively.

(iii) The susceptible hosts (animals or humans) were assumed to acquire infection upon being bitten by an infectious tsetse fly and as a result the following forces of infection were proposed:

$$\lambda_h(t) = \frac{\beta_{vh} I_v(t)}{N_v(t)}, \qquad \lambda_a(t) = \frac{\beta_{va} I_v(t)}{N_v(t)}. \tag{3.1}$$

In (3.1), parameter β_{vi} $(i = a, h)$ denotes the transmission rate of the infection from an infected tsetse fly to a susceptible host i given that effective contact between the two occurs. Upon infection, the host was considered to progress to the infectious stage where they remained for an average period of $1/\alpha_i$ days before recovery with temporary immunity. It was assumed that this immunity waned at rate γ_i after-which they became susceptible to infection again.

(iv) Susceptible vectors were assumed to acquire infection whenever they bite infectious hosts and the following force of infection accounts for disease transmission in this case:

$$\lambda_v(t) = \frac{\beta_{hv} I_h(t)}{N_h(t)} + \frac{\beta_{av} I_a(t)}{N_a(t)}. \tag{3.2}$$

In (3.2) parameter β_{iv} is the rate of infection transmission from an infected host i to a susceptible vector given that effective contact between the two occurs. Upon infection, vectors were assumed to move to the infectious stage where they were considered to remain for their entire life span.

Based on the above assumptions, the following system of nonlinear ODEs was considered:

$$\left.\begin{array}{rcl}
\frac{dS_h}{dt} &=& \mu_h N_h - \lambda_h S_h - (\mu_h + \theta_h) S_h + \gamma_h R_h, \\
\frac{dI_h}{dt} &=& \lambda_h S_h - (\mu_h + \alpha_h + d_h) I_h, \\
\frac{dR_h}{dt} &=& \theta_h S_h + \alpha_h I_h - (\mu_h + \gamma_h) R_h, \\
\frac{dS_a}{dt} &=& \mu_a N_a - \lambda_a S_a - \mu_a S_a + \gamma_a R_a, \\
\frac{dI_a}{dt} &=& \lambda_a S_a - (\mu_a + \alpha_a + d_a) I_a, \\
\frac{dR_a}{dt} &=& \alpha_a I_a - (\mu_a + \gamma_a) R_a, \\
\frac{dS_v}{dt} &=& \mu_v N_v - \lambda S_v - \mu_v S_v, \\
\frac{dI_h}{dt} &=& \lambda S_v - \mu_v I_v.
\end{array}\right\} \tag{3.3}$$

The flow diagram for model (3.3) is depicted in Fig. 4.

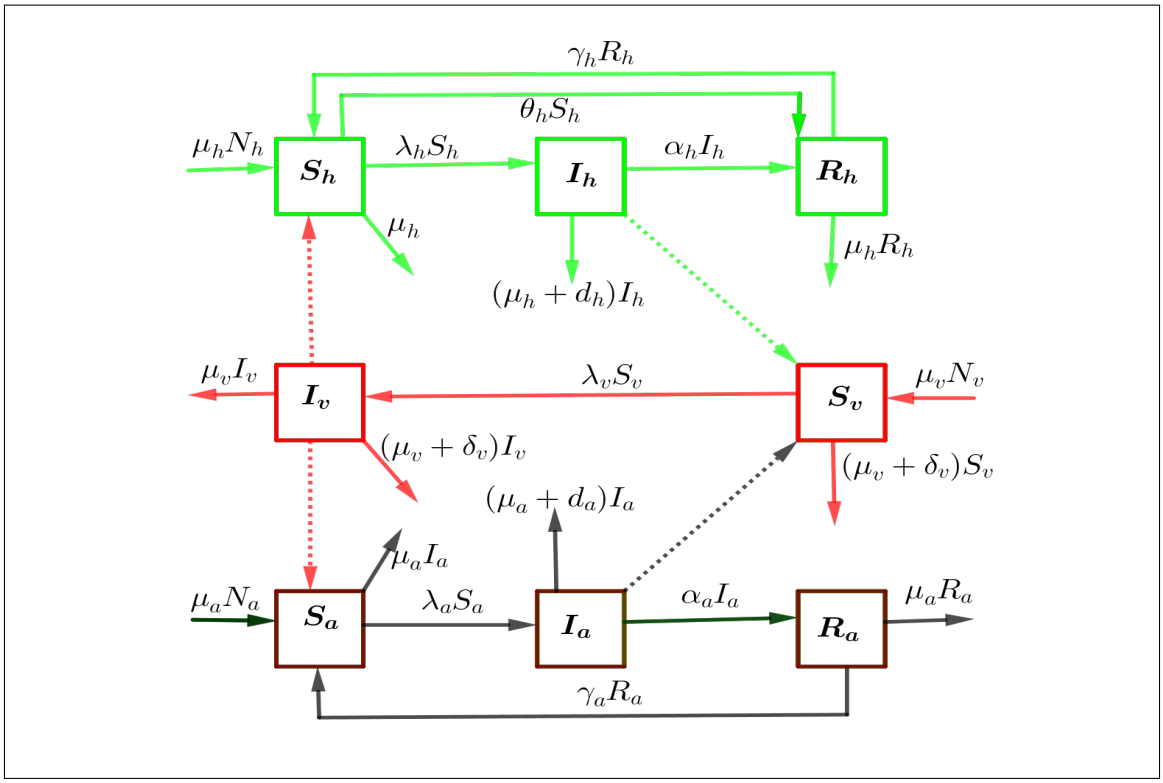

Figure 4: Schematic diagram of model (3.3)

To analyze the dynamics of model (3.3) more easily, the fractional quantities instead of actual populations by scaling the population of each class by the total species population has been considered. Let

$$\left.\begin{array}{rcl}
s_h &=& \frac{S_h}{N_h}, \quad i_h = \frac{I_h}{N_h}, \quad r_h = \frac{R_h}{N_h}, \quad s_a = \frac{S_a}{N_a}, \\
i_a &=& \frac{I_a}{N_a}, \quad r_a = \frac{R_a}{N_a}, \quad s_v = \frac{S_v}{N_v}, \quad i_v = \frac{I_v}{N_v}.
\end{array}\right\} \tag{3.4}$$

Differentiation of the scaling equations (3.4) leads to the following rescaled model:

$$\left.\begin{array}{rcl}
\frac{ds_h}{dt} &=& \mu_h - \beta_{vh} i_v s_h - (\mu_h + \theta_h) s_h + \gamma_h r_h, \\
\frac{di_h}{dt} &=& \beta_{vh} i_v s_h - (\mu_h + \alpha_h + d_h) i_h, \\
\frac{dr_h}{dt} &=& \theta_h s_h + \alpha_h i_h - (\mu_h + \gamma_h) r_h, \\
\frac{ds_a}{dt} &=& \mu_a - \beta_{va} i_v s_a - \mu_a s_a(t) + \gamma_a r_a, \\
\frac{di_a}{dt} &=& \beta_{va} i_v s_a - (\mu_a + \alpha_a + d_a) i_a, \\
\frac{dr_a}{dt} &=& \alpha_a i_a - (\mu_a + \gamma_a) r_a, \\
\frac{ds_v}{dt} &=& \mu_v - (\beta_{hv} i_h + \beta_{av} i_a) s_v - \mu_v s_v, \\
\frac{di_v}{dt} &=& (\beta_{hv} i_h + \beta_{av} i_a) s_v - \mu_v i_v.
\end{array}\right\} \tag{3.5}$$

By using the relations $r_h = 1 - s_h - i_h$, $s_a = 1 - i_a - r_a$ and $s_v = 1 - i_v$ system (3.5) reduces to:

$$\left.\begin{array}{rl}
\frac{ds_h}{dt} &= \mu_h - \beta_{vh} i_v s_h - (\mu_h + \theta_h) s_h + \gamma_h (1 - s_h - i_h), \\
\frac{di_h}{dt} &= \beta_{vh} i_v s_h - (\mu_h + \alpha_h + d_h) i_h \\
\frac{di_a}{dt} &= \beta_{va} i_v (1 - i_a - r_a) - (\mu_a + \alpha_a + d_a) i_a \\
\frac{dr_a}{dt} &= \alpha_a i_a - (\mu_a + \gamma_a) r_a, \\
\frac{di_v}{dt} &= (\beta_{hv} i_h + \beta_{av} i_a)(1 - i_v) - \mu_v i_v.
\end{array}\right\} \tag{3.6}$$

Since model (3.6) monitors human, animal and vector populations it was essential to investigate its biological and mathematical feasibility. Comprehensive analysis on bounded and positivity of solutions for model (3.6) is in Appendix 2 and a summary of the results are in Theorem 3.1.

Theorem 3.1

Assuming that the initial conditions of model (3.6) are nonnegative then the system of equations for model (3.6) has a unique solution that exists and remains in the domain Ω (3.7) for all time $t \geq 0$:

$$\Omega = \left\{ \left(s_h, i_h, i_a, r_a, i_v \right) \in \mathbb{R}^5_+ \;\middle|\; \begin{array}{l} s_h \geq 0,\ i_h \geq 0,\ s_h + i_h \leq 1, \\ i_a \geq 0,\ r_a \geq 0, \\ i_a + r_a \leq 1,\ 0 \leq i_v \leq 1. \end{array} \right\}. \tag{3.7}$$

3.2.1 The basic reproduction number and model equilibria

The $\mathscr{R}_0$ is an important metric for infectious disease models. It demonstrates the power of the disease to invade the population. There are several ways of computing this metric, however, in this dissertation, the next-generation matrix method proposed in Van den Driessche (2002) was considered (see Appendix 2 for the derivation). The $\mathscr{R}_0$ for model (3.6) was obtained as follows :

$$\begin{aligned}\mathscr{R}_0 &= \sqrt{\left(\frac{\beta_{vh}\beta_{vh}(\mu_h+\gamma_h)}{(\mu_h+\alpha_h+d_h)(\mu_h+\gamma_h+\theta_h)\mu_v}\right)+\left(\frac{\beta_{av}\beta_{va}}{\mu_v(\mu_a+\alpha_a+d_a)}\right)} \\ &= \sqrt{\mathscr{R}_{0h}+\mathscr{R}_{0a}}. \end{aligned} \tag{3.8}$$

In (3.8), $\mathscr{R}_{0h}$ represents the secondary cases of infection generated from human-vector interaction and $\mathscr{R}_{0a}$ is the secondary cases of infection from animal-vector interaction. For the vector-borne diseases, the generation of secondary cases require two transmission process, therefore the $\mathscr{R}_0$ computed using the next generation method give number of new infections per generation process (hence the square root).

Further dynamical analysis on the existence and stability of the equilibria for model (3.6) was determined (see Appendix 2) and the model (3.6) admits:

(i) a unique endemic equilibrium $\mathscr{E}^*$ if $\mathscr{R}_0 > 1$ and part 2 and 4 are both holds,

(ii) more than one endemic equilibrium if $\mathscr{R}_0 < 1$ and part 1 and case of part 3 satisfied ,

(iii) no endemic equilibrium if $\mathscr{R}_0 < 1$, and part 1 and case of part 3 are holds.

3.2.2 The optimal control problem

Results of model (3.6) exhibits a backward bifurcation. A backward bifurcation is a phenomenon in which stable endemic equilibrium point co-exists with a stable disease-free equilibrium point for $\mathscr{R}_0 < 1$. This phenomenon has also been observed in numerous epidemiological settings (Gumel, 2012). The existence of a backward bifurcation implies that reducing the $\mathscr{R}_0$ to levels below unity no-longer guarantees disease elimination. Hence disease elimination can be attained through the implementation of time-dependent intervention strategies.

To assess the impact time-dependent intervention strategies model, (3.6) was extended to include two controls $u_1(t)$ and $u_2(t)$, which represent time-dependent media campaigns and insecticide use. The use of insecticides was assumed to enhance the mortality rate of vectors, hence an addition constant parameter δ_v was introduced into the model. Thus, δ_v accounted for the mortality rate of tsetse flies due to insecticide use. Making use of similar variables and parameters (3.6) the new model with controls was considered as follows:

$$\left.\begin{aligned}\tfrac{ds_h}{dt} &= \mu_h-\beta_{vh}i_v s_h-(\mu_h+u_1(t)\theta_h)s_h+\gamma_h(1-s_h-i_h),\\ \tfrac{di_h}{dt} &= \beta_{vh}i_v s_h-(\mu_h+\alpha_h)i_h,\\ \tfrac{di_a}{dt} &= \beta_{va}i_v(1-i_a-r_a)-(\mu_a+\alpha_a)i_a,\\ \tfrac{dr_a}{dt} &= \alpha_a i_a-(\mu_a+\gamma_a)r_a,\\ \tfrac{di_v}{dt} &= (\beta_{hv}i_h+\beta_{av}i_a)(1-i_v)-(\mu_v+u_2(t)\delta_v)i_v.\end{aligned}\right\} \tag{3.9}$$

In this case, a successful control strategy was thought to be one capable of reducing the proportion of infected humans and animals at minimal costs. Therefore, the following objective functional was proposed:

$$J(u_1(t),u_2(t)) = \int_0^{t_f} \left[c_1 i_h(t) + c_2 i_a(t) + \frac{w_1}{2}u_1^2(t) + \frac{w_2}{2}u_2^2(t)\right] dt. \tag{3.10}$$

subject to the constraints of the ODEs in system (3.9) and where c_1, c_2, w_1 and w_2 are non-negative constants known as the balancing coefficients and their goal is to transfer the integral into monetary quantity over a finite time interval $[0, t_f]$.

In (3.10), control efforts are assumed to be nonlinear-quadratic, since a quadratic structure in the control has mathematical advantages such as: if the control set is compact and convex, it follows that the Hamiltonian attains its minimum over the control set at a unique point (Silva *et al.*, 2016). Further, the goal was to find a control pair $(u_1^*, u_2^*) \in U$ such that condition (3.11) is attained:

$$J(u_1^*(t), u_2^*(t)) = \inf_{(u_1,u_2)\in U} J(u_1(t), u_2(t)), \tag{3.11}$$

for the admissible set $U = \{(u_1,u_2) \in (L^\infty(0,t_f))^2 : 0 \le u_i \le q_i; q_i \in \mathbb{R}^+, i = 1,2\}$, where q_i represents the upper bound of the control functions. Derivations on the existence of an optimal control pair as well as the necessary conditions that must be satisfied by optimal control solutions of system (3.9) are summarized in Theorem 3.2 (see Appendix 1 for detailed computations):

Theorem 3.2

Given an optimal control pair $u = (u_1, u_2) \in U$ and corresponding states (s_h, i_h, i_a, r_a), there exist adjoint functions $\lambda_1(t)$, $\lambda_2(t)$,$\lambda_3(t)$,$\lambda_4(t)$, and $\lambda_5(t)$ (Lenhart, 2007) satisfying (3.12):

$$\left.\begin{array}{rcl}
\frac{d\lambda_1(t)}{dt} &=& \lambda_1(\mu_h + u_1(t)\theta_h + \gamma_h + \beta_{vh} i_v) - \lambda_2 \beta_{vh} i_v, \\
\frac{d\lambda_2(t)}{dt} &=& -c_1 + \lambda_1 \gamma_h + \lambda_2(\mu_h + \alpha_h + d_h) - \lambda_5 \beta_{hv}(1 - i_h), \\
\frac{d\lambda_3(t)}{dt} &=& -c_2 + \lambda_3(\mu_a + \alpha_a + d_a + \beta_{va} i_v) - \lambda_4 \alpha_a - \lambda_5 \beta_{av}(1 - i_v), \\
\frac{d\lambda_4(t)}{dt} &=& \lambda_3 \beta_{va} i_v + \lambda_4(\mu_a + \gamma_a), \\
\frac{d\lambda_5(t)}{dt} &=& (\lambda_1 - \lambda_2)\beta_{vh} - \lambda_3 \beta_{va}(1 - i_a - r_a) + \lambda_5(\mu_v + u_2(t)\delta + \beta_{hv} i_h + \beta_{av} i_a).
\end{array}\right\} \tag{3.12}$$

In (3.12) $\lambda_j(t_f) = 0,\ j = 1,2,3,4,5$, models the transversality. Furthermore, these optimal

controls are characterized by:

$$\left.\begin{aligned} u_1 &= \min\left\{q_1, \max\left(0, \frac{\theta_h s_h \lambda_1}{w_1}\right)\right\}, \\ u_2 &= \min\left\{q_2, \max\left(0, \frac{\delta_v i_v \lambda_5}{w_2}\right)\right\}. \end{aligned}\right\} \tag{3.13}$$

Note that (3.13) follows from the standard arguments on bounds of controls (Lenhart, 2007).

3.3 Rhodesiense model with seasonal effects

Seasonal variations in climatic factors such as rainfall and temperature have a strong influence on the life cycle of tsetse flies thereby affecting their distribution and abundance (Nnko *et al.*, 2017). To account for this aspect, the basic model (3.6) was extended into a non-autonomous system, that is, model parameters in Table 2 which are influenced by seasonal effects were now considered to be periodic functions. In particular, the rhodesiense model with seasonal effects was formulated based on the following assumptions:

(i) An additional compartment for exposed population was included in the host (human and animal) and vector population, such that the total population of the host at time t was governed by $N_i(t) = S_i(t) + E_i(t) + I_i(t) + R_i(t)$ for $i = a, h$. Meanwhile, the total tsetse fly's population at time t was also governed by $N_v(t) = S_v(t) + E_v(t) + I_v(t)$. The addition of this new compartment meant that, upon infection the host and vector would now incubate the disease for a certain duration before becoming infectious. In particular, the host and vector were assumed to incubate the disease for an average time $1/\kappa_j$, with, $j = a, h, v$.

(ii) The forces of infection to account for vector-to-host disease transmission were remodeled as follows:

$$\left.\begin{aligned} \lambda_h(t) &= \frac{\sigma_v(t)N_v(t)\sigma_h}{\sigma_v(t)N_v(t)+\sigma_h N_h(t)}\beta_{vh}\frac{I_v(t)}{N_v(t)}, \\ \lambda_a(t) &= \frac{\sigma_v(t)N_v(t)\sigma_a}{\sigma_v(t)N_v(t)+\sigma_a N_a(t)}\beta_{va}\frac{I_v(t)}{N_v(t)}. \end{aligned}\right\} \tag{3.14}$$

In (3.14), parameter β_{vi} accounted for the probability of disease transmission from an infectious vector to a susceptible host i given that a contact between the two occurs, σ_a and σ_h represents the maximum number of vector bites an animal host and human host can sustain per unit time, respectively. The parameter:

$$\sigma_v(t) = \sigma_{v0}\left\{1 - \sigma_{v1}\cos\left(\frac{2\pi}{365}(t+\tau)\right)\right\}, \tag{3.15}$$

modeled the frequency of feeding activity by the tsetse flies and is also known as the

vector biting rate. Further, in (3.15), σ_{v0} is the average vector biting rate, and σ_{v1} defines the amplitude of seasonal variations (degree of periodic forcing, $0 < \sigma_{v1} < 1$), τ is a phase-shifting parameter to capture the timing of seasonality. Also note that a one-year cycle has been considered, that is, $\omega = \frac{2\pi}{365}$.

(iii) The force of infection to model host-to-vector disease transmission was reformulated as follows:

$$\lambda_v(t) = \frac{\sigma_v(t)\sigma_h N_h(t)}{\sigma_v(t)N_v(t) + \sigma_h N_h(t)}\beta_{hv}\frac{I_h(t)}{N_h(t)} + \frac{\sigma_v(t)\sigma_a N_a(t)}{\sigma_v(t)N_v(t) + \sigma_a N_a(t)}\beta_{va}\frac{I_a(t)}{N_a(t)}. \tag{3.16}$$

In (3.16), model parameter β_{hv} accounted for the likelihood of infection transmission from an infected human to a susceptible vector provided that there is a contact between the two species, β_{av} modeled the probability that disease transmission occurs whenever there is sufficient contact between a susceptible vector and infected animal.

(iv) Recruitment rate of vector b_v, natural mortality of vectors μ_v, and incubation rate for vectors were assumed to be no-longer constant but periodic functions and were defined as follows:

$$\left.\begin{array}{rcl} b_v(t) &=& b_{v0}[1 - b_{v1}\cos(\omega t + \tau)], \\ \mu_v(t) &=& \mu_{v0}[1 - \mu_{v1}\cos(\omega t + \tau)], \\ \kappa_v(t) &=& \kappa_{v0}[1 - \kappa_{v1}\cos(\omega t + \tau)]. \end{array}\right\} \tag{3.17}$$

In (3.17), b_{v0}, μ_{v_0} denotes the average birth and natural mortality rates, respectively, and b_{v_1} $(0 < b_{v_1} < 1)$ μ_{v_1} $(0 < \mu_{v_1} < 1)$ is the amplitude of the seasonal variation. Similarly, κ_{v_0} denotes the average incubation rate in the absence of seasonal variations and κ_{v_1} $(0 < \kappa_{v_1} < 1)$ is the amplitude of the seasonal variation.

Based on assumptions, the extended model was considered as follows:

$$\left.\begin{array}{rcl} \frac{dS_h}{dt} &=& b_h N_h(t) - \lambda_h(t)S_h(t) - \mu_h S_h(t) + \gamma_h R_h(t), \\ \frac{dE_h}{dt} &=& \lambda_h(t)S_h(t) - (\mu_h + \kappa_h)E_h(t), \\ \frac{dI_h}{dt} &=& \kappa_h E_h(t) - (\mu_h + \alpha_h + d_h)I_h(t), \\ \frac{dR_h}{dt} &=& \alpha_h I_h(t) - (\mu_h + \gamma_h)R_h(t), \\ \frac{dS_a}{dt} &=& b_a N_a(t) - \lambda_a(t)S_a(t) - \mu_a S_a(t) + \gamma_a R_a(t), \\ \frac{dE_a}{dt} &=& \lambda_a(t)S_a(t) - (\mu_a + \kappa_a)E_a(t), \\ \frac{dI_a}{dt} &=& \kappa_a E_a(t) - (\mu_a + \alpha_a + d_a)I_a(t), \\ \frac{dR_a}{dt} &=& \alpha_a I_a(t) - (\mu_a + \gamma_a)R_a(t), \\ \frac{dS_v}{dt} &=& b_v(t)N_v(t) - \lambda_v(t)S_v(t) - \mu_v(t)S_v(t), \\ \frac{dE_v}{dt} &=& \lambda_v(t)S_v(t) - (\kappa_v(t) + \mu_v(t))E_v(t), \\ \frac{dI_v}{dt} &=& \kappa_v(t)E_v(t) - \mu_v(t)I_v(t), \end{array}\right\} \tag{3.18}$$

subject to the initial conditions (3.19):

$$\left.\begin{array}{llll} S_h(0) = S_{h0} \geq 0, & E_h(0) = E_{h0} \geq 0, & I_h(0) = I_{h0} \geq 0, \\ R_h(0) = R_{h0} \geq 0, & S_a(0) = S_{a0} \geq 0, & E_a(0) = E_{a0} \geq 0, \\ I_a(0) = I_{a0} \geq 0, & R_a(0) = R_{a0} \geq 0, & S_v(0) = S_{v0} \geq 0, \\ E_v(0) = E_{v0} \geq 0, & I_v(0) = I_{v0} \geq 0. & \end{array}\right\} \tag{3.19}$$

From the detailed computations in Appendix 3, it was noted that that the solutions $(S_h(t), E_h(t), I_h(t), R_h(t), S_a(t), E_a(t), I_a(t), R_a(t), S_v(t), E_v(t), I_v(t))$ of the model (3.18) are uniformly and ultimately bounded in:

$$\Omega = \left\{ \left(\begin{array}{c} S_h(t) + E_h(t) + I_h(t) + R_h(t) \\ S_a(t) + E_a(t) + I_a(t) + R_a(t) \\ S_v(t) + E_v(t) + I_v(t) \end{array} \right) \in \mathbb{R}^{11}_{+} \middle| \begin{array}{l} N_h(t) \leq N_{h0}, \\ N_a(t) \leq N_{a0}, \\ N_v(t) \leq N_{v0} \end{array} \right\}, \tag{3.20}$$

with $N_h(0) = N_{h0}$, $N_a(0) = N_{a0}$ and $N_v(0) = N_{v0}$. Based on (3.20), one can conclude that model (3.18) is epidemiologically and mathematically well-posed in the region Ω for all $t \geq 0$. The flow diagram for model (3.18) is depicted in Fig. 5.

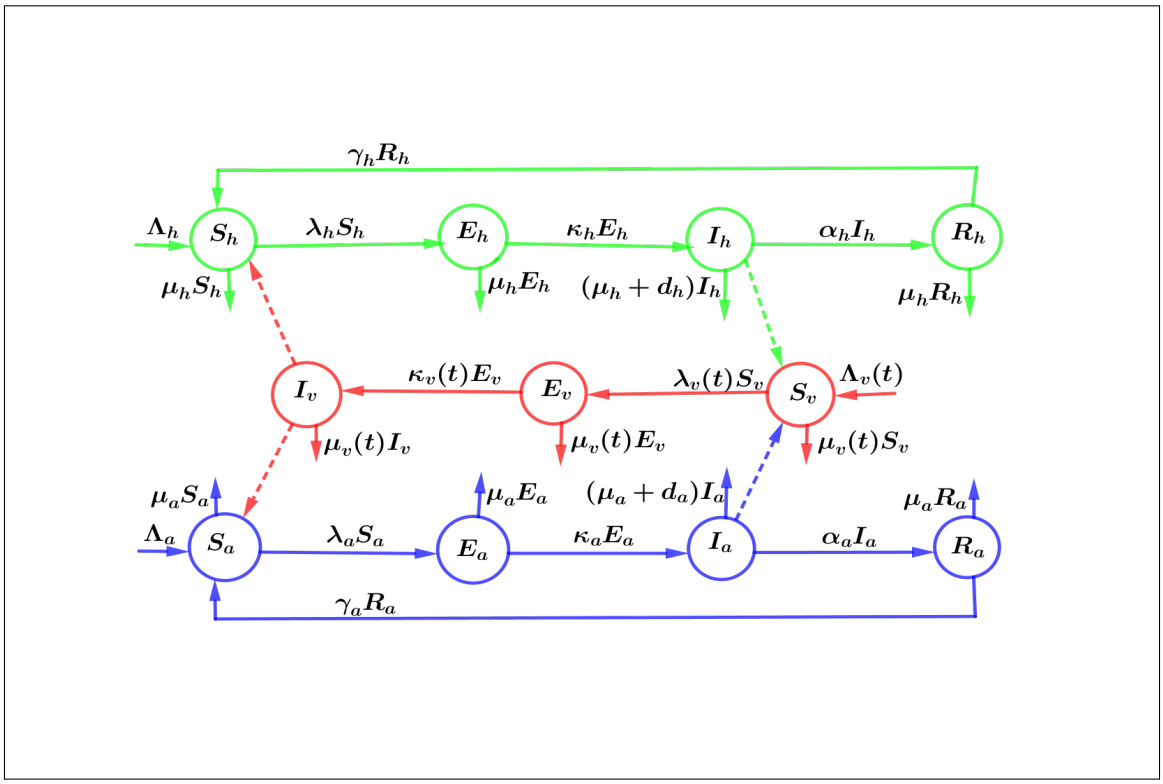

Figure 5: Schematic diagram of model (3.18)

3.3.1 Extinction and uniform persistence of the disease

To determine the extinction and uniform persistence of the disease, the basic reproduction number $\mathscr{R}_0$ of system (3.18) was computed using the next-generation matrix method proposed by Van den Driessche (2002). Based on the computations in appendix 3, the $\mathscr{R}_0$ of the time-averaged autonomous system was obtained as follows:

$$[\mathscr{R}_0] = \sqrt{\mathscr{R}_{0h} + \mathscr{R}_{0a}}, \tag{3.21}$$

where

$$\mathscr{R}_{0h} = \left(\frac{\kappa_h \beta_{vh} N_{h0} \kappa_{v0} \beta_{hv} N_{v0}}{\mu_{v0}(\kappa_{v0}+\mu_{v0})(\kappa_h+\mu_h)(\mu_h+\alpha_h+d_h)}\right)\left(\frac{\sigma_h \sigma_{v0}}{\sigma_{v0} N_{v0}) + \sigma_h N_{h0}}\right)^2,$$

$$\mathscr{R}_{0a} = \left(\frac{\kappa_a \beta_{va} N_{a0} \kappa_{v0} \beta_{av} N_{v0}}{\mu_{v0}(\kappa_{v0}+\mu_{v0})(\kappa_a+\mu_a)(\mu_a+\alpha_a+d_a)}\right)\left(\frac{\sigma_a \sigma_{v0}}{\sigma_{v0} N_{v0} + \sigma_a N_{a0}}\right)^2.$$

In (3.21), the threshold quantities $\mathscr{R}_{0h}$ and $\mathscr{R}_{0a}$ represent the power of the disease to invade the human and animal hosts, respectively. Due to several time-dependent parameters in model (3.18), a detailed derivation of the seasonal reproduction number has been presented in Appendix 3 together with results on stability of the model. In particular, results on the stability of the model equilibria for model (3.18) are summarized in Theorem 3.3.

Theorem 3.3
If $R_0 < 1$, then the disease-free equilibrium $\mathscr{E}_0$ of system (3.18) is globally asymptotically stable. However, if $R_0 > 1$, then system (3.18) admits at least one positive ω-periodic solution, and solutions of system (3.18) are uniformly persistent.

3.3.2 The optimal control problem for a seasonality model

Prior studies suggest that time-dependent intervention strategies have more impact on disease management compared to non-time dependent (Lenhart, 2007). To infer on this assertion, model (3.18) was extended to incorporate two controls $u_1(t)$ and $u_2(t)$, which modeled time-dependent media campaigns and insecticide use. The controls were assigned reasonable lower and upper bounds to reflect their limitations. Due to the unavailability of baseline values for these bounds in literature most of them were evaluated through simulations to demonstrate their impact. Utilizing the same variables and parameter names as in (3.18), the extended model with controls

had the form:

$$\left.\begin{array}{rcl}
\frac{dS_h}{dt} &=& b_h N_h(t) - \lambda_h(t) S_h(t) - \mu_h S_h(t) - u_1(t) S_h(t) + \gamma_h R_h(t), \\
\frac{dE_h}{dt} &=& \lambda_h(t) S_h(t) - (\mu_h + \kappa_h) E_h(t), \\
\frac{dI_h}{dt} &=& \kappa_h E_h(t) - (\mu_h + \alpha_h + d_h) I_h(t), \\
\frac{dR_h}{dt} &=& u_1(t) S_h(t) + \alpha_h I_h(t) - (\mu_h + \gamma_h) R_h(t), \\
\frac{dS_a}{dt} &=& b_a N_a(t) - \lambda_a(t) S_a(t) - \mu_a S_a(t) + \gamma_a R_a(t), \\
\frac{dE_a}{dt} &=& \lambda_a(t) S_a(t) - (\mu_a + \kappa_a) E_a(t), \\
\frac{dI_a}{dt} &=& \kappa_a E_a(t) - (\mu_a + \alpha_a + d_a) I_a(t), \\
\frac{dR_a}{dt} &=& \alpha_a I_a(t) - (\mu_a + \gamma_a) R_a(t), \\
\frac{dS_v}{dt} &=& b_v(t) N_v(t) - \lambda_v(t) S_v(t) - (\mu_v(t) + u_2(t)) S_v(t), \\
\frac{dE_v}{dt} &=& \lambda_v(t) S_v(t) - (\kappa_v(t) + \mu_v(t) + u_2(t))) E_v(t), \\
\frac{dI_v}{dt} &=& \kappa_v(t) E_v(t) - (\mu_v(t) + u_2(t)) I_v(t),
\end{array}\right\} \tag{3.22}$$

subject to the initial values:

$$\left.\begin{array}{rcllll}
S_h(0) &=& S_{h0} \geq 0, & E_h(0) = E_{h0} \geq 0, & I_h(0) = I_{h0} \geq 0, \\
R_h(0) &=& R_{h0} \geq 0, & S_a(0) = S_{a0} \geq 0, & E_a(0) = E_{a0} \geq 0, \\
I_a(0) &=& I_{a0} \geq 0, & R_a(0) = R_{a0} \geq 0, & S_v(0) = S_{v0} \geq 0, \\
E_v(0) &=& E_{v0} \geq 0, & I_v(0) = I_{v0} \geq 0.
\end{array}\right\}. \tag{3.23}$$

As one can note, in system (3.22), it is assumed that humans who become aware of the disease have negligible chances of acquiring it and also insecticide use affects all epidemiological classes of the vector populations. Furthermore, it was assumed that $u_i(t)$ ranges between 0 and q_i, that is $0 \leq u_i(t) \leq q_i < 1$, such that $u_i = 0$ reflects the absence of time-dependent controls and q_i represents the upper bound of the control. The control set is:

$$U = \left\{ (u_1, u_2) | \in (L^{\infty}(0, t_f)) : 0 \leq u_i \leq q_i < 1, \quad q_i \in \mathbb{R}^+, \quad i = 1, 2. \right\}. \tag{3.24}$$

In developing response plans for the effective management of diseases, policymakers seek optimal responses/strategies that can minimize the incidence and/or disease-related mortality rates while considering the costs involved. Here, the main goal was to minimize the number of infectious hosts (humans and animals) with minimal implementation costs. Thus, the following objective functional was considered:

$$J(u_1(t), u_2(t)) = \int_0^{t_f} \left(C_1 I_h(t) + C_2 I_a(t) + \frac{W_1}{2} u_1^2(t) + \frac{W_2}{2} u_2^2(t) \right) dt. \tag{3.25}$$

Equation (3.25) was considered subject to the constraints of the ODEs in system (3.22), with C_1, C_2, W_1 and W_2 as positive constants also known as the balancing coefficients. These balancing coefficients transfers the integral into a monetary quantity over a finite time interval $[0, t_f]$.

In (3.25), control efforts were assumed to be nonlinear-quadratic. The quadratic structure in the control has mathematical advantages such as: if the control set is a compact and convex, it follows that the Hamiltonian attains its minimum over the control set at a unique point. Using (3.25) and (3.22), derivations on the existence of an optimal control pair as well as the necessary conditions that must be satisfied by optimal control solutions of system (3.22) are in Appendix3.

3.4 Rhodesiense model with memory and temperature effects

3.4.1 Model formulation and assumptions

Memory effects are inherent in many biological phenomena (Kheiri, 2019), and prior studies suggest, that they have a significant influence on short-and long-term *T. brucei rhodesiense* dynamics. In addition, prior laboratory experiments have shown that temperature has an integral role on *T. brucei rhodesiense* dynamics (Phelps, 1973; Coetzer *et al.*, 2004; Alderton *et al.*, 2018). In particular, Coetzer *et al.* (2004) noted that temperature does not only alter the different developmental periods of the vector but it also plays a huge role in the fly's flight activity. To investigate the combined effects of memory and temperature on *T. brucei rhodesiense* dynamics, model (3.6) was extended to incorporate the early development stages of tsetse flies as well as temperature-dependent model parameters.

To capture memory effects, mathematical model for *T. brucei rhodesiense* disease was formulated using fractional-order derivatives. A Caputo derivative was considered since it is the commonly used to model biological phenomena (Gashirai *et al.*, 2021). Moreover, unlike other derivatives such the Riemann-Liouville, the Caputo derivative deals properly with initial value problems and also the Caputo derivative for a constant is equivalent to zero. Additional assumptions that were considered for the extended model are as follows:

(i) The life cycle of the tsetse flies was incorporated and was accounted for by the following system of equations:

$$\left.\begin{aligned} {}^{c}_{t_0}D^{\alpha}_{t} L(t) &= b^{\alpha}_{l} W N_v \left(1 - \tfrac{L}{K^{\alpha}_{l}}\right) - (\sigma^{\alpha}_{l} + \mu^{\alpha}_{p}) L, \\ {}^{c}_{t_0}D^{\alpha}_{t} N_v(t) &= \sigma^{\alpha}_{l} L - \mu^{\alpha}_{v} N_v. \end{aligned}\right\} \tag{3.26}$$

In (3.26), the $L(t)$ modeled the pupal stage of the tsetse, and $N_v(t)$ denotes the total adult vector population at time t, which comprised of susceptible $S_v(t)$, and infectious $I_v(t)$

adults such that, $N_v = S_v + I_v$. In addition, all model parameters and variables in system (3.26) were considered to be nonnegative. Furthermore, other model parameters were defined as follows: b_l denoted the rate at which female flies gave birth to larvae; W accounted for a fraction of female flies in the population of adult flies; K_l modeled the pupal carrying capacity of the nesting site; σ_l modeled the transition from the pupal stage into an adult fly. In addition μ_p and μ_v accounted for the mortality rate of pupae and adult flies, respectively.

(ii) To incorporate the effects of temperature on the development of tsetse flies, model parameters of system (3.26) were remodeled as functions of temperature (T). In these functions were adapted from the worked of Hargrove (1994) and Lord *et al.* (2018). Thus, the rate at which female flies give birth was reformulated as follows:

$$b_l(T) = d_1 + d_2(T - T_0). \tag{3.27}$$

In (3.27), b_l denotes the rate in which the tsetse flies giving birth and T_0 was set to 20°C (Lord *et al.*, 2018). The function (3.27) was derived by Hargrove (1994) when the author used ovarian dissection data from marked and released *G. m. morsitans* and *G. pallidipes* at Rekomitjie and suggested that the larviposition rate per day increases linearly between 20 and 30°C.

(iii) Adult fly mortality rate was redefined as follows:

$$\mu_v(T) = \begin{cases} a_1 & T \leq 25, \\ a_1 e^{a_2(T-25)} & T > 25, \end{cases} \tag{3.28}$$

In (3.28), μ_v denotes the adult mortality rate, T modeled the temperature in °C, and a_2 accounted for an increase in temperature. Further, based on the laboratory experiments performed by Phelps (1973), pupal survival to adulthood was found to dependent on temperature variations and it was noted to be highest for temperatures between about 20 and 30°C. It was also observed that as temperatures shift from this range, the mortality was rose sharply, leading to a U-shaped curve and a suitable function to represent this relation was proposed as follows:

$$\mu_p(T) = b_1 + b_2\exp(-b_3(T - T_2)) + b_4\exp(b_5(T - T_3)). \tag{3.29}$$

In (3.29), T accounted for the temperature in °C, T_2 and T_3 are not parameters but are constants which were selected to ensure that the coefficients b_3 and b_5 respectively in a convenient range and in our simulation these will be set to 16°C and 32°C as in Lord *et al.* (2018).

(iv) Another important result from the work of Phelps (1973) was the quantification of the daily rate of pupal development in *G. m. morsitans* as a function of constant temperature. The following function was considered to be the best representation of pupal emergence and temperature variations:

$$\sigma_l(T) = \frac{c_1}{1+\exp(c_2+c_3T)}. \tag{3.30}$$

In (3.30), σ_L denotes the growth rate of tsetse flies from pupal to an adult stage, T accounted for the mean daily temperature and c_1, c_2 and c_3 modeled pupal hatching rate (Lord *et al.*, 2018).

(v) Apart from modeling early development stages of the vector a temperature-dependent functions, in the extended model, disease transmission from infectious vectors to susceptible hosts is modelled by a non-linear incidence rate and the function $f(I_v)$ is equivalent to $f(I_v) = I_v/(1+\theta I_v$ where θ is a positive constant. This type of infection is sometimes referred to as 'incidence rate with psychological effect' because the effect of θ stems from epidemic control (taking appropriate preventive measures and awareness) and the rate of infection decreases as the inhibitory coefficient θ increases (Ghosh *et al.*, 2019).

The above assumptions led to the following system of equations:

$$\left.\begin{aligned}
{}^{c}_{t_0}D^{\alpha}_{t}L(t) &= b^{\alpha}_{l}WN_v\left(1-\tfrac{L}{K^{\alpha}_{l}}\right)-(\sigma^{\alpha}_{l}+\mu^{\alpha}_{p})L,\\
{}^{c}_{t_0}D^{\alpha}_{t}N_v(t) &= \sigma^{\alpha}_{l}L-\mu^{\alpha}_{v}N_v,\\
{}^{c}_{t_0}D^{\alpha}_{t}S_v(t) &= \sigma^{\alpha}_{l}L-(\beta^{\alpha}_{hv}I_h+\beta^{\alpha}_{av}I_a)S_v-\mu^{\alpha}_{v}S_v,\\
{}^{c}_{t_0}D^{\alpha}_{t}I_v(t) &= (\beta^{\alpha}_{hv}I_h+\beta^{\alpha}_{av}I_a)S_v-\mu^{\alpha}_{v}I_v,\\
{}^{c}_{t_0}D^{\alpha}_{t}S_h(t) &= \Lambda^{\alpha}_{h}-\beta^{\alpha}_{vh}f(I_v)S_h-\mu^{\alpha}_{h}S_h,\\
{}^{c}_{t_0}D^{\alpha}_{t}I_h(t) &= \beta^{\alpha}_{vh}f(I_v)S_h-(\mu^{\alpha}_{h}+\gamma^{\alpha}_{h})I_h,\\
{}^{c}_{t_0}D^{\alpha}_{t}S_a(t) &= \Lambda^{\alpha}_{a}-\beta^{\alpha}_{va}f(I_v)S_a-\mu^{\alpha}_{a}S_a,\\
{}^{c}_{t_0}D^{\alpha}_{t}I_a(t) &= \beta^{\alpha}_{va}f(I_v)S_a-(\mu^{\alpha}_{a}+\gamma^{\alpha}_{a})I_a,\\
{}^{c}_{t_0}D^{\alpha}_{t}R_h(t) &= \gamma^{\alpha}_{h}I_h-\mu^{\alpha}_{h}R_h,\\
{}^{c}_{t_0}D^{\alpha}_{t}R_a(t) &= \gamma^{\alpha}_{a}I_a-\mu^{\alpha}_{a}R_a.
\end{aligned}\right\} \tag{3.31}$$

Note that, to avoid flaws regarding the time dimension, we introduced α in the model parameters (right-hand side) of model (3.31), so that the dimensions of these parameters become $(time)^{-\alpha}$ which is in agreement with the left-hand side of the model. Comprehensive definitions of the model variables and parameters can be found in Table 1 and 2, respectively. The flow diagram for model (3.31) is depicted in Fig. 6.

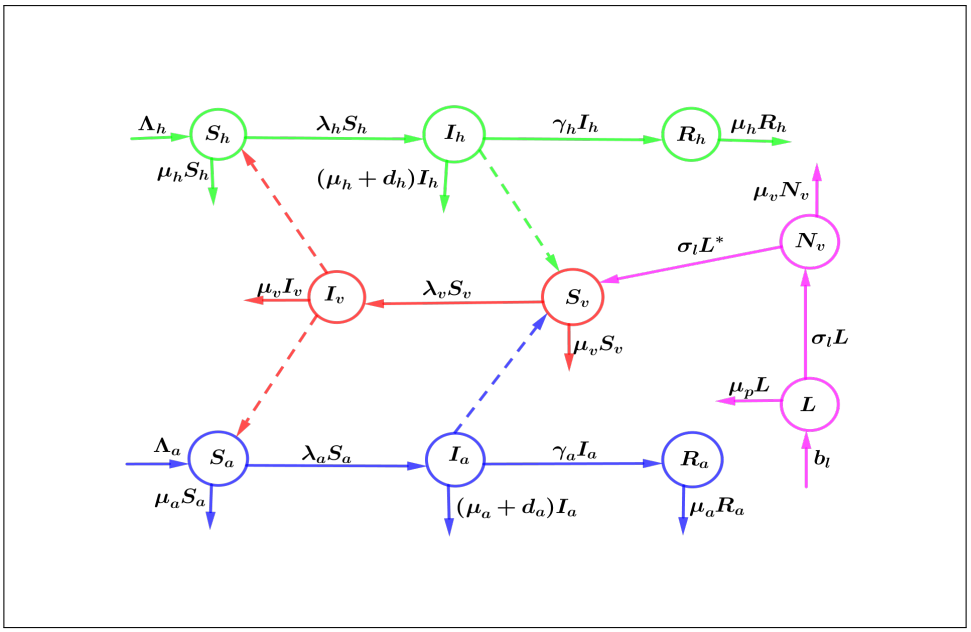

Figure 6: Schematic diagram of model (3.31)

3.4.2 Analysis of the tsetse fly dynamical growth model

Before the analysis of model (3.31), there was need to investigate the conditions for extinction and persistence of the tsetse fly population at an early stage. Hence analysis of model (3.26) was conducted first. It was noted that model (3.26) is biologically meaningful and all model solutions are unique, Theorem 3.4 (see Appendix 4).

Theorem 3.4

Let $\mathscr{X}(t) = (L(t), N_v(t))$ be the unique of the model (3.26) for $t \geq 0$. Then, the solution $\mathscr{X}(t)$ is bounded above, that is, $\mathscr{X}(t) \in \Omega$ where Ω denotes the feasible region and is given by:

$$\Omega = \left\{ \left(L, N_v \right) \in \mathbb{R}^2_+ \middle| 0 \leq L \leq K_l^{\alpha}, \;\; 0 \leq N_v \leq C \right\}. \tag{3.32}$$

where $C = \max \left\{ \frac{\sigma_l^{\alpha} K_l^{\alpha}}{\mu_v^{\alpha}}, N_v(0) \right\}$.

Based on the outcome of Theorem 3.4, the equilibrium points of model (3.26) were computed and their stability was also investigated. The computations revealed that model (3.26) has two equilibrium points, namely the a trivial $(L, N_v) = (0, 0)$ and a non-trivial:

$$\{L^*, N_v^*\} = \left\{ \left(1 - \frac{1}{r} \right) K_l^{\alpha}, \frac{\sigma_l^{\alpha}}{\mu_v^{\alpha}} \left(1 - \frac{1}{r} \right) K_l^{\alpha} \right\}, \tag{3.33}$$

where:

$$r = \frac{\sigma_l^\alpha}{\sigma_l^\alpha + \mu_p^\alpha} \frac{b_l^\alpha}{\mu_v^\alpha} W. \tag{3.34}$$

From (3.33) and (3.34), it was noted that r is a threshold quantity that determines the growth of the tsetse fly population. It is defined as the likelihood of the fly to survive the pupal stage multiplied by the surviving population of female flies (Ndondo *et al.*, 2016). A comprehensive analysis on the stability of the two equilibrium points of model (3.26) revealed the results summarized in Theorem 3.5 (See Appendix 4 for detailed computation).

Theorem 3.5
For $\alpha \in (0,1)$, and $r \leq 1$, model (3.26) has a sole equilibrium point $(0,0)$ which is globally (uniformly) asymptotically stable in Ω. However, if $r > 1$, then model (3.26) admits a unique equilibrium (L^*, N_v^*) is also globally (uniformly) asymptotically stable in the interior of Ω.

3.4.3 Analysis of the full rhodesiense model (3.31)

Based on the results in Theorem 3.4 and 3.5, an analysis of the full rhodesiense model (3.31) was conducted. Making use of the next-generation matrix method proposed in Van den Driessche (2002) the basic reproduction number of of model (3.31) was obtained as follows:

$$\mathscr{R}_0 = \sqrt{K_l^\alpha \frac{\sigma_l^\alpha}{\mu_v^\alpha} \left(1 - \frac{1}{r}\right) \left(\frac{\beta_{vh}^\alpha \beta_{hv}^\alpha \Lambda_h^\alpha}{\mu_v^\alpha \mu_h^\alpha (\mu_h^\alpha + \gamma_h^\alpha)} + \frac{\beta_{av}^\alpha \beta_{va}^\alpha \Lambda_a^\alpha}{\mu_v^\alpha \mu_a^\alpha (\mu_a^\alpha + \gamma_a^\alpha)} \right)}. \tag{3.35}$$

The $\mathscr{R}_0$ in (3.35) accounted for the expected number of secondary cases (vector or host) produced in a completely susceptible population, by one infectious individual (vector or host, respectively) during its lifetime. It was noted that $\mathscr{R}_0$ is an integral epidemiological metric for understanding *T. brucei rhodesiense* persistence and extinction. It was also noted that this metric depends of disease transmission parameters β_{ij} for $i \neq j = a,h,v$, the average infectious period of the vector (host) $\frac{1}{(\mu_i^\alpha + \gamma_i^\alpha)}$, vector competence and survival $\frac{\sigma_l^\alpha}{\mu_v^{2\alpha}} \left(1 - \frac{1}{r}\right) K_l^\alpha$. Further dynamics analysis of model (3.31) revealed the results in Theorem 3.6 (see., Appendix for detailed computations).

Theorem 3.6
For $\alpha \in (0,1)$, $r > 1$, and $\mathscr{R}_0 < 1$, model system (3.31) admits a unique disease-free equilibrium which is globally (uniformly) asymptotically stable. However, if $\mathscr{R}_0 > 1$, the disease-free equilibrium becomes unstable and there exists a unique globally (uniformly) asymptotically stable endemic equilibrium point.

3.5 Rhodesiense model with time delay and heterogeneity in human population

Various biological reasons lead to the introduction of time delays in models of disease transmission. Precisely, biological processes have intrinsic delays which can represent temporary immunity, latency in a vector,gestation periods, immune activation, and incubation periods in infectious diseases (Mushayabasa, 2015, 2016; Ding *et al.*, 2016). There is growing interest among researchers to understand the implications of time delays on the dynamics of infectious and non-infectious diseases.

Despite several studies on HAT dynamics, several important questions regarding the transmission and control of sleeping sickness remain unanswered (Kajunguri, 2013; Ndondo *et al.*, 2016; Rock *et al.*, 2015). For example, how to characterize the role of incubation period in vector population? Cognizant that the incubation period in tsetse vectors is close their life span, there is a need to assess its influence on the short-and long-term dynamics of the disease. Another question is: to what extent does heterogeneity exposure to tsetse vectors in the human population influence the short-and long-term dynamics of the disease?

Considering that sleeping sickness is predominant in poor populations in sub-Saharan Africa (Stone, 2015), there is a need to understand the combined effects of heterogeneous exposure to the tsetse vector and the incubation period of the vectors on the short-and long-term dynamics of the disease. Motivated by the two aforementioned research questions, model (3.31) was extended to include latency delay in tsetse flies and heterogeneity in human population. However, it is worth noting that here, an integer order differentiation was considered. The proposed model

was governed by the following system of equations:

$$\left.\begin{aligned}
L'(t) &= b_P W N_V(t)\left(1-\tfrac{L(t)}{K_L}\right)-(\sigma_L+\mu_P)L(t),\\
N_V'(t) &= \sigma_P L(t)-\mu_P N_V(t),\\
S_V'(t) &= \sigma_L L(t)-\beta_{HV}[I_{H1}(t)+(1-\varepsilon_H)I_{H2}(t)]S_V(t)\\
&\quad -\beta_{AV}I_A(t)S_V(t)-\mu_V S_V(t),\\
I_V'(t) &= [\beta_{HV}(I_{H1}(t-\tau)+(1-\varepsilon_H)I_{H2}(t-\tau))\\
&\quad +\beta_{AV}I_A(t-\tau)]S_V(t-\tau)e^{-\mu_V\tau}-\mu_V I_V(t),\\
S_{H1}'(t) &= \mu_H p_H N_H-\beta_{VH}f(I_V(t))S_{H1}(t)-\mu_H S_{H1}(t),\\
I_{H1}'(t) &= \beta_{VH}f(I_V(t))S_{H1}(t)-(\mu_H+\gamma_H)I_{H1}(t),\\
S_{H2}'(t) &= \mu_H(1-p_H)N_H-\beta_{VH}(1-\varepsilon_H)f(I_V(t))S_{H2}(t)-\mu_H S_{H2}(t),\\
I_{H2}'(t) &= \beta_{VH}(1-\varepsilon_H)f(I_V(t))S_{H2}(t)-(\mu_H+\gamma_H)I_{H2}(t),\\
S_A'(t) &= \mu_A N_A-\beta_{VA}f(I_V(t))S_A(t)-\mu_A S_A(t),\\
I_A'(t) &= \beta_{VA}f(I_V(t))S_A(t)-(\mu_A+\gamma_A)I_A(t),\\
R_{H1}'(t) &= \gamma_H I_{H1}(t)-\mu_H R_{H1}(t),\\
R_{H2}'(t) &= \gamma_H I_{H2}(t)-\mu_H R_{H2}(t),\\
R_A'(t) &= \gamma_A I_A(t)-\mu_A R_A(t).
\end{aligned}\right\} \tag{3.35}$$

All other variables and parameters retain definitions presented in Table 1 and 2, respectively. However, to account for heterogeneity in the human population, all the previously considered human compartments (in model 3.31) have an additional one, for example S_{H1} and S_{H2} modeled susceptible human populations in patch 1 and patch 2, respectively. Individuals in these two patches were assumed to have an unequal degree of risk of infection based on their socio-economic status and geographical location. For the distinction individuals in patch 2, were assumed to be at low-risk compared to those in patch 1. Hence, the factor $(1-\varepsilon_H)$, accounted for the assumed reduction in disease transmission between the low-risk individuals and vector, with $0<\varepsilon_H<1$. For the human population, a fraction p_H of new recruits was assumed to occur in the high risk-group and the remainder $(1-p_H)$ occur in the low risk group. In addition, the time delay factor, $\tau \geq 0$ modeled the incubation period in the tsetse fly population. Thus, $0<e^{-\mu_V\tau}\leq 1$ represented the survival rate of the exposed vectors. Figure 7 illustrate the model flow diagram.

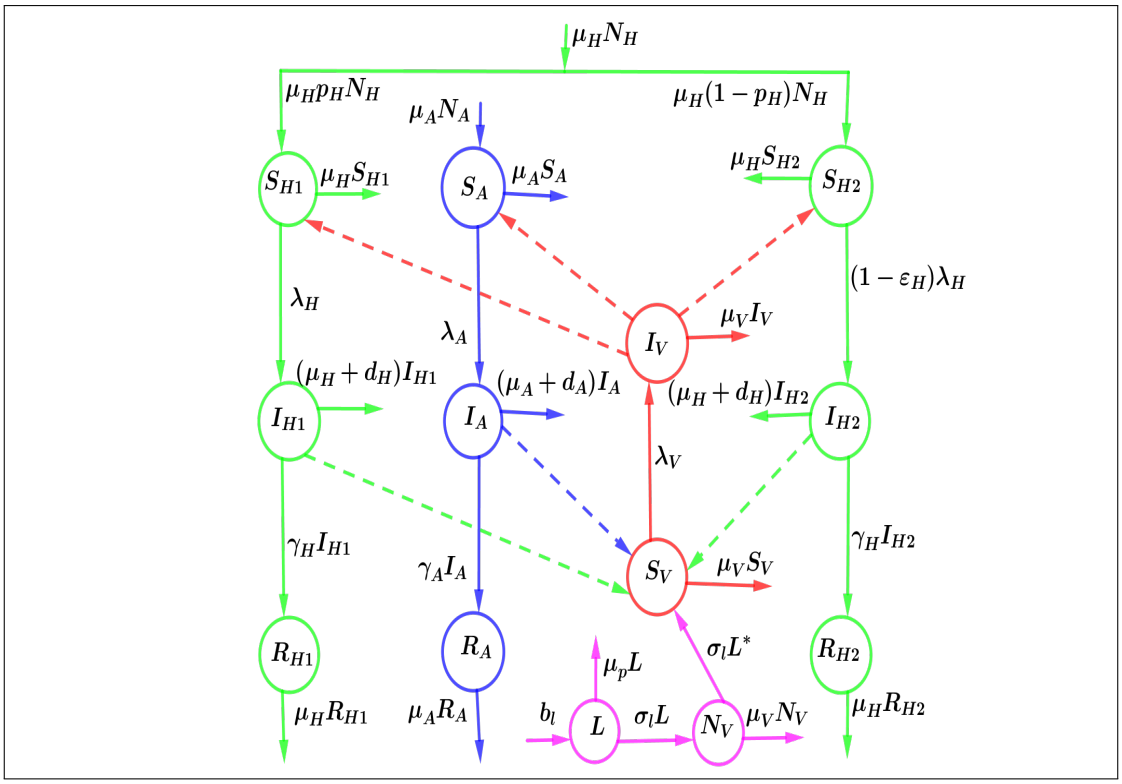

Figure 7: Schematic diagram of model (3.5)

3.5.1 Initial conditions and positivity of solutions

The appropriate space for system (3.5) is $X = \mathscr{C}([-\tau,0],\mathbb{R}^{13}_+)$ the Banach space of continuous functions mapping the interval $[-\tau,0]$ into $\mathbb{R}^{13}_+$ equipped with sub-norm where $\tau \geq 0$. From the standard results of functional differential equations (Hale *et al.*, 1993), it follows that, given any initial conditions $x_0 \in X$ there exists a unique solution $\phi(t,x_0) = (L(t,x_0),N_V(t,x_0),S_i(t,x_0),I_i(t,x_0),R_i(t,x_0))$, $i = A,V,H1,H2$, of system (3.5), which satisfies $\phi_0 = x_0$, the initial conditions are given by:

$$\left.\begin{array}{llll} L(\theta) = x_0^1(\theta), & N_V(\theta) = x_0^2(\theta), & S_V(\theta) = x_0^3(\theta), \\ I_V(\theta) = x_0^4(\theta), & S_{H1}(\theta) = x_0^5(\theta), & I_{H1}(\theta) = x_0^6(\theta), \\ R_{H1}(\theta) = x_0^7(\theta), & S_{H2}(\theta) = x_0^8(\theta), & I_{H2}(\theta) = x_0^9(\theta), \\ R_{H2}(\theta) = x_0^{10}(\theta), & S_A(\theta) = x_0^{11}(\theta), & I_A(\theta) = x_0^{12}(\theta), \\ R_A(\theta) = x_0^{13}(\theta), & -\tau \leq \theta \leq 0. & \end{array}\right\}. \tag{3.35}$$

In (3.5.1) $x_0 = x_0^i \in X$ with $x_0^i(\theta) \geq 0$ $(\theta \in [-\tau,0])$, $i = 1,2,3,...,13$. By summing all the equations that represent the human population one can easily note that, the total human population considered in this study is constant, that is; $N'_H(t) = S'_i(t) + I'_i(t) = 0$, for $i = H1,H2$. This implies that $N_H(t) = N_H$, where N_H is a positive constant. Similarly, by summing the equations for the animal population one can also demonstrate that $N'_A(t) = S'_A(t) + I'_A(t) = 0$, such that

$N_A(t) = N_A$. For the proposed system to be biologically meaningful the solutions of the first equation in (3.5) need to be bounded in the region, $0 \leq L \leq K_L$. Hence, it follows that solutions for the equations that describe the adult tsetse vector population will be bounded in the region $0 \leq N_V \leq \frac{\sigma_L}{\mu_v} K_L$. From this, it was concluded that all feasible solutions of the system (3.5) are bounded and enter the region (3.5.1):

$$\Omega = \left\{ \begin{pmatrix} L(t) \\ N_V(t) \\ N_H(t) \\ N_A(t) \end{pmatrix} \in \mathbb{R}^{13}_{+} \middle| \begin{array}{l} 0 \leq L \leq K_L, \\ N_v(t) \leq \frac{\sigma_L}{\mu_v} K_L, \\ N_H(t) = N_H, \\ N_A(t) = N_A \end{array} \right\}, \tag{3.35}$$

Hence it was concluded that the solutions of model (3.5) determined from initial conditions (3.5.1) remain positive for $t \geq 0$ and are bounded and lie in the region Ω which is positively invariant with respect to model (3.5).

3.5.2 The basic reproduction number and model equilibria

Following the next-generation matrix method proposed by Van den Driessche (2002), the $\mathscr{R}_0$ of model (3.5) was found to be (see Appendix 5 for the derivation) (3.36):

$$\mathscr{R}_0 = \sqrt{\left(\mathscr{R}_H + \mathscr{R}_A\right)\left(1 - \frac{1}{r}\right)\frac{\sigma_L e^{-\mu_v \tau}}{\mu_V} K_L}, \tag{3.36}$$

with $\mathscr{R}_H = \frac{\beta_{VH}\beta_{HV} N_H [p_H + (1-p_H)(1-\varepsilon_H)^2]}{\mu_V(\mu_H + \gamma_H)}$, $\mathscr{R}_A = \frac{\beta_{AV}\beta_{VA} N_A}{\mu_V(\mu_A + \gamma_A)}$ and $r = \frac{\sigma_l^{\alpha}}{\sigma_l^{\alpha} + \mu_p^{\alpha}} \frac{b_l^{\alpha}}{\mu_v^{\alpha}} W$. The $\mathscr{R}_0$ (3.36) was defined as the measure of the expected number of secondary cases (vector or host) produced in a completely susceptible population by one infectious individual (vector or host, respectively) during its lifetime as infectious. Further dynamical analysis of model (3.5) on the stability of model equilibria revealed outcomes summarized in Theorem 3.7.

Theorem 3.7
If $\mathscr{R}_0 \leq 1$ model (3.5) admits a diease-free equilibrium which is globally asymptotically stable. However, if $\mathscr{R}_0 > 1$ the disease-free equilibrium is unstable and there exists a unique endemic equilibrium point that is globally asymptotically stable.

3.6 Chapter overview

In this chapter, four mathematical models meant to understand the transmission dynamics of *T. brucei rhodesiense* dynamics were formulated and analyzed. In the first model, the effects

of educational campaigns were considered. It was noted that due to educational campaigns, the model undergoes a backward bifurcation, that is, a stable disease-free equilibrium co-exists with one or more stable endemic equilibria when the associated reproduction number is less than unity. In the second model, the effects of seasonality on tsetse fly development and feeding were investigated. Among the several outcomes, it was observed that if the model $\mathscr{R}_0$ is less than unity, the model has a sole equilibrium point, the disease-free equilibrium which is globally asymptotically stable. However, whenever the $\mathscr{R}_0$ is greater than unity the non-autonomous model admits at least one positive ω-periodic solution, and solutions of the model are considered to be uniformly persistent. In the third model, effects of temperature and memory effects of *T. brucei rhodesiense* dynamics were investigated. The results showed that indeed memory and temperature have significant effects on the extinction and persistence of the disease in the community. In the fourth model, it was noted that time delay and heterogeneity have a significant impact on the stability of the model's steady states. In the next chapter, simulation were carried out to support the analytical results presented in this chapter.

CHAPTER FOUR

RESULTS AND DISCUSSION

4.1 Introduction

In this chapter, the results obtained after the proposed mathematical models were simulated are presented and comprehensively discussed. A majority of baseline values for the model parameters were drawn from literature and sources from which they were obtained have been acknowledged. In circumstances where baseline values were not found in literature, an assumed baseline value and the justification were provided.

4.2 Numerical results of model with educational campaigns

4.2.1 Data fitting and model validation

Tanzania is one of the countries in sub-Saharan Africa were *T. brucei rhodesiense* cases have been recorded since 1990 (Franco *et al.*, 2014*a*). WHO report *T. brucei rhodesiense* data for Tanzania as shown in Table 3 was used to calibrate and validate model (3.6). Making use of the least square method was conducted in MATLAB programming Language during model calibration process. Cumulative yearly infections (human) predicted by the proposed model, $C(t)$, were defined by equation (4.1):

$$\frac{dC}{dt} = \beta_{vh} i_v(t) s_h(t) \tag{4.1}$$

Thus, the estimation of confirmed cumulative *T. brucei rhodesiense* cases over a fixed time interval $t_{k-1} \leq t \leq t_k$ (where t_0 and T marks the beginning and end of the time interval, respectively) from the model output is computed using equation (4.2):

$$C_k = \int_{t_{k-1}}^{t_k} \beta_{vh} i_v(\tau) s_h(\tau) d\tau. \tag{4.2}$$

During the fitting process model, five (5) parameters θ_h, βvh, β_{va}, β_{hv} and β_{av} were determined by fitting the model, while the remainder of parameters assumed baseline values as presented in Table 2.

Table 1: *T. brucei rhodesiense* data for Tanzania, 1990-2017 (Franco *et al.*, 2014*a*)

Year	1990	1991	1992	1993	1994	1995	1996	1997
Observed cases	187	177	366	262	319	422	400	354
Rescaled data	0.10	0.09	0.18	0.08	0.16	0.2	0.2	0.18
Year	1998	1999	2000	2001	2002	2003	2004	2005
Observed cases	299	288	350	277	228	113	159	186
Rescaled data	0.15	0.14	0.18	0.14	0.11	0.06	0.08	0.09
Year	2006	2007	2008	009	2010	2011	2012	2013
Observed cases	126	126	59	14	5	1	4	
Rescaled data	0.06	0.06	0.003	0.007	0.003	0.0005	0.0005	0.002
Year	2014	2015	2016	2017				
Observed cases	1	2	3	4				
Rescaled data	0.0005	0.001	0.0015	0.002				

Table 2: Baseline values for parameters of model (3.6)

Symbol	Parameter baseline value	Units	Source
γ_h	$1/90$	Day^{-1}	Rogers (1988); Moore *et al.* (2012*a*)
γ_a	$1/75$	Day^{-1}	Rogers (1988); Moore *et al.* (2012*a*)
μ_h	$1/(365 \times 50)$	Day^{-1}	Kajunguri (2013); Ndondo *et al.* (2016)
μ_a	$1/(365 \times 15)$	Day^{-1}	Kajunguri (2013); Ndondo *et al.* (2016)
μ_v	$1/33$	Day^{-1}	Artzrouni (1996*c*); Ndondo *et al.* (2016)
α_h	$1/30$	Day^{-1}	Rogers (1988); Ndondo *et al.* (2016)
α_a	$1/25$	Day^{-1}	Rogers (1988); Ndondo *et al.* (2016)
β_{hv}	0.011715	Day^{-1}	Fitting
β_{av}	0.011715	Day^{-1}	Fitting
β_{vh}	0.002739	Day^{-1}	Fitting
β_{va}	0.002739	Day^{-1}	Fitting
θ_h	0.2	Day^{-1}	Fitting

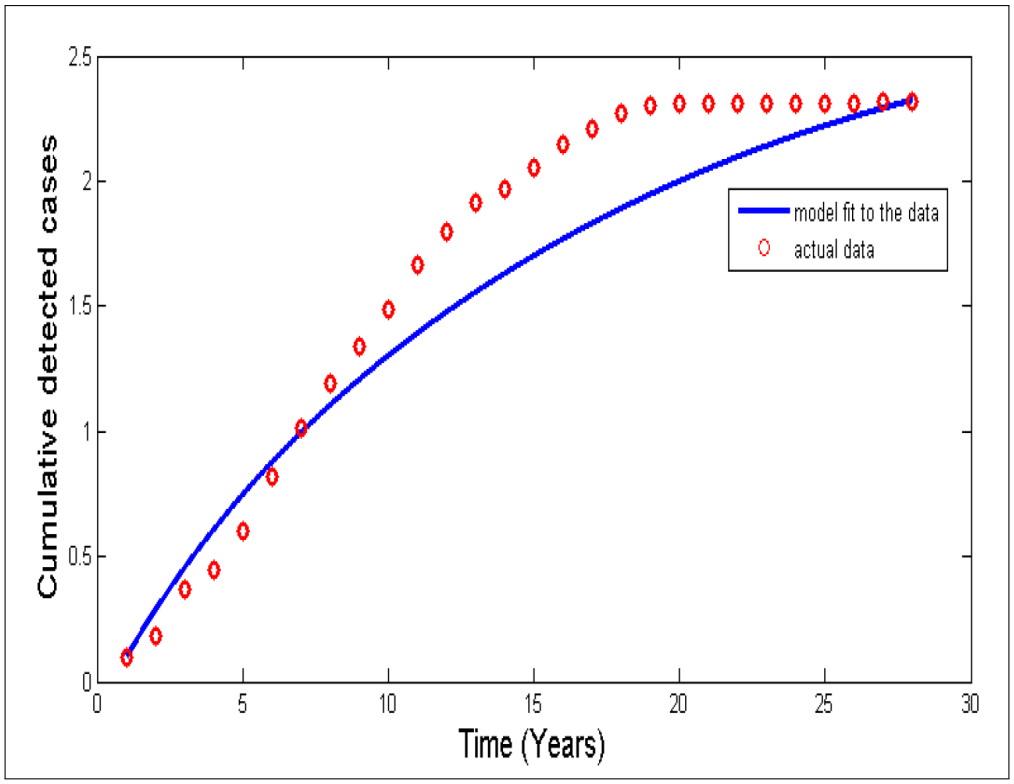

Figure 1: Data fitting result for the cumulative confirmed *T. brucei rhodesiense* cases in Tanzania from 1990-2017

Figure 1 presents a graph of cumulative confirmed cases fitted to the model. The circles (in red) denote the reported cases and the solid line (in blue) denotes the fitting result. To measure the goodness-of-fit, the normalized root-mean-square error (NRMSE) was computed using the formula (4.3) at it was found to be 0.2842. This shows that the proposed model had 28.42% deviations from observed values. It was concluded that the model was approximately 71.58% efficient.

$$\text{NRMSE} = \sqrt{\sum_{i=1}^{28} (\text{Real data} - \text{Estimated cases})^2}. \tag{4.3}$$

To further test the efficiency of the model, residuals were computed and plotted against time (Fig. 2). It was observed that the residuals did not follow any particular path (exhibit random pattern), implying that the model was a good fit to observed cases.

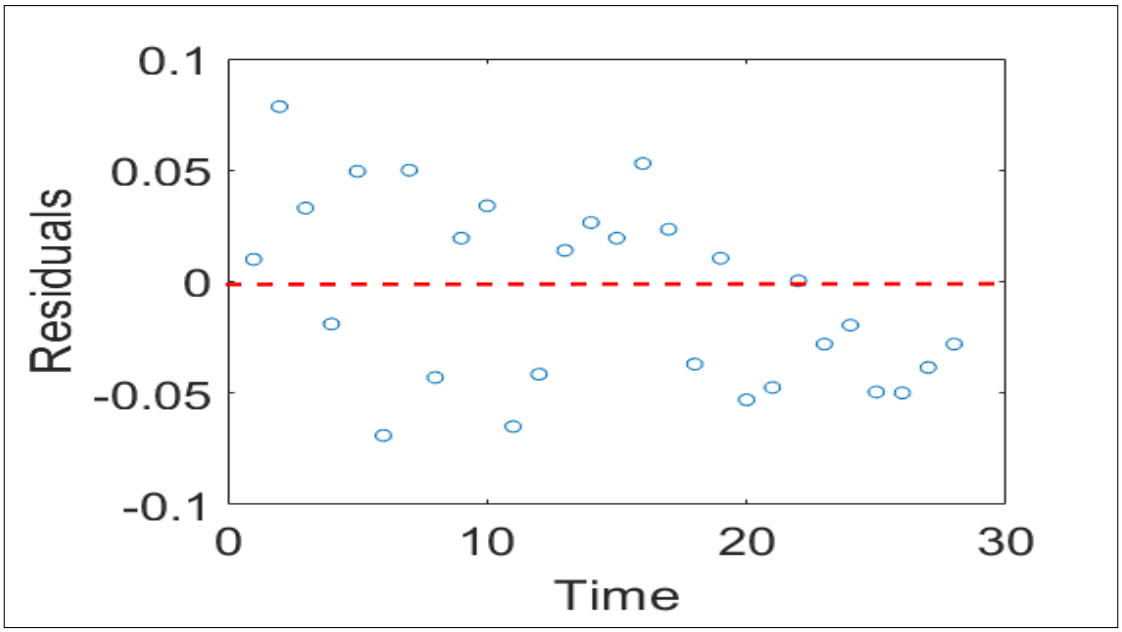

Figure 2: A time series plot of residuals against time

4.2.2 Sensitivity analysis of the basic reproduction number

To investigate the influence of model parameters on generation on secondary cases, sensitivity analysis of the $\mathscr{R}_0$ was performed following the approach by Arriola (2007). In general, Arriola defined the sensitivity as follows:

Definition 4.1
The normalized forward sensitivity index of the $\mathscr{R}_0$ which depends on the differentiable of the model parameter ω is defined as

$$\frac{\omega}{\mathscr{R}_0} \times \frac{\partial \mathscr{R}_0}{\partial \omega}. \tag{4.3}$$

Making use of formula (4.1), computations for the sensitivity analysis of model (3.6) was done and the output is in Table 4.1.

Table 3: Sensitivity analysis of model parameters in system (3.6)

Parameter	β_{hv}	β_{av}	β_{vh}	β_{va}	γ_h	θ_h	μ_h	γ_a
Index	+0.029	+0.47	+0.029	+0.47	+0.028	-0.028	-8×10^{-5}	+0.021
Parameter	γ_a	μ_a	μ_v	α_h	α_a			
Index	+0.021	-0.002	-0.50	-0.029	-0.468			

From the results in Table 3, it was noted that model parameters β_{hv}, β_{av}, β_{vh}, γ_h and γ_a have a positive influence on the $\mathscr{R}_0$, that is., whenever they are increased the $\mathscr{R}_0$ increases. For instance an increase in β_{av} by 10% will lead to an increase in the magnitude of the $\mathscr{R}_0$ by 4.7%.

Model parameters μ_h, μ_v, μ_a and θ_h were observed to have a negative influence on the $\mathscr{R}_0$, thus, whenever they were increased the magnitude of the $\mathscr{R}_0$ decreased.

4.2.3 Backward bifurcation

Analytical results of model (3.6) revealed that the model admits multiple equilibrium point when the model reproduction number is less than unity (Theorem 5.12). This phenomenon is known as the backward bifurcation. Precisely, a backward bifurcation is a phenomenon in which a stable endemic equilibrium point co-exists with a stable disease-free equilibrium point for $\mathscr{R}_0 < 1$. This phenomenon has also been observed in epidemiological settings (Gumel, 2012). To investigate the possibility of this phenomenon, the discriminant of equation ($B^2 - 4AC = 0$) was determined from through the computation of the model's endemic equilibrium (see Appendix 2), The equation was solved to determine the critical value of $\mathscr{R}_0$, denoted by $\mathscr{R}_{0c}$, as follows:

$$\mathscr{R}_{0c} = \sqrt{1 - \frac{B^2}{4Am_2m_4m_5m_6(m_1 + \gamma_h)}}. \tag{4.4}$$

Using parameter values in Table 2 illustration in Fig. 3.

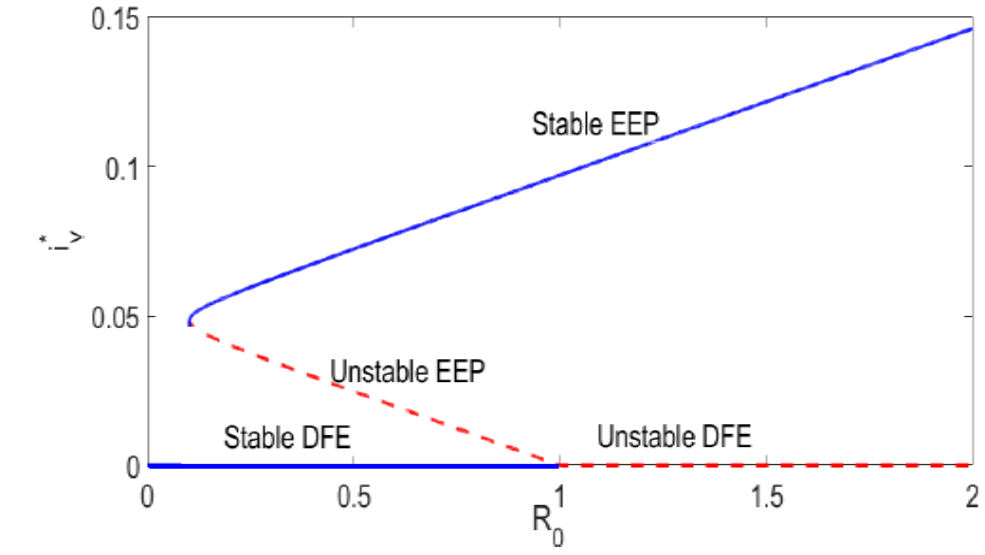

(a)

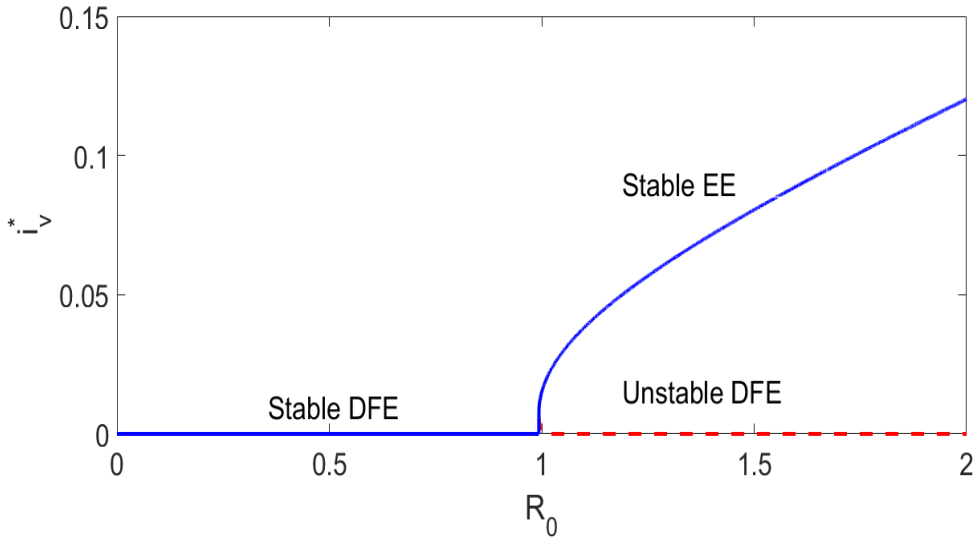

(b)

Figure 3: Graphical results for the possibility of bifurcations for model system (3.6)

Simulation results in Fig. 3 were generated for different values of awareness campaigns θ_h with parameters taken from Table 2. Further parameters different than those listed in Table 2 are $\beta_{hv} = \beta_{av} = 0.65$, $\beta_{vh} = \beta_{va} = 0.4$. In (a), it was assumed that $\theta_h = 0.764$ and in (b) $\theta_h = 0.857$. For $\mathscr{R}_0 < 1$, the model has two endemic equilibria: one stable and the other unstable. As $\mathscr{R}_0$ approaches one, the unstable endemic equilibrium looses its nature and coalesce with the disease-free equilibrium at $\mathscr{R}_0 = 1$. Therefore, it was concluded that the model admits a backward bifurcation whenever $\mathscr{R}_0 < 1$ and a forward bifurcation for $\mathscr{R}_0 > 1$.

4.2.4 Optimal control results

The Forward-backward sweep algorithm as outlined in Lenhart (2007) was used to generate simulation results for the optimal control problem (3.9). From the proposed objective functional

(3.25), parameters c_1 and c_2 were set as follows $c_1 = 2c_2$. This supposition implied that the minimization of the infected humans has more importance/weight compared to that of infected animals.

It is worth noting that the initial level and upper bound for each control reflects practical limitations on the maximum rate of control that can be implemented in a given time. These bounds and initial levels do not exist in literature since a primary study would have to be conducted first and ascertain them. However, to demonstrate the possible outcomes from the model, these bounds and initial levels were varied and possible outcomes were not and comparison was made. Recall that the minimum level of each control is zero, implying the absence of time-dependent controls and the maximum is unity, implying 100% implementation of time-dependent controls. For example, by setting $u_1 = 0.30$ with a bound of $q_1 = 0.6$ implies that the assumed initial value of u_1 is 0.30, however, since u_1 is a variable that also requires to be bounded, then the expected maximum success rate is 60%. For each set of bounds and initial control values chosen, the number of infections averted was computed using equations (4.5) and (4.6).

Further, due to the environmental effects associated with insecticide use, their intensity was assumed to be always lower or equivalent to that of awareness. It was also hypothetically assumed that the cost of insecticide use was higher than awareness campaign costs. The initial population levels which were used in the simulations were set as follows $s_h = 0.99$, $i_h = 0.01$, $r_h = 0$, $i_a = 0.01$, $r_a = 0$, $i_v = 0.01$, that is, each species comprise of 1% infectives initially and no recoveries for the hosts. It was also assumed that $\delta_v = 1$ per day. The total number of new infections generated to within the human population in the presence and absence of optimal control was defined in (4.5) as follows:

$$T_h = \int_0^{t_f} \left(\beta_{vh} i_v(t) N_v s_v(t) N_h \right) dt. \tag{4.5}$$

Similarly, the total number of new infections generated in within the animal population in the presence and absence of optimal control was considered in (4.6) as:

$$T_a = \int_0^{t_f} \left(\beta_{va} i_v(t) N_v (1 - i_a(t) - r_a(t)) N_a \right) dt, \tag{4.6}$$

where N_h, N_a and N_v are constants and are equivalent to 1×10^5, 1×10^4 and 5×10^4, respectively. Equations (4.5) and (4.6) were used to estimate the power of the controls to avert the disease.

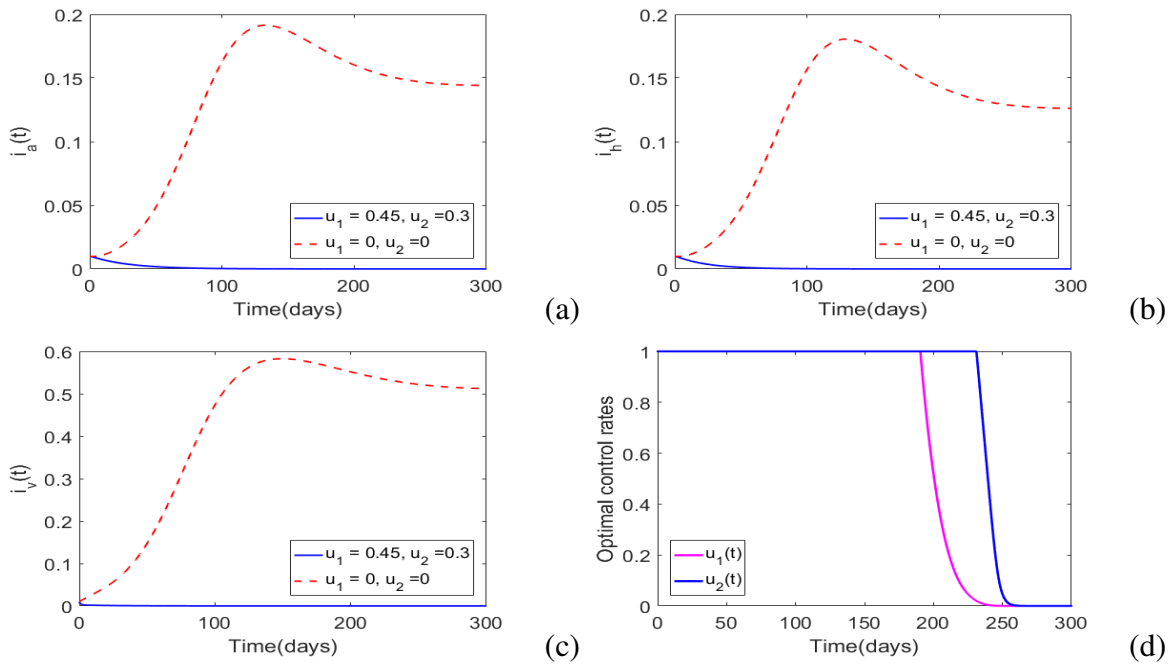

Figure 4: Simulations of model system (3.9) with the initial guesses $u_1 = 0.45$ and $u_2 = 0.3$

Simulation results in Fig. 4 showed the dynamics of *T. brucei rhodesiense* with, $u_1 = 0.45$ and $u_2 = 0.3$. The bounds of the controls were assumed to be $q_1 = q_2 = 1$. The weight constants were set as follows $w_1 = 10$, $w_2 = 100$ and the model parameter values were adopted from Table 2. It was noted that in the presence of optimal intervention strategies, the proportion of infectious hosts and vectors may never exceed the initially assumed population levels (1%). In particular, in the presence of optimal awareness and insecticide use, the population levels for the hosts and vectors converge to the disease-free equilibrium suggesting that the aforementioned optimal control mechanisms can lead to disease eradication. Precisely, the results showed that, in the presence of optimal control the total numbers of new infections for the human and animal population generated over 300 days are 2.5635×10^5, 9.7×10^4, respectively, and the total cost is $J = 6.5028 \times 10^4$. However, in the absence of optimal controls, that is, $u_1 = u_2 = 0$, one can observe that the disease persists. In Fig. 4 (d), it was observed that the control profiles of u_1 and u_2 start at the maximum, and they remain there for approximately 200 and 250 days, respectively, suggesting that awareness campaigns can essentially be ceased after 200 days of implementation while insecticides use need to maintained at maximum strength for an additional 50 days.

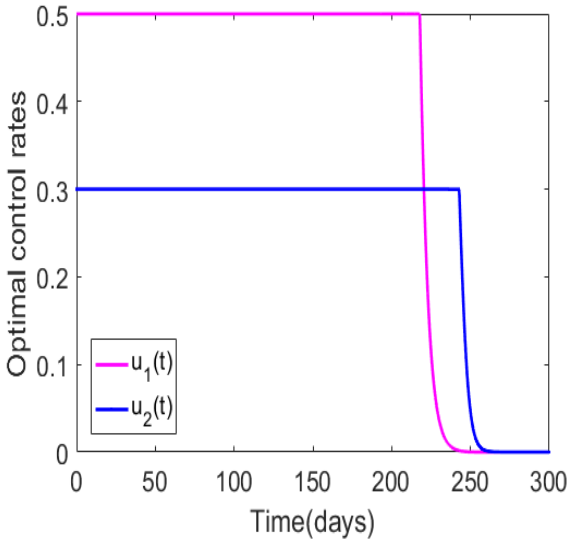

Figure 5: Simulation results for controls $u_1(t)$ and $u_2(t)$ with bounds less than 1

Figure 5 shows the optimal control profiles for u_1 and u_2 when the upper bound for these controls are less than unity, that is, $q_1 = 0.5$ and $q_2 = 0.3$, with initial guesses of the controls set to $u_1 = 0.45$ and $u_2 = 0.3$. It was noted that both u_1 and u_2 starts from their maxima, and they stay at the maximum strength for much longer periods of time than the previous case (compare to Fig. 4), due to the reduced intensity bounds. When the upper bounds of the controls are reduced, the population levels for all the infected species will converge to zero within the defined time interval, $t_f = 300$ (the Figures were omitted since their behaviour is analogous to that of Fig. 4). The results also showed that by reducing the bounds for the controls, the total cost $J(= 5.3582 \times 10^4)$ is reduced 17.6%, compared to that of Fig. 4.

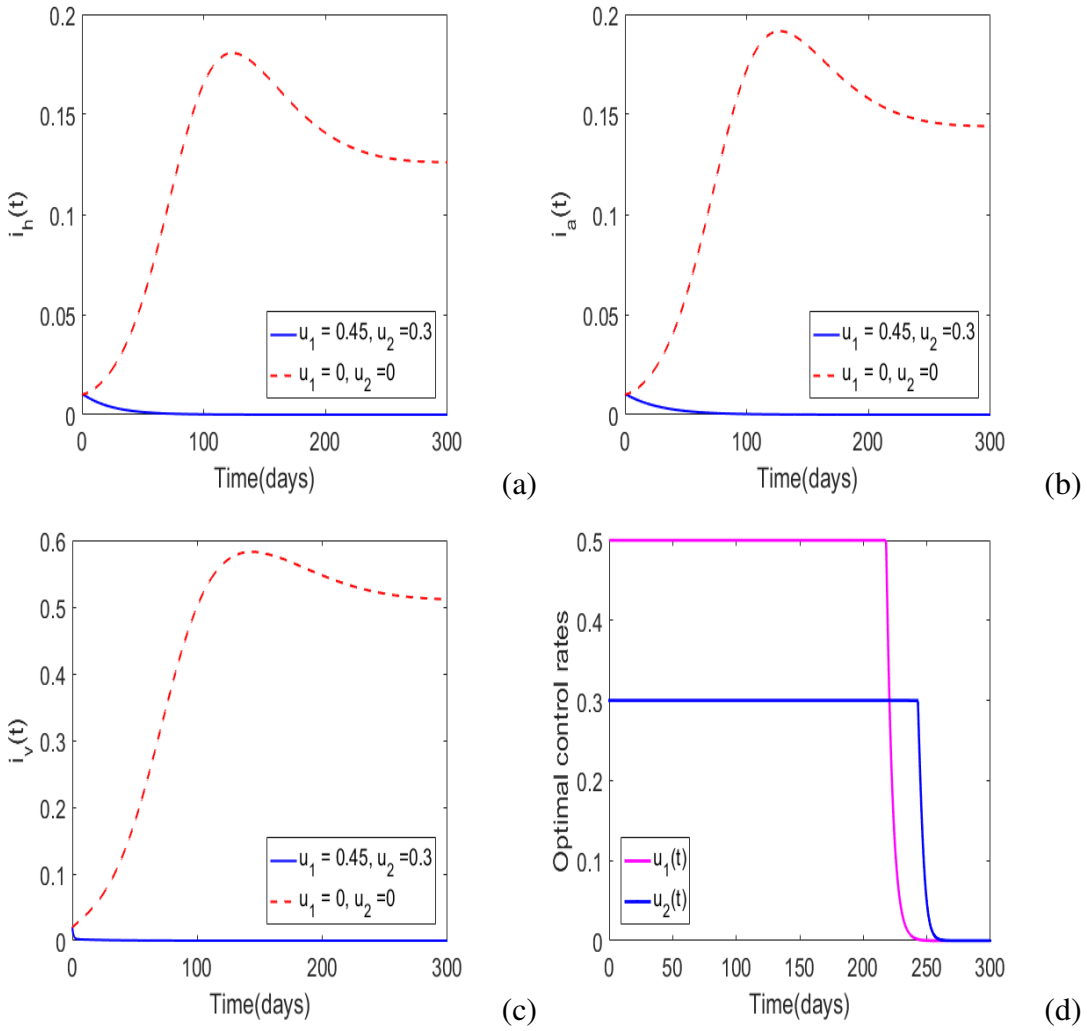

Figure 6: Simulations of model (3.9) with the initial guesses $u_1 = 0.45$ and $u_2 = 0.3$

Numerical results in Fig.6 shows the dynamics of *T. brucei rhodesiense* disease. When the population of infectious vectors is 3%, and the hosts' infectious population is 1% each and the controls have the following bounds set to: $q_1 = 0.5$, $q_2 = 0.3$ and the initial guesses of the controls were set to $u_1 = 0.45$ and $u_2 = 0.3$. The rest of the model parameter values were adopted from Table 2. Again, one can note that the population levels will converge to the disease-free equilibrium in the presence of optimal control, whereas in the absence of optimal control the disease persists. The total numbers of new infections for the human and animal population generated over 300 days are 3.7167×10^5 and 1.1232×10^4 respectively, and the total cost is $J = 5.4726 \times 10^4$. In Fig. 6 (d), it was noted that the control profiles for u_1 and u_2 exhibits a similar behaviour to the one illustrated in Fig. 5. Comparing the results in Fig. 3 and Fig. 6, one can observe that even if the total number of new infections for the hosts increases due to an increase in the population of infectious vector population, the total cost will still be lower by approximately 15.8%.

Next, the effects of extremely low-intensity controls on *T. brucei rhodesiense* disease dynamics in Fig. 7 was investigated. The initial control values was assigned to be $u_1 = 0.15$, $u_2 = 0.01$ and the upper bounds of the controls to $q_1 = 0.15$ and $q_2 = 0.01$. The weights constants were set to $w_1 = 10$, and $w_2 = 100$ and the rest of the model parameter values are as in Table 2. Furthermore, the initial population-levels and the weight constants was defined as $i_h = i_a = 0.01$, $i_v = 0.03$, $r_h = r_a = 0$, $s_h = 1 - i_h - r_h$, $s_a = 1 - i_a - r_a$, $s_v = 1 - i_v$, $w_1 = 10$, and $w_2 = 100$. Although the Figures of the population level effects are not displayed since their behaviour is similar to that of Fig. 6, it was noted that in the presence of optimal control, the infected population levels will converge to the disease-free equilibrium and the reverse occurs in the absence of optimal control. The total numbers of new infections for the human and animal population generated over 300 days are 4.8695×10^5 and 1.2764×10^4 respectively, and the total cost is $J = 5.4519 \times 10^4$. From these simulation results, it was observed that for effective disease management, the control profiles will have to be maintained at their maximum intensity for the greater part of the implementation period. Even though we have considered insecticide control as more expensive compared to the awareness control, in addition to that this control has to be maintained at its maximum intensity for a slightly longer time even after the awareness control has been dropped.

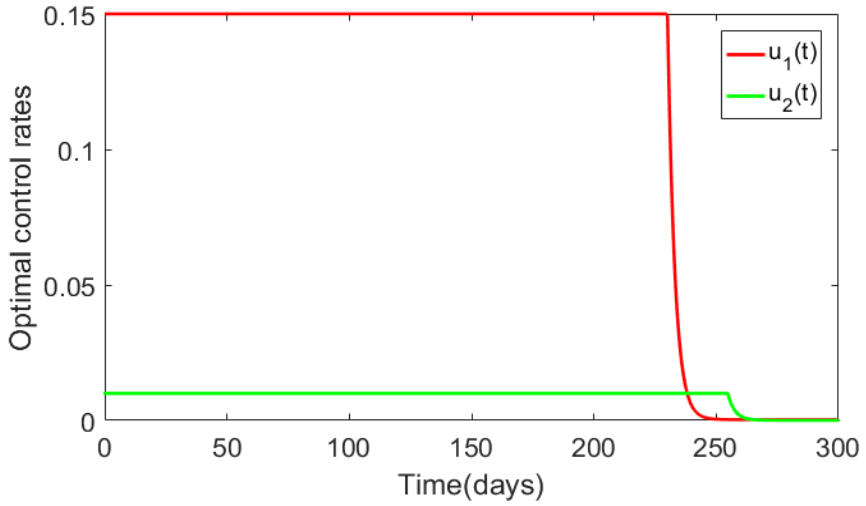

Figure 7: Simulations of model (3.9) with the initial guesses $u_1 = 0.15$ and $u_2 = 0.01$

In what follows, the formulas (4.5) and (4.6) was used to determine the number of new infections averted by the implementation of optimal control. This was determined by taking the difference between the total numbers of new infections observed in the absence of optimal control and those recorded when optimal control is implemented, the results are displayed in Table 4. The total numbers of new infections generated in the human and animal population in the absence of optimal control are 1.0866×10^7 and 7.7237×10^7 respectively.

Table 4: Infection reduction due to implementation of optimal control functions

Case	Host	T_1	T_2
Fig. 4	Human population	2.5635×10^5	1.0097×10^7
	Animal population	9.7000×10^4	7.7141×10^7
Fig. 6	Human population	3.7197×10^5	1.04943×10^7
	Animal population	1.1232×10^4	7.7226×10^7
Fig. 7	Human population	4.8695×10^5	1.03791×10^7
	Animal population	1.2764×10^4	7.7224×10^7

From Table 4, T_1 represents the total number of new infections, and T_2 denotes the number of infections averted due to the implementation of control functions. It was observed that the number of infections averted is extremely high even when the intensity of the optimal controls is low, and this clearly shows the strength of optimal control strategies on minimizing the spread of the disease.

4.3 Numerical results of model with seasonality

To support the analytical findings for the rhodesiense model with seasonality, model (3.22) was numerically solved using the forward-backward sweep method outlined by (Lenhart, 2007). In brief, in the forward-backward sweep method, one has to start with an initial guess for the optimal controls and solve the optimal state system forward in time and then solve the adjoint state backward in time using ode45 in MATLAB. Then these optimal controls are updated for optimality using the Hamiltonian of the optimal system. For this purpose, the steepest descent method of optimization discussed in Kirk (2004) was also utilized.

On simulating system (3.22), the following initial population levels was assumed: $S_h = 1 \times 10^4$, $E_h = 0$, $I_h = 5 \times 10^2$, $R_h = 0$, $S_a = 5 \times 10^3$, $E_a = 0$, $I_a = 3.5 \times 10^2$, $R_a = 0$, $S_v = 2 \times 10^4$, $E_v = 0$, $I_v = 1 \times 10^3$. Since no specific weights are in literature for this particular problem, the weight constants W_1 and W_2 were varied and the different outcomes obtained were discussed accordingly. Without loss of generality, it was assumed that the periodic forcing in all seasonal parameters at 0.8. Baseline values for non-periodic parameters were obtained from Table 2. The baseline values of additional parameters are in Table 5:

Table 5: Baseline values for additional model parameters in model (3.22)

Symbol	Description	Unit	Source
b_h, b_a	$\frac{1}{50\times365}$, $\frac{1}{15\times365}$	Day^{-1}	Moore *et al.* (2012*a*); Ndondo *et al.* (2016)
b_{v0}	$\frac{1}{33}$	Day^{-1}	Rogers (1988); Moore *et al.* (2012*a*)
d_a, d_h	$0.0008, \frac{1}{108}$	Day^{-1}	Moore *et al.* (2012*a*); Ndondo *et al.* (2016)
κ_{v0}	$\frac{1}{25}(\frac{1}{25}-\frac{1}{30})$	Day^{-1}	Artzrouni (1996*c*); Ndondo *et al.* (2016)
κ_a, κ_h	$\frac{1}{12}(\frac{1}{10}-\frac{1}{14})$	Day^{-1}	Rogers (1988); Ndondo *et al.* (2016)
σ_{v0}	$\frac{1}{4}(\frac{1}{10}-\frac{1}{3})$	Day^{-1}	Rogers (1988); Ndondo *et al.* (2016)
σ_a, σ_h	$0.62, 0.7$	Day^{-1}	Rogers (1988); Ndondo *et al.* (2016)
β_{va}, β_{vh}	0.62		Rogers (1988); Ndondo *et al.* (2016)
β_{av}, β_{hv}	0.01		Rogers (1988); Ndondo *et al.* (2016)

For model (3.22), the total number of new infections in the human and cattle population was determined by the formulas in (4.7) and (4.8), respectively:

$$T_h = \int_0^{t_f} \left(\frac{\sigma_v(t) N_v \sigma_h}{\sigma_v(t) N_v + \sigma_h N_h} \beta_{vh} \frac{I_v}{N_v} S_h \right) dt, \tag{4.7}$$

$$T_a = \int_0^{t_f} \left(\frac{\sigma_v(t) N_v \sigma_a}{\sigma_v(t) N_v + \sigma_a N_a} \beta_{va} \frac{I_v}{N_v} S_a \right) dt. \tag{4.8}$$

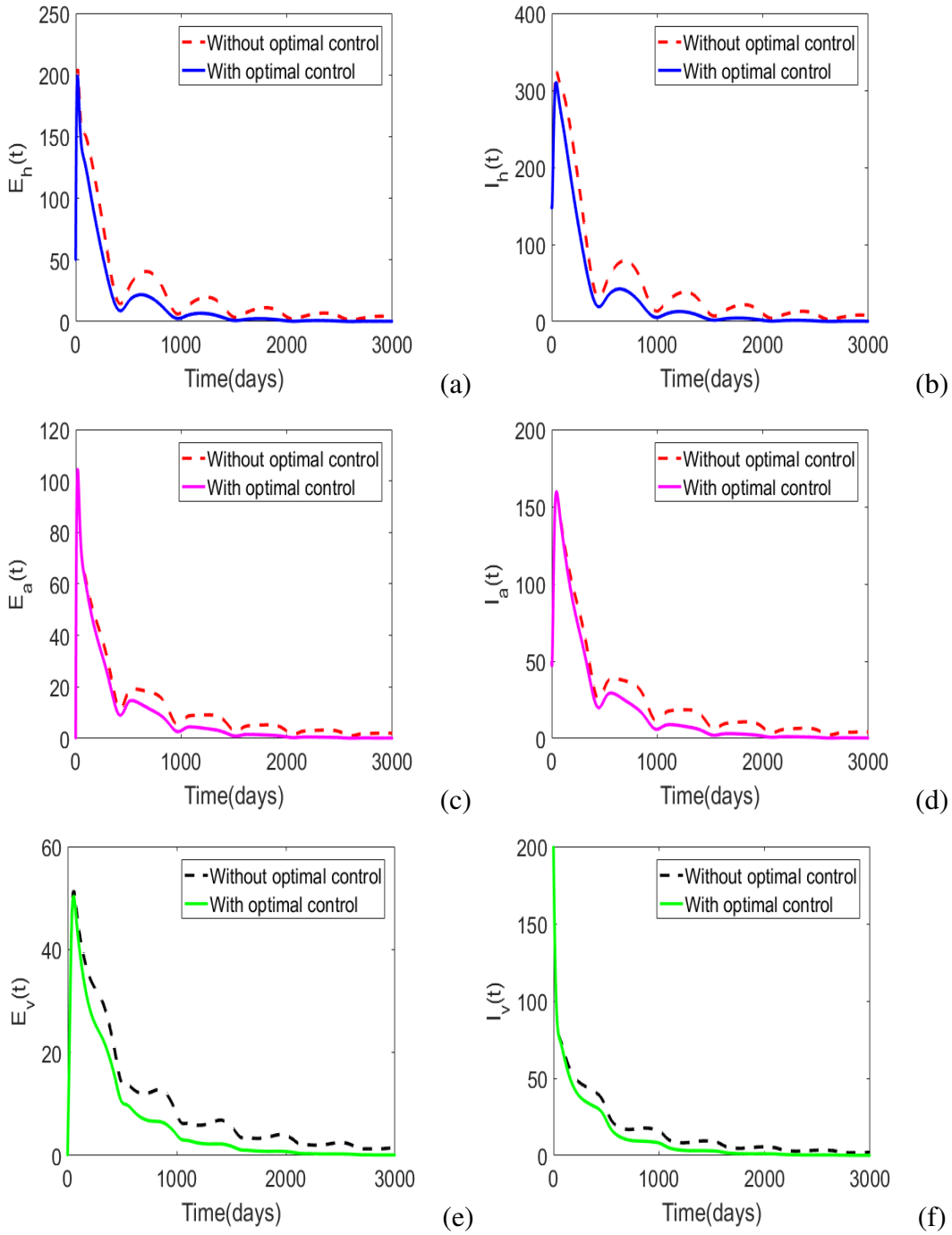

Figure 8: Simulations of model (3.22) with and without optimal controls

Simulation results in Fig. 8 illustrate *T. brucei rhodesiense* dynamics in the host and vector populations in the presence of human awareness only, that is $0 \leq u_1(t) \leq 0.003$ and $u_2(t) = 0$. The weight constants were assumed to be $W_1 = 0.1$ and $W_2 = 0$. Overall, it was observed that in the presence of optimal human awareness, the numbers of infected hosts and vectors is low compared to without optimal control. Furthermore, with optimal control, the numbers of infected host and vector converge to the disease-free equilibrium in a short time than when there

is no optimal control. In addition, the result showed that the total number of infected human and animal without control over a 3×10^3 day is 5.7×10^3 and 3.013×10^3, respectively, while in the presence of optimal human awareness campaigns only, the total number of infected human and animal populations for the same period is 3.662×10^3 and 2.146×10^3, respectively and the associated total costs of implementing the strategy is $J = 2.3535 \times 10^4$. Based on these results, one can conclude that the presence of optimal human awareness leads to a reduction in cumulative infections for the human and animal hosts by 2.038×10^3 and 8.67×10^2, respectively. Comparing the reduction of infection relative to the total number of infections recorded in without optimal control, it follows that, there is a 36% and 29% reduction in the human and animal populations respectively.

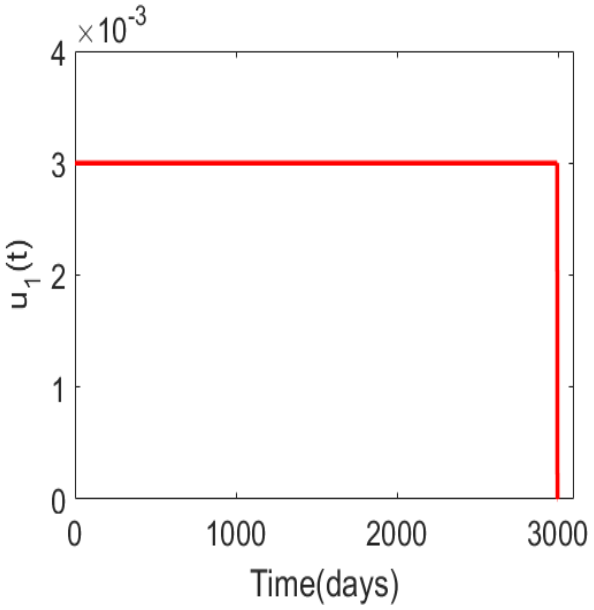

Figure 9: Control profile for $u_1(t)$, $(0 \leq u_1(t) \leq 0.003)$, $u_2(t) = 0$ and $w_1 = 0.1$

Figure 9 illustrates the control profile of $u_1(t)$, (note that $u_2(t) = 0$). From the numerical simulation the results demonstrated that, the control profile starts at its maxima and remains there for the entire time horizon. This signifies that to attain the above results, the control will have to be maintained at its maximum intensity for the entire time horizon.

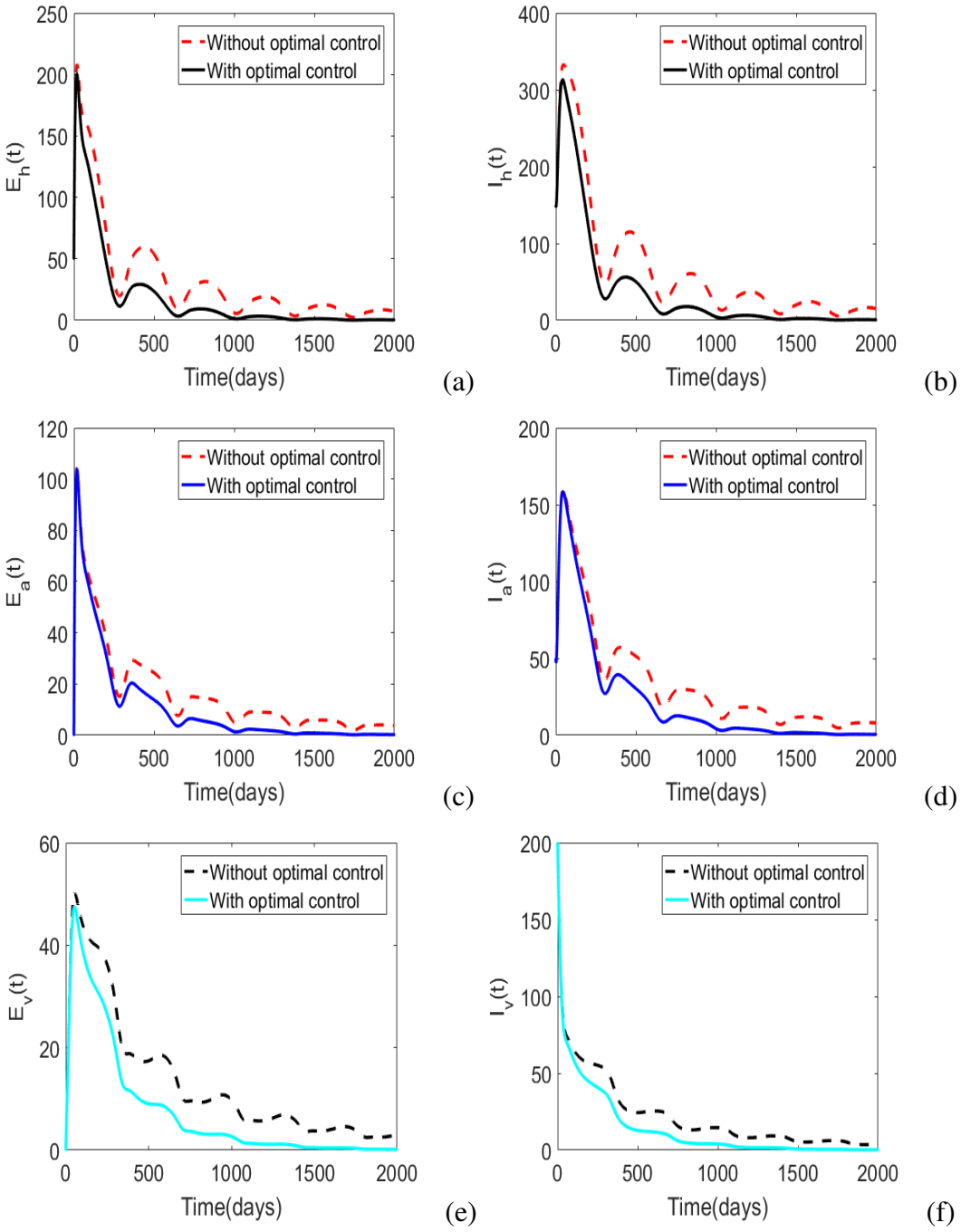

Figure 10: Simulations of model (3.22) with and without optimal controls for 2000 days

Numerical results in Fig. 10, illustrates the effects of combining optimal human awareness and insecticide use on long term *T. brucei rhodesiense* dynamics in a periodic environment over 2000 days (we set $0 \leq u_1(t) \leq 0.003$ and $0 \leq u_1(t) \leq 0.001$, with $W_1 = 0.1$ and $W_2 = 1 \times 10^2$). Once again, it was observed that with optimal control strategies in place, a few infections will be recorded compared to when there are no optimal control strategies. Precisely, with optimal control strategies in place, the total number of new infections over 2×10^3 days is 2.368×10^3

and 1.741×10^3, for the human and animal populations, respectively, and the associated costs of implementation is $J = 19,264$. The results also demonstrated that without optimal control strategies, the total number of new infections for the human and animal host over 2000 days is 5.336×10^3 and 2.703×10^3 respectively.

It follows that the optimal control strategies associated would have averted 2.368×10^3 and 9.62×10^2 infections in human and animal populations respectively. This represents approximately 44 and 36% reduction of infections in human and animal populations respectively, relative to when there are no controls. Comparing the results in Fig. 8 and Fig. 10, it was observed that combining optimal human awareness and insecticide use leads to effective disease management in a short period (convergence of solutions to the disease-free equilibrium in Fig. 10 takes less time than in Fig. 8) compared to when there is optimal human awareness alone.

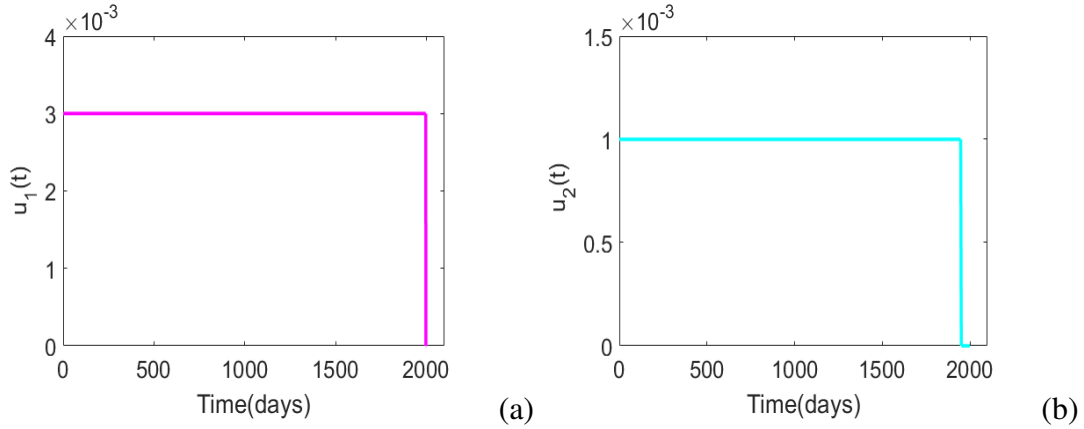

Figure 11: Numerical results illustrating the control profiles for $u_1(t)$, $(0 \leq u_1(t) \leq 0.003)$ and $u_2(t)$ $(0 \leq u_2(t) \leq 0.001)$, with $W_1 = 0.1$ and $W_2 = 100$

Simulation results in Fig. 11 depict the control profiles for $u_1(t)$ and $u_2(t)$ over 2000 days. The overall results showed that, all the control profiles start at their respective maximums and remain so for the greater part of the time horizon. In particular, the control profile for $u_1(t)$ drops on the final time while that of $u_2(t)$ drops just before the final time. These results suggest that for this scenario, both controls can be maintained at their respective maximum intensities in order to effectively manage the spread of the disease.

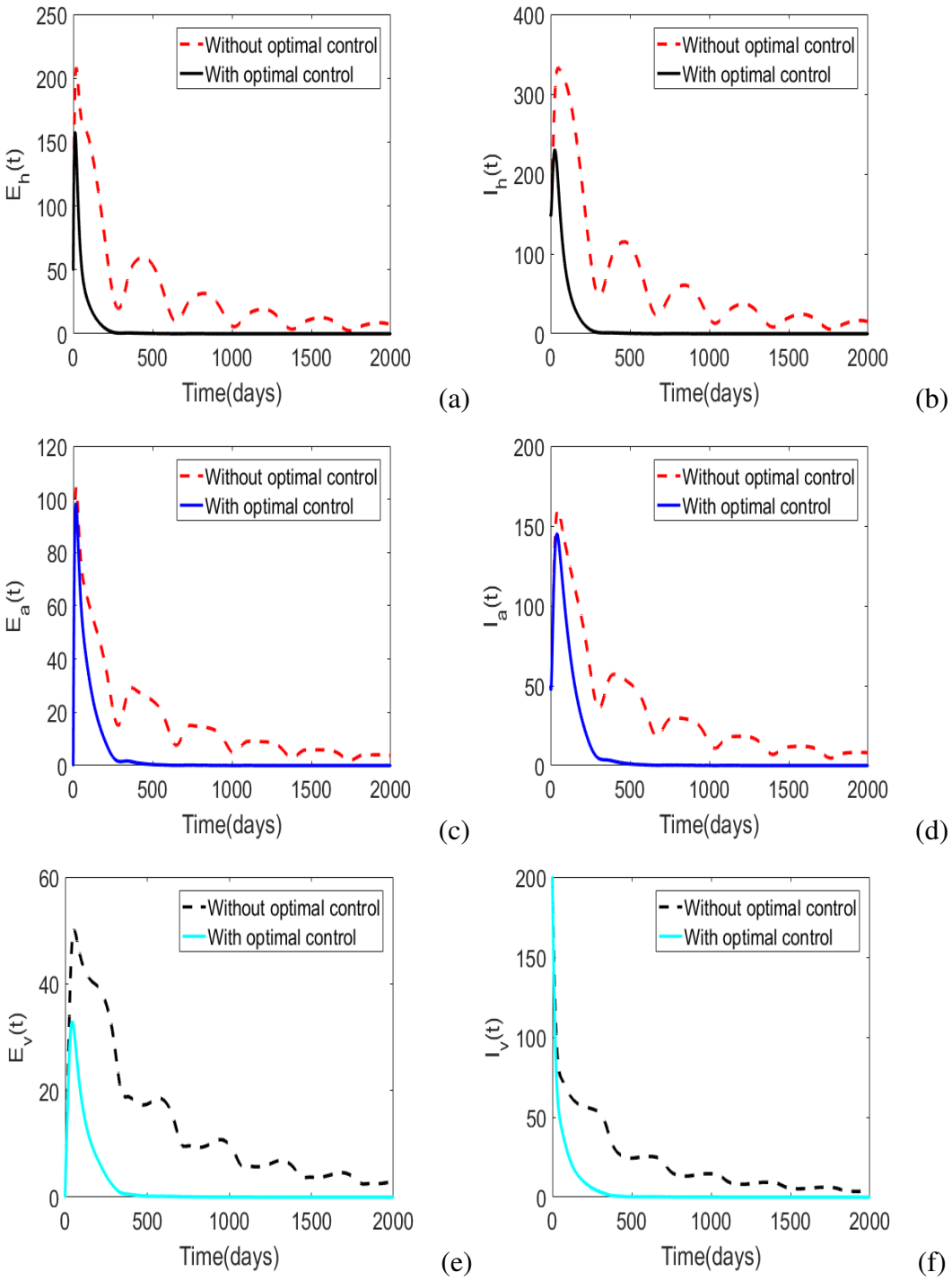

Figure 12: Simulations of model (3.22) with and without optimal human awareness and insecticides use over 2000 days

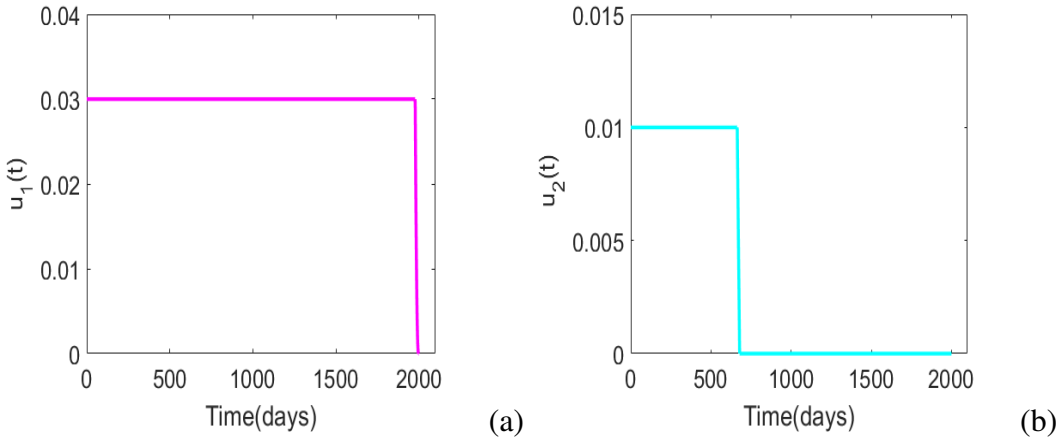

Figure 13: Numerical results illustrating the control profiles for $u_1(t)$, $(0 \leq u_1(t) \leq 0.03)$ and $u_2(t)$ $(0 \leq u_2(t) \leq 0.01)$, with $W_1 = 0.1$ and $W_2 = 10^3$

In Fig. 12, the bounds of the controls; human awareness $u_1(t)$ and insecticide use $u_2(t)$. Further, it was assumed that $0 \leq u_1(t) \leq 0.03$ and $0 \leq u_1(t) \leq 0.01$, with $W_1 = 0.1$ and $W_2 = 1000$. Under this scenario, it was noted that the total number of new infections generated in human and animal populations in the presence of the controls over 2000 days will be 667 and 716, respectively, implying that optimal control strategies will avert approximately $4,669$ and $1,988$ infections in human and animal populations, respectively. Relative to the total number of infections in the absence of controls, the presence of controls will be associated with 88 and 74% reductions for human and animal populations, respectively. Comparing with earlier scenarios (Fig. 8 and Fig. 8), it was observed that this scenario will have more impact on disease management. In addition, the control profiles associated with this scenario (Fig. 13) suggest that for these results to be attained, control $u_1(t)$ will have to be maintained at its maximum intensity from the start to the final day, while control $u_2(t)$ can be maintained at a maximum intensity from the start till the 750^{th} day, there after can be ceased. Thus at higher costs and intensity, control $u_2(t)$ cannot be maintained at its maximum intensity from the start till the final day.

4.4 Numerical results of model with memory and temperature effects

4.4.1 Temperature-dependent model parameters

In this section, numerical experiments conducted using MATLAB programing language to support the analytical findings of model (3.31) are presented. For the numerical implementation of fractional derivatives, the Adam-Bashforth-Moulton (ABM) scheme (Garrappa, 2011) was used for the model simulation. It is worth noting that the construction of model (3.31) was proposed by the outcomes from a recent laboratory experiment conducted by Lord *et al.* (2018). Hence all temperature-dependent parameters used in model (3.31) had their baseline values and function adapted from Lord *et al.* (2018) and no other source. To the best of the author's knowledge, this

is the most recent experiment of tsetse flies. Other model parameters are as in Table 2 and 5.

Table 6: Description and baseline values of temperature-depedent parameters used in model (3.31). All the baseline values were adopted from the work of Lord *et al.* (2018)

Parameter	Function or parameter definition	Range	Baseline value
d_1	Larviposition rate (b_l)	0.1046 ± 0.0004	0.1050
d_2	Larviposition rate (b_l)	0.0052 ± 0.0001	0.0053
a_1	Adult mortality rate (μ_v)	0.027 ± 0.001	0.027
a_2	Adult mortality rate (μ_v)	0.153 ± 0.020	0.153
b_1	Pupal mortality rate (μ_p)	0.0019 ± 0.0004	0.0019
b_2	Pupal mortality rate (μ_p)	0.006 ± 0.001	0.006
b_3	Pupal mortality rate (μ_p)	1.481 ± 0.681	1.4881
b_4	Pupal mortality rate (μ_p)	0.003 ± 0.001	0.003
b_5	Pupal mortality rate (μ_p)	1.211 ± 0.117	1.094
c_1	Pupal emergence rate (σ_l)	0.05884 ± 0.00289	0.05884
c_2	Pupal emergence rate (σ_l)	4.8829 ± 0.0993	4.8829
c_3	Pupal emergence rate (σ_l)	-0.2159 ± 0.0050	-0.2159

4.4.2 Model calibration and validation

The observed HAT cases in Table 1 were used to calibrate model (3.31). The least-squares method (4.9) was used to determine a fractional-order that gives the best fit. Since the fractional-order lies between zero and unity $0 < \alpha \leq 1$, the values of the fractional-order were varied till the best fit was obtained. The least squares method used is given:

$$\text{RMSE} = \sqrt{\sum_{i=1}^{28} (\text{Real data} - \text{Estimated cases})^2}. \tag{4.9}$$

The graphical illustration in Fig. 14 show the outcome of different fractional-orders versus the observed data. It was observed that $\alpha = 0.62$ gives a good fit, hence it was plotted as a single graph in Fig. 15.

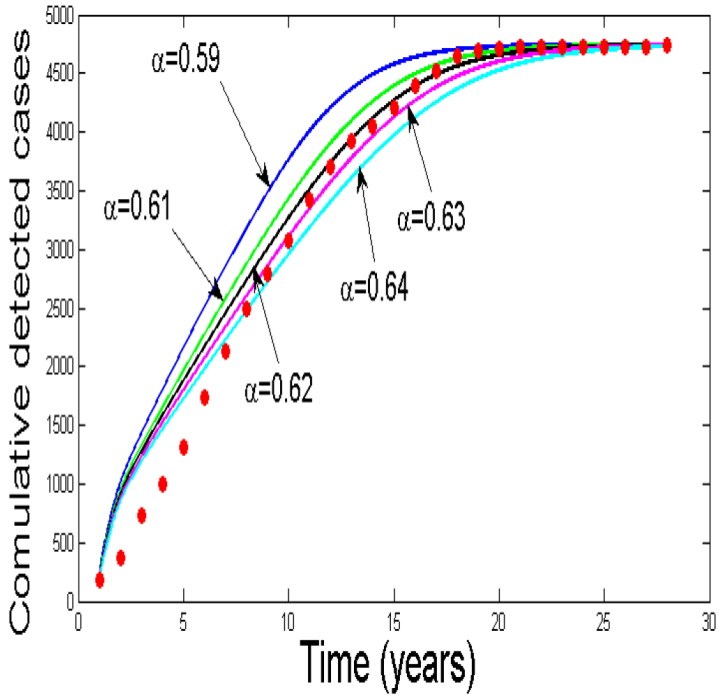

Figure 14: Model system (3.31) fitted to r-HAT cases in Tanzania

Figure 14 illustrates the cumulative confirmed cases versus the model fitting curve with $\alpha =$ 0.59, 0.61, 0.62, 0.63, and 0.64. The results demonstrated that, the model formulated fit well with r-HAT cases in Tanzania. To measure the goodness-of-fit, the model was fitted at $\alpha = 0.62$ as shown in Fig. 15 and the normalized root-mean-square error (RMSE) was computed using the formula (4.9) at it was found to be 0.1301. This shows that the proposed model had 13.01% deviations. Hence it was concluded that the model was approximately 86.99% efficient. To further illustrate the efficiency of the model residuals were computed and plotted against time (Fig. 16). It was noted that residuals did not appear to follow a particular path. Precisely the plot showed that residuals have no pattern and this imply that model was really a good fit.

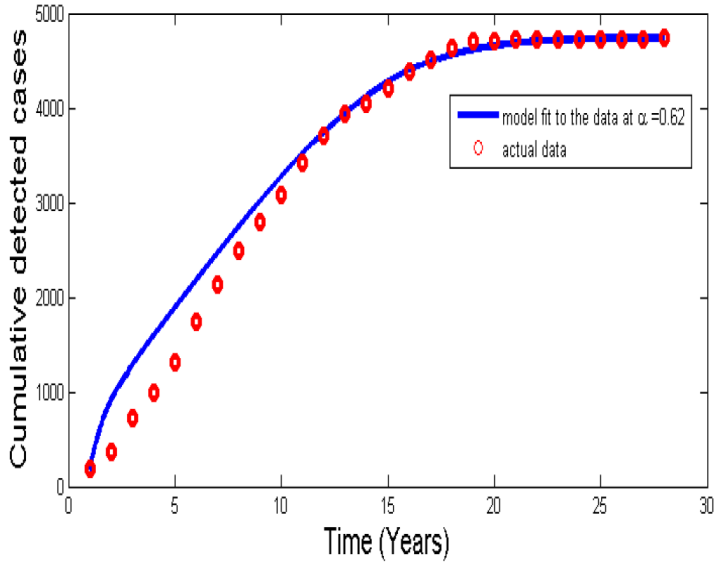

Figure 15: Model system (3.31) fitted to r-HAT cases in Tanzania at $\alpha = 0.62$

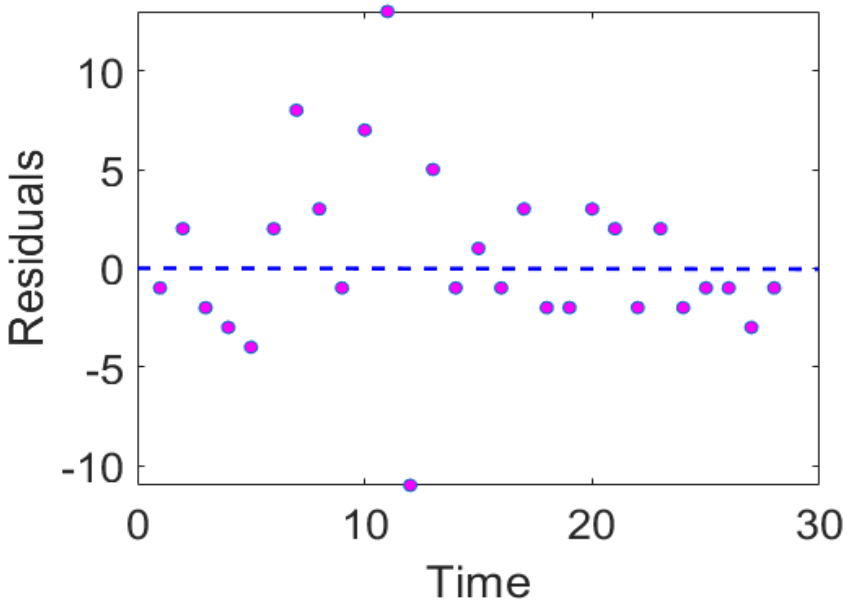

Figure 16: A time series plot of residuals against time

4.4.3 Effects of temperature variation the basic reproduction number

Since model (3.31) has temperature-dependent parameters the effects of temperature on the $\mathscr{R}_0$ needed to be determined. Numerical simulations were carried out and the results are sown in Fig. 17.

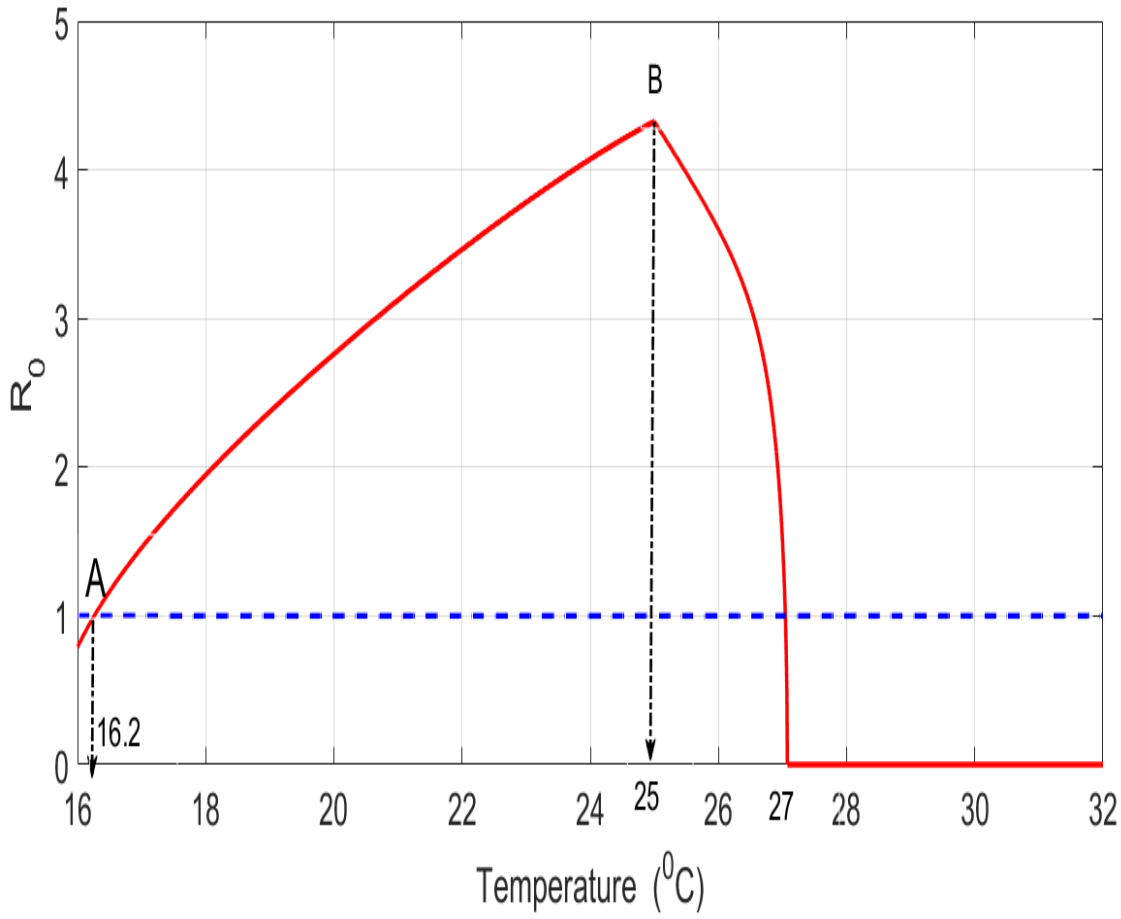

Figure 17: The relationship between the $\mathscr{R}_0$ and temperature T. for model (3.22)

The numerical results in Fig. 17 demonstrate the relationship between the $\mathscr{R}_0$ and temperature in °C. It was set that $K_l = 1300$, $N_h = 1000$, $N_a = 500$, $N_v = 1500$ and varied the temperature from 16-27 °C. The results demonstrated that as temperature increases from the critical minimum $T = 16$°C, the $\mathscr{R}_0$ gradually increases till the highest value is attained at optimum temperature $T = 25$°C, thereafter $\mathscr{R}_0$ sharply declines. Furthermore, It was observed that when $T < 16$°C then $\mathscr{R}_0 < 1$.

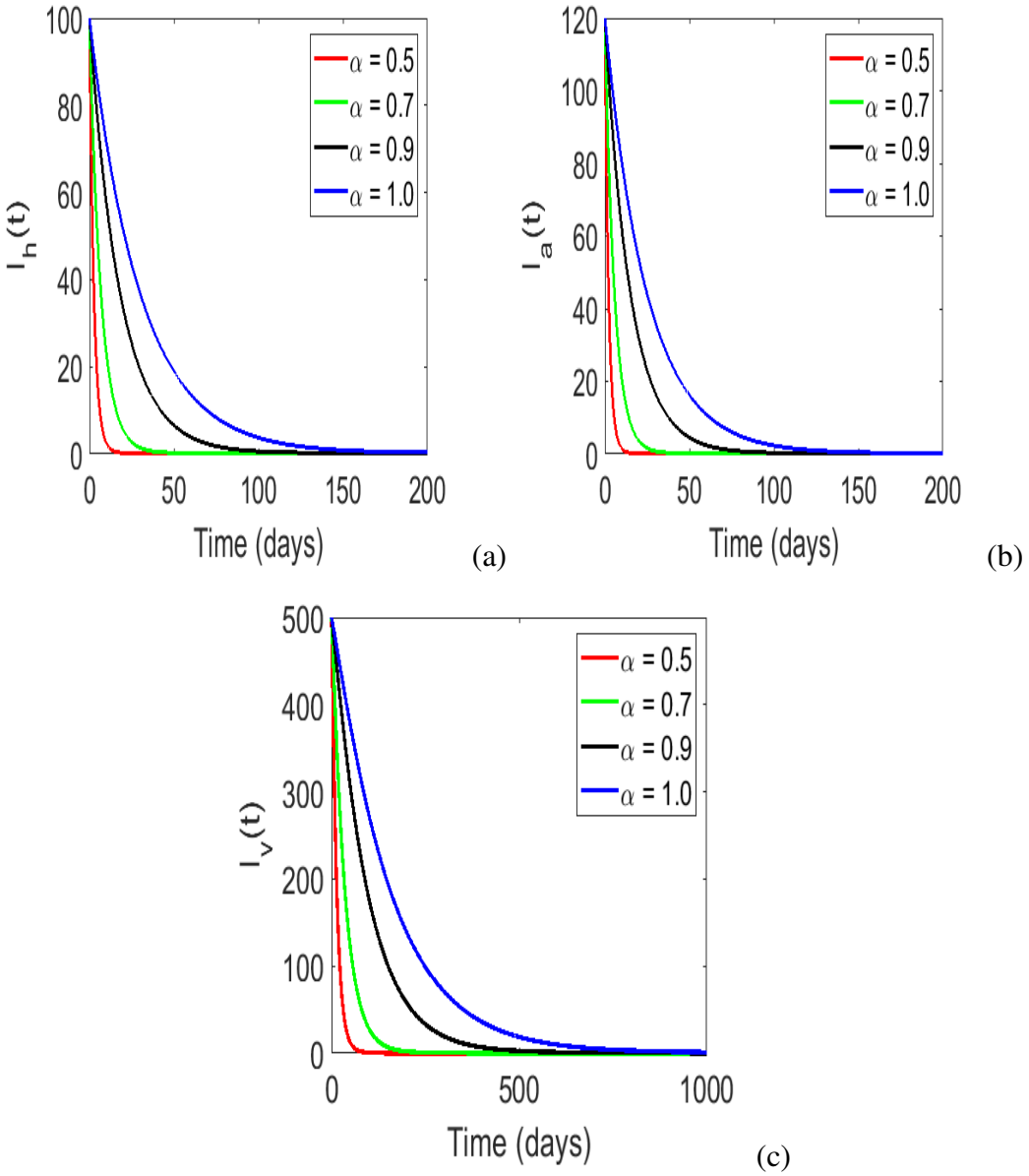

Figure 18: Numerical results of model system (3.31) for $\mathscr{R}_0 \leq 1$

The numerical results in Fig. 18 illustrate the dynamics of the infected population when for $\mathscr{R}_0 \leq 1$ to demonstrate the convergence of infected species at the disease-free equilibrium point. On the construction of the simulations, the initial population levels was assumed as discussed earlier while baseline values for the model parameters are as in Table 2 and 6. In addition, it was assumed that $T = 16.5°C$ and $K = 3.3 \times 10^3$, giving $\mathscr{R}_0 = 1.0$. From the numerical results, it was concluded that all populations converged to the disease-free equilibrium, irrespective of the chosen value of α. These results concur with the analytical findings presented in Theorem 3.6 that whenever $\mathscr{R}_0 \leq 1$, the proposed model is stable and the disease dies out in the community.

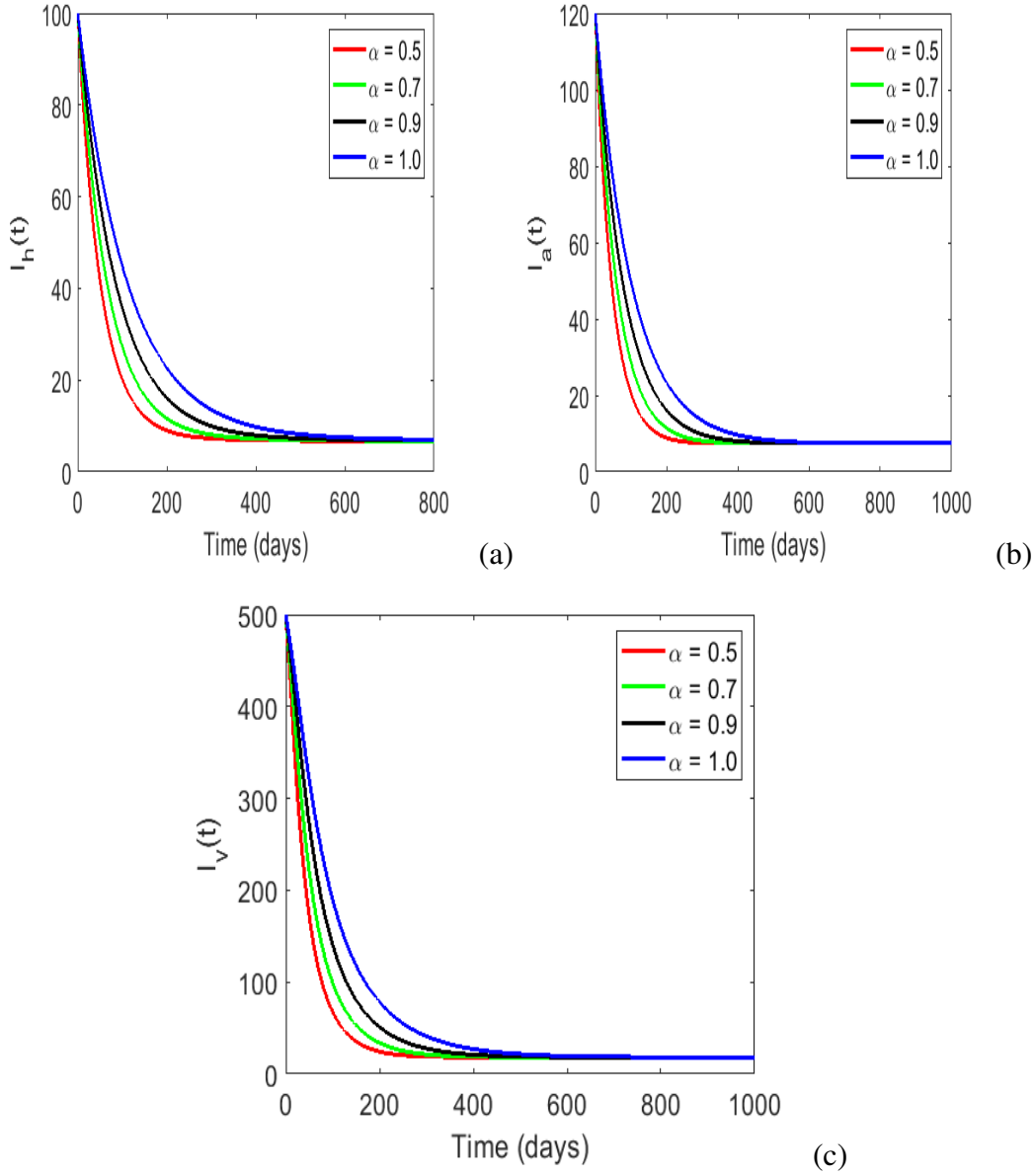

Figure 19: Numerical results of system (3.31) demonstrating the convergence of infected population to the endemic equilibrium for $\mathscr{R}_0 > 1$

The simulation results in Fig. 19 show the solution of model (3.31) at different levels of $\alpha = (0.5, 0.7, 0.9, 1.0)$ for $\mathscr{R}_0 = 3.7 > 1$. The temperature was set to be $T = 25^{\circ}C$, and $K_l = 3.3 \times 10^3$. From the graphical illustration, it was noted that the solutions profiles converge to a non-zero equilibrium point, implying that whenever $\mathscr{R}_0 > 1$, the model is stable and admits a unique endemic equilibrium point. Biologically, this means that if $\mathscr{R}_0 > 1$, the disease persists in the community. These simulation results support analytical findings presented in Theorem 3.6.

4.4.4 Effects of screening and vector control

In this section, the effects of screening infected hosts and vector control on disease dynamics was investigated. Detection and treatment of humans has been a primary control strategy for HAT. Detection of cases can be carried out either periodically (usually large-scale screening) or continually (usually small scale) at health care centres. To explore the potential effects of continuous detection and treatment the study closely followed the approach used by Artzrouni (1996*a*). This author proposed that the rate of exit of infected hosts to the recovery stage can be presented as a composite of the intrinsic underlying disease progression (say, γ_{int}) in (4.10) and the removal rate by treatment (extrinsic , say γ_{ext}) such that:

$$\gamma_h = \gamma_{\text{int}} + \gamma_{\text{ext}}, \tag{4.10}$$

then the monthly percent detection is given in (4.11) by:

$$C_h = 100[1 - \exp(-30\gamma_{\text{ext}})]. \tag{4.11}$$

Consequently, (4.10) and (4.11) lead to the exit rate from the infected class for human hosts to be:

$$\gamma_h = \gamma_{\text{int}} - \frac{1}{30}\ln\left(1 - \frac{C_h}{100}\right). \tag{4.12}$$

From (4.12), it was noted observed that linear detection of an infected individual does not result in linear changes in γ_h. Rock *et al.* (2015) opines that this representation of the recovery rate leads to a meaningful way in which the

influence of the parameter on the $\mathscr{R}_0$ can be extensively explored. Although there are several methods to control the density of tsetse such as aerial spraying and the deployment of natural or artificial baits, essentially altering the total population parameter N_v, birth rate and natural mortality rate will alter the density of the tsetse population. Cognisant of these fundamental parameters, Artzrouni (1996*a*) hypothesized that tsetse control will affect mortality rate but not the population size. Hence in an analogous approach to mdelling detection and treatment of human, they model 'natural' mortality rate of the vectors a follows in (4.13):

$$\mu_v = \mu_{v,\text{int}} + \mu_{v,\text{ext}}, \tag{4.13}$$

where $\mu_{v,\text{int}}$ accounts for the mortality experienced by flies in their environment and $\mu_{v,\text{ext}}$ describes an additional death rate that occurs as a result of control strategies. Furthermore, it was suggested that this death rate μ_v is related to the daily percentage of flies killed as denoted

here in (4.14) by:

$$C_v = 100[1 - \exp(-30\mu_{v,\text{ext}})]. \tag{4.14}$$

With C_v denotes the daily percentage killing of tsetse flies. Thus, the total mortality rate of vectors due to 'natural' and control measures is given in (4.15) by:

$$\mu_v = \mu_{v,\text{int}} - \ln\left(1 - \frac{C_v}{100}\right), \tag{4.15}$$

Note that Artzrouni (1996*a*) used rates with 3 days as the unit of time on equation (4.15).

In what follows, we numerically explore the effectiveness of case detection and vector controls on the spread of the disease. Precisely, the contour plot to determine the influence of c_h and c_v on the $\mathscr{R}_0$ was used, since it an integral epidemiological metric for understanding the power of *T. brucei rhodesiense* to invade the community.

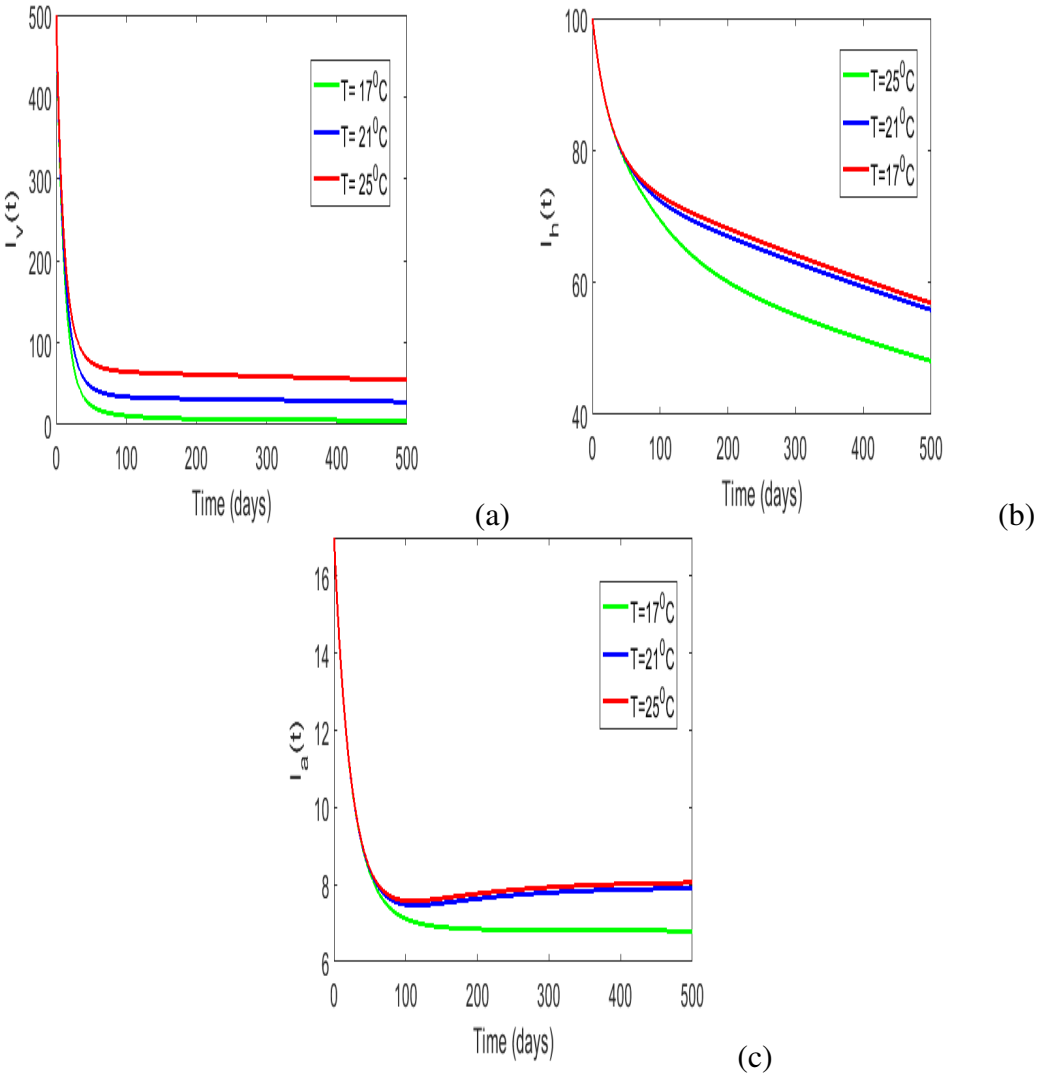

Figure 20: Simulation for model system (3.31) at different temperature levels

Figure 20 shows the number of infected vectors, humans and animals at different temperature values for 500 days. It was assumed that $\alpha = 0.7$, $K_l = 1 \times 10^3$, $N_h = 1 \times 10^3$, $N_a = 5 \times 10^2$, $L = 1.3 \times 10^3$, $N_v = 1.5 \times 10^3$, $S_v = 1 \times 10^3$, $I_v = 5 \times 10^2$, $I_h = 1 \times 10^2$, $S_a = 3.8 \times 10^3$ and $I_a = 17$. From the graphical illustration it was noted that low-temperature values ($T < 25°$C) were associated with low infection levels and as the temperature increased to the optimum value replay $T = 25°$C, the number of infections increased over time. Furthermore, it was observed that for $t < 100$ days the impact of different temperature values on populations are not extremely distinct. However, thereafter there was a significant distinction.

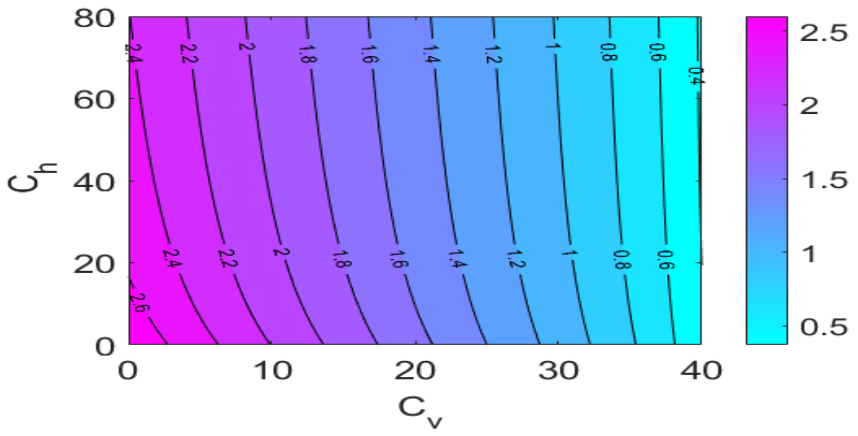

Figure 21: A contour plot illustrating the effects of human detection and vector control on *T. brucei rhodesiense* dynamics

The contour plot in Fig. 21 illustrates the impact of human case detection and vector control on *T. brucei rhodesiense* dynamics at $T = 20^{\circ}$C. In this case, the temperature was assumed to be $T = 20^{\circ}$C, and the other parameters were defined as $K_l = 1 \times 10^3$, $\beta_{hv} = \beta_{av} = 3.55 \times 10^{-4}$, $\beta_{vh} = \beta_{va} = 8.3 \times 10^{-4}$, $N_h = 1 \times 10^3$, $N_a = 5 \times 10^2$, $\gamma_{\text{int}} = 0.009$ and $\mu_{v,\text{int}} = 0.027$. It has been shown that an increase in both case detection and vector control percentages leads to a decrease in the magnitude of $\mathscr{R}_0$. The results also demonstrated that vector control has a strong influence on minimizing the magnitude of $\mathscr{R}_0$ compared to human detection. In particular, whenever, $C_v > 30$, then $\mathscr{R}_0 < 1$, despite any value of C_h.

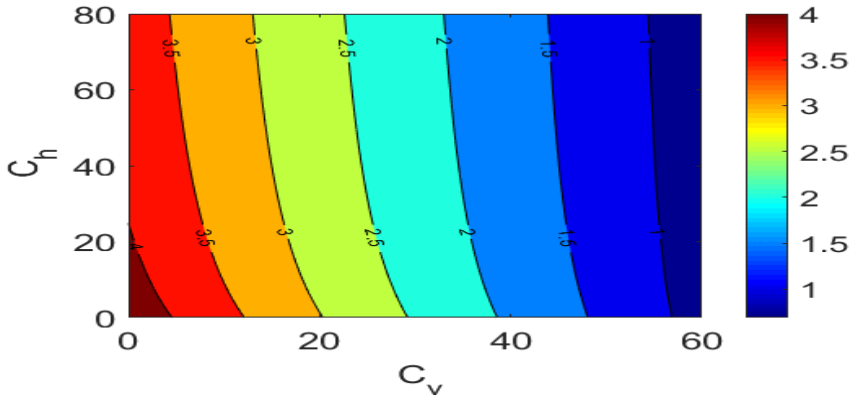

Figure 22: A contour plot illustrating the effects of human detection and vector control on *T. brucei rhodesiense* dynamics

The contour plot in Fig. 22 demonstrates the impact of C_h and C_v on the transmission dynamics of *T. brucei rhodesiense* at $T = 25^{\circ}$C. Comparing the results in Fig. 22 and Fig. 22, it has been assumed that $T = 25^{\circ}$C, $K_l = 1 \times 10^3$, $N_h = 1 \times 10^3$, $N_a = 5 \times 10^2$, $\gamma_{\text{int}} = 0.009$ and $\mu_{v,\text{int}} = 0.027$. From numerical simulations, the results show that at optimum temperature, $T = 25^{\circ}$C, vector control needs to be greater than fifty ($C_v > 50$) in order to reduce the magnitude of the

basic $\mathscr{R}_0$ to values less than unit whereas in Fig. 22, $C_v > 30$ is sufficient to obtain $\mathscr{R}_0 < 1$. Therefore, it was concluded that if the average temperature in the community is very close to the optimum temperature, then the intensity of vector control needs to be at least 50%.

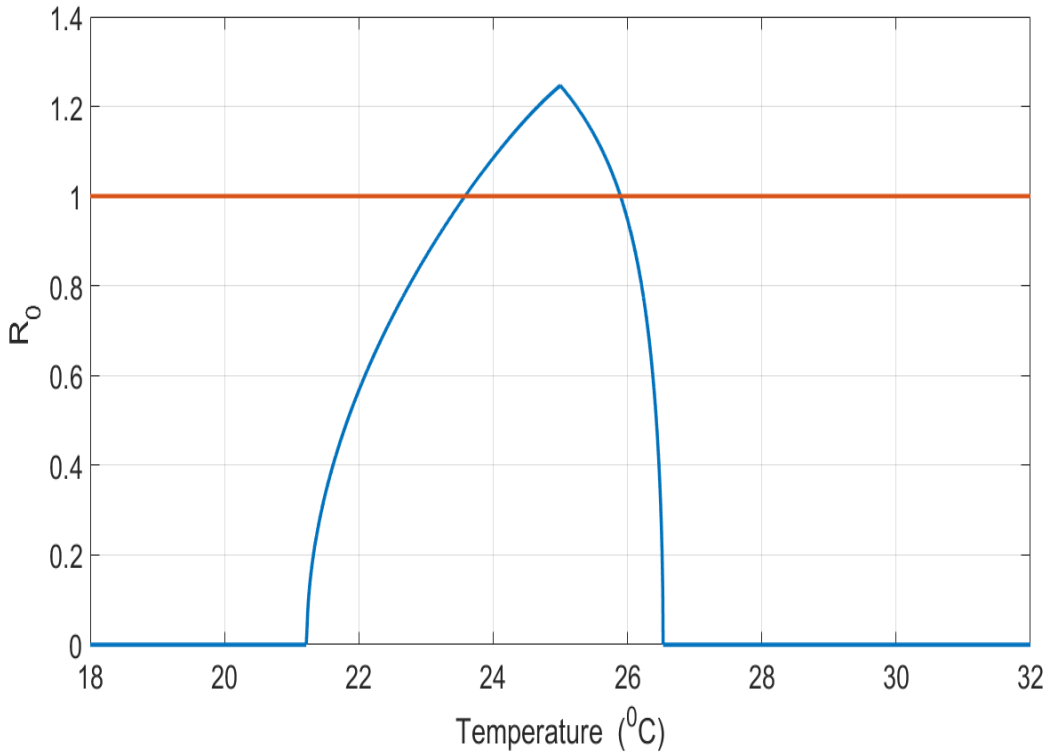

Figure 23: Simulation results showing the effects of temperature on $\mathscr{R}_0$

In Fig. 23, the relationship between temperature and $\mathscr{R}_0$ in the presence of human screening and vector control was investigated. It was set that $C_h = C_v = 50$, $K_l = 1 \times 10^3$, $N_h = 1 \times 10^3$, $N_a = 5 \times 10^2$, $L = 1.3 \times 10^3$, $N_v = 1.5 \times 10^3$, $S_v = 1 \times 10^3$, $I_v = 5 \times 10^2$, $I_h = 1 \times 10^2$, $S_a = 3.8 \times 10^2$, $I_a = 17$, and the rest of the parameter values are as in Table 2. From the illustration, it was observed that $\mathscr{R}_0 > 1$, for $23 < T < 26$°C. This implies that at 50% human detection and 50% killing of vectors, the disease can only persist in the community when the average temperature is between 23 and 26°C, otherwise, the disease dies out. However, by setting $C_h = 50$ and $C_v = 55$, (Fig. 23), the disease is not persist even at optimum temperature, $T = 25$°C .

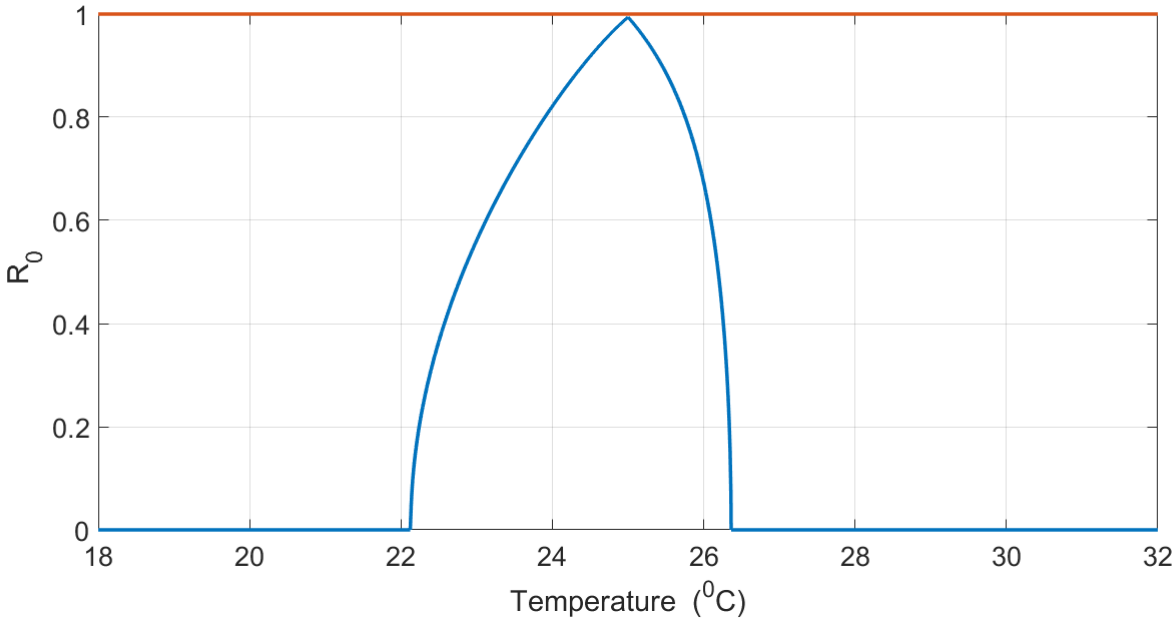

Figure 24: Simulation results showing the effects of temperature on $\mathscr{R}_0$

In Fig. 24, the relationship between temperature and $\mathscr{R}_0$ in the presence of human screening and vector control was investigated. It was assumed that $C_h = C_v = 50$. The results showed that $\mathscr{R}_0 > 1$ for $23 < T < 26^{\circ}$C. Next, the control was set to be $C_h = 50$, $C_v = 55$, with $k_l = 1 \times 10^3$, $N_h = 1 \times 10^3$, $N_a = 500$, $L = 1.3 \times 10^3$, $N_v = 1.5 \times 10^3$, $S_v = 1 \times 10^3$, $I_v = 5 \times 10^2$, $I_h = 100$, $S_a = 3.8 \times 10^3$ and $I_a = 17$, and the rest of the parameter values are as in Table 5. The results demonstrated that at 50% human detection and 50% killing of vectors, the disease can only persist in the community when the average temperature is between 23 and 26°C, otherwise, it dies out. However, if $C_h = 50$ and $C_v = 55$, (Fig. 24), the disease will not persist even at optimum temperature, $T = 25^{\circ}$C.

4.5 Numerical results of model with time delay and heterogeneity

In this section, numerical illustrations which were carried out to support the analytical results of model (3.5) are presented. Baseline values for model parameters are in Table 2 and 5. Fig. 25 illustrates a contour plot of $\mathscr{R}_0$ as a function of p_H (proportion of new recruits in the high-risk population) and ε_H (modification factor). The values of other model parameters are based on Table 2 and 5. It was observed that for small values of p_H and ε_H, the number of secondary infections generated is high and the reverse is equally true. In addition, the results also showed that even with small initial population levels considered $P_H = \varepsilon_H = 1$ (100%) may not be associated with the value of $\mathscr{R}_0$ less than unity.

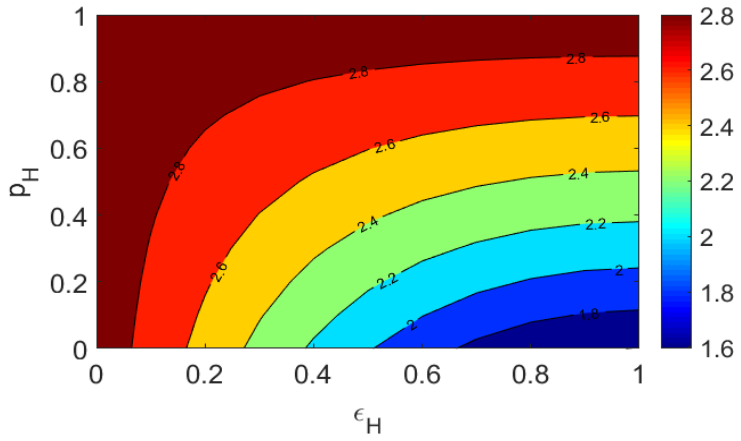

Figure 25: Contour plot of $\mathscr{R}_0$ as a function of p_H (proportion of new recruits in the high-risk population) and ε_H (modification factor)

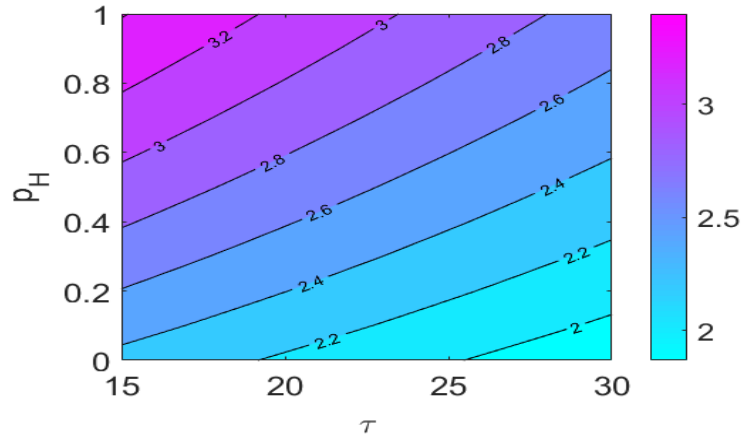

Figure 26: Contour plot of $\mathscr{R}_0$ as a function of p_H (proportion of new recruits in the high-risk population) and τ (time delay factor)

A contour plot of $\mathscr{R}_0$ as a function of p_H (proportion of new recruits in the high-risk population) and τ (time delay factor) is presented in Fig. 26. The results suggest that the time delay factor τ has more influence on the outcome of $\mathscr{R}_0$ compared to p_H. For high values of τ the outcomes of $\mathscr{R}_0$ are low even when the values of P_H are small. This further suggests that the time delay factor may be an important component in the transmission and control of the disease.

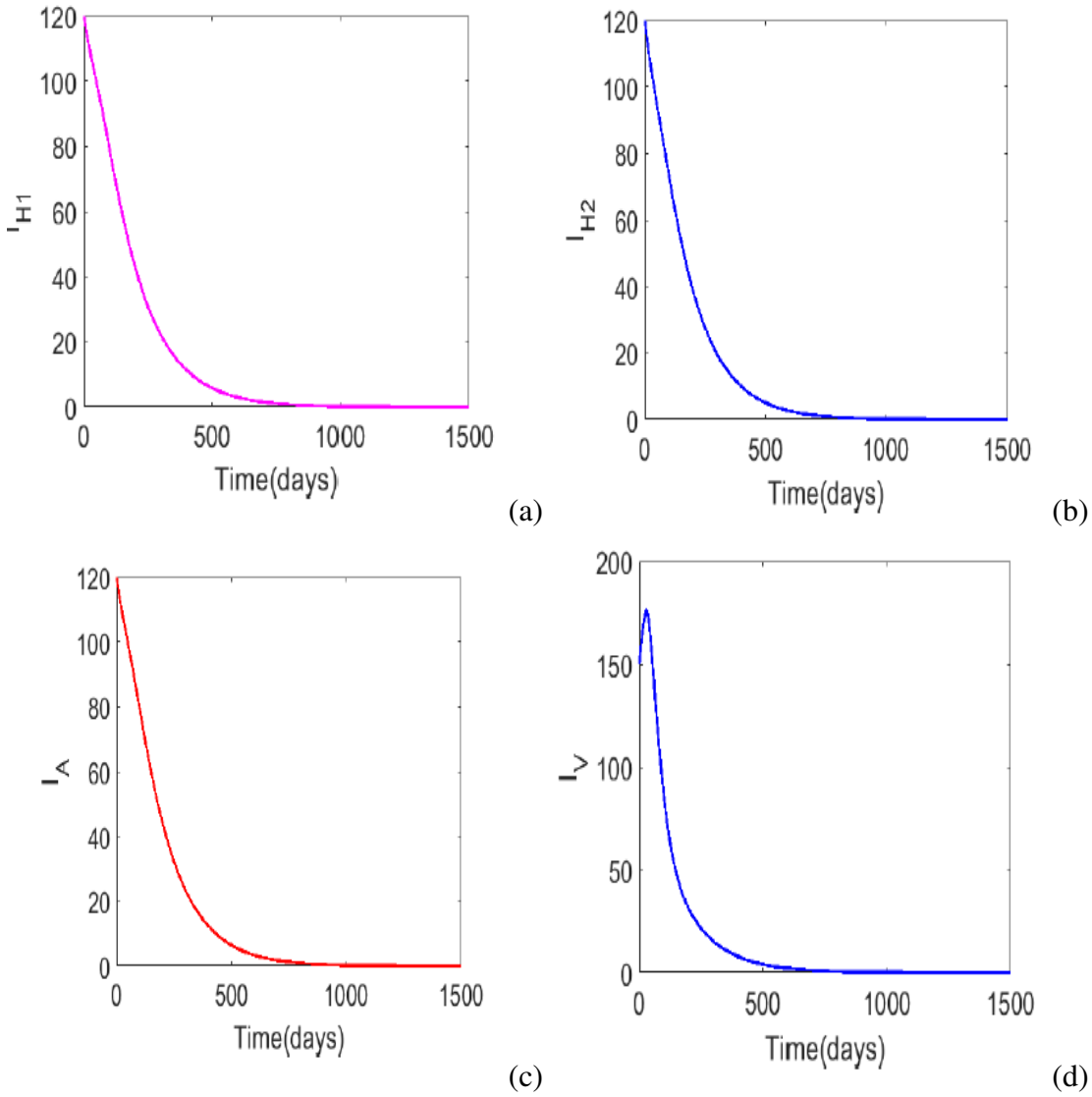

Figure 27: Simulation results of system 3.5 at the disease-free-equilibrium $\mathscr{E}^0$

Figure 27 demonstrates the convergence of the infected populations to the disease-free equilibrium for $\mathscr{R}_0 < 1$. The value of $\mathscr{R}_0$ in this case, is $\mathscr{R}_0 = 0.59 < 1$ and it is evident that all the infected populations die out after 500 days which is in agreement with the analytical results summarized by Theorem 3.7.

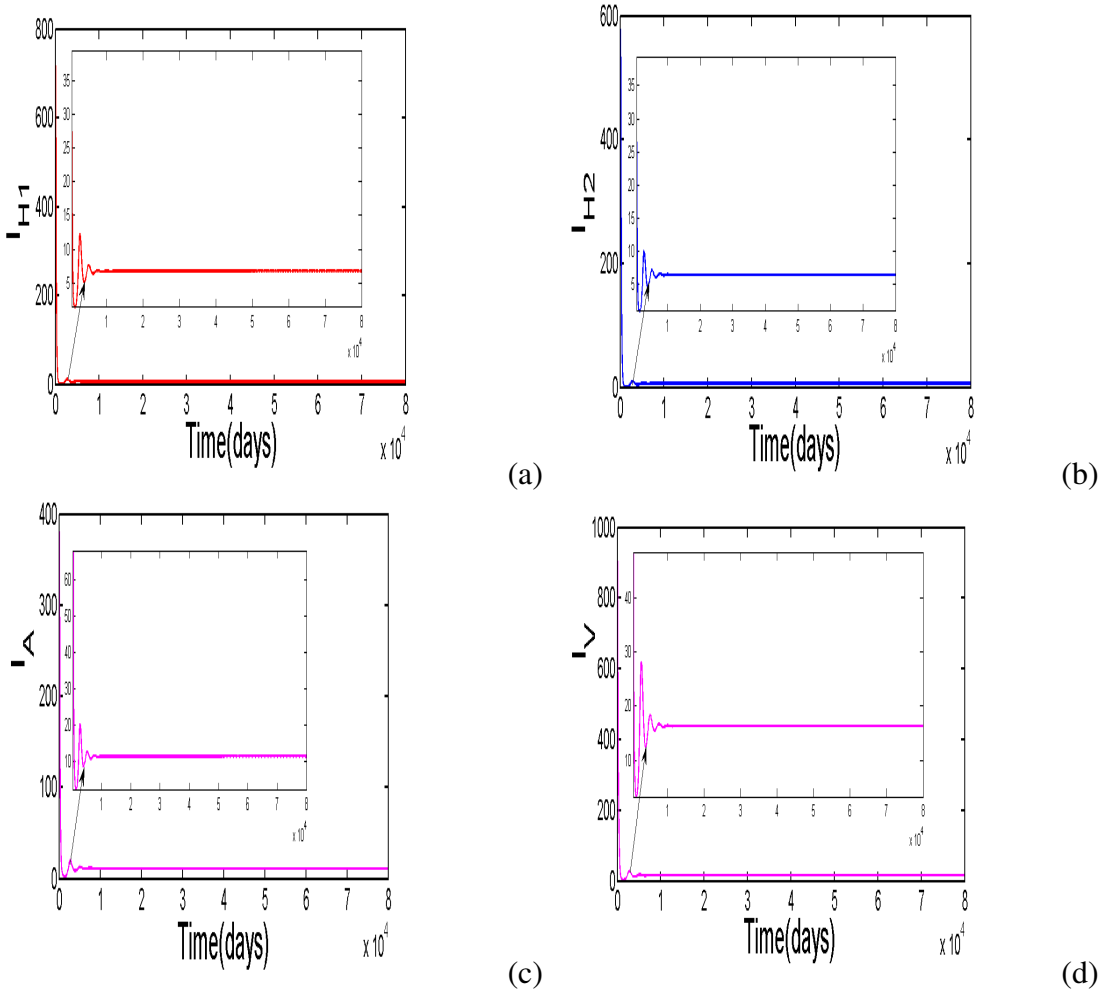

Figure 28: Simulations of system (3.5) at the endemic equilibrium point $\mathscr{E}^*$

The numerical results in Fig. 28 illustrate the trajectories of system (3.5) at an endemic equilibrium point. The results were obtained using parameter values in Table 2 and 5 coupled with $\beta_{HV} = \beta_{AV} = 3.55 \times 10^{-5}$, $\beta_{VH} = \beta_{VA} = 8.3 \times 10^{-5}$, giving $\mathscr{R}_0 = 7.23$. In addition, the population levels were assumed as follows: $L(0) = 1300$, $S_V(0) = 5 \times 10^3$, $I_V(0) = 3 \times 10^2$, $S_{H1}(0) = 1 \times 10^3, I_{H1}(0) = 150$, $S_{H2}(0) = 5 \times 10^2$, $I_{H2}(0) = 150$, $S_A(0) = 5 \times 10^2$, $I_A(0) = 100$, and $R_H(0) = R_A(0) = 0$. It was evidenced that all the trajectories present some periodic oscillations from the start for a considerable time frame before they finally converge to a unique equilibrium point. These results showed that the inclusion of the time delay factor destabilizes the endemic equilibrium point for a certain period of time leading to periodic oscillations due to the existence of Hopf bifurcations. In the following illustrations (Fig. 30 and 31), it was investigated the effects of the size of the initial population levels on the period and amplitude of the periodic oscillations.

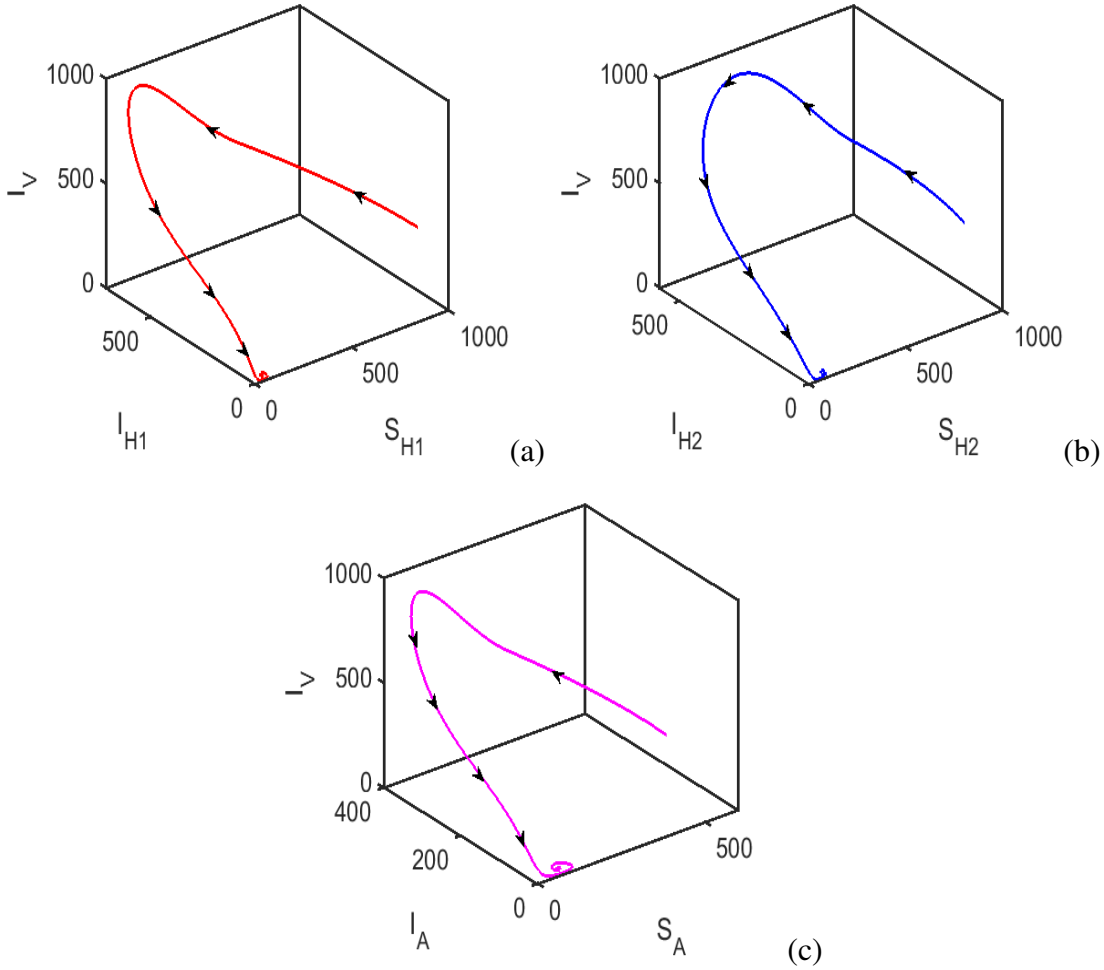

Figure 29: Numerical simulations to demonstrating the Hopf bifurcations of that arise due to the inclusion of the time delay factor in the model (3.5)

The simulation results in Fig. 30 depict the persistence of the disease at an endemic equilibrium, that is., for $\mathscr{R}_0 > 1$. The results were obtained by setting $\beta_{HV} = \beta_{AV} = 3.55 \times 10^{-5}$, $\beta_{VH} = \beta_{VA} = 8.3 \times 10^{-5}$ and the rest of the model parameters are as in Table 2 and 5, leading to $\mathscr{R}_0 = 2.51$. From the numerical simulations, it was observed that the solution profiles for all the populations (susceptible and infected) undergo periodic oscillations for a certain time before they finally converging to the endemic equilibrium point $\mathscr{E}^*$. Thus, the time delay factor τ factor leads to some periodic oscillations from the start for a considerable time frame before finally converging to a unique equilibrium point. Therefore, one can note that, adding the time delay in the model system destabilizes the solution profile of the system, leading to some periodic solutions.

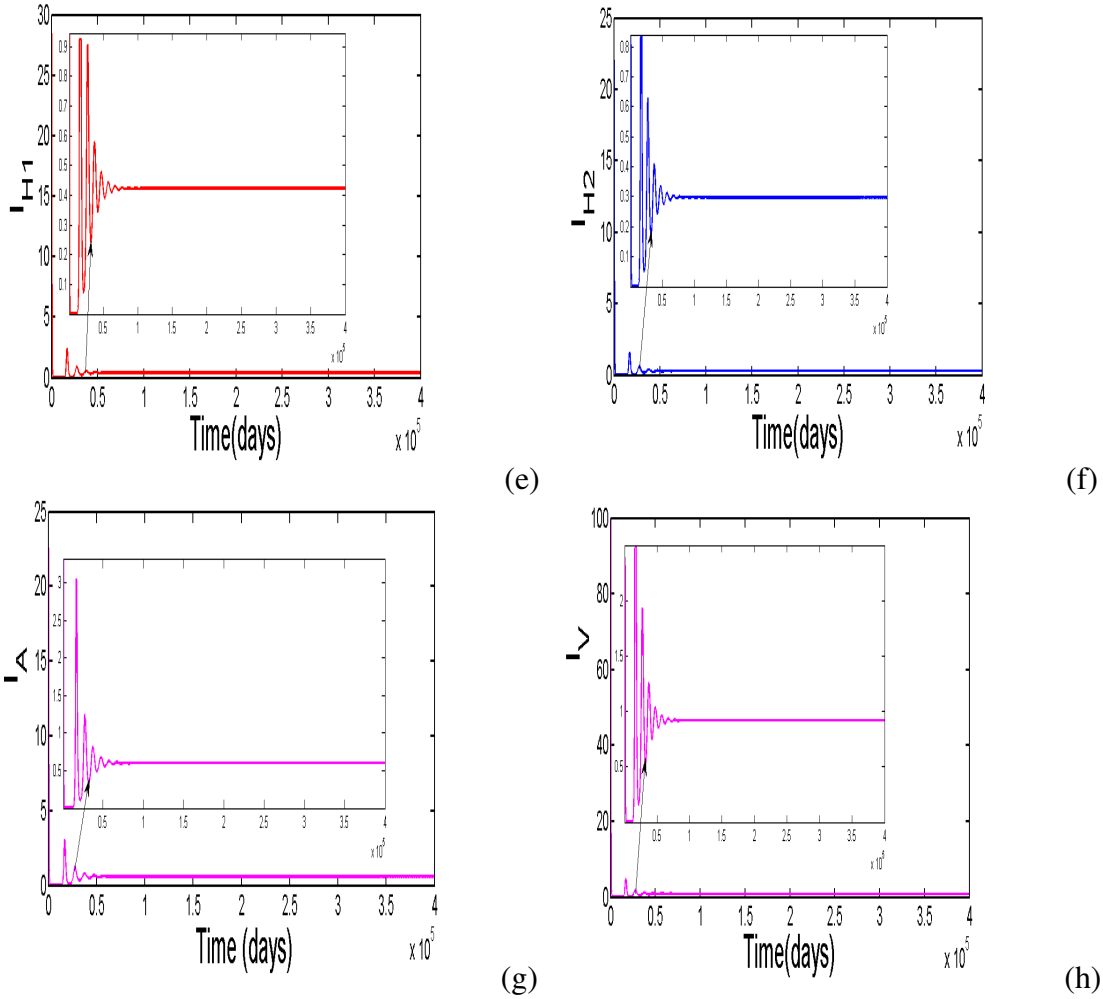

Figure 30: Numerical results of system (3.5) depicting the persistence of the disease of $\mathscr{R}_0 > 1$

To further support the analytical results in Fig. 31, the Hopf bifurcation plots were presented in Fig. 29. The plots further demonstrate the existence of periodic solutions which are arise due to Hopf bifurcations caused by the time delay factor. Comparing the results in Fig. 28 and 30, it was observed that small initial population levels are associated with more pronounced periodic oscillations with large amplitude in comparison to high initial population levels. Moreover, the existence of periodic oscillations solutions arising due to Hopf bifurcations caused by the time delay factor may cause challenges in planning the control strategies for dynamics of the sleeping sickness disease.

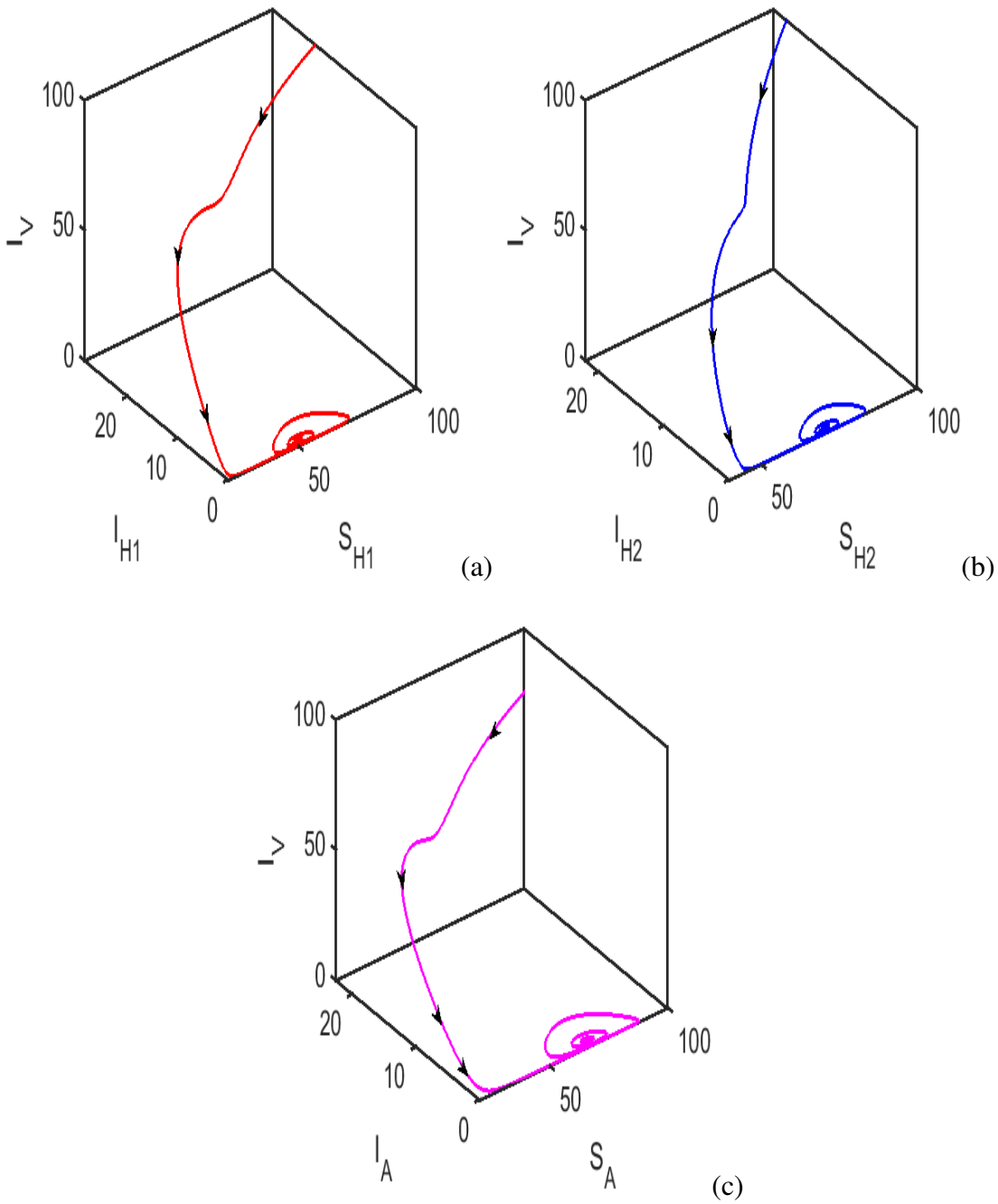

Figure 31: Dynamics of model system (3.5) illustrating stability of endemic equilibrium

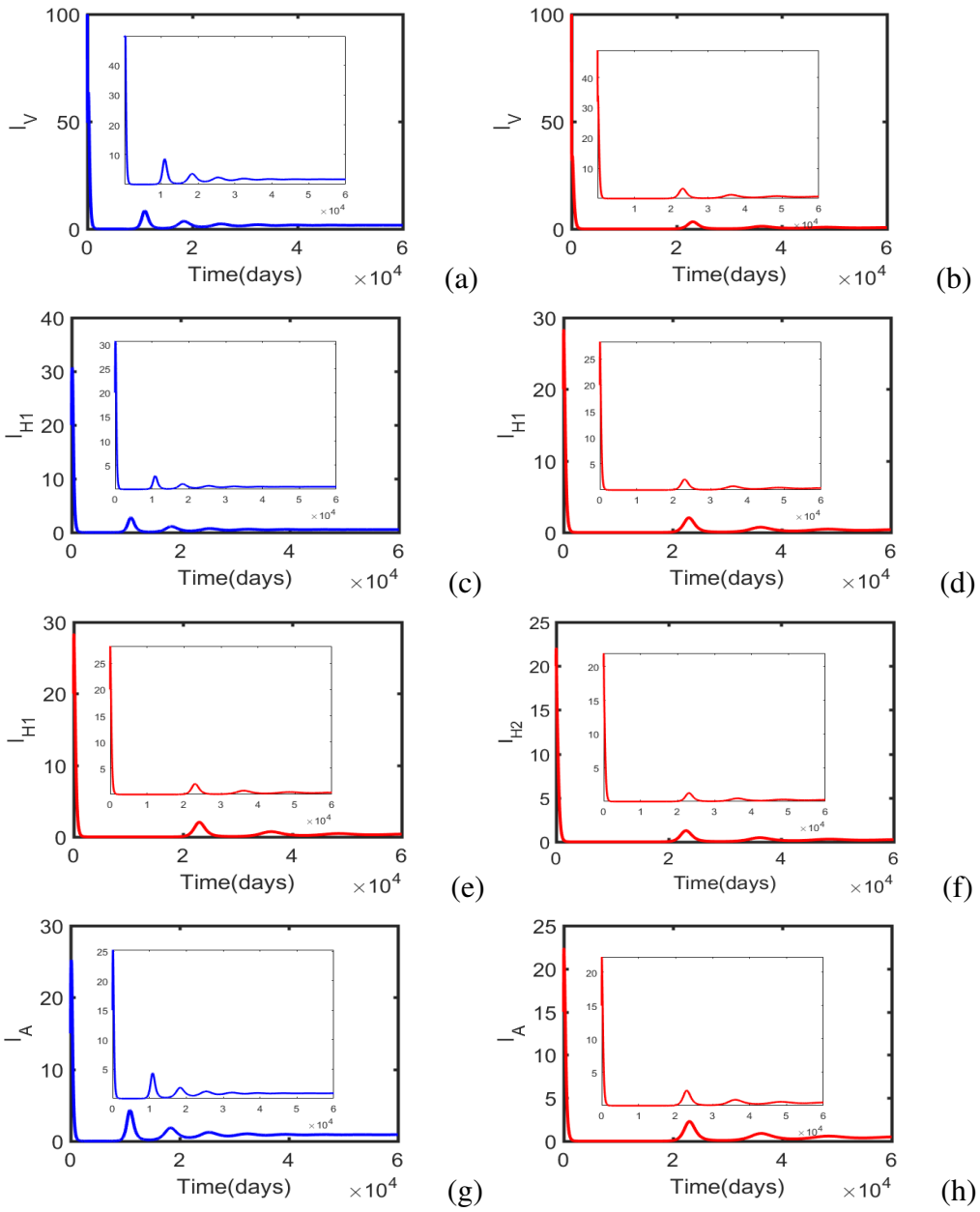

Figure 32: Numerical results of system (3.5) demonstrating the effects of the time delay factor $\tau = 30$ on the dynamics of the disease

Numerical simulations in Fig. 32 illustrate the effect of the time delay factor τ, on the period and amplitude of the oscillations. It was also considered that, $\tau = 15$ and $\tau = 30$ and compared the results with those in Fig. 30 where τ is set to 25. For all the plots in blue was set to be $\tau = 15$ and for those in red $\tau = 30$. All the other parameter values and initial population levels were fixed. Overall, the results showed that the period and amplitude of the periodic solutions become is smaller for both $\tau = 15$ and $\tau = 30$ compared to $\tau = 25$.

4.6 Chapter overview

In this chapter, the numerical results and discussions on the results for the four proposed models have been presented. From the first model, rhodesiense with educational campaigns, it was noted that the model admits multiple equilibrium points when the $\mathscr{R}_0$ is less than unity. Hence, it was concluded that the model undergoes a backward bifurcation. It was also noted that time-dependent educational campaigns and insecticide use could significantly reduce new cases of the disease when they are implemented at less than 100% intensity. From the second framework, rhodesiense with seasonality, it was observed that seasonality plays an important role in shaping the long-term dynamics of the disease which subsequently impact the design of its optimal control strategies. In the third model, rhodesiense with memory and temperature effects, it was noted that at temperature less than 16°C, the tsetse population could become extinct even in the absence of intervention strategies. The simulation results from the rhodesiense with time delay and heterogeneity showed that the inclusion of the time delay factor in the model destabilized the endemic equilibrium point leading to periodic solutions for a certain time frame. It was also observed that as the time delay exceed 15 days, the amplitude of the oscillations decreases significantly. Overall, the numerical results presented in this chapter have not only reaffirmed some of the existing hypothesis on tsetse fly epidemiology but also demonstrated the implications of educational campaigns, seasonality, memory effects, temperature effects, heterogeneity in human population and time delay in tsetse fly population, on the short-and long-term dynamics of *T. brucei rhodesiense* disease

CHAPTER FIVE

CONCLUSION AND RECOMMENDATIONS

5.1 Conclusion

Increased understanding of the ecological, environmental and behavioral drivers of HAT transmission is critical to designing effective control programs that maximize the probability of achieving elimination. The present study aimed to utilize mathematical model to investigate the effects of different factors (educational campaigns, seasonality, memory and temperature effects, time-delay effects due to the incubation period of vector population and heterogeneity of the human population) on the short-and long-term dynamics of *T. brucei rhodesiense* disease. Hence, four new comprehensive mathematical frameworks (which extend many of the published models in the literature) were designed and rigorously analyzed.

The first mathematical proposed model, assessed the implications of educational campaigns and insecticide use on *T. brucei rhodesiense* dynamics. Dynamical analysis of the model showed that due to educational campaigns admits multiple equilibrium point whenever the $\mathscr{R}_0$ of this model was less than unity. When a model admits multiple equilibrium points for $\mathscr{R}_0 < 1$, it implies that it undergoes a backward bifurcation. Making use of the numerical illustrations, the existence of the backward bifurcation for this framework was illustrated.

Backward bifurcation makes disease elimination difficult (since, effective disease control or elimination is dependent on the initial sizes of the sub-populations of the model). Hence, it was imperative to investigate the implications of time-dependent educational campaigns (control $u_1(t)$ and insecticide use (control $u_2(t)$). An optimal control problem whose objective was to minimize the number of infected human populations over the defined time horizon, at minimal implementation costs the aforementioned disease intervention strategies were proposed. In the entire analysis, the intensity of awareness campaigns was assumed to be higher than that of insecticide use since the excessive use of insecticides has some residual effects.

Analysis of the optimal model problem was done with the population levels for the hosts (humans and animals) fixed at 1% while the vector population was varied from 1 to 3%. The results showed that optimal control awareness campaigns and insecticide use have the potential to eliminate the disease in the community, whereas in the absence of optimal control, the disease may not be reduced to levels close to zero. It was observed that when the bounds of the control were high, the associated costs were also high, and the reverse was true. In particular, it was noted that reducing the upper bound of u1 from 1 to 0.5 and u_2 from 1 to 0.3 could lead to a reduction in costs by 17.6%. Overall, the study demonstrated that optimal awareness and

insecticide use have the potential to reduce the population levels of infected species to levels close to zero, and for this to be attained insecticide control has to be implemented for a slightly longer period compared to the awareness control.

The effects of seasonal variations on the epidemiology of *T. brucei rhodesiense* disease are well documented. In particular, seasonal variations alter vector development rates and behavior, thereby in influencing the transmission dynamics of the disease. To investigate the effects of seasonality on the short-and long-term dynamics of *T. brucei rhodesiense* disease, a non-autonomous framework that incorporates relevant biological details, (human, animal and vector populations) was proposed. Owing to the importance of understanding the effective ways of managing the spread of the disease, this framework included time-dependent educational campaigns as well as tine-dependent insecticide use.

In developing response plans for effective management of diseases, policymakers seek optimal responses that can minimize the incidence and/or disease-related mortality rate while considering the costs involved. Hence, on this model the aim of this model was to minimize the number of people who become infected, while minimizing the costs associated with strategy implementation. Overall the study showed that seasonality plays an important role in shaping the short-and long-term dynamics of the disease which subsequently impacts the design of its optimal control strategies. Although insecticide usage is associated with adverse effects on the environment, the results from this study suggest that by totally neglecting insecticide use, effective disease management may present a formidable challenge. However, if human awareness is combined with low insecticide usage, then the disease can be effectively be managed.

Over the past few decades, many scientists have demonstrated that fractional models can more accurately describe natural phenomena than classical integer order. Unlike integer differential equations, fractional derivatives can capture memory effects that are inherent in real world problems from fields such as engineering, biology, and social sciences. To investigate the effects of memory on *T. brucei rhodesiense* transmission and control dynamics, a mathematical model based on Caputo derivative was proposed and analyzed. The proposed model also incorporated temperature-dependent parameters to investigate their effects on the short-and long-term dynamics of the disease.

Among the several outcomes obtained, the study showed that when daily averaged temperature is around $T = 20^{\circ}C$ then destruction of 30% or more vectors in 3 days will reduce the $\mathscr{R}_0$ to levels below unity, despite any level of human detection. In addition, it was observed that if human detection is around 50% and vector control is 55% or more, then the disease will die out in the community even at the optimum temperature $T = 25^{\circ}C$. Overall, the findings from

this study have demonstrated the impact of temperature and control strategies on the long term dynamics of *T. brucei rhodesiense* and the outcomes enhance our understanding of the effective management of the disease.

The last model considered in this dissertation aimed to investigate the effects of time delay and heterogeneity of human population on *T. brucei rhodesiense* transmission and control dynamics. To account for heterogeneity in the human population, a two patch structure for the human population was considered. Individuals were subdivided into two distinct patches, patch 1 (high-risk individuals) and patch (low-risk individuals). Since the life span of tsetse flies is extremely short of approximately 33 days (Ndondo *et al.*, 2016) compared to that of humans and animals, it was imperative to investigate the effects of the needed incubation period for an infected vector to become infectious. Hence the time delay factor considered in the proposed frame work was due to latency in the tsetse fly population. Dynamical analysis of the model revealed that the model admits a globally asymptotically stable disease-free equilibrium whenever the basic reproduction number is less than unity. It was also noted that a unique endemic equilibrium which is globally asymptotically stable exists whenever the $\mathscr{R}_0$ is greater than unity. Results from simulations showed that whenever the $\mathscr{R}_0$ is greater than unity the model solutions will be associated with periodic oscillations for a considerable time scale from the start before attaining stability. This suggests that, the inclusion of the time delay factor destabilized the endemic equilibrium point leading to periodic solutions for a certain time frame due to Hopf bifurcations.

5.2 Recommendations

Sleeping sickness or HAT is a neglected disease that impacts 70 million people living in 1.55 million km^2 in sub-Saharan Africa (Aksoy *et al.*, 2017). Several modelling studies have been undertaken to assess the feasibility of the WHO's goal of eliminating the disease by 2030. However, these studies overlooked the effects of time-dependent use of educational campaigns (awareness) and insecticides, heterogeneity in the human population and memory effects. In this study, mathematical models were proposed and analyzed to assess the effects of the aforementioned factors on *T. brucei rhodesiense* elimination. Based on outcomes from this study the following recommendations are made:

(i) Coupling of time-dependent educational campaigns and insecticides use be considered and mathematical model be utilized to evaluate the success after a defined time horizon. In addition, insecticide be applied at an intensity lower than that of educational campaigns all the time. From the study, it was observed that educational campaigns alone even at an intensity higher than 50% may not be sufficient to eliminate the disease.

(ii) The intensity of intervention strategies needs to be varied based on the season since sea-

sonality plays an important role in shaping the short-and long-term dynamics of the disease.

(iii) Policymakers need to pay more attention to heterogeneity in the human population when designing ways of effectively managing the disease. The study showed that heterogeneity could possibly be one of the several factors complicating the elimination of the disease. In particular, it was noted that an increase of the risk population beyond a certain threshold could lead to the persistence of the disease.

(iv) Mathematical models be utilized alongside medical interventions to infer and make forecasts on the success and possible elimination of the disease. Since mathematical models have proved to be important tools that can aid our understanding and provide solutions to phenomena which are complex to measure in the field. Combining mathematical models with other approaches could shed light on the feasibility of the WHO's goal of eliminating the disease by 2030.

5.2.1 Limitation of the study and possible future works

Although this study adds to the existing body of knowledge on *T. brucei rhodesiense* transmission and control, it has some limitations which need to be acknowledged. These limitations is regarded as the areas of future work:

(i) Effects of host and vector migrations were not factored in all the four frameworks considered. Both tsetse flies and hosts are capable of migrating from one place to another in time. Hence partial differential equations (PDEs) could be used to formulate a spatial *T. brucei rhodesiense*.

(ii) Considered intervention strategies could be coupled with cattle treatment (use of trypanocide). In all the formulated mathematical models and analyzed in this study animals were assumed to recover from the infection naturally (as suggested by Stone & Chitnis (2015)). However, according to Hargrove *et al.* (2012) use of trypanocide could significantly aid on the effective management of the *T. brucei rhodesiense*.

(iii) On some of the objectives, deterministic model was used to evaluate the effects of certain intervention strategies on disease elimination. Though such modeling approach captures the average behavior of the system, it may miss some aspects of disease transmission, especially in the context of small populations and low infection prevalence where stochastic fade-out or take-off may be significant.

(iv) Multiple animal hosts could also be considered since the disease affects both wild and domesticated animals.

REFERENCES

Ackley, Sarah F & Hargrove, J. W. (2017). A dynamic model for estimating adult female mortality from ovarian dissection data for the tsetse fly glossina pallidipes austen sampled in zimbabwe. *PLoS Neglected Tropical Diseases*. **11**(8).

Agaba, G., Kyrychko, Y. & Blyuss, K. (2017). Mathematical model for the impact of awareness on the dynamics of infectious diseases. *Mathematical Biosciences*. **286**: 22–30.

Aguila-Camacho, N., Duarte-Mermoud, M. A. & Gallegos, J. A. (2014). Lyapunov functions for fractional order systems. *Communications in Nonlinear Science and Numerical Simulation*. **19**(9): 2951–2957.

Aksoy, S., Buscher, P., Lehane, M., Solano, P. & Van Den Abbeele, J. (2017). Human african trypanosomiasis control: achievements and challenges. *PLoS Neglected Tropical Diseases*. **11**(4).

Alderton, S., Macleod, E. T., Anderson, N. E., Palmer, G., Machila, N., Simuunza, M., Welburn, S. C. & Atkinson, P. M. (2018). An agent-based model of tsetse fly response to seasonal climatic drivers: Assessing the impact on sleeping sickness transmission rates. *PLoS Neglected Tropical Diseases*. **12**(2).

Alderton, S., Macleod, E. T., Anderson, N. E., Schaten, K., Kuleszo, J., Simuunza, M., Welburn, S. C. & Atkinson, P. M. (2016). A multi-host agent-based model for a zoonotic, vector-borne disease. a case study on trypanosomiasis in eastern province, zambia. *PLoS Neglected Tropical Diseases*. **10**(12): e0005252.

Allahviranloo, Tofigh & Salahshour, S. (2011). Euler method for solving hybrid fuzzy differential equation. *Soft Computing*. **15**(7): 1247–1253.

Arriola, Leon M & Hyman, J. M. (2007). Being sensitive to uncertainty. *Computing in Science & Engineering*. **9**(2): 10–20.

Artzrouni, Marc & Gouteux, J.-P. (1996*a*). A compartmental model of sleeping sickness in central africa. *Journal of Biological Systems*. **4**(04): 459–477.

Artzrouni, Marc & Gouteux, J.-P. (1996*b*). Control strategies for sleeping sickness in central africa: a model-based approach. *Tropical Medicine & International Health*. **1**(6): 753–764.

Artzrouni, Marc & Gouteux, J.-P. (1996*c*). Control strategies for sleeping sickness in central africa: a model-based approach. *Tropical Medicine & International Health*. **1**(6): 753–764.

Beretta, G. P. (1986). A theorem on lyapunov stability for dynamical systems and a conjecture on a property of entropy. *Journal of Mathematical Physics*. **27**(1): 305–308.

Bhatia, Nam Parshad & Szegö, G. P. (2002). Stability theory of dynamical systems. Springer Science & Business Media.

Blaszak, M. (2012). Multi-Hamiltonian theory of dynamical systems. Springer Science & Business Media.

Brin, Michael & Stuck, G. (2002). Introduction to dynamical systems. Cambridge University Press.

Büscher, P., Cecchi, G., Jamonneau, V. & Priotto, G. (2017*a*). Human african trypanosomiasis. *The Lancet*. **390**(10110): 2397–2409.

Büscher, P., Cecchi, G., Jamonneau, V. & Priotto, G. (2017*b*). Human african trypanosomiasis. *The Lancet*. **390**(10110): 2397–2409.

Caputo, M. (1967). Linear models of dissipation whose q is almost frequency independent—ii. *Geophysical Journal International*. **13**(5): 529–539.

Cartwright, Julyan HE & Piro, O. (1992). The dynamics of runge–kutta methods. *International Journal of Bifurcation and Chaos*. **2**(03): 427–449.

Chalvet-Monfray, K., Artzrouni, M., Gouteux, J.-P., Auger, P. & Sabatier, P. (1998). A two-patch model of gambian sleeping sickness: application to vector control strategies in a village and plantations. *Acta Biotheoretica*. **46**(3): 207–222.

Chen, X & Liu, B. (2010). Existence and uniqueness theorem for uncertain differential equations. *Fuzzy Optimization and Decision Making*. **9**(1): 69–81.

Cheng, A. K. (2009). Mathematical modelling and real life problem solving. *In:* Mathematical Problem Solving: Yearbook 2009, Association of Mathematics Educators. World Scientific. pp. 159–182.

Chitnis, N., Hyman, J. M. & Cushing, J. M. (2008). Determining important parameters in the spread of malaria through the sensitivity analysis of a mathematical model. *Bulletin of Mathematical Biology*. **70**(5): 1272.

Coetzer, J., Tustin, R. *et al.* (2004). Infectious diseases of livestock, volume one.. *Infectious Diseases of Livestock, Volume One.*. (Ed. 2).

Cressman, R. (2013). The stability concept of evolutionary game theory: a dynamic approach. Vol. 94. Springer Science & Business Media.

Diekmann, O., Heesterbeek, J. A. P. & Metz, J. A. (1990). On the definition and the computation of the basic reproduction ratio r 0 in models for infectious diseases in heterogeneous populations. *Journal of Mathematical Biology*. **28**(4): 365–382.

Diethelm, K. (2010). The analysis of fractional differential equations: An application-oriented exposition using differential operators of Caputo type. Springer Science & Business Media.

Ding, C., Tao, N., Sun, Y. & Zhu, Y. (2016). The effect of time delays on transmission dynamics of schistosomiasis. *Chaos, Solitons & Fractals*. **91**: 360–371.

Eperon, G., Balasegaram, M., Potet, J., Mowbray, C., Valverde, O. & Chappuis, F. (2014). Treatment options for second-stage gambiense human african trypanosomiasis. *Expert Review of Anti-Infective Therapy*. **12**(11): 1407–1417.

Faizullah, F. (2017). Existence and uniqueness of solutions to sfdes driven by g-brownian motion with non-lipschitz conditions. *Journal of Computational Analysis & Applications*. **2**(23): 344–354.

Fleming, Wendell H & Rishel, R. W. (1976). Deterministic and stochastic optimal control. *Bulletin of the American Mathematical Society*. **82**: 869–870.

Franco, J. R., Cecchi, G., Priotto, G., Paone, M., Diarra, A., Grout, L., Simarro, P. P., Zhao, W. & Argaw, D. (2020). Monitoring the elimination of human african trypanosomiasis at continental and country level: Update to 2018. *PLoS Neglected Tropical Diseases*. **14**(5): e0008261.

Franco, J. R., Simarro, P. P., Diarra, A. & Jannin, J. G. (2014*a*). Epidemiology of human african trypanosomiasis. *Clinical Epidemiology*. **6**: 257.

Franco, J. R., Simarro, P. P., Diarra, A. & Jannin, J. G. (2014*b*). Epidemiology of human african trypanosomiasis. *Clinical Epidemiology*. **6**: 257.

Funk, S., Nishiura, H., Heesterbeek, H., Edmunds, W. J. & Checchi, F. (2013). Identifying transmission cycles at the human-animal interface: the role of animal reservoirs in maintaining gambiense human african trypanosomiasis. *PLoS Computational Biology*. **9**(1).

Gao, Y. (2012). Existence and uniqueness theorem on uncertain differential equations with local lipschitz condition. *Journal of Uncertain Systems*. **6**(3): 223–232.

Garrappa, R. (2011). Predictor-corrector pece method for fractional differential equations. *MATLAB Central File Exchange [File ID: 32918]*. .

Gashirai, T. B., Hove-Musekwa, S. D. & Mushayabasa, S. (2021). Dynamical analysis of a fractional-order foot-and-mouth disease model. *Mathematical Sciences*. **15**(1): 65–82.

Gear, C. (1974). Multirate methods for ordinary differential equations. Technical report. Illinois Univ., Urbana (USA). Dept. of Computer Science.

Ghosh, J. K., Ghosh, U., Biswas, M. & Sarkar, S. (2019). Qualitative analysis and optimal control strategy of an sir model with saturated incidence and treatment. *Differential Equations & Dynamical Systems*. pp. 1–15.

Gilbert, J. A., Medlock, J., Townsend, J. P., Aksoy, S., Mbah, M. N. & Galvani, A. P. (2016). Determinants of human african trypanosomiasis elimination via paratransgenesis. *PLoS Neglected Tropical Diseases*. **10**(3).

Glover, P. (1967). The importance of ecological studies in the control of tsetse flies. *Bulletin of the World Health Organization*. **37**(4): 581.

Greenhalgh, D., Rana, S., Samanta, S., Sardar, T., Bhattacharya, S. & Chattopadhyay, J. (2015). Awareness programs control infectious disease–multiple delay induced mathematical model. *Applied Mathematics & Computation*. **251**: 539–563.

Griffiths, David F & Higham, D. J. (2010). Euler's method. *In:* Numerical Methods for Ordinary Differential Equations. Springer. pp. 19–31.

Gumel, A. (2012). Causes of backward bifurcations in some epidemiological models. *Journal of Mathematical Analysis and Applications*. **395**(1): 355–365.

Habbema, J., Oostmarssen, G. & Plaisier, A. (1996). The onchosim model and its use in decision support for river blindness control. *In:* Models for Infectious Human Diseases. Their Structure & Relation to Data. Cambridge University Press Cambridge. pp. 360–380.

Hairer, Ernst & Wanner, G. (2015). Euler methods, explicit, implicit, symplectic. *Encyclopedia of Applied & Computational Mathematics*. (1): 451–455.

Hale, J. K., Lunel, S. M. V., Verduyn, L. S. & Lunel, S. M. V. (1993). Introduction to functional differential equations. Vol. 99. Springer Science & Business Media.

Hargrove, J. (1994). Reproductive rates of tsetse flies in the field in zimbabwe. *Physiological Entomology*. **19**(4): 307–318.

Hargrove, J. W., Ouifki, R., Kajunguri, D., Vale, G. A. & Torr, S. J. (2012). Modeling the control of trypanosomiasis using trypanocides or insecticide-treated livestock. *PLoS Negl Trop Dis*. **6**(5): e1615.

Hide, G. (1999). History of sleeping sickness in east africa. *Clinical Microbiology Reviews*. **12**(1): 112–125.

Igor, P. (1999). Fractional differential equations. *Mathematics in Science & Engineering*. **198**.

Jleli, M., Nieto, J. & Samet, B. (2017). Lyapunov-type inequalities for a higher order fractional differential equation with fractional integral boundary conditions. *Electronic Journal of Qualitative Theory of Differential Equations*. **2017**(16): 1–17.

Kajunguri, D. (2013). Modelling the control of tsetse and African trypanosomiasis through application of insecticides on cattle in Southeastern Uganda. PhD thesis. Stellenbosch: Stellenbosch University.

Kajunguri, D., Hargrove, J. W., Ouifki, R., Mugisha, J., Coleman, P. G. & Welburn, S. C. (2014). Modelling the use of insecticide-treated cattle to control tsetse and trypanosoma brucei rhodesiense in a multi-host population. *Bulletin of Mathematical Biology*. **76**(3): 673–696.

Kalman, R. (1963). The theory of optimal control and the calculus of variations. *In:* Mathematical Optimization Techniques. University of California Press Los Angeles, CA. pp. 309–331.

Keeling, M. J. (2005). Models of foot-and-mouth disease. *Proceedings of the Royal Society B: Biological Sciences*. **272**(1569): 1195–1202.

Kennedy, P. G. (2013). Clinical features, diagnosis, and treatment of human african trypanosomiasis (sleeping sickness). *The Lancet Neurology*. **12**(2): 186–194.

Kexue, Li & Jigen, P. (2011). Laplace transform and fractional differential equations. *Applied Mathematics Letters*. **24**(12): 2019–2023.

Khalil, H. K. (2009). Lyapunov stability. *Control Systems, Robotics & AutomatioN–Volume XII: Nonlinear, Distributed, and Time Delay Systems-I*. p. 115.

Kheiri, Hossein & Jafari, M. (2019). Stability analysis of a fractional order model for the hiv/aids epidemic in a patchy environment. *Journal of Computational & Applied Mathematics*. **346**: 323–339.

Kirk, D. E. (2004). Optimal control theory: an introduction. Courier Corporation.

Kumar, A., Srivastava, P. K. & Takeuchi, Y. (2017). Modeling the role of information and limited optimal treatment on disease prevalence. *Journal of Theoretical Biology*. **414**: 103–119.

Lakshmikantham, Vangipuram & Leela, S. (1969). Differential and Integral Inequalities: Theory and Applications: Volume I: Ordinary Differential Equations. Academic Press.

Lapidus, L. & Seinfeld, J. H. (1971). Numerical solution of ordinary differential equations. Academic Press.

LaSalle, J. P. (1976). The stability of dynamical systems. Vol. 25. Siam.

LaSalle, J. P. *et al.* (1960). The time optimal control problem. *Contributions to the Theory of Nonlinear Oscillations*. **5**: 1–24.

Leak, S. G. (1999). Tsetse biology and ecology: their role in the epidemiology and control of trypanosomosis. ILRI (Aka ILCA & ILRAD).

Lee, Ernest Bruce & Markus, L. (1967). Foundations of optimal control theory. Technical report. Minnesota Univ Minneapolis Center For Control Sciences.

Lenhart, Suzanne & Workman, J. T. (2007). Optimal control applied to biological models. CRC press.

Liang, S., Wu, R. & Chen, L. (2015). Laplace transform of fractional order differential equations. *Electron. J. Differ. Equ*. **139**: 1–15.

Lord, J. S., Hargrove, J. W., Torr, S. J. & Vale, G. A. (2018). Climate change and african trypanosomiasis vector populations in zimbabwe's zambezi valley: a mathematical modelling study. *PLoS Medicine*. **15**(10): e1002675.

Lukes, D. L. & DL, L. (1982). Differential equations: classical to controlled. . .

Lutumba, P., Makieya, E., Shaw, A., Meheus, F. & Boelaert, M. (2007). Human african trypanosomiasis in a rural community, democratic republic of congo. *Emerging Infectious Diseases*. **13**(2): 248.

Macdonald, G. *et al.* (1950). The analysis of infection rates in diseases in which super infection occurs.. *Tropical Diseases Bulletin*. **47**: 907–915.

Madsen, T., Wallace, D. & Zupan, N. (2013*a*). Seasonal fluctuation in tsetse fly populations and human african trypanosomiasis: A mathematical model. *In:* BIOMAT 2012. World Scientific. pp. 56–69.

Madsen, T., Wallace, D. & Zupan, N. (2013*b*). Seasonal fluctuation in tsetse fly populations and human african trypanosomiasis: A mathematical model. *In:* BIOMAT 2012. World Scientific. pp. 56–69.

Magez, S., Caljon, G., Tran, T., Stijlemans, B. & Radwanska, M. (2010). Current status of vaccination against african trypanosomiasis. *Parasitology*. **137**(14): 2017–2027.

McKenzie, F. E. (2000). Why model malaria?. *Parasitology Today*. **16**(12): 511–516.

Mehdi, S. A. & Kareem, R. S. (2017). Using fourth-order runge-kutta method to solve lü chaotic system. *Am. J. Eng. Res*. **6**: 72–77.

Meisner, J., Barnabas, R. V. & Rabinowitz, P. M. (2019). A mathematical model for evaluating the role of trypanocide treatment of cattle in the epidemiology and control of trypanosoma brucei rhodesiense and t. b. gambiense sleeping sickness in uganda. *Parasite Epidemiology and Control*. **5**: e00106.

Milligan, PJM & Baker, R. (1988). A model of tsetse-transmitted animal trypanosomiasis. *Parasitology*. **96**(1): 211–239.

Monitoring, C. G. (2011). A research agenda for malaria eradication: monitoring, evaluation, and surveillance. *PLoS Medicine*. **8**(1).

Moore, S., Shrestha, S., Tomlinson, K. W. & Vuong, H. (2012*a*). Predicting the effect of climate change on african trypanosomiasis: integrating epidemiology with parasite and vector biology. *Journal of the Royal Society Interface*. **9**(70): 817–830.

Moore, S., Shrestha, S., Tomlinson, K. W. & Vuong, H. (2012*b*). Predicting the effect of climate change on african trypanosomiasis: integrating epidemiology with parasite and vector biology. *Journal of the Royal Society Interface*. **9**(70): 817–830.

Mulenga, G. M., Henning, L., Chilongo, K., Mubamba, C., Namangala, B. & Gummow, B. (2020). Insights into the control and management of human and bovine african trypanosomiasis in zambia between 2009 and 2019—a review. *Tropical Medicine & Infectious Disease*. **5**(3): 115.

Musa, S. S., Qureshi, S., Zhao, S., Yusuf, A., Mustapha, U. T. & He, D. (2021). Mathematical modeling of covid-19 epidemic with effect of awareness programs. *Infectious Disease Modelling*. **6**: 448–460.

Mushayabasa, S. (2015). Global stability of an anthrax model with environmental decontamination and time delay. *Discrete Dynamics in Nature & Society*. **2015**.

Mushayabasa, S. (2016). Dynamics of an anthrax model with distributed delay. *Acta Applicandae Mathematicae*. **144**(1): 77–86.

Mushayabasa, S & Bhunu, C. (2013). Modeling the impact of early therapy for latent tuberculosis patients and its optimal control analysis. *Journal of Biological Physics*. **39**(4): 723–747.

Ndeffo-Mbah, M. L., Pandey, A., Atkins, K. E., Aksoy, S. & Galvani, A. P. (2019). The impact of vector migration on the effectiveness of strategies to control gambiense human african trypanosomiasis. *PLoS Neglected Tropical Diseases*. **13**(12).

Ndondo, A., Munganga, J., Mwambakana, J., Saad-Roy, C., Van den Driessche, P. & Walo, R. (2016). Analysis of a model of gambiense sleeping sickness in humans and cattle. *Journal of Biological Dynamics*. **10**(1): 347–365.

Niu, J., Ding, Y., Zhu, L. & Ding, H. (2014). Runge–kutta methods for a semi-analytical prediction of milling stability. *Nonlinear Dynamics*. **76**(1): 289–304.

Nnko, H. J., Ngonyoka, A., Salekwa, L., Estes, A. B., Hudson, P. J., Gwakisa, P. S. & Cattadori, I. M. (2017). Seasonal variation of tsetse fly species abundance and prevalence of trypanosomes in the maasai steppe, tanzania. *Journal of Vector Ecology*. **42**(1): 24–33.

Nsoesie, E. O., Brownstein, J. S., Ramakrishnan, N. & Marathe, M. V. (2014). A systematic review of studies on forecasting the dynamics of influenza outbreaks. *Influenza & Other Respiratory Viruses*. **8**(3): 309–316.

Ochoche, A. (2007). Improving the modified euler method. *Leonardo Journal of Sciences*. **10**: 1–8.

Pandey, A., Atkins, K. E., Bucheton, B., Camara, M., Aksoy, S., Galvani, A. P. & Ndeffo-Mbah, M. L. (2015). Evaluating long-term effectiveness of sleeping sickness control measures in guinea. *Parasites & Vectors*. **8**(1): 550.

Phelps, R. (1973). The effect of temperature on fat consumption during the puparial stages of glossina morsitans morsitans westw.(dipt., glossinidae) under laboratory conditions, and its implication in the field. *Bulletin of Entomological Research*. **62**(3): 423–438.

Podlubny, I. (1999). An introduction to fractional derivatives, fractional differential equations, to methods of their solution and some of their applications. *Mathematics in Science & Engineering*. **198**: xxiv+–340.

Podlubny, I., Dorcak, L. & Kostial, I. (1997). On fractional derivatives, fractional-order dynamic systems and pi/sup/spl lambda//d/sup/spl mu//-controllers. In: *Proceedings of the 36th IEEE Conference on Decision and Control*. Vol. 5. IEEE. pp. 4985–4990.

Pontryagin, L. S. (2018*a*). Mathematical theory of optimal processes. Routledge.

Pontryagin, L. S. (2018*b*). Mathematical theory of optimal processes. Routledge.

Ranjbarian, F. (2017). Targets and strategies for drug development against human African sleeping sickness. PhD thesis. Umeå University.

Rock, K. S., Stone, C. M., Hastings, I. M., Keeling, M. J., Torr, S. J. & Chitnis, N. (2015). Mathematical models of human african trypanosomiasis epidemiology. *In:* Advances in parasitology. Vol. 87. Elsevier. pp. 53–133.

Rogers, D. (1988). A general model for the african trypanosomiases. *Parasitology*. **97**(1): 193–212.

Rogers, D., Hendrickx, G., Slingenbergh, J. *et al.* (1994). Tsetse flies and their control. *Revue Scientifique et Technique-Office International Des Epizooties*. **13**: 1075–1075.

Rosenbrock, H. H. (1963). A lyapunov function with applications to some nonlinear physical systems. *Automatica*. **1**(1): 31–53.

Ross, R. (1916). An application of the theory of probabilities to the study of a priori pathometry.—part i. *Proceedings of the Royal Society of London. Series A, Containing Papers of a Mathematical and Physical Character*. **92**(638): 204–230.

Ruo-Shi, Y., Yi-An, M., Bo, Y. & Ping, A. (2013). Lyapunov function as potential function: A dynamical equivalence. *Chinese Physics B*. **23**(1): 010505.

Shereni, W., Anderson, N. E., Nyakupinda, L. & Cecchi, G. (2016). Spatial distribution and trypanosome infection of tsetse flies in the sleeping sickness focus of zimbabwe in hurungwe district. *Parasites & Vectors*. **9**(1): 605.

Silva, C. J., Maurer, H. & Torres, D. F. (2016). Optimal control of a tuberculosis model with state and control delays. *ArXiv Preprint ArXiv:1606.08721*. .

Steverding, D. (2008). The history of african trypanosomiasis. *Parasites & Vectors*. **1**(1): 3.

Stone, C. M. & Chitnis, N. (2015). Implications of heterogeneous biting exposure and animal hosts on trypanosomiasis brucei gambiense transmission and control. *PLoS Comput Biol*. **11**(10): e1004514.

Stone, Chris M & Chitnis, N. (2015). Implications of heterogeneous biting exposure and animal hosts on trypanosomiasis brucei gambiense transmission and control. *PLoS Computational Biology*. **11**(10).

Thomson, GR & Tustin, R. (1994). Infectious Diseases of Livestock: With Special Reference to Southern Africa. Oxford University Press, Incorporated.

Todorov, E. (2006). Optimal control theory. *Bayesian brain: Probabilistic Approaches to Neural Coding*. pp. 269–298.

Vale, G. (1971). Artificial refuges for tsetse flies (glossina spp.). *Bulletin of Entomological Research*. **61**(2): 331–350.

Van den Driessche, P & Watmough, J. (2008). Further notes on the basic reproduction number. *In:* Mathematical Epidemiology. Springer. pp. 159–178.

Van den Driessche, Pauline & Watmough, J. (2002). Reproduction numbers and sub-threshold endemic equilibria for compartmental models of disease transmission. *Mathematical Biosciences*. **180**(1-2): 29–48.

Vargas-De-León, C. (2015). Volterra-type lyapunov functions for fractional-order epidemic systems. *Communications in Nonlinear Science and Numerical Simulation*. **24**(1-3): 75–85.

Wang, Wendi & Zhao, X.-Q. (2008). Threshold dynamics for compartmental epidemic models in periodic environments. *Journal of Dynamics and Differential Equations*. **20**(3): 699–717.

Wei, Fengying & Cai, Y. (2013). Existence, uniqueness and stability of the solution to neutral stochastic functional differential equations with infinite delay under non-lipschitz conditions. *Advances in Difference Equations*. **2013**(1): 151.

Yanagimoto, T. (2005). Teaching modelling as an alternative approach to school mathematics. *Teaching Mathematics & Its Applications: International Journal of the IMA*. **24**(1): 1–13.

Zhang, J., Mokhtari, A., Sra, S. & Jadbabaie, A. (2018). Direct runge-kutta discretization achieves acceleration. In: *Advances in Neural Information Processing Systems*. pp. 3900–3909.

Zhao, X.-Q. (2003*a*). Dynamical systems in population biology. 2003.

Zhao, X.-Q. (2003*b*). Dynamical systems in population biology springer-verlag. *New York*. .

APPENDICES

Appendix 1: Basic mathematical concepts

Dynamical system and equilibrium point

If q_i is the group of any population of living organisms at a time i, then the notation $q_{i+1} = h(q_i)$ is called a dynamical system and the point q^* is an equilibrium point of the dynamical system if and only if $h(q^*) = q^*$ (Brin, 2002) (See Appendix 5.25).

Stability of the dynamical system

The stability of any system implies that any solution that is initially selected close to the critical point ξ of the system must remain to the point ξ for the entire period of infection (Cressman, 2013).

Definition 5.2
(See, Bhatia & Szego, 2002; Beretta, 1986). Let ξ be the critical point of the system $\dot{g(t)} = h(g(t))$, the following definition is true (See in Appendices 5.101, 5.105 and 5.126):

(i) The critical point ξ is said to be stable if for all $\varepsilon > 0$, there exist $\delta > 0$ such that the solution of $\dot{g(t)} = h(g(t))$ satisfy the condition that $|g(0) - \xi| \leq \delta \rightarrow |g(t) - \xi| \leq \varepsilon$ for all $t \geq 0$.

(ii) The critical point ξ is said to be asymptotically stable if the point ξ is stable and there exist $\delta > 0$ such that the solution of $\dot{g(t)} = h(g(t))$ satisfy the condition that $|g(0) - \xi| \leq \delta \rightarrow \lim_{\rightarrow\infty} g(t) = \xi$.

Basic reproduction number

The basic reproduction number ($\mathscr{R}_0$) is the average number of secondary cases that is produced when a single infected individual is introduced in a population of full susceptible for the entire period of infection (Van den Driessche, 2008). The $\mathscr{R}_0$ provides the necessary conditions for the existence of the disease in the population as well as the stability of the equilibrium points, in particular the following is true (See Appendix 5.23):

(i) When $\mathscr{R}_0 < 1$, the disease dies in the population and the disease free-equilibrium point is asymptotically stable.

(ii) When $\mathscr{R}_0 >, 1$ the disease exist in the population and the disease-free equilibrium point is unstable.

Next-generation matrix method

The next-generation matrix is a popular method for the computation of basic reproduction. This technique was first introduced by Diekmann *et al.* (1990) and further extended in Van den Driessche (2002). The following are the procedures for computation of $\mathscr{R}_0$ using the next-generation matrix method; Suppose the number of individuals in each compartment of a dynamical $x = (x_1, x_2, x_3 ..... x_n)^T$ for which $m < n$ compartments contain the infected individuals whereby x_0 is a disease-free equilibrium point which exists and is stable, then the system $(x_1, x_2, x_3 ..... x_n)^T$ in (5.1) can be expressed in the following form 5.1 (See Appendix 5.123):

$$\frac{dx_i}{dt} = \mathscr{F}_i(x) - \mathscr{V}_i(x), \tag{5.1}$$

where $\mathscr{F}_i(x)$ denotes the rate of new appearance of infection in the compartment and $\mathscr{V}_i(x)$ is the new transfer rate between compartment i and infected compartments with $i = 1, 2, 3, ...m$. Therefore this is defined in 5.2 (See also Appendix 5.42):

$$F = \frac{\partial \mathscr{F}_i(x_0)}{\partial x_j}, \qquad \text{and} \qquad V = \frac{\partial \mathscr{V}_i(x_0)}{\partial x_j}. \tag{5.2}$$

In this case, $\mathscr{R}_0$ is given by $\mathscr{R}_0 = \rho(FV^{-1})$, where ρ represents the maximum eigenvalue of the matrix (FV^{-1}) called the spectral radius (Van den Driessche, 2008).

Lyapunov function

(See, (Ruo-Shi *et al.*, 2013; Rosenbrock, 1963; Lakshmikantham, 1969)). Let the function $N(y,z)$ be continuous and differentiable on an open interval containing the origin, then the function is said to be Lyapunov function of any dynamical system if it satisfies the following conditions (See Appendix 5.133):

(i) $N(0,0) = 0$.

(ii) $N(y,z) > 0$ for all value of y,z except 0.

(iii) $\dot{N}(y,z) \leq 0$ for all values of y,z except 0.

Lyapunov stability theorem

(See, (Khalil, 2009; Jleli *et al.*, 2017)). Let $\dot{Y} = f(Y)$ be any dynamical system with an equilibrium point at Y^* such that $f : D \to \mathscr{R}^n$ and let $N : D \to \mathscr{R}$ be continuous and differentiable function then the following is true (See Appendix 5.103):

(i) If $\dot{N}(y,z) \leq 0$ for all value of y,z except 0 then the equilibrium point Y^* is Lyapunov stable.

(ii) If $\dot{N}(y,z) < 0$ for all value of y,z except 0 then the point Y^* is asymptotically stable .

(iii) $\dot{N}(y,z) > 0$ for all values of y,z except 0 then the point Y^* is unstable.

Optimal control problem

(See, (LaSalle *et al.*, 1960; Lee, 1967)), suppose $\dot{z(t)} = f(z,\mu,t)$ is any system $y(t) \in \Re^n$ and control $\mu(t) \in \mu\Re^m$ where μ is convex and compact in $\Re^m$, in this case the optimal control problem is defined as follows in (5.3) (See Appendix 5.73):

$$J(z_0) = M(z(t),T) + \int_0^T L(z(t),\mu(t),t)dt, \tag{5.3}$$

whereby $[0,T]$ is the finite time interval, $M(z(T),T)$ is the terminal state and $L(z(t),\mu(t),t)$ is any constant called weight balance, with aim of transferring the integral into monitory quantity.

Hamiltonian function

(See, (Blaszak, 2012; Kalman, 1963; Todorov, 2006)), The function $H(t,y(t),\nu(t),\lambda(t))$ defined in (5.4) (See Appendix 5.77):

$$(t,z(t),\nu(t),\lambda(t)) = f(t,z(t),\nu(t),\lambda(t)) + \lambda(t)g(t,z(t),\nu(t)), \tag{5.4}$$

which satisfy the following Euler-Langragian equations (5.5) (See Appendix 5.89):

$$\frac{\partial z}{\partial t} = \frac{\partial H}{\partial z}, \qquad \frac{\partial \lambda}{\partial t} = -\frac{\partial H}{\partial z}, \qquad \frac{\partial H}{\partial \nu} = 0. \tag{5.5}$$

is called Hamiltonian function whereby $\lambda(t)$ is adjoin function.

Existence and uniqueness theorem

Consider the dynamical system $\dot{y} = g(t,x)$, such that $y(t_0) = a$, this problem has a unique solution $y(t)$ for $a \leq t \leq b$ if and only if $g(t,y)$ is continuous on the domain $\Re = \{a \leq t \leq b, \quad \infty \leq t \leq \infty\}$ and satisfies the following condition (5.6), (See Appendix 5.25):

$$|g(t,y) - g(t,y^*)| \leq K|y - y^*|, \tag{5.6}$$

for which $(y,t),(t,y^*) \in \Re$ (see, (Chen, 2010; Gao, 2012; Faizullah, 2017; Wei, 2013)). On the other hand, the condition $|g(t,y) - g(t,y^*)| \leq K|y - y^*|$ is called Lipschitz condition and the constant K is Lipschitz constant.

Definitions of the Caputo fractional calculus

Definition 5.3

Suppose that $\alpha > 0, t > a, \alpha, a, t \in \mathbb{R}$, the Caputo fractional derivative of order $\alpha \in (0,1]$ is given by the following equation (5.7) (Vargas-De-León, 2015; Caputo, 1967; Diethelm, 2010):

$$ {}_a^c D_t^\alpha f(t) \frac{1}{\Gamma(n-\alpha)} \int_a^t \frac{f^n(\xi)}{(t-\xi)^{\alpha+1-n}} d\xi, \quad n-1 < \alpha, n \in \mathbb{N}. \tag{5.7} $$

Definition 5.4

Consider (Linearity property) $g(t), h(t) : [a,b] \to \mathbb{R}$ such that ${}_a^c D_t^\alpha g(t)$ and ${}_a^c D_t^\alpha h(t)$ are both exist everywhere and let $c_1, c_2 \in \mathbb{R}$ Then, ${}_a^c D_t^\alpha (c_1 g(t)) + {}_a^c D_t^\alpha (c_2 h(t))$ exists everywhere and the following equation (5.8) is true (Vargas-De-León, 2015):

$$ {}_a^c D_t^\alpha (c_1 g(t) + c_2 h(t)) = c_1 \, {}_a^c D_t^\alpha g(t) + c_2 \, {}_a^c D_t^\alpha h(t). \tag{5.8} $$

Definition 5.5

The Caputo fractional order derivative of any constant function $g(t) = k$ is zero as shown in (5.9) (Podlubny, 1999), that is:

$$ {}_a^c D_t^\alpha k = 0. \tag{5.9} $$

Definition 5.6

The Caputo derivative of fractional order $\alpha \in (0,1]$ for any dynamical system is given by the following equation (5.10) (Podlubny *et al.*, 1997; Aguila-Camacho *et al.*, 2014):

$$ {}_{t_0}^c D_t^\alpha y(t) = g(t, y(t)), \qquad \alpha \in (0,1) \tag{5.10} $$

where by $y_0 = y(t_0)$.

Definition 5.7

The Caputo fractional dynamic system (5.10) has an equilibrium point x^* if and only if, $f(t, x^*) = 0$ (see (Vargas-De-León, 2015)).

Theorem 5.8

(Uniform Asymptotic Stability), Let y^* be an equilibrium point for the non-autonomous fractional-order differential equation (5.10) and $\Omega \subset \mathbb{R}^n$ be a domain containing y^* as shown in (5.11) and (5.12). Let $M : [0, \infty) \times \Omega \to \mathbb{R}$ be a continuously differentiable function (Vargas-

De-León, 2015; Diethelm, 2010)) such that:

$$N_1(y) \leq M(t, y(t)) \leq N_2(y) \tag{5.11}$$

and

$${}_a^c D_t^{\alpha} M(t, y(t)) \leq -N_3(y) \tag{5.12}$$

for every $\alpha \in (0,1)$ and every $y \in \Omega$, for $N_1(y)$, $N_2(y)$ and $N_3(y)$ are continuous non-negative definite functions on Ω. Thus, the equilibrium point of system (5.10) is uniformly asymptotically stable.

Definition 5.8

Let $x(\cdot)$ be any function which is differentiable and continuous with condition that $x(t) \in \mathbb{R}_+$. Then, the Volterra-type Lyapunov function for fractional-order differential equations for the disease dynamics is given by the following expression(5.13) (See Appendix 5.109):

$${}_{t_0}^c D_t^{\alpha} \left(x(t) - x^* - x^* \ln \frac{x(t)}{x^*} \right) \leq \left(1 - \frac{x^*}{x(t)} \right) {}_{t_0}^c D_t^{\alpha} x(t), \quad x^* \in \mathbb{R}^+, \quad \forall \alpha \in (0,1). \tag{5.13}$$

Theorem 5.9

Suppose that $f(t), f'(t), ..., f^{(n-1)}(t)$ are continuous on $[t_0, \infty)$ and the exponential order and that ${}_{t_0}^c D_t^{\alpha} f(t)$ is piecewise continuous on $[t_0, \infty)$ (Liang *et al.*, 2015). Let $\alpha > 0$, $n-1 < \alpha < n \in \mathbb{N}$. Then the following equation (5.14) is true:

$$\mathscr{L}\{{}_{t_0}^c D_t^{\alpha} f(t)\} = s^{\alpha} \mathscr{F}(s) - \sum_{k=0}^{n-1} s^{\alpha-k-1} f^{(k)}(t_0) \tag{5.14}$$

where $\mathscr{F}(s) = \mathscr{L}\{f(t)\}$.

Theorem 5.10

Let $\mathbb{C}$ be the complex plane. For any $\alpha > 0$ $\beta > 0$, and $A \in \mathbb{C}^{n \times n}$, one get the following equation (5.15) (Kexue, 2011):

$$\mathscr{L}\{t^{\beta-1} E_{\alpha,\beta}(At^{\alpha})\} = s^{\alpha-\beta}(s^{\alpha} - A)^{-1}, \tag{5.15}$$

for $\mathscr{R}s > \|A\|^{\frac{1}{\alpha}}$, where $\mathscr{R}s$ denotes the part of complex number s which real part, and $E_{\alpha,\beta}$ is called Mittag-Leffler function (Igor, 1999).

Euler method

The Euler method is used to approximate the solution of the dynamical system $\dot{y} = g(t,y)$ with $y(t_0) = a, \quad a \leq t_i \leq b$. This method is derive from Taylor series expansion of the function $y(t)$. The Taylor series expansion for the function $y(t)$ of order n at y_{i+1} as in(5.16) is given by (5.16) (Ochoche, 2007; Hairer, 2015; Allahviranloo, 2011; Griffiths, 2010):

$$\begin{aligned} y(t_{i+1}) &= y(t_i) + (t_{i+1} - t_i)\frac{dy(t_i)}{dt} + \frac{(y_{i+1} - y_i)^2}{2!}\frac{dy^2(t_i)}{dt^2} + \cdots + \frac{(t_{i+1} - t_i)^n}{n!}\frac{dy^n(t_i)}{dt} \\ &\quad + \frac{(t_{i+1} - t_i)^{n+1}}{(n+1)!}\frac{dy^{n+1}(t_i)}{dt^{n+1}}(\xi), \end{aligned} \tag{5.16}$$

with $\xi \in (t_i, t_{i+1})$. Therefore, for $n = 1$ we have $y(t_{i+1}) = y(t_i) + h\frac{dy(t_i)}{dt} + \frac{h^2}{2}\frac{dy^2}{dt^2}(\xi)$ in which the term $\frac{h^2}{2}\frac{dy^2}{dt^2}(\xi)$ is the remainder. The Euler-method is obtained by neglecting the remainder theorem.

Definition 5.9

The Euler-method for dynamical system $\dot{y} = g(t,y)$ with $y(t_0) = a, \quad a \leq t_i \leq b$ is defined as follows in (5.17) (Gear, 1974; Lapidus & Seinfeld, 1971):

$$\begin{aligned} y_{i+1} &= y_i + h\dot{y}(t_i) \\ &= y_i + hg(t_i, t_{i+1}). \end{aligned} \tag{5.17}$$

Runge-Kutta methods

The Runge-Kutta Methods are used to approximate solution of initial value problems of higher-order Taylor series expansion without considering the higher-order derivatives. For the dynamical system $\dot{y} = g(t,y)$ with $y(t_0) = a, \quad a \leq t_i \leq b$, the scheme for computation is defined as follows in (5.18) (Cartwright, 1992; Zhang *et al.*, 2018; Niu *et al.*, 2014):

$$\begin{aligned} L_1 &= g(t_n, y_n), \\ L_2 &= g(t_n + k_2 h, y_n + h a_{21} L_1), \\ L_3 &= g(t_n + k_3 h, y_n + h(a_{31} L_1 + a_{32} L_2)), \\ &\vdots \\ L_s &= g(t_n + k_s h, y_n + h \sum_{j=1}^{s-1} a_{sj} L_j). \end{aligned} \tag{5.18}$$

This implies that $y_{n+1} = y_n + h\sum_{j=1}^{s} b_i L_i$ for which ki, a_{ij} and b_i are arbitrary constants. Therefore the Runge-Kutta Method of order 4 for approximating the initial value problem $\dot{y} = g(t,y)$

with $y(t_0) = a, \quad a \leq t_i \leq b$ is defined in (5.19) and (5.20) (Mehdi & Kareem, 2017):

$$y_{n+1} = y_n + \frac{h}{6}(L_1 + 2L_2 + 2L_3 + L_4), \tag{5.19}$$

with:

$$\begin{aligned} L_1 &= g(t_n, y_n), \\ L_2 &= g(t_n + \frac{h}{2}, y_n + \frac{h}{2}L_1), \\ L_3 &= g(t_n + \frac{h}{2}, y_n + \frac{h}{2}L_2), \\ L_4 &= g(t_n + h, y_n + hL_3). \end{aligned} \tag{5.20}$$

Appendix 2: Model with educational campaigns

Positivity and boundedness of model solutions

Since model (3.6) monitors human, animal and vector population it was essential to investigate its biological and mathematical feasibility and this was done in Theorem 3.1.

Theorem 5.11
Assuming that the initial conditions of model (3.6) are non-negative, then the system of equations for model (3.6) has a unique solution that exists and remains in the domain Ω (5.21) for all time $t \geq 0$:

$$\Omega = \left\{ \left(s_h, i_h, i_a, r_a, i_v \right) \in \mathbb{R}^5_+ \left| \begin{array}{l} s_h \geq 0,\ i_h \geq 0,\ s_h + i_h \leq 1, \\ i_a \geq 0,\ r_a \geq 0, \\ i_a + r_a \leq 1,\ 0 \leq i_v \leq 1. \end{array} \right. \right\}. \tag{5.21}$$

Proof. The partial derivatives of the model differential equations (3.6) is continuous in ω, therefore system (3.6) has a unique solution. In this case it was showed that ω is forward-invariant. It can easily be observed from (3.6) that if $s_h = 0$, then $s_h' = \mu_h + \gamma_h(1 - i_h) \geq 0$; if $i_h = 0$, then $i_h' = \beta_{vh} i_v s_h \geq 0$; if $i_a = 0$, then $i_a' = \beta_{va} i_v (1 - r_a) \geq 0$; if $r_a = 0$, then $r_a' = \alpha_a i_a \geq 0$; and if $i_v = 0$, then $i_v' = (\beta_{hv} i_h + \beta_{av} i_a) \geq 0$. this is also true that if $s_h + i_h = 1$ then $s_h' + i_h' < 0$, if $i_a + r_a = 1$ then $i_a' + r_a' < 0$ and if $i_v = 1$ then $i_v' < 0$. This shows that no orbits can leave Ω and hence a unique solution exists for all time. □

The derivation of basic reproduction number $\mathscr{R}_0$

In the absence of the disease in the community, the disease-free equilibrium of model (3.6) was found to be denoted by $\mathscr{E}^0$ which is given by:

$$\mathscr{E}^0 : \left(s_h^0, i_h^0, i_a^0, r_a^0, i_v^0 \right) = \left(\frac{(\mu_h + \gamma_h)}{(\mu_h + \theta_h + \gamma_h)}, 0, 0, 0, 0 \right). \tag{5.22}$$

Following the next-generation matrix method proposed in Van den Driessche (2002) the basic reproduction is computed after one identifies matrices $\mathscr{F}$ (that denotes the generation of new infection) and $\mathscr{V}$ (non-singular matrix $\mathscr{V}$ that denotes the disease transfer among compartments). To determine the matrix $\mathscr{F}$ and $\mathscr{V}$, equations of model (3.6) that model infected species were considered and evaluated using the disease-free equilibrium (5.22) and the following outcomes

were obtained:

$$\mathscr{F} = \begin{pmatrix} 0 & 0 & \frac{\beta_{vh}(\mu_h+\gamma_h)}{(\mu_h+\gamma_h+\theta_h)} \\ 0 & 0 & \beta_{va} \\ \beta_{hv} & \beta_{av} & 0 \end{pmatrix} \quad \text{and} \quad \mathscr{V} = \begin{pmatrix} \mu_h+\alpha_h+d_h & 0 & 0 \\ 0 & \mu_a+\alpha_a+d_a & 0 \\ 0 & 0 & \mu_v \end{pmatrix}. \tag{5.23}$$

From (5.23) it follows that the spectral radius of model (3.5), that is, $\rho(\mathscr{F}\mathscr{V}^{-1})$, and is given by:

$$\begin{aligned} \mathscr{R}_0 &= \sqrt{\left(\frac{\beta_{vh}\beta_{vh}(\mu_h+\gamma_h)}{(\mu_h+\alpha_h+d_h)(\mu_h+\gamma_h+\theta_h)\mu_v}\right)+\left(\frac{\beta_{av}\beta_{va}}{\mu_v(\mu_a+\alpha_a+d_a)}\right)} \\ &= \sqrt{\mathscr{R}_{0h}+\mathscr{R}_{0a}}. \end{aligned} \tag{5.24}$$

where $\mathscr{R}_{0h}$ represents the secondary cases of infection generated from human-vector interaction and $\mathscr{R}_{0a}$ is the secondary cases of infection from animal-vector interaction. For the vector borne diseases, the generation of secondary cases require two transmission process, therefore the $\mathscr{R}_0$ computed using the next generation method give number of new infections per generation process (hence the square root).

Existence and uniqueness of the endemic equilibria

Suppose $\mathscr{E}^* = (s_h^*, i_h^*, i_a^*, r_a^*, i_v^*)$ is the endemic equilibrium point of the system (3.6). Therefore, by solving the first four equations of the system (3.6) expressed inform of i_v^* as follows:

$$\left.\begin{aligned} s_h^* &= \tfrac{m_2 m_3}{m_2(m_1+\gamma_h)+\beta_{vh}i_v^*(m_2+\gamma_h)}, \qquad i_h^* = \tfrac{\beta_{vh}i_v^* m_3}{m_2(m_1+\gamma_h)+\beta_{vh}i_v^*(m_2+\gamma_h)}, \\ i_a^* &= \tfrac{\beta_{va}i_v^* m_5}{m_4 m_5+\beta_{va}i_v^*(\alpha_a+m_5)}, \qquad r_a^* = \tfrac{\beta_{va}i_v^*\alpha_a}{m_4 m_5+\beta_{va}i_v^*(\alpha_a+m_5)}, \end{aligned}\right\}. \tag{5.25}$$

with:

$$\begin{aligned} m_1 &= (\mu_h+\theta_h), \qquad m_2 = (\mu+\alpha_h+d_h), \qquad m_3 = (\mu_h+\gamma_h), \\ m_4 &= (\mu_a+\alpha_a+d_a), \qquad m_5 = (\mu_a+\gamma_a), \qquad m_6 = \mu_v. \end{aligned} \tag{5.26}$$

Substituting i_h^* and i_a^* from (5.25) into the last equation of the system (3.6) one gets the following:

$$g(i_v^*) = A(i_v^*)^2 + Bi_v^* + C = 0, \tag{5.27}$$

with:

$$\begin{aligned}
A &= \beta_{vh}\beta_{va}[m_2(\alpha_a m_6 + m_5(m_6+\beta_{av})) + \beta_{hv}m_3(\alpha_a+m_5) + \gamma_h(\alpha_a m_6 + m_5(m_6+\beta_{av}))],\\
B &= \beta_{va}(m_1 m_2(m_6\alpha_a + m_5(m_6+\beta_{av})) - \beta_{vh}\beta_{hv}m_3(\beta_{va}(\alpha_a+m_5) - m_4 m_5)\\
&\quad -\beta_{vh}m_5\gamma_h(\beta_{av}\beta_{va} - m_4 m_6) + m_2(m_4 m_5 m_6\beta_{vh} + \beta_{va}(m_6\alpha_a\gamma_h\\
&\quad +m_5(m_6\gamma_h + \beta_{av}(\gamma_h - \beta_{vh})))) - \beta_{vh}(\beta_{hv}+\beta_{av})))] + \alpha_h m_4 m_3\beta_{vh}\mu_v - \beta_{va}\beta_{av}),\\
C &= m_2 m_4 m_5 m_6(m_1+\gamma_h)(1-\mathscr{R}_0^2). \qquad (5.28)
\end{aligned}$$

Based on the fact that all parameters in (3.6) are positive for $t \geq 0$, it follows from (5.27) that $A > 0$. Furthermore, $C > 0$ when $\mathscr{R}_0 < 1$. Therefore, the number of possible positive real roots the polynomial (5.27) depends on the signs of B and C. By applying the Descartes rule of signs on the quadratic equation $g(i_v^*) = 0$, given in (5.27), I present a list of various possibilities for the roots of $g(i_v^*)$ in Table 7.

Table 7: The possibility of non-negative real roots of $g(i_v^*)$ given in (5.27) for $\mathscr{R}_0 < 1$ and $\mathscr{R}_0 > 1$.

Case	A	B	C	Basic reproduction number, $\mathscr{R}_0$	No. of sign changes	No. of possible positive real roots
1	+	+	+	$\mathscr{R}_0 < 1$	0	0
2	+	+	-	$\mathscr{R}_0 > 1$	1	1
3	+	-	+	$\mathscr{R}_0 < 1$	2	0,2
4	+	-	-	$\mathscr{R}_0 > 1$	1	1

Outcomes from Table 7 are summarized in Theorem 5.12.

Theorem 5.12
The model (3.6) admits:

(i) a unique endemic equilibrium $\mathscr{E}^*$ if $\mathscr{R}_0 > 1$ and part 2 and 4 are both holds,

(ii) more than one endemic equilibrium if $\mathscr{R}_0 < 1$ and part 1 and case of part 3 satisfied,

(iii) no endemic equilibrium if $\mathscr{R}_0 < 1$, and part 1 and case of part 3 are holds.

Existence and uniqueness results on the optimal control problem

Theorem 5.13 states the existence of the solution of the system (3.9) as well as their non-negativity and boundedness.

Theorem 5.13

There exists an optimal control pair $(u_1^*, u_2^*) \in U$ with corresponding positive states $(s_h^*, i_h^*, I_a^*, r_a^*, i_v^*)$ such that the objective functional $J(u_1, u_2)$ is minimum.

Proof. Since our control functions and the state variables are both bounded and positive on the finite interval $[0, t_f]$, therefore a minimum sequence (u_1^n, u_2^n) exists such that:

$$\lim_{n\to\infty} J(u_1^n, u_2^n) = \inf_{(u_1,u_2)\in U} J(u_1, u_2). \tag{5.29}$$

Let $(s_h, i_h, i_a, r_a, i_v)$ be the state variables corresponding to the sequence. Since the state variables and control functions are both bounded, then the first derivative of all the state variables are also bounded. It follows that the Lipschitz conditions with its constant holds for all state variables. In this case, the sequence $(s_h, i_h, i_a, r_a, i_v)$ is uniformly continuous in $[0, t_f]$. By the Arzela–Ascoli Theorem (Lukes, D. L., 1982), it implies that the state sequence has a subsequence that converges uniformly to $(s_h, i_h, i_a, r_a, i_v)$ in $[0, t_f]$.

In addition, it was demonstrated that the control sequence $u^n = (u_1^n, u_2^n)$ has a subsequence that converges weakly in $L^2(0, t_f)$. Let $(u_1^*, u_2^*) \in U$ be such that $u_i^n \rightharpoonup u_i^*$ weakly in $L^2(0, t_f)$ for $i = 1, 2$. Using the lower semi-continuity of norms in weak L^2, one get the following:

$$\|u_i^*\|_{L^2}^2 \leq \liminf_{n\to\infty} \|u_i^n\|_{L^2}^2, \qquad \text{for} \quad i = 1, 2. \tag{5.30}$$

Hence:

$$\begin{aligned} J(u_1^*, u_2^*) &\leq \lim_{n\to\infty} \int_0^{t_f} \left(c_1 i_h^n(t) + c_2 i_a^n(t) + \frac{w_1}{2} u_1^n(t) + \frac{w_2}{2} u_2^n(t) \right) dt \\ &= \lim_{n\to\infty} J(u_1^n, u_2^n). \end{aligned} \tag{5.31}$$

Therefore, it was concluded that there exists a pair of controls (u_1^*, u_2^*) that minimizes the objective functional $J(u_1, u_2)$. □

By utilizing the results from Lukes (1982) existence and uniqueness of solutions for the state system (3.9) with a given control pair can easily be verified. Since there exists an optimal control from appendix 1, the Pontryagin's Maximum Principle (Pontryagin, 2018*a*) was used to further analyze the optimal control problem. Thus, the optimal control system (3.9) was converted into an equivalent problem of minimizing the Hamiltonian $H(t)$:

$$\begin{aligned} H(t) &= c_1 i_h(t) + c_2 i_a(t) + \frac{w_1}{2} u_1^2(t) + \frac{w_2}{2} u_2^2(t) \\ &\quad + \lambda_1 \Big[\mu_h - \beta_{vh} i_v s_h - (\mu_h + u_1(t)\theta_h) s_h + \gamma_h (1 - s_h - i_h) \Big] \\ &\quad + \lambda_2 \Big[\beta_{vh} i_v s_h - (\mu_h + \alpha_h + d_h) i_h \Big] \end{aligned}$$

$$
\begin{aligned}
&+\lambda_3\Big[\beta_{va}i_v(1-i_a-r_a)-(\mu_a+\alpha_a+d_a)i_a\Big]\\
&+\lambda_4\Big[\alpha_a i_a-(\mu_a+\gamma_a)r_a\Big]\\
&+\lambda_5\Big[(\beta_{hv}i_h+\beta_{av}i_a)(1-i_v)-(\mu_v+u_2(t)\delta_v)i_v\Big].
\end{aligned}
\tag{5.32}
$$

From (5.32) $\lambda_1(t)$, $\lambda_2(t)$,$\lambda_3(t)$,$\lambda_4(t)$, and $\lambda_5(t)$, denote the adjoint functions associated with the states s_h, i_h, i_a, r_a, respectively. Note that, in H, each adjoint function multiplies the right-hand side of the differential equation of its corresponding state function. The first term in H comes from the integrand of the objective functional.

Given an optimal control pair $u=(u_1,u_2)\in U$ and corresponding states (s_h, i_h, i_a, r_a), there exist adjoint functions $\lambda_1(t)$, $\lambda_2(t)$,$\lambda_3(t)$,$\lambda_4(t)$, and $\lambda_5(t)$ (Lenhart, 2007) satisfying (5.33):

$$
\left.
\begin{aligned}
\tfrac{d\lambda_1(t)}{dt} &= -\tfrac{dH}{ds_h}\\
&= \lambda_1(\mu_h+u_1(t)\theta_h+\gamma_h+\beta_{vh}i_v)-\lambda_2\beta_{vh}i_v,\\
\tfrac{d\lambda_2(t)}{dt} &= -\tfrac{dH}{di_h}\\
&= -c_1+\lambda_1\gamma_h+\lambda_2(\mu_h+\alpha_h+d_h)-\lambda_5\beta_{hv}(1-i_h),\\
\tfrac{d\lambda_3(t)}{dt} &= -\tfrac{dH}{di_a}\\
&= -c_2+\lambda_3(\mu_a+\alpha_a+d_a+\beta_{va}i_v)-\lambda_4\alpha_a-\lambda_5\beta_{av}(1-i_v),\\
\tfrac{d\lambda_4(t)}{dt} &= -\tfrac{dH}{dr_a}\\
&= \lambda_3\beta_{va}i_v+\lambda_4(\mu_a+\gamma_a),\\
\tfrac{d\lambda_5(t)}{dt} &= -\tfrac{dH}{di_v}\\
&= (\lambda_1-\lambda_2)\beta_{vh}-\lambda_3\beta_{va}(1-i_a-r_a)+\lambda_5(\mu_v+u_2(t)\delta+\beta_{hv}i_h+\beta_{av}i_a).
\end{aligned}
\right\}
\tag{5.33}
$$

with transversality conditions $\lambda_j(t_f)=0$ for $j=1,2,3,4,5$. Moreover, the optimal solutions of the Hamiltonian were determined by taking the partial derivatives of the function $H(t)$ in (5.32) with respect to control functions u_1, and u_2, followed by setting the resultant equation to zero and then solve for u_1 and u_2, as follows:

$$
\frac{\partial H}{\partial u_1} = u_1w_1-\lambda_1\theta_h s_h, \tag{5.34}
$$

$$
\frac{\partial H}{\partial u_2} = u_2w_2-\lambda_5\delta_v i_v. \tag{5.35}
$$

Setting (5.34) and (5.35) to zero and solve for u_1 and u_2 leading to (5.36):

$$
u_1=\frac{\theta_h s_h\lambda_1}{w_1}, \qquad u_2=\frac{\delta_v i_v\lambda_5}{w_2}. \tag{5.36}
$$

Thus:

$$u_1 = \min\left\{q_1, \max\left(0, \frac{\theta_h s_h \lambda_1}{w_1}\right)\right\}, \;\; u_2 = \min\left\{q_2, \max\left(0, \frac{\delta_v i_v \lambda_5}{w_2}\right)\right\}. \tag{5.37}$$

Note that (5.37) follows from the standard arguments on bounds of controls (Lenhart, 2007).

Appendix 3: Model with seasonality

Positivity and boundedness of solutions

Theorem 5.14

The solutions $(S_h(t),\ E_h(t),\ I_h(t),\ R_h(t),\ S_a(t),\ E_a(t),\ I_a(t),\ R_a(t),\ S_v(t),\ E_v(t),\ I_v(t))$ of the model (3.18) are uniformly and ultimately bounded in

$$\Omega = \left\{ \begin{pmatrix} S_h(t)+E_h(t)+I_h(t)+R_h(t) \\ S_a(t)+E_a(t)+I_a(t)+R_a(t) \\ S_v(t)+E_v(t)+I_v(t) \end{pmatrix} \in \mathbb{R}_+^{11} \middle| \begin{array}{l} N_h(t) \leq N_{h0}, \\ N_a(t) \leq N_{a0}, \\ N_v(t) \leq N_{v0} \end{array} \right\}, \tag{5.38}$$

with $N_h(0) = N_{h0}$, $N_a(0) = N_{a0}$ and $N_v(0) = N_{v0}$.

Proof. For the *Trypanosoma brucei rhodesiense* model (3.18) to be epidemiologically meaningful, it is important to demonstrate that all its state variables are non-negative for all $t \geq 0$. In other words, one needs to show that solutions of system (3.18) with non-negative initial data will remain non-negative for all $t \geq 0$. Let the initial data $S_i(0) \geq 0$, $E_i(0) \geq 0$, $I_i(0) \geq 0$, $R_i(0) \geq 0$, for $i = a, h$, and $S_v(0) \geq 0$, $E_v(0) \geq 0$, and $I_v(0) \geq 0$, such that from the second equation of model (3.18) one gets

$$E_h(t) = e^{-(\mu_h+\kappa_h)t}\left(E_h(0) + \int_0^t \lambda_h(s)S_h(s)ds\right), \qquad t \geq 0. \tag{5.39}$$

Thus, $E_h(t) \geq 0$ for all $t \geq 0$. A similar approach can be utilized to show that all the other variables of model (3.18) are positive for all $t \geq 0$. In what follows, the feasible region of model (3.18) was determined. It can easily be verified that rate of change of the total host populations N_i, $(i = a, h)$ is

$$N_i'(t) = (b_i - \mu_i)N_i(t) - d_iI_i(t) \leq (b_i - \mu_i)N_i(t), \qquad \text{where} \qquad \mu_i \leq b_i. \tag{5.40}$$

As suggested by Moore *et al.* (2012*b*) the following condition was set $b_i = \mu_i$, otherwise the population will grow without bound or become extinct. Therefore, $N_i(t) \leq N_i(0)$. Similarly, by adding all the last three equations of model (3.18), and setting $b_v(t) = \mu_v(t)$ as in (Moore *et al.*, 2012*b*), one gets $N(t) \leq N_{v0}$. Thus, the feasible region for model (3.18) was obtained as follows:

$$\Omega = \left\{ \begin{pmatrix} S_h(t)+E_h(t)+I_h(t)+R_h(t) \\ S_a(t)+E_a(t)+I_a(t)+R_a(t) \\ S_v(t)+E_v(t)+I_v(t) \end{pmatrix} \in \mathbb{R}_+^{11} \middle| \begin{array}{l} N_h(t) \leq N_{h0}, \\ N_a(t) \leq N_{a0}, \\ N_v(t) \leq N_{v0} \end{array} \right\}, \tag{5.41}$$

with $N_h(0) = N_{h0}$, $N_a(0) = N_{a0}$ and $N_v(0) = N_{v0}$. Based on the analysis above, it was concluded that the proposed model is epidemiologically and mathematically well-posed in the domain Ω. This completes the proof of Theorem. □

Extinction and uniform persistence of the disease

Having determined the positivity and boundedness of solutions of model (3.18), the next step was to determine the $\mathscr{R}_0$. Following the next generation method proposed in (Van den Driessche, 2002). In the absence of infection it was found that model (3.18) admits an infection-free equilibrium given by $\mathscr{E}^0 : (S_h^0, E_h^0, I_h^0, R_h^0, S_a^0, E_a^0, I_a^0, R_a^0, S_v^0, E_v^0, I_v^0) = (N_{h0}, 0, 0, 0, 0, N_{a0}, 0, 0, 0, N_{v0}, 0, 0)$.

In the model (3.18) the infected compartments are $(E_j(t), I_j(t))$ classes, for $j = h, a, v$. Using the next-generation matrix method, the positive matrix $F(t)$ of the infection terms and the non-singular matrix, $V(t)$ of the transfer terms evaluated at $\mathscr{E}^0$ were obtained as follows:

$$F(t) = \begin{bmatrix} 0 & 0 & 0 & 0 & 0 & \frac{\sigma_v(t)\sigma_h\beta_{vh}N_{h0}}{\sigma_v(t)N_v(t)+\sigma_hN_{h0}} \\ 0 & 0 & 0 & 0 & 0 & 0 \\ 0 & 0 & 0 & 0 & 0 & \frac{\sigma_v(t)\sigma_a\beta_{va}N_{a0}}{\sigma_v(t)N_v(t)+\sigma_aN_{a0}} \\ 0 & 0 & 0 & 0 & 0 & 0 \\ 0 & \frac{\sigma_h\sigma_v(t)\beta_{hv}N_v(t)}{\sigma_v(t)N_v(t)+\sigma_hN_{h0}} & 0 & \frac{\sigma_a\sigma_v(t)\beta_{va}N_v(t)}{\sigma_v(t)N_v(t)+\sigma_aN_{a0}} & 0 & 0 \\ 0 & 0 & 0 & 0 & 0 & 0 \end{bmatrix}, \quad (5.42)$$

and

$$V(t) = \begin{bmatrix} \kappa_h+\mu_h & 0 & 0 & 0 & 0 & 0 \\ -\kappa_h & m_1 & 0 & 0 & 0 & 0 \\ 0 & 0 & \kappa_a+\mu_a & 0 & 0 & 0 \\ 0 & 0 & -\kappa_a & m_2 & 0 & 0 \\ 0 & 0 & 0 & 0 & \kappa_v(t)+\mu_v(t) & 0 \\ 0 & 0 & 0 & 0 & -\kappa_v(t) & \mu_v(t) \end{bmatrix}, \quad (5.43)$$

with:

$$m_1 = (\mu_h+\alpha_h+d_h), \qquad m_2 = (\mu_a+\alpha_a+d_a). \quad (5.44)$$

Upon evaluating (5.43) the spectral radius of model (3.18) was obtained as:

$$[\mathscr{R}_0] = \sqrt{\mathscr{R}_{0h}+\mathscr{R}_{0a}}. \quad (5.45)$$

where:

$$\begin{aligned}
\mathscr{R}_{0h} &= \left(\frac{\kappa_h\beta_{vh}N_{h0}\kappa_{v0}\beta_{hv}N_{v0}}{\mu_{v0}(\kappa_{v0}+\mu_{v0})(\kappa_h+\mu_h)(\mu_h+\alpha_h+d_h)}\right)\left(\frac{\sigma_h\sigma_{v0}}{\sigma_{v0}N_{v0}+\sigma_hN_{h0}}\right)^2,\\
\mathscr{R}_{0a} &= \left(\frac{\kappa_a\beta_{va}N_{a0}\kappa_{v0}\beta_{av}N_{v0}}{\mu_{v0}(\kappa_{v0}+\mu_{v0})(\kappa_a+\mu_a)(\mu_a+\alpha_a+d_a)}\right)\left(\frac{\sigma_a\sigma_{v0}}{\sigma_{v0}N_{v0}+\sigma_aN_{a0}}\right)^2. \qquad (5.46)
\end{aligned}$$

Making use of the result in the work of work of Wang and Zhao Wang (2008), the $\mathscr{R}_0$ of the non-autonomous model (3.18) was determined. In particular, Wang (2008) in their computation of the $\mathscr{R}_0$ for a non-autonomous model proposed next-infection operator L as follows:

$$(L\phi)(t) = \int_0^\infty Y(t,t-s)F(t-s)\phi(t-s)ds \qquad (5.47)$$

where $Y(t,s),\ t \geq s$, represent the evolution operator of the linear ω-periodic system $\frac{dy}{dt} = -V(t)y$ and $\phi(t)$, is the function known as the initial distribution of infected host, is ω-periodic which is non-negative. By evaluating (5.47) the spectral radius of the non-autonomous model (3.18) was found to be:

$$\mathscr{R}_0 = \rho(L). \qquad (5.48)$$

To explicitly present (5.48), I solved the system of differential equations $\frac{dy}{dt} = -V(t)y$ using the initial condition $Y(s,s) = I_{6\times 6}$ to determine the evolution operator and the following results were obtained:

$$Y(t,s) = \begin{bmatrix}
y_{11}(t,s) & 0 & 0 & 0 & 0 & 0\\
y_{21}(t,s) & y_{22}(t,s) & 0 & 0 & 0 & 0\\
0 & 0 & y_{33}(t,s) & 0 & 0 & 0\\
0 & 0 & y_{43}(t,s) & y_{44}(t,s) & 0 & 0\\
0 & 0 & 0 & 0 & y_{55}(t,s) & 0\\
0 & 0 & 0 & 0 & y_{65}(t,s) & e^{-\mu_v(t-s)}
\end{bmatrix}. \qquad (5.49)$$

where:

$$\begin{aligned}
y_{11}(t,s) &= e^{-(\mu_h+\kappa_h)(t-s)},\\
y_{21}(t,s) &= \frac{\kappa_h}{d_h+\alpha_h-\kappa_h}\left(e^{-(\mu_h+\kappa_h)(t-s)} - e^{-(\mu_h+d_h+\alpha_h)(t-s)}\right),\\
y_{22}(t,s) &= e^{-(\mu_h+d_h+\alpha_h)(t-s)},\\
y_{33}(t,s) &= e^{-(\mu_a+\gamma_a)(t-s)},
\end{aligned}$$

$$
\begin{aligned}
y_{43}(t,s) &= \frac{\kappa_a}{d_a+\alpha_a-\kappa_a}\left(e^{-(\mu_a+\gamma_a)(t-s)}-e^{-(\mu_a+d_a+\alpha_a)(t-s)}\right),\\
y_{44}(t,s) &= e^{-(\mu_a+d_a+\alpha_a)(t-s)},\\
y_{44}(t,s) &= e^{-(\mu_a+d_a+\alpha_a)(t-s)},\\
y_{55}(t,s) &= \exp-\left\{\kappa_{vo}(t-s)+\frac{2\kappa_{v0}\kappa_{v1}}{\omega}\cos\left(\frac{\omega}{2}(t+\tau+s)\right)\sin\left(\frac{\omega}{2}(t+\tau-s)\right)\right.\\
&\quad \left.+\mu_{vo}(t-s)+\frac{2\mu_{v0}\mu_{v1}}{\omega}\cos\left(\frac{\omega}{2}(t+\tau+s)\right)\sin\left(\frac{\omega}{2}(t-s)\right)\right\},\\
y_{65}(t,s) &= \left(e^{-\int_0^t\mu_v(s)ds}\right)\int_s^t e^{\mu_v(x)}\kappa_v(x)y_{55}(x,s)dx,\\
y_{66}(t,s) &= \exp-\left\{\mu_{vo}(t-s)+\frac{2\mu_{v0}\mu_{v1}}{\omega}\cos\left(\frac{\omega}{2}(t+\tau+s)\right)\right.\\
&\quad \left.\times\sin\left(\frac{\omega}{2}(t+\tau-s)\right)\right\}.
\end{aligned}
\tag{5.50}
$$

Based on results in Wang (2008) Lemma 5.1 was proposed.

Lemma 5.1

Theorem 2.2 in Wang and Zhao Wang (2008). Let $x(t)=(E_i(t),I_i(t))$, $i=a,h,v$, denote the infected vector species of all states of the system (3.18), such that the linearization of system (3.18) at disease-free equilibrium $\mathscr{E}^0$ is

$$\dot{x}(t)=(F(t)-V(t))x(t), \tag{5.51}$$

where $F(t)$ and $V(t)$ are defined earlier on equation (5.43). Furthermore, let $\Phi_{F-V(t)}$ and $\rho(\Phi_{F-V(\omega)}$ be the monodromy matrices of the variable system (5.51) and the spectral radius of $\Phi_{F-V(t)}(\omega)$, respectively, then the following statements are valid:

(i) $\mathscr{R}_0=1$, if and only if $\rho(\Phi_{F-V}(\omega))=1$;

(ii) $\mathscr{R}_0>1$, if and only if $\rho(\Phi_{F-V}(\omega))>1$;

(iii) $\mathscr{R}_0<1$, if and only if $\rho(\Phi_{F-V}(\omega))<1$.

Thus, the disease-free equilibrium $\mathscr{E}^0$ of system (3.18) is locally asymptotically stable if $\mathscr{R}_0<1$ and unstable if $\mathscr{R}_0>1$.

Using Lemma 5.1 exticntion and persistence of the disease in a periodic environment was considered.

Theorem 5.15

For the model system (3.18), the its disease-free equilibrium $\mathscr{E}^0$ is globally asymptotically stable in Ω If $\mathscr{R}_0 < 1$.

Proof. According to Lemma 5.1, if $\mathscr{R}_0 < 1$, then the disease-free equilibrium $\mathscr{E}^0$ of system (3.18) is locally asymptotically stable. Hence, it was necessary to demonstrate for $\mathscr{R}_0 < 1$, the disease-free equilibrium is a global attractor. Assuming that $\mathscr{R}_0 < 1$, it follows that $\rho(\Phi_{F-V}(\omega)) < 1$. From the second, third, sixth, seventh, tenth and eleventh equations of model (3.18) the following results were obtained:

$$\left.\begin{array}{rcl}
\dot{E}_h(t) &\leq& \left(\frac{\sigma_v(t)\sigma_h\beta_{vh}I_v}{\sigma_v(t)N_v(t)+\sigma_hN_h}\right)S_h^0-(\mu_h+\kappa_h)E_h,\\
\dot{I}_h(t) &=& \kappa_hE_h-(\mu_h+d_h+\alpha_h)I_h,\\
\dot{E}_a(t) &\leq& \left(\frac{\sigma_v(t)\sigma_a\beta_{va}I_v}{\sigma_v(t)N_v(t)+\sigma_aN_a}\right)S_a^0-(\mu_a+\kappa_a)E_a,\\
\dot{I}_a(t) &=& \kappa_aE_a-(\mu_a+d_a+\alpha_a)I_a,\\
\dot{E}_v(t) &\leq& \left(\frac{\sigma_v(t)\sigma_h\beta_{hv}I_h}{\sigma_v(t)N_v(t)+\sigma_hN_h}+\frac{\sigma_v(t)\sigma_a\beta_{va}I_a}{\sigma_v(t)N_v(t)+\sigma_aN_a}\right)S_v^0-(\kappa_v(t)+\mu_v(t))E_v,\\
\dot{I}_v(t) &=& \kappa_v(t)E_v-\mu_v(t)I_v,
\end{array}\right\} \tag{5.52}$$

for $t \geq 0$. Consider the following auxiliary system:

$$\left.\begin{array}{rcl}
\dot{\widetilde{E}}_h(t) &=& \left(\frac{\sigma_v(t)\sigma_h\beta_{vh}\widetilde{I}_v}{\sigma_v(t)\widetilde{N}_v+\sigma_h\widetilde{N}_h}\right)S_h^0-(\mu_h+\kappa_h)\widetilde{E}_h,\\
\dot{\widetilde{I}}_h(t) &=& \kappa_h\widetilde{E}_h-(\mu_h+d_h+\alpha_h)\widetilde{I}_h,\\
\dot{\widetilde{E}}_a(t) &=& \left(\frac{\sigma_v(t)\sigma_a\beta_{va}\widetilde{I}_v}{\sigma_v\widetilde{N}_v+\sigma_a\widetilde{N}_a}\right)S_a^0-(\mu_a+\kappa_a)\widetilde{E}_a,\\
\dot{\widetilde{I}}_a(t) &=& \kappa_a\widetilde{E}_a(t)-(\mu_a+d_a+\alpha_a)\widetilde{I}_a(t),\\
\dot{\widetilde{E}}_v(t) &=& \left(\frac{\sigma_v(t)\sigma_h\beta_{hv}\widetilde{I}_h}{\sigma_v(t)\widetilde{N}_v(t)+\sigma_h\widetilde{N}_h}+\frac{\sigma_v(t)\sigma_a\beta_{va}\widetilde{I}_a}{\sigma_v(t)\widetilde{N}_v(t)+\sigma_a\widetilde{N}_a}\right)S_v^0-(\kappa_v(t)+\mu_v(t))\widetilde{E}_v,\\
\dot{\widetilde{I}}_v(t) &=& \kappa_v(t)\widetilde{E}_v-\mu_v(t)\widetilde{I}_v.
\end{array}\right\} \tag{5.53}$$

Following the standard comparison principle and Lemma 5.1, there exist a function $\widetilde{x}(t)$ with a positive $\omega-$periodic such that $x(t) \leq \widetilde{x}(t)e^{pt}$, where $\widetilde{x}(t) = (\widetilde{E}_i(t), \widetilde{I}_i(t))^{\mathrm{T}}$, for $i = a,h,v$, and $p = \frac{1}{\omega}\ln\rho\left(\Phi_{(F-V)(\cdot)}(\omega)\right) < 0$. Thus, we conclude that $x(t) \to 0$ as $t \to \infty$, that is,

$$\lim_{t\to\infty} E_i(t) = 0, \ \lim_{t\to\infty} I_i(t) = 0, \ \lim_{t\to\infty} R_a(t) = 0, \ \text{and} \ \lim_{t\to\infty} R_h(t) = 0, \ i = a,h,v. \tag{5.54}$$

Hence it follows that:

$$\lim_{t\to\infty} S_i(t) = S_i^0, \qquad \text{and} \qquad \lim_{t\to\infty} N_h(t) = N_i^0, \qquad i = a,h,v. \tag{5.55}$$

Therefore, the disease-free equilibrium $\mathscr{E}^0$ of the model system (3.18) is globally asymptotically stable. □

Theorem 5.16

If $R_0 > 1$, then system (3.18) is uniformly persistent, i.e., there exists a positive constant η, such that for all initial values of $(S_i(0), E_i(0), I_i(0), R_k(0))\mathbb{R}^5_+ \times \text{Int}(\mathbb{R}_+)^6$, $(i = a, h, v,\ k = a, h)$ the solution of model (3.18) satisfies:

$$\liminf_{t\to\infty} S_i(t) \geq \eta, \quad \liminf_{t\to\infty} E_i(t) \geq \eta, \quad \liminf_{t\to\infty} I_i(t) \geq \eta, \quad \liminf_{t\to\infty} R_k(t) \geq \eta. \tag{5.56}$$

Proof. Let us define

$$Y = \mathbb{R}^{11}_+; \qquad Y_0 = \mathbb{R}^5_+ \times \text{Int}(\mathbb{R}_+)^6; \qquad \partial Y_0 = Y \backslash Y_0. \tag{5.57}$$

Let $P : Y \longrightarrow Y$ be the Poincaré map corresponding to the model system (3.18) such that $P(y_0) = u(\omega, y_0)\ \forall y_0 \in Y$, where $u(t, y_0)$ represents the unique solution of the dynamical system $u(0, y_0) = y_0$.

To begin with, it was demonstrated that P is uniformly persistent with respect to $(Y_0, \partial Y_0)$. It can easily be deduced from model (3.18) that, Y and Y_0 are non-negative invariant. However, ∂Y_0 is a relatively closed set in Y. Following the Theorem 5.2.1 that solutions of model(3.18) uniformly and ultimately bounded. This show that the semiflow P is point dissipative on $\mathbb{R}^{11}_+$, and $P : \mathbb{R}^{11}_+ \to \mathbb{R}^{11}_+$ is compact. By Theorem 3.4.8 in (Zhao, 2003*b*), it shows that the the point P admits a global attractor, which attracts every bounded set in $\mathbb{R}^{11}_+$.
Define

$$\begin{aligned} M_\partial = \{&(S_i(0), E_i(0), I_i(0), R_k(0)) \in \partial Y_0 : \\ &P^m(S_i(0), E_i(0), I_i(0), R_k(0)) \in \partial Y_0,\ \forall m \geq 0\}, \end{aligned} \tag{5.58}$$

for $i = a, h, v, \quad k = a, h$.
Next, it was assumed that $M_\partial = \{(S_h(0), 0, 0, R_h(0), S_a(0), 0, 0, R_a(0), S_v(0), 0, 0) : S_i \geq 0, R_k \geq 0\}$. Clearly, $\widetilde{M} = \{(S_h(0), 0, 0, R_h(0), S_a(0), 0, 0, R_a(0), S_v(0), 0, 0) : S_i \geq 0, R_k \geq 0\} \subseteq M_\partial$.
Now, for every $(S_i(0), E_i(0), I_i(0), R_k(0)) \in \partial Y_0 \backslash M$; if $E_h(0) = I_h(0) = 0$, it follows that $S_i(0) > 0$, $R_h(0) > 0$, $E_a(0) > 0$, $I_a(0) > 0$, $R_a(0) > 0$, $E_v(0) > 0$, $I_v(0) > 0$, $\dot{E}_h(0) = \lambda_h(0) S_h(0) > 0$, and $\dot{I}_h(0) = 0$. If $E_a(0) = I_a(0) = 0$, it follows that $S_i(0) > 0$, $E_h(0) > 0$, $I_h(0) > 0$, $R_h(0) > 0$, $R_a(0) = 0$, $E_v(0) > 0$, $I_v(0) > 0$, $\dot{E}_a(0) = \lambda_a(0) S_a(0) > 0$, and $\dot{I}_a(0) = 0$. If $E_v(0) = I_v(0) = 0$, it follows that $S_i(0) > 0$, $E_h(0) = 0$, $I_h(0) = 0$, $R_h(0) > 0$, $E_a(0) = 0$, $I_a(0) = 0$, $R_a(0) = 0$, $\dot{E}_v(0) = 0$, and $\dot{I}_a(0) = 0$. Thus, we have $(S_i(0), E_i(0), I_i(0), R_k(0)) \notin \partial Y_0$ for $0 < t \ll 1$. By using the non-negative set of Y_0, this implies that $P^m(S_i(0), E_i(0), I_i(0), R_k(0)) \notin \partial Y_0$ for $m \geq 1$, hence $(S_i(0), E_i(0), I_i(0), R_k(0)) \notin M_\partial$, and thus $M_\partial = \{(S_h(0), 0, 0, R_h(0), S_a(0), 0, 0, R_a(0), S_v(0), 0, 0) : S_i \geq 0, R_k \geq 0\}$.

In what follows, it was assumed the following fixed point $M_0 = (S_h^0, 0, 0, R_h^0, S_a^0, 0, 0, 0, S_v^0, 0, 0)$ of the Poincaré map P, and defined $W^S(M_0) = \{y_0 : P^m(y_0) \to M_0, m \to \infty\}$, then the next step was to demonstrate that:

$$W^S(M_0) \cap Y_0 = \emptyset. \tag{5.59}$$

Following the solution for continuity with initial conditions, for every $\varepsilon > 0$, it was noted that there exists $\delta > 0$ with small such that for each $(S_i(0), E_i(0), I_i(0), R_k(0)) \in Y_0$ with $||(S_i(0), E_i(0), I_i(0), R_k(0)) - M_0|| \leq \delta$, thus

$$||u(t, (S_i(0), E_i(0), I_i(0), R_k(0)) - u(t, M_0)|| < \varepsilon, \quad \forall t \in [0, \omega]. \tag{5.60}$$

To obtain (5.59), the following claim was considered:

$$\limsup_{m\to\infty} ||P^m(S_i(0), E_i(0), I_i(0), R_k(0)) - M_0|| \geq \delta, \quad \forall (S_i(0), E_i(0), I_i(0), R_k(0)) \in Y_0. \tag{5.61}$$

The above claim was proved using contradiction. First it was assumed that:

$$\limsup_{m\to\infty} ||P^m(S_i(0), E_i(0), I_i(0), R_k(0)) - M_0|| < \delta, \tag{5.62}$$

for some $(S_i(0), E_i(0), I_i(0), R_k(0)) \in Y_0$. Without loss of generality, it was further assumed that: $||P^m(S_i(0), E_i(0), I_i(0), R_k(0)) - M_0|| < \delta, \ \forall m \geq 0$. Thus,

$$||u(t, P^m(S_i(0), E_i(0), I_i(0), R_k(0)) - u(t, M_0)|| < \varepsilon, \quad \forall t \in [0, \omega] \text{ and } m \geq 0. \tag{5.63}$$

Moreover, for any $t \geq 0$, one has $t = t_0 + q\omega$ with $t_0 \in [0, \omega)$ and $q = [\frac{t}{\omega}]$, the greatest integer less than or equal to $\frac{t}{\omega}$. Hence the following result was obtained:

$$\begin{aligned} ||u(t, (S_i(0), E_i(0), I_i(0), R_k(0)) - u(t, M_0)|| &= ||u(t_0, P^m(S_i(0), E_i(0), I_i(0), R_k(0)) \\ &\quad - u(t_0, M_0)|| < \varepsilon \end{aligned} \tag{5.64}$$

for any $t \geq 0$. Let $(S_i(t), E_i(t), I_i(t), R_k(t)) = u(t, (S_i(0), E_i(0), I_i(0), R_k(0))$. It follows that $N_{i0} - \varepsilon < S_i(t) < N_{i0} + \varepsilon$, $0 < E_i(t) < \varepsilon$, $0 < I_i(t) < \varepsilon$, and $0 < R_k(t) < \varepsilon$. Therefore using the second equation of the model system (3.18) one gets the following:

$$\begin{aligned} \frac{dE_h}{dt} &= \frac{\sigma_v(t)\sigma_h\beta_{vh}I_vS_h}{\sigma_v(t)N_v + \sigma_hN_h} - (\mu_h + \kappa_h)E_h, \\ &\geq \frac{\sigma_v(t)\sigma_h\beta_{vh}I_v(N_{h0} - \varepsilon)}{\sigma_v(t)(N_{v0} + \varepsilon) + \sigma_h(N_{h0} + \varepsilon)} - (\mu_h + \kappa_h)E_h, \end{aligned}$$

$$= \left(\frac{\sigma_v(t)\sigma_h\beta_{vh}N_{h0}}{\sigma_v(t)N_{v0}+\sigma_hN_{h0}}\right)\left(1-\frac{2\varepsilon\sigma_h\left(1+\frac{\sigma_v(t)}{2\sigma_h}+\frac{\sigma_v(t)N_{v0}}{2\sigma_hN_{h0}}\right)}{\sigma_v(t)\left(N_{v0}+\varepsilon\right)+\sigma_h\left(N_{h0}+\varepsilon\right)}\right)I_v$$

$$-(\mu_h+\kappa_h)E_h, \tag{5.65}$$

The seventh equation of system (3.18) has the form:

$$\dot{I}_a(t) = \kappa_aE_a-(\mu_a+\alpha_a+d_a)I_a. \tag{5.66}$$

The ninth equation of system (3.18) satisfies:

$$\begin{aligned}\frac{dE_v}{dt} &\geq \frac{\sigma_v(t)\sigma_h\beta_{hv}I_h(N_{v0}-\varepsilon)}{\sigma_v(t)(N_{v0}+\varepsilon)+\sigma_h(N_{h0}+\varepsilon)}+\frac{\sigma_v(t)\sigma_a\beta_{av}I_a(N_{v0}-\varepsilon)}{\sigma_v(t)(N_{v0}+\varepsilon)+\sigma_a(N_{a0}+\varepsilon)}\\ &\quad -(\mu_v(t)+\kappa_v(t))E_v,\\ &= +\left(\frac{\sigma_v(t)\sigma_h\beta_{hv}N_{v0}}{\sigma_v(t)N_{v0}+\sigma_hN_{h0}}\right)\left(1-\frac{2\varepsilon\sigma_v(t)\left(1+\frac{\sigma_h}{2\sigma_v(t)}+\frac{\sigma_hN_{h0}}{2\sigma_v(t)N_{v0}}\right)}{\sigma_v(t)\left(N_{v0}+\varepsilon\right)+\sigma_h\left(N_{h0}+\varepsilon\right)}\right)I_h\\ &\quad +\left(\frac{\sigma_v(t)\sigma_a\beta_{av}N_{v0}}{\sigma_v(t)N_{v0}+\sigma_aN_{a0}}\right)\left(1-\frac{2\varepsilon\sigma_v(t)\left(1+\frac{\sigma_a}{2\sigma_v(t)}+\frac{\sigma_aN_{a0}}{2\sigma_v(t)N_{v0}}\right)}{\sigma_v(t)\left(\frac{\Lambda_v}{\mu_v(t)}+\varepsilon\right)+\sigma_a\left(N_{a0}+\varepsilon\right)}\right)I_a\\ &\quad -(\mu_v(t)+\kappa_v(t))E_v(t).\end{aligned} \tag{5.67}$$

Recall that the tenth equation of system (3.18) has the form:

$$\dot{I}_v(t) = \kappa_v(t)E_v-\mu_v(t)I_v. \tag{5.68}$$

Let:

$$M_\varepsilon = \begin{bmatrix} 0 & 0 & 0 & 0 & 0 & n_1\\ 0 & 0 & 0 & 0 & 0 & 0\\ 0 & 0 & 0 & 0 & 0 & n_2\\ 0 & 0 & 0 & 0 & 0 & 0\\ 0 & n_3 & 0 & n_4 & 0 & 0\\ 0 & 0 & 0 & 0 & 0 & 0 \end{bmatrix}, \tag{5.69}$$

with:

$$\left.\begin{array}{rcl} n_1 &=& \dfrac{2\varepsilon\sigma_h\left(1+\frac{\sigma_v(t)}{2\sigma_h}+\frac{\sigma_v(t)N_{v0}}{2\sigma_h N_{h0}}\right)}{\sigma_v(t)(N_{v0}+\varepsilon)+\sigma_h(N_{h0}+\varepsilon)}, \quad n_2 = \dfrac{2\varepsilon\sigma_a\left(1+\frac{\sigma_v(t)}{2\sigma_a}+\frac{\sigma_v(t)N_{v0}}{2\sigma_a N_{a0}}\right)}{\sigma_v(t)(N_{v0}+\varepsilon)+\sigma_a(N_{a0}+\varepsilon)}, \\ n_3 &=& \dfrac{2\varepsilon\sigma_v(t)\left(1+\frac{\sigma_h}{2\sigma_v(t)}+\frac{\sigma_h N_{h0}}{2\sigma_v(t)N_{v0}}\right)}{\sigma_v(t)(N_{v0}+\varepsilon)+\sigma_h(N_{h0}+\varepsilon)}, \quad n_4 = \dfrac{2\varepsilon\sigma_v(t)\left(1+\frac{\sigma_a}{2\sigma_v(t)}+\frac{\sigma_a N_{a0}}{2\sigma_v(t)N_{v0}}\right)}{\sigma_v(t)\left(\frac{\Lambda_v}{\mu_v(t)}+\varepsilon\right)+\sigma_a(N_{a0}+\varepsilon)}, \end{array}\right\} \tag{5.70}$$

such that

$$[\dot{E}_h,\, \dot{I}_h,\, \dot{E}_a,\, \dot{I}_a,\, \dot{E}_v,\, \dot{I}_v]^{\mathrm{T}} \geq [F-V-M_\varepsilon][E_h,\, I_h,\, E_a,\, I_a,\, E_v,\, I_v]^{\mathrm{T}}. \tag{5.71}$$

Again based on (Wang, 2008, Theorem 2.2), if $\rho(\Phi_{F-V}(\omega)) > 1$, then there exists ε which is small enough such that $\rho(\Phi_{F-V-M_\varepsilon}(\omega)) > 1$. Also from the (Wang, 2008, Theorem 2.2) and the standard comparison principle, one can choose a non-negative $\omega-$ periodic function $v(t)$ such that $y(t) \geq \widetilde{y}_1(t)e^{p_1 t}$, with $\widetilde{y}_1(t) = (\widetilde{E}_i(t), \widetilde{I}_i(t))^{\mathrm{T}}$, for $i = a,h,v$, and $p_1 = \frac{1}{\omega}\ln\rho\left(\Phi_{(F-V-M_\varepsilon)}(\omega)\right) > 0$ this show that:

$$\lim_{t\to\infty} E_i(t) = \infty, \qquad \text{and} \qquad \lim_{t\to\infty} I_i(t) = \infty, \quad i = a,h,v.. \tag{5.72}$$

which is a contradiction in M_∂ since M_∂ always tend to M_0. and M_0 is cyclic in M_∂. By (Zhao, 2003*a*, Theorem 1.3.1), for a stronger repelling property of ∂Y_0, therefore it was concluded that P is uniformly persistent with respect to $(Y_0, \partial Y_0)$, which show that there exists a uniform persistence of the solutions of the model system (3.18) with respect to $(Y_0, \partial Y_0)$ (Zhao, 2003*a*, Theorem 3.1.1). Now following the Theorem 3.1.1 in (Zhao, 2003*a*) it was shown that the solution of (3.18) is uniformly persistent. □

Optimal control framework

In this section, an optimal control problem for a seasonal *T. brucei rhodesiense* model (3.22) was formulated and analyzed. The main goal being to minimize the population of infected humans at a minimal cost of implementation. The following objective functional was considered:

$$J(u_1(t), u_2(t)) = \int_0^{t_f} \left(I_h(t) + \frac{W_1}{2}u_1^2(t) + \frac{W_2}{2}u_2^2(t)\right) dt. \tag{5.73}$$

The optimal control problem becomes seeking an optimal functions, $U^* = (u_1^*(t), u_2^*(t))$, such that

$$J(u_1^*(t), u_2^*(t)) = \inf_{(u_1,u_2)\in U} J(u_1(t), u_2(t)), \tag{5.74}$$

for the admissible set $U = \{(u_1(t), u_2(t)) \in (L^\infty(0,t_f))^2 : 0 \leq u_i(t) \leq q_i; q_i \in \mathbb{R}^+, i = 1,2\}$, where q_i denotes the upper bound of the controls.
In what follows, the existence of an optimal control pair based on the work of Fleming (1976) was considered.

Theorem 5.17
There exists an optimal control U^* to the problem (3.22).

Proof. Suppose that $\mathbf{f}(t,\mathbf{x},\mathbf{u})$ be the right-hand side of the (3.22) where by $\mathbf{x} = (S_h,\ E_h,\ I_h,\ R_h,\ S_a,\ E_a,\ I_a,\ R_a,\ S_v,\ E_v,\ I_v$ and $\mathbf{u} = u_1(t)$ represent the vector of state variables and control functions respectively. The following list shows the requirements for the existence of optimal control as presented in Fleming (1976):

(i) The function $\mathbf{f}$ is of class C^1 and there exists a constant C such that $|\mathbf{f}(t,0,0)| \leq C, |\mathbf{f}_\mathbf{x}(t,\mathbf{x},\mathbf{u})| \leq C(1+|\mathbf{u}|), |\mathbf{f}_\mathbf{u}(t,\mathbf{x},\mathbf{u})| \leq C$;

(ii) the admissible set of all solutions to system (3.22) with corresponding control in Ω is nonempty;

(iii) $\mathbf{f}(t,\mathbf{x},\mathbf{u}) = \mathbf{a}(t,\mathbf{x}) + \mathbf{b}(t,\mathbf{x})\mathbf{u}$;

(iv) the control set $U = [0, u_{1\max}] \times [0, u_{2\max}]$ is closed, convex and compact;

(v) the integrand of the objective functional is convex in U.

In order ton verify these conditions we write:

$$\mathbf{f}(t,\mathbf{x},\mathbf{u}) = \begin{bmatrix} b_h N_h(t) - \lambda_h(t)S_h(t) - \mu_h S_h(t) - u_1(t)S_h(t) + \gamma_h R_h(t) \\ \lambda_h(t)S_h(t) - (\mu_h + \kappa_h)E_h(t) \\ \kappa_h E_h(t) - (\mu_h + \alpha_h + d_h)I_h(t) \\ u_1(t)S_h(t) + \alpha_h I_h(t) - (\mu_h + \gamma_h)R_h(t) \\ b_a N_a(t) - \lambda_a(t)S_a(t) - \mu_a S_a(t) + \gamma_a R_a(t) \\ \lambda_a(t)S_a(t) - (\mu_a + \kappa_a)E_a(t) \\ \kappa_a E_a(t) - (\mu_a + \alpha_a + d_a)I_a(t) \\ \alpha_a I_a(t) - (\mu_a + \gamma_a)R_a(t) \\ b_v(t)N_v(t) - \lambda_v(t)S_v(t) - (\mu_v(t) + u_2(t))S_v(t) \\ \lambda_v(t)S_v(t) - (\kappa_v(t) + \mu_v(t) + u_2(t)))E_v(t) \\ \kappa_v(t)E_v(t) - (\mu_v(t) + u_2(t))I_v(t) \end{bmatrix}. \tag{5.75}$$

From (5.75), it was observed that $\mathbf{f}(t,\mathbf{x},\mathbf{u})$ is of class C^1 and $|\mathbf{f}(t,\mathbf{0},\mathbf{0})| = 0$. In addition, it can easily be verified that $|\mathbf{f}_\mathbf{x}(t,\mathbf{x},\mathbf{u})|$ and $|\mathbf{f}_\mathbf{u}(t,\mathbf{x},\mathbf{u})|$ leading to

$$|\mathbf{f}(t,\mathbf{0},\mathbf{0})| \leq C, \quad |\mathbf{f}_\mathbf{x}(t,\mathbf{x},\mathbf{u})|, \leq C(1+|\mathbf{u}|) \quad |\mathbf{f}_\mathbf{u}(t,\mathbf{x},\mathbf{u})| \leq C. \tag{5.76}$$

Due to the condition 1, the existence of the unique solution for condition 2 for bounded control is satisfied. on the other hand, the quantity $\mathbf{f}(t,\mathbf{x},\mathbf{u})$ is expressed as linear function of control variables which satisfy the condition 3. □

Optimal system

To characterize the optimal control functions, the Pontryagin's Maximum Principle (Pontryagin, 2018*b*) was considered. Thus, system (3.22) was converted into an equivalent problem, namely the problem of minimizing the Hamiltonian $H(t)$ given by:

$$\left.\begin{aligned} H(t) &= I_h(t) + \tfrac{W_1}{2}u_1^2(t) + \tfrac{W_2}{2}u_2^2(t) \\ &\quad +\lambda_1(t)\big[b_h N_h(t) - \lambda_h(t)S_h(t) - (u_1(t)+\mu_h)S_h + \gamma_h R_h(t)\big] \\ &\quad +\lambda_2(t)\big[\lambda_h(t)S_h(t) - (\mu_h+\kappa_h)E_h(t)\big] \\ &\quad +\lambda_3(t)\big[\kappa_h E_h(t) - (\mu_h+d_h+\alpha_h)I_h(t)\big] \\ &\quad +\lambda_4(t)\big[u_1(t)S_h(t) + \alpha_h I_h(t) - (\mu_h+\gamma_h)R_h(t)\big] \\ &\quad +\lambda_5(t)\big[\Lambda_a - \lambda_a(t)S_a(t) - \mu_a S_a(t) + \gamma_a R_a(t)\big] \\ &\quad +\lambda_6(t)\big[b_a N_a(t) - \lambda_a(t)S_a - (\mu_a+\kappa_a)E_a(t)\big] \\ &\quad +\lambda_7(t)\big[\kappa_a E_a(t) - (\mu_a+d_a+\alpha_a)I_a(t)\big] \\ &\quad +\lambda_8(t)\big[\alpha_a I_a(t) - (\mu_a+\gamma_a)R_a(t)\big] \\ &\quad +\lambda_9(t)\big[b_v(t)N_v(t) - \lambda_v(t)S_v(t) - (\mu_v(t)+u_2(t))S_v(t)\big] \\ &\quad +\lambda_{10}(t)\big[\lambda_v(t)S_v - (\mu_v(t)+\kappa_v(t)+u_2(t))E_v(t)\big] \\ &\quad +\lambda_{11}(t)\big[\kappa_v(t)E_v - (\mu_v(t)+u_2(t))I_v(t)\big]. \end{aligned}\right\} \tag{5.77}$$

Note that the first part of the terms in $H(t)$ came from the integrand of the objective functional. Given an optimal control solution (u^*) and the corresponding state solutions (S_h, E_h, I_h, R_h, S_a, E_a, I_a, R_a,S_v,E_v,I_v) there exist adjoint functions $\lambda_i(t)$, $(i = 1,2,3,\cdots,11)$ (Lenhart, 2007) satisfying

$$\frac{\partial \lambda_i}{dt} = \frac{\partial H}{\partial \mathbf{x}}, \tag{5.78}$$

with transversality condition $\lambda(t_f) = 0$. Thus the adjoint system is:

$$\begin{aligned} \frac{d\lambda_1}{dt} &= \lambda_1\mu_h + u_1(t)(\lambda_1-\lambda_4) + (\lambda_1-\lambda_2)\frac{\sigma_v(t)\sigma_h\beta_{vh}I_v}{\sigma_v(t)N_v+\sigma_h N_h} \\ &\quad +(\lambda_2-\lambda_1)\frac{\sigma_v(t)\sigma_h^2\beta_{vh}I_vS_h}{(\sigma_v(t)N_v+\sigma_h N_h)^2} + (\lambda_{10}-\lambda_9)\frac{\sigma_v(t)\sigma_h^2\beta_{hv}I_hS_v}{(\sigma_v(t)N_v+\sigma_h N_h)^2}, \qquad (5.79) \\ \frac{d\lambda_2}{dt} &= \lambda_2\mu_h + (\lambda_2-\lambda_3)\kappa_h + (\lambda_2-\lambda_1)\frac{\sigma_v(t)\sigma_h^2\beta_{vh}I_vS_h}{(\sigma_v(t)N_v+\sigma_h N_h)^2} \end{aligned}$$

$$+(\lambda_{10}-\lambda_9)\frac{\sigma_v(t)\sigma_h^2\beta_{hv}I_hS_v}{(\sigma_v(t)N_v+\sigma_hN_h)^2}, \tag{5.80}$$

$$\begin{aligned}\frac{d\lambda_3}{dt} &= -1+\lambda_3(\mu_h+d_h)+\alpha_h(\lambda_3-\lambda_4)+(\lambda_2-\lambda_1)\frac{\sigma_v(t)\sigma_h^2\beta_{vh}I_vS_h}{(\sigma_v(t)N_v+\sigma_hN_h)^2}\\ &\quad+(\lambda_9-\lambda_{10})\frac{\sigma_v(t)\sigma_h\beta_{hv}S_v}{\sigma_v(t)N_v+\sigma_hN_h}+(\lambda_{10}-\lambda_9)\frac{\sigma_v(t)\sigma_h^2\beta_{hv}I_hS_v}{(\sigma_v(t)N_v+\sigma_hN_h)^2},\end{aligned} \tag{5.81}$$

$$\begin{aligned}\frac{d\lambda_4}{dt} &= \lambda_4\mu_h+(\lambda_4-\lambda_1)\gamma_h+(\lambda_2-\lambda_1)\frac{\sigma_v(t)\sigma_h^2\beta_{vh}I_vS_h}{(\sigma_v(t)N_v+\sigma_hN_h)^2}\\ &\quad+(\lambda_{10}-\lambda_9)\frac{\sigma_v(t)\sigma_h^2\beta_{hv}I_hS_v}{(\sigma_v(t)N_v+\sigma_hN_h)^2},\end{aligned} \tag{5.82}$$

$$\begin{aligned}\frac{d\lambda_5}{dt} &= \lambda_5\mu_a+(\lambda_5-\lambda_6)\frac{\sigma_v(t)\sigma_a\beta_{va}I_v}{\sigma_v(t)N_v+\sigma_aN_a}+(\lambda_6-\lambda_5)\frac{\sigma_v(t)\sigma_a^2\beta_{va}I_vS_a}{(\sigma_v(t)N_v+\sigma_aN_a)^2}\\ &\quad+(\lambda_{10}-\lambda_9)\frac{\sigma_v(t)\sigma_a^2\beta_{av}I_aS_v}{(\sigma_v(t)N_v+\sigma_aN_a)^2},\end{aligned} \tag{5.83}$$

$$\begin{aligned}\frac{d\lambda_6}{dt} &= \lambda_6\mu_a+(\lambda_6-\lambda_7)\kappa_a+(\lambda_6-\lambda_5)\frac{\sigma_v(t)\sigma_a^2\beta_{va}I_vS_a}{(\sigma_v(t)N_v+\sigma_aN_a)^2}\\ &\quad+(\lambda_{10}-\lambda_9)\frac{\sigma_v(t)\sigma_a^2\beta_{av}I_aS_v}{(\sigma_v(t)N_v+\sigma_aN_a)^2},\end{aligned} \tag{5.84}$$

$$\begin{aligned}\frac{d\lambda_7}{dt} &= \lambda_7(\mu_a+d_a)+\alpha_a(\lambda_7-\lambda_8)+(\lambda_6-\lambda_5)\frac{\sigma_v(t)\sigma_a^2\beta_{va}I_vS_a}{(\sigma_v(t)N_v+\sigma_aN_a)^2}\\ &\quad+(\lambda_9-\lambda_{10})\frac{\sigma_v(t)\sigma_a\beta_{av}S_v}{\sigma_v(t)N_v+\sigma_aN_a}+(\lambda_{10}-\lambda_9)\frac{\sigma_v(t)\sigma_a^2\beta_{av}I_aS_v}{(\sigma_v(t)N_v+\sigma_aN_a)^2},\end{aligned} \tag{5.85}$$

$$\begin{aligned}\frac{d\lambda_8}{dt} &= \lambda_8\mu_a+(\lambda_8-\lambda_5)\gamma_a+(\lambda_6-\lambda_5)\frac{\sigma_v(t)\sigma_a^2\beta_{va}I_vS_a}{(\sigma_v(t)N_v+\sigma_aN_a)^2}\\ &\quad+(\lambda_{10}-\lambda_9)\frac{\sigma_v(t)\sigma_a^2\beta_{av}I_aS_v}{(\sigma_v(t)N_v+\sigma_aN_a)^2},\end{aligned} \tag{5.86}$$

$$\begin{aligned}\frac{d\lambda_9}{dt} &= \lambda_9(\mu_v(t)+u_2(t))+(\lambda_2-\lambda_1)\frac{\sigma_v^2(t)\sigma_h\beta_{vh}I_vS_h}{(\sigma_v(t)N_v+\sigma_hN_h)^2}\\ &\quad+(\lambda_6-\lambda_5)\frac{\sigma_v^2(t)\sigma_a\beta_{va}I_vS_a}{(\sigma_v(t)N_v+\sigma_aN_a)^2}+(\lambda_9-\lambda_{10})\frac{\sigma_v(t)\sigma_h\beta_{hv}I_h}{\sigma_v(t)N_v+\sigma_hN_h}\\ &\quad+(\lambda_9-\lambda_{10})\frac{\sigma_v(t)\sigma_a\beta_{av}I_a}{\sigma_v(t)N_v+\sigma_aN_a}+(\lambda_{10}-\lambda_9)\frac{\sigma_v^2\sigma_a\beta_{av}I_aS_v}{(\sigma_vN_v+\sigma_aN_a)^2}\\ &\quad+(\lambda_{10}-\lambda_9)\frac{\sigma_v^2(t)\sigma_h\beta_{hv}I_hS_v}{(\sigma_v(t)N_v+\sigma_hN_h)^2},\end{aligned} \tag{5.87}$$

$$\begin{aligned}
\frac{d\lambda_{10}}{dt} &= \lambda_{10}(\mu_v(t)+u_2(t))+\kappa_v(t)(\lambda_{10}-\lambda_{11})+(\lambda_2-\lambda_1)\frac{\sigma_v^2(t)\sigma_h\beta_{vh}I_vS_h}{(\sigma_v(t)N_v+\sigma_hN_h)^2} \\
&\quad +(\lambda_6-\lambda_5)\frac{\sigma_v^2(t)\sigma_a\beta_{va}I_vS_a}{(\sigma_v(t)N_v+\sigma_aN_a)^2} \\
&\quad +(\lambda_{10}-\lambda_9)\frac{\sigma_v^2(t)\sigma_a\beta_{av}I_aS_v}{(\sigma_v(t)N_v+\sigma_aN_a)^2}+(\lambda_{10}-\lambda_9)\frac{\sigma_v^2(t)\sigma_h\beta_{hv}I_hS_v}{(\sigma_v(t)N_v+\sigma_hN_h)^2}, \qquad (5.88) \\
\frac{d\lambda_{11}}{dt} &= \lambda_{11}(\mu_v(t)+u_2(t))+(\lambda_1-\lambda_2)\frac{\sigma_v(t)\sigma_h\beta_{vh}S_h}{\sigma_v(t)N_v+\sigma_hN_h} \\
&\quad +(\lambda_2-\lambda_1)\frac{\sigma_v^2(t)\sigma_h\beta_{vh}I_vS_h}{(\sigma_v(t)N_v+\sigma_hN_h)^2}+(\lambda_5-\lambda_6)\frac{\sigma_v(t)\sigma_a\beta_{va}S_a}{\sigma_v(t)N_v+\sigma_aN_a} \\
&\quad +(\lambda_6-\lambda_5)\frac{\sigma_v^2(t)\sigma_a\beta_{va}I_vS_a}{(\sigma_v(t)N_v+\sigma_aN_a)^2}+(\lambda_{10}-\lambda_9)\frac{\sigma_v^2(t)\sigma_a\beta_{av}I_aS_v}{(\sigma_v(t)N_v+\sigma_aN_a)^2} \\
&\quad +(\lambda_{10}-\lambda_9)\frac{\sigma_v^2(t)\sigma_h\beta_{hv}I_hS_v}{(\sigma_v(t)N_v+\sigma_hN_h)^2}. \qquad (5.89)
\end{aligned}$$

In addition, the optimal solution of the Hamiltonian are determined by taking the partial derivatives of the function $H(t)$ in (5.77) with respect to control functions u_i, followed by setting the resultant equation to zero and then solve for u_i^*, $i = 1,2$ follows:

$$\begin{aligned}
\frac{\partial H}{\partial u_1} &= u_1^*W_1-(\lambda_1-\lambda_4)S_h. \qquad (5.90) \\
\frac{\partial H}{\partial u_2} &= u_2^*W_2-(\lambda_9S_v+\lambda_{10}E_v+\lambda_{11}I_v). \qquad (5.91)
\end{aligned}$$

Observe that $\frac{\partial^2 H}{\partial u^i} = W_i > 0$ and this demonstrates that the optimal control problem has minimum value at the optimal solution $U^*(t)$. Furthermore by setting (5.91) to zero and solve for u_i^* gives

$$u_1^* = \frac{(\lambda_1-\lambda_4)S_h}{W_1}, \quad u_2^* = \frac{(S_v\lambda_9+E_v\lambda_{10}+I_v\lambda_{11})}{W_2}. \qquad (5.92)$$

By applying the the standard arguments and the bounds for the controls the following arguments on characterization of the optimal controls was obtained:

$$u_i = \min\left\{q_i, \max\left(0, u_i^*\right)\right\}. \qquad (5.93)$$

Appendix 4: Model with memory and temperature effects

Basic properties of the model

Theorem 5.18
Let $\mathscr{X}(t) = (L(t), N_v(t))$ be the unique of the model (3.26) for $t \geq 0$. Then, the solution $\mathscr{X}(t)$ remains in $\mathbb{R}^2_+$.

Proof. In order to demonstrate that the solution $\mathscr{X}(t)$ of model (3.26) s non-negative there was need to investigate the direction of the vector field given by the right hand side of (3.26) on each space and determine whether the vector field points to the interior of $\mathbb{R}^2_+$ or is tangent to the coordinate space. Since,

$$
\begin{aligned}
{}^{c}_{t_0}D^{\alpha}_{t} L(t)\,|_{L=0} &= b^{\alpha}_{l} W N_v \geq 0, && (5.94)\\
{}^{c}_{t_0}D^{\alpha}_{t} N_v(t)\,|_{N_v=0} &= \sigma^{\alpha}_{l} L \geq 0. && (5.95)
\end{aligned}
$$

The results presented implied that the vector field given by the right hand side of (3.26) on each coordinate plane is either tangent to the coordinate plane or points to the interior of $\mathbb{R}^2_+$. Hence, the domain $\mathbb{R}^2_+$ is a positively invariant region. Moreover, if the initial conditions of system (3.26) are non-negative then it follows that the corresponding solutions of model (3.26) are non-negative. □

Theorem 5.19
Let $\mathscr{X}(t) = (L(t), N_v(t))$ be the unique of the model (3.26) for $t \geq 0$. Then, the solution $\mathscr{X}(t)$ is bounded above, that is, $\mathscr{X}(t) \in \Omega$ where Ω denotes the feasible region and is given by

$$
\Omega = \left\{ \begin{pmatrix} L, N_v \end{pmatrix} \in \mathbb{R}^2_+ \middle| 0 \leq L \leq K^{\alpha}_{l},\ \ 0 \leq N_v \leq C \right\}. \tag{5.96}
$$

Proof. For model (3.26) to be biological meaningful all model solutions need to be positive. Hence, from the first equation of model (3.26), one can easily note that for all solutions of this equation to remain positive the following condition must hold $0 \leq L(t) \leq K^{\alpha}_{l}$, otherwise the solutions will be negative and biological irrelevant. From the bounds of $L(t)$ it follows that

$$
\begin{aligned}
{}^{c}_{t_0}D^{\alpha}_{t} N_v(t) &= \sigma^{\alpha}_{l} L - \mu^{\alpha}_{v} N_v \\
&\leq \sigma^{\alpha}_{l} K^{\alpha}_{l} - \mu^{\alpha}_{v} N_v. && (5.97)
\end{aligned}
$$

Applying the Laplace transform lead to

$$
s^{\alpha}\mathscr{L}(N_V(t)) - s^{\alpha-1} N_v(0) \leq \frac{\sigma^{\alpha}_{l} K^{\alpha}_{l}}{s} - \mu^{\alpha}_{v}\mathscr{L}(N_v(t)). \tag{5.98}
$$

Combining the like terms I got:

$$\begin{aligned}\mathscr{L}(N_v(t)) &\leq \sigma_l^\alpha K_l^\alpha \frac{s^{-1}}{s^\alpha+\mu_v^\alpha} + N_v(0)\frac{s^{\alpha-1}}{s^\alpha+\mu_v^\alpha} \\ &= \sigma_l^\alpha K_l^\alpha \frac{s^{\alpha-(1+\alpha)}}{s^\alpha+\mu_v^\alpha} + N_v(0)\frac{s^{\alpha-1}}{s^\alpha+\mu_v^\alpha}. \end{aligned} \tag{5.99}$$

Applying the inverse Laplace transform lead:

$$\begin{aligned} N_v(t) &\leq \mathscr{L}^{-1}\left\{\sigma_l^\alpha K_l^\alpha \frac{s^{\alpha-(1+\alpha)}}{s^\alpha+\mu_v^\alpha}\right\} + \mathscr{L}^{-1}\left\{N_v(0)\frac{s^{\alpha-1}}{s^\alpha+\mu_v^\alpha}\right\} \\ &\leq \sigma_l^\alpha K_l^\alpha t^\alpha E_{\alpha,\alpha+1}(-\mu_v t^\alpha) + N_V(0)E_{\alpha,1}(-\mu_v t^\alpha) \\ &\leq \frac{\sigma_l^\alpha K_l^\alpha}{\mu_v^\alpha}\mu_v^\alpha t^\alpha E_{\alpha,\alpha+1}(-\mu_v t^\alpha) + N_V(0)E_{\alpha,1}(-\mu_v t^\alpha) \\ &\leq \max\left\{\frac{\sigma_l^\alpha K_l^\alpha}{\mu_v^\alpha}, N_v(0)\right\}(\mu_v^\alpha t^\alpha E_{\alpha,\alpha+1}(-\mu_v t^\alpha) + E_{\alpha,1}(-\mu_v t^\alpha)) \\ &= \frac{C}{\Gamma(1)} = C, \end{aligned} \tag{5.100}$$

where $C = \max\{\frac{\sigma_l^\alpha K_l^\alpha}{\mu_v^\alpha}, N_v(0)\}$. Thus, $N_V(t)$ is bounded from above. Hence, one can conclude that the solution $X_1(t)$ is bounded above. □

Equilibrium points and their stability

This section constitute the fundamental results of model (3.26) that were derived following the comprehensive dynamical analysis of the model. In particular, it was noted that model (3.26) has two equilibrium points, a trivial $(L, N_v) = (0,0)$ and a non-trivial

$$\{L^*, N_v^*\} = \left\{\left(1-\frac{1}{r}\right)K_l^\alpha, \frac{\sigma_l^\alpha}{\mu_v^\alpha}\left(1-\frac{1}{r}\right)K_l^\alpha\right\}, \tag{5.101}$$

where

$$r = \frac{\sigma_l^\alpha}{\sigma_l^\alpha+\mu_p^\alpha}\frac{b_l^\alpha}{\mu_v^\alpha}W, \tag{5.102}$$

r is a threshold quantity that determines growth of the tsetse fly population.

(i) If $r \leq 1$, then the equilibrium point $(0,0)$ is the sole equilibrium point of system (3.26) and it is globally (uniformly) asymptotically stable in Ω.

(ii) If $r > 1$, then the equilibrium (L^*, N_v^*) is globally (uniformly) asymptotically stable in int(Ω).

Proof. Lyapunov functionals were used to demonstrate that Theorem (5.59) holds.

(i) To investigate the first part of Theorem (5.59) the following Lyapunov function was considered:

$$U_1(t) = \frac{\mu_v^\alpha}{b_l^\alpha W} L(t) + N_v(t). \tag{5.103}$$

Taking the fractional derivative of (5.103) leads to:

$$\begin{aligned} {}_{t_0}^{c}D_t^\alpha U_1(t) &= \frac{\mu_v^\alpha}{b_l^\alpha W} {}_{t_0}^{c}D_t^\alpha L(t) + {}_{t_0}^{c}D_t^\alpha N_v(t) \\ &= \frac{\mu_v^\alpha}{b_l^\alpha W}\left[b_l^\alpha W N_v\left(1 - \frac{L}{K_l^\alpha}\right) - (\sigma_l^\alpha + \mu_p^\alpha)L\right] + \sigma_l^\alpha L - \mu_v^\alpha N_v \\ &= -\frac{\mu_v^\alpha N_v L}{K_l^\alpha} - \frac{\sigma_l^\alpha}{r}(1-r). \end{aligned} \tag{5.104}$$

Since ${}_{t_0}^{c}D_t^\alpha U(t) < 0$, for $r < 1$, it was concluded that the equilibrium point $(0,0)$ is globally (uniformly) asymptotically stable in Ω. The next step was to demonstrate item (ii) hold.

(ii) To demonstrate that item (ii) hold the following Lyapunov function was considered:

$$\begin{aligned} U_2(t) &= a_1\left[L(t) - L^* - L^* \ln\left(\frac{L(t)}{L^*}\right)\right] \\ &\quad + a_2\left[N_v(t) - N_v^* - N_v^* \ln\left(\frac{N_v(t)}{N_v^*}\right)\right], \end{aligned} \tag{5.105}$$

where a_1 and a_2 are positive constants to be determined. After taking the fractional derivatives the following results were obtained:

$$\begin{aligned} {}_{t_0}^{c}D_t^\alpha U_2(t) &\leq a_1\left(1 - \frac{L^*}{L(t)}\right) {}_{t_0}^{c}D_t^\alpha L(t) + a_2\left(1 - \frac{N_v^*}{N_v(t)}\right) {}_{t_0}^{c}D_t^\alpha N_v(t) \\ &= a_1\left(1 - \frac{L^*}{L(t)}\right)(g(N_v, L) - (\sigma_l^\alpha + \mu_p^\alpha)L) \\ &\quad + a_2\left(1 - \frac{N_v^*}{N_v(t)}\right)(\sigma_l^\alpha L - \mu_v^\alpha N_v), \end{aligned} \tag{5.106}$$

with $g(N_v,L) = b_l^\alpha W N_v\left(1-\frac{L}{K_l^\alpha}\right)$. Setting $a_1 = 1$ and $a_2 = g(N_v^*,L^*) > 0$, with $g(N_v^*,L^*) = b_l^\alpha W N_v\left(1-\frac{L^*}{K_l^\alpha}\right)$. Furthermore by utilizing the identities $g(N_v^*,L^*) = (\sigma_l^\alpha + \mu_p^\alpha)L^*$ and $\sigma_l^\alpha L^* = \mu_v^\alpha N_v^*$ one gets

$$\begin{aligned} {}_{t_0}^{c}D_t^\alpha U_2(t) &\leq g(N_v^*,L^*)\Bigg(2-\frac{N_v}{N_v^*}-\frac{LN_v^*}{L^*N_v}-\frac{L^*}{L}\frac{g(N_v,L)}{g(N_v^*,L^*)} \\ &\quad +\frac{g(N_v,L)}{g(N_v^*,L^*)}\Bigg). \end{aligned} \tag{5.107}$$

Let $\Phi(x) = 1-x+\ln x$, for $x>0$. It follows that $\Phi(x)\leq 0$, with the equality satisfied if and only if $x=1$. Using this relation one get the following:

$$\left.\begin{aligned} &2-\tfrac{N_v}{N_v^*}-\tfrac{LN_V^*}{L^*N_V}-\tfrac{L^*}{L}\tfrac{g(N_V,L)}{g(N_V^*,L^*)}+\tfrac{g(N_V,L)}{g(N_V^*,L^*)} \\ &= \Phi\left(\tfrac{LN_V^*}{L^*N_V}\right)+\Phi\left(\tfrac{L^*}{L}\tfrac{g(N_V,L)}{g(N_V^*,L^*)}\right)-\tfrac{N_v}{N_v^*}+\tfrac{g(N_V,L)}{g(N_V^*,L^*)} \\ &\quad -\ln\left(\tfrac{N^*g(N_V,L)}{Ng(N_V^*,L^*)}\right) \\ &\leq \ln\left(\tfrac{N_v}{N_v^*}\right)-\tfrac{N_v}{N_v^*}+\tfrac{g(N_V,L)}{g(N_V^*,L^*)}-\ln\left(\tfrac{g(N_V,L)}{g(N_V^*,L^*)}\right) \\ &\leq 0. \end{aligned}\right\} \tag{5.108}$$

Hence, it was concluded that if $r>1$, then the equilibrium (L^*,N_v^*) is globally (uniformly) asymptotically stable in int(Ω). From the above analytical results we can also deduce that if $r<1$, then the tsetse vector population will become extinct and for $r>1$ it will persist. Based on these results the analysis of the full model (3.31) was performed considering $r>1$ implying that the tsetse flies are at the equilibrium (L^*,N_v^*).

□

Theorem 5.20

For $\alpha\in(0,1)$, the disease-free equilibrium of system (3.31) is globally (uniformly) asymptotically stable for $\mathscr{R}_0<1$.

Proof. The Lyapunov functional was considered:

$$\begin{aligned}\mathscr{L}_0(t) &= c_1\left\{S_h(t)-S_h^0-S_h^0\ln\frac{S_h(t)}{S_h^0}\right\}+c_1I_h(t)+c_2\left\{S_a(t)-S_a^0-S_a^0\ln\frac{S_a(t)}{S_a^0}\right\}\\ &\quad +c_2I_a(t)+c_3\left\{S_v(t)-S_v^0-S_v^0\ln\frac{S_v(t)}{S_v^0}+I_v(t)\right\},\end{aligned} \tag{5.109}$$

where c_1, c_2 and c_3 are positive constants to be determined. Thus

$$\begin{aligned}{}_{t_0}^{c}D_t^{\alpha}\mathscr{L}_0(t) &\leq c_1\left(1-\frac{S_h^0}{S_h}\right){}_{t_0}^{c}D_t^{\alpha}S_h+\ c_1\,{}_{t_0}^{c}D_t^{\alpha}I_h+c_2\left(1-\frac{S_a^0}{S_a}\right){}_{t_0}^{c}D_t^{\alpha}S_a\\ &\quad c_2\,{}_{t_0}^{c}D_t^{\alpha}I_a+c_3\left(1-\frac{S_v^0}{S_v}\right){}_{t_0}^{c}D_t^{\alpha}S_v+\ c_3\,{}_{t_0}^{c}D_t^{\alpha}I_v.\end{aligned} \tag{5.110}$$

Setting

$$\begin{aligned}c_1 &= \mu_v^{\alpha}\beta_{hv}^{\alpha}(\mu_a^{\alpha}+\gamma_a^{\alpha}), \qquad c_2=\mu_v^{\alpha}\beta_{av}^{\alpha}(\mu_h^{\alpha}+\gamma_h^{\alpha}),\\ c_3 &= \left(\frac{\beta_{hv}^{\alpha}\beta_{vh}^{\alpha}\Lambda_h^{\alpha}(\mu_a^{\alpha}+\gamma_a^{\alpha})}{\mu_h^{\alpha}}+\frac{\beta_{va}^{\alpha}\beta_{av}^{\alpha}\Lambda_a^{\alpha}(\mu_h^{\alpha}+\gamma_h^{\alpha})}{\mu_a^{\alpha}}\right),\end{aligned} \tag{5.111}$$

and simplifying one gets:

$$\left.\begin{aligned}{}_{t_0}^{c}D_t^{\alpha}\mathscr{L}_0(t) \leq\ & -\mu_v^{\alpha}\mu_h^{\alpha}\beta_{hv}^{\alpha}(\mu_a^{\alpha}+\gamma_a^{\alpha})\tfrac{(S_h-S_h^0)^2}{S_h}-\mu_v^{\alpha}\mu_a^{\alpha}\beta_{av}^{\alpha}(\mu_h^{\alpha}+\gamma_h^{\alpha})\tfrac{(S_a-S_a^0)^2}{S_a}\\ & -\left(\tfrac{\beta_{hv}^{\alpha}\beta_{vh}^{\alpha}\Lambda_h^{\alpha}(\mu_a^{\alpha}+\gamma_a^{\alpha})\mu_v^{\alpha}}{\mu_h^{\alpha}}+\tfrac{\beta_{va}^{\alpha}\beta_{av}^{\alpha}\Lambda_a^{\alpha}(\mu_h^{\alpha}+\gamma_h^{\alpha})\mu_v^{\alpha}}{\mu_a^{\alpha}}\right)\tfrac{(S_v-S_v^0)^2}{S_v}\\ & -\left(\tfrac{\beta_{hv}^{\alpha}\beta_{vh}^{\alpha}\Lambda_h^{\alpha}(\mu_a^{\alpha}+\gamma_a^{\alpha})\mu_v^{\alpha}}{\mu_h^{\alpha}}+\tfrac{\beta_{va}^{\alpha}\beta_{av}^{\alpha}\Lambda_a^{\alpha}(\mu_h^{\alpha}+\gamma_h^{\alpha})\mu_v^{\alpha}}{\mu_a^{\alpha}}\right)\theta f(I_v)I_v\\ & -\mu_v^{\alpha}(\mu_a^{\alpha}+\gamma_a^{\alpha})(\mu_h^{\alpha}+\gamma_h^{\alpha})(\beta_{hv}^{\alpha}I_h+\beta_{av}^{\alpha}Ia)(1-\mathscr{R}_0^2).r\end{aligned}\right\} \tag{5.112}$$

Since all the parameters and variables in system (3.31) are non-negative, it follows that ${}_{t_0}^{c}D_t^{\alpha}\mathscr{L}_0(t)<0$ holds if $\mathscr{R}_0<1$. Therefore by the Lasalle Invariance principle (LaSalle, 1976), we conclude that the DFE of system (3.31) is globally (uniformly) asymptotically stable whenever $\mathscr{R}_0<1$. This completes the proof. Biologically, this implies that whenever $\mathscr{R}_0<1$ then the disease dies out in the community. □

Theorem 5.21

Let $\mathscr{E}^*=(S_i^*,I_i^*)$ for $i=a,h,v$, be the endemic equilibrium point of system (3.31). Then for $\alpha\in(0,1)$ and $\mathscr{R}_0>1$, the endemic equilibrium point $\mathscr{E}^*$ is globally (uniformly) asymptotically stable.

Proof. Consider the following Lyapunov functional

$$\begin{aligned}\mathscr{L}_1(t) &= b_1\left(S_h(t)-S_h^*-S_h^*\ln\frac{S_h(t)}{S_h^*}\right)+b_2\left(I_h(t)-I_h^*-I_h^*\ln\frac{I_h(t)}{I_h^*}\right)\\ &+b_3\left(S_a(t)-S_a^*-S_a^*\ln\frac{S_a(t)}{S_a^*}\right)+b_4\left(I_a(t)-I_a^*-I_a^*\ln\frac{I_a(t)}{I_a^*}\right)\\ &+b5\left(S_v(t)-S_v^*-S_v^*\ln\frac{S_v(t)}{S_v^*}\right)\\ &+b_6\left(I_v(t)-I_v^*-I_v^*\ln\frac{I_v(t)}{I_v^*}\right),\end{aligned} \tag{5.113}$$

where $b_i=$, $i=1,2,3,..,6$, are positive constants to be determined, Applying Lemma **??** leads to:

$$\begin{aligned}{}_{t_0}^{c}D_t^{\alpha}\mathscr{L}_1(t) &\leq b_1\left(1-\frac{S_h^*}{S_h}\right){}_{t_0}^{c}D_t^{\alpha}S_h+b_2\left(1-\frac{I_h^*}{I_h}\right){}_{t_0}^{c}D_t^{\alpha}I_h+b_3\left(1-\frac{S_a^*}{S_a}\right){}_{t_0}^{c}D_t^{\alpha}S_a\\ &+b_4\left(1-\frac{I_a^*}{I_a}\right){}_{t_0}^{c}D_t^{\alpha}I_a+b_5\left(1-\frac{S_v^*}{S_v}\right){}_{t_0}^{c}D_t^{\alpha}S_v\\ &+b_6\left(1-\frac{I_v^*}{I_v}\right){}_{t_0}^{c}D_t^{\alpha}I_v.\end{aligned} \tag{5.114}$$

Setting $b_i=1$, for $i=1,2,3,4$ and $b_5=b_6=\frac{\beta_{vh}^{\alpha}f(I_v^*)S_h^*}{\beta_{hv}^{\alpha}I_h^*S_v^*}+\frac{\beta_{va}^{\alpha}f(I_v^*)S_a^*}{\beta_{av}^{\alpha}I_a^*S_v^*}$ and utilising the following identities (which exists at the endemic point)

$$\left.\begin{array}{lll}\Lambda_h^{\alpha} &= \beta_{vh}^{\alpha}f(I_v^*)S_h^*+\mu_h^{\alpha}S_h^*, & (\mu_h^{\alpha}+\gamma_h^{\alpha})I_h^*=\beta_{vh}^{\alpha}f(I_v^*)S_h^*,\\ \Lambda_a^{\alpha} &= \beta_{va}^{\alpha}f(I_v^*)S_a^*+\mu_a^{\alpha}S_a^*, & (\mu_a^{\alpha}+\gamma_a^{\alpha})I_a^*=\beta_{va}^{\alpha}f(I_v^*)S_a^*,\\ \sigma_l^{\alpha}L^* &= (\beta_{hv}^{\alpha}I_h^*+\beta_{av}^{\alpha}I_a^*)S_v^*+\mu_v^{\alpha}S_v^*, & \mu_v^{\alpha}I_v^*=(\beta_{hv}^{\alpha}I_h^*+\beta_{av}^{\alpha}I_a^*(t))S_v^*,\end{array}\right\} \tag{5.115}$$

one gets

$$\begin{aligned}D^{\alpha}\mathscr{L}_1(t) &\leq \mu_h^{\alpha}S_h^*\underbrace{\left(2-\frac{S_h}{S_h^*}-\frac{S_h^*}{S_h}\right)}_{(1)}+\beta_{va}^{\alpha}f(I_v^*)S_a^*\frac{\beta_{hv}^{\alpha}I_h^*}{\beta_{av}^{\alpha}I_a^*}\underbrace{\left(2-\frac{S_v^*}{S_v}-\frac{I_v}{I_v^*}-\frac{S_vI_v^*I_h}{S_v^*I_vI_h^*}+\frac{I_h}{I_h^*}\right)}_{(2)}\\ &+\beta_{vh}^{\alpha}f(I_v^*)S_h^*\underbrace{\left(4-\frac{S_h^*}{S_h}-\frac{S_hI_h^*f(I_v)}{S_h^*I_hf(I_v^*)}-\frac{S_v^*}{S_v}-\frac{I_v}{I_v^*}-\frac{S_vI_v^*I_h}{S_v^*I_vI_h^*}+\frac{f(I_v)}{f(I_v^*)}\right)}_{(3)}\end{aligned}$$

$$+\mu_a^\alpha S_a^* \underbrace{\left(2-\frac{S_a}{S_a^*}-\frac{S_a^*}{S_a}\right)}_{(4)}+\beta_{vh}^\alpha f(I_v^*)S_h^*\frac{\beta_{av}^\alpha I_a^*}{\beta_{hv}^\alpha I_h^*}\underbrace{\left(2-\frac{S_v^*}{S_v}-\frac{I_v}{I_v^*}-\frac{S_vI_v^*I_a}{S_v^*I_vI_a^*}+\frac{I_a}{I_a^*}\right)}_{(5)}$$
$$+\beta_{va}^\alpha f(I_v^*)S_a^*\underbrace{\left(4-\frac{S_a^*}{S_a}-\frac{S_aI_a^*f(I_v)}{S_a^*I_af(I_v^*)}-\frac{S_v^*}{S_v}-\frac{I_v}{I_v^*}-\frac{S_vI_v^*I_a}{S_v^*I_vI_a^*}+\frac{f(I_v)}{f(I_v^*)}\right)}_{(6)}$$
$$+\mu_v^\alpha S_v^*\left(\frac{\beta_{vh}^\alpha f(I_v^*)S_h^*}{\beta_{hv}^\alpha I_h^*S_v^*}+\frac{\beta_{va}^\alpha f(I_v^*)S_a^*}{\beta_{av}^\alpha I_a^*S_v^*}\right)\underbrace{\left(2-\frac{S_v}{S_v^*}-\frac{S_v^*}{S_v}\right)}_{(7)}. \tag{5.116}$$

Since the arithmetic mean is greater than or equal to the geometric mean, it follows that for brackets (1), (4) and (7) satisfies:

$$\left(2-\frac{S_i}{S_i^*}-\frac{S_i^*}{S_i}\right)\leq 0. \tag{5.117}$$

Furthermore, let $\Phi(x)=1-x+\ln x$, for $x>0$. It follows that $\Phi(x)\leq 0$, with equality if and only if $x=1$. Utilizing, the aforementioned properties of $\Phi(x)$ we can demonstrate that the terms in the brackets are less or equal to zero. Let $k=a,h$, so that from brackets (2) and (5) we can write:

$$\begin{aligned}
&2-\frac{S_v^*}{S_v}+\frac{I_k}{I_k^*}-\frac{I_v}{I_v^*}-\frac{S_vI_v^*I_k}{S_v^*I_vI_k^*},\\
&=\Phi\left(\frac{S_v^*}{S_v}\right)+\Phi\left(\frac{S_vI_v^*I_k}{S_v^*I_vI_k^*}\right)-\ln\left(\frac{I_v^*I_k}{I_vI_k^*}\right)+\frac{I_k}{I_k^*}-\frac{I_v}{I_v^*}\\
&\leq\frac{I_k}{I_k^*}-\ln\left(\frac{I_k}{I_k^*}\right)-\frac{I_v}{I_v^*}+\ln\left(\frac{I_v}{I_v^*}\right)\\
&\leq 0.
\end{aligned} \tag{5.118}$$

In addition, from brackets (3) and (6) we have:

$$\begin{aligned}
&4-\frac{S_k^*}{S_k}-\frac{S_kI_k^*f(I_v)}{S_k^*I_kf(I_v^*)}-\frac{S_v^*}{S_v}-\frac{I_v}{I_v^*}-\frac{S_vI_v^*I_k}{S_v^*I_vI_k^*}+\frac{f(I_v)}{f(I_v^*)},\\
&=\Phi\left(\frac{S_k^*}{S_k}\right)+\Phi\left(\frac{S_v^*}{S_v}\right)+\Phi\left(\frac{S_kI_k^*f(I_v)}{S_k^*I_kf(I_v^*)}\right)+\Phi\left(\frac{S_vI_v^*I_k}{S_v^*I_vI_k^*}\right)\\
&\quad-\frac{I_v}{I_v^*}+\frac{f(I_v)}{f(I_v^*)}-\ln\left(\frac{f(I_v)I_v^*}{f(I_v^*)I_v}\right)
\end{aligned}$$

$$\leq \ln\left(\frac{I_v}{I_v^*}\right) - \frac{I_v}{I_v^*} + \frac{f(I_v)}{f(I_v^*)} - \ln\left(\frac{f(I_v)}{f(I_v^*)}\right)$$
$$\leq 0. \tag{5.119}$$

From (5.117), (5.118) and (5.119), it follows that $D^{\alpha}\mathscr{L}_1(t) \leq 0$ whenever $\mathscr{R}_0 > 1$. Therefore, by the invariant principle of LaSalles (LaSalle, 1976), system (3.31) admits a globally (uniformly) asymptotically stable endemic equilibrium for $\mathscr{R}_0 > 1$. In a nutshell, the result implies that whenever $\mathscr{R}_0 > 1$ the disease will persist, unless intervention strategies that are capable of reducing $\mathscr{R}_0$ to value less than unity are implemented. □

Appendix 5: Model with heterogeneity and time delay

The derivation of basic reproduction number $\mathscr{R}_0$

Through direct calculations it was noted that in the absence of the disease in the community system (3.5) admits a disease-free equilibrium (DFE) given by:

$$\begin{aligned}\mathscr{E}^0 \quad : \quad & \left(S_V^0, I_V^0, S_{H1}^0, I_{H1}^0, S_{H2}^0, I_{H2}^0, S_A^0, I_A^0\right) \\ & = \left(\frac{\sigma_L L^*}{\mu_V}, 0, p_H N_H, 0, (1-p_H)N_H, 0, N_A, 0\right),\end{aligned} \tag{5.120}$$

with $L^* = K_L\left(1-\frac{1}{r}\right)$. Following the next generation matrix approach as used in Van den Driessche (2002), the non-negative matrix $\mathscr{F}$ that denotes the generation of new infection and the non-singular matrix $\mathscr{V}$ that denotes the disease transfer among compartments evaluated at $\mathscr{E}^0$ are, respectively given by:

$$\mathscr{F} = \begin{bmatrix} 0 & z_1 & z_2 & z_3 \\ \beta_{VH} p_H N_H & 0 & 0 & 0 \\ (1-\varepsilon_H)\beta_{VH}(1-p_H)N_H & 0 & 0 & 0 \\ \beta_{VA} N_A & 0 & 0 & 0 \end{bmatrix}, \tag{5.121}$$

$$\mathscr{V} = \begin{bmatrix} \mu_H+\gamma_H & 0 & 0 & 0 \\ 0 & \mu_H+\gamma_H & 0 & 0 \\ 0 & 0 & \mu_A+\gamma_A & 0 \\ 0 & 0 & 0 & \mu_V \end{bmatrix}. \tag{5.122}$$

$$\mathscr{V} = \begin{bmatrix} \mu_H+\gamma_H & 0 & 0 & 0 \\ 0 & \mu_H+\gamma_H & 0 & 0 \\ 0 & 0 & \mu_A+\gamma_A & 0 \\ 0 & 0 & 0 & \mu_V \end{bmatrix}. \tag{5.123}$$

with:

$$\begin{aligned} z_1 &= \frac{\beta_{HV}\sigma_L L^* e^{-\mu_V \tau}}{\mu_V}, \qquad z_2 = \frac{\beta_{HV}(1-\varepsilon)\sigma_L L^* e^{-\mu_v \tau}}{\mu_V} \\ z_3 &= \frac{\beta_{AV}\sigma_L L^* e^{-\mu_V \tau}}{\mu_V} \end{aligned} \tag{5.124}$$

From (5.123), it follows that the basic reproduction number $\mathscr{R}_0$ of system (3.5) is:

$$\mathscr{R}_0 = \sqrt{\left(\mathscr{R}_H + \mathscr{R}_A\right)\left(1 - \frac{1}{r}\right)\frac{\sigma_L e^{-\mu_v \tau}}{\mu_V} K_L}, \tag{5.125}$$

with $\mathscr{R}_H = \frac{\beta_{VH}\beta_{HV}N_H[p_H+(1-p_H)(1-\varepsilon_H)^2]}{\mu_V(\mu_H+\gamma_H)}$ and $\mathscr{R}_A = \frac{\beta_{AV}\beta_{VA}N_A}{\mu_V(\mu_A+\gamma_A)}$. The basic reproduction number $\mathscr{R}_0$ is defined to be the expected number of secondary cases (vector or host) produced in a completely susceptible population, by one infectious individual (vector or host, respectively) during its lifetime as infectious.

Model equilibria and their stability

Having determined the basic reproduction number of model (3.5) the next step was to determine the existence of the endemic equilibrium point.

Theorem 5.22
If $\mathscr{R}_0 > 1$ system (3.5) admits a unique equilibrium poin.t

Proof. Let $\mathscr{E}_H^*$ denote the endemic equilibrium of system (3.5) with $\mathscr{E}_H^* = (S_{H1}^*, I_{H1}^*, S_{H2}^*, I_{H2}^*, S_A^*, I_A^*, S_V^*, I_V^*)$. Solving the first seven equations of the system (3.5) in-terms of I_V^* one gets:

$$\left.\begin{aligned}
&S_{H1}^*(I_V^*) = \tfrac{\mu_H p_H N_H}{[\beta_{VH} f(I_V^*)+\mu_H]}, \qquad S_{H2}^*(I_V^*) = \tfrac{(1-p_H)\mu_H N_H}{[(1-\varepsilon_H)\beta_{VH} f(I_V^*)+\mu_H]},\\
&I_{H1}^*(I_V^*) = \tfrac{p_H \mu_H N_H \beta_{VH} f(I_V^*)}{[\beta_{VH} f(I_V^*)+\mu_H][\mu_H+\gamma_H]},\\
&I_{H2}^*(I_V^*) = \tfrac{(1-p_H)\mu_H N_H (1-\varepsilon_H)\beta_{VH} f(I_V^*)}{[(1-\varepsilon_H)\beta_{VH} f(I_V^*)+\mu_H][\mu_H+\gamma_H]},\\
&S_A^*(I_V^*) = \tfrac{\mu_A N_A}{[\beta_{VA} f(I_V^*)+\mu_A]}, \qquad I_A^*(I_V^*) = \tfrac{\mu_A N_A \beta_{VA} f(I_V^*)}{[\beta_{VA} f(I_V^*)+\mu_A][\mu_A+\gamma_A]},\\
&S_V^*(I_V^*) = \tfrac{\sigma_L L^*}{\beta_{AV} I_A^* + \beta_{HV} I_{H1}^* + (1-\varepsilon_H)\beta_{HV} I_{H2}^* + \mu_V}.
\end{aligned}\right\} \tag{5.126}$$

Substituting the expressions present in (5.126) into the second equation of system (3.5) one gets:

$$\begin{aligned} G(I_V) \;=\; & \left[\beta_{HV} g_{H1}(I_V) + (1-\varepsilon_H)\beta_{HV} g_{H2}(I_V) + \beta_{AV} g_A(I_V)\right] g_V(I_V) e^{-\mu_V \tau} \\ & - \mu_V I_V, \end{aligned} \tag{5.127}$$

with:

$$\left.\begin{array}{rcl} g_{H1}(I_V) & = & \frac{p_H\beta_{VH}\mu_H N_H}{[\mu_H+\gamma_H]}\frac{f(I_V)}{[\beta_{VH}f(I_V)+\mu_H]}, \\ g_{H2}(I_V) & = & \frac{(1-p_H)\mu_H N_H\beta_{VH}}{[\mu_H+\gamma_H])}\frac{f(I_V)}{[(1-\varepsilon_H)\beta_{VH}f(I_V)+\mu_H]}, \\ g_A(I_V) & = & \frac{\beta_{VA}\mu_A N_A}{[\mu_A+\gamma_A]}\frac{f(I_V)}{[\beta_{VA}f(I_V)+\mu_A]}, \\ g_V(I_V) & = & \frac{\sigma_L L^*}{\beta_{AV}g_A(I_V)+\beta_{HV}(g_{H1}(I_V)+(1-\varepsilon_H)g_{H2}(I_V))+\mu_V} \end{array}\right\}. \tag{5.128}$$

Taking the derivatives of the $g_{H1}(I_V)$, $g_{H2}(I_V)$, $g_A(I_V)$, and $g_V(I_V)$ with respect to I_V leads to:

$$\left.\begin{array}{rcl} g'_{H1}(I_V) & = & \frac{p_H\beta_{VH}\mu_H N_H}{[\mu_H+\gamma_H]}\frac{\mu_H f'(I_V)}{[\beta_{VH}f(I_V)+\mu_H]^2}, \\ g'_{H2}(I_V) & = & \frac{(1-p_H)\mu_H N_H\beta_{VH}}{[\mu_H+\gamma_H])}\frac{\mu_H f(I_V)}{[(1-\varepsilon_H)\beta_{VH}f(I_V)+\mu_H]^2}, \\ g'_A(I_V) & = & \frac{\beta_{VA}\mu_A N_A}{[\mu_A+\gamma_A]}\frac{f(I_V)}{[\beta_{VA}f(I_V)+\mu_A]}, \\ g'_V(I_V) & = & -\frac{[\beta_{AV}g'_A(I_V)+\beta_{HV}g'_{H1}(I_V)+(1-\varepsilon_H)g'_{H2}(I_V)]\sigma_L L^*}{[\beta_{AV}g_A(I_V)+\beta_{HV}(g_{H1}(I_V)+(1-\varepsilon_H)g_{H2}(I_V))+\mu_V]^2}. \end{array}\right\}. \tag{5.129}$$

Taking the derivative of $G(I_V)$ with respect to I_V results in:

$$\begin{aligned} G'(I_V) = & \left[\beta_{HV}g_{H1}(I_V)+(1-\varepsilon_H)\beta_{HV}g_{H2}(I_V)+\beta_{AV}g_A(I_V)\right]g'_V(I_V)e^{-\mu_V\tau} \\ & -\mu_V\left[1-\frac{\beta_{HV}g'_{H1}(I_V)+(1-\varepsilon_H)\beta_{HV}g'_{H2}(I_V)+\beta_{AV}g'_A(I_V)}{\mu_V}\right. \\ & \left.\times e^{-\mu_V\tau}g_V(I_v)\right], \end{aligned} \tag{5.130}$$

Recall that the saturation function $f(I_V)$ has the following properties: $f(0)=0$, $f'(I_V)>0$, and $\lim_{I_V\to+\infty}f(I_V)=1$. Hence, it follows that:

$$\text{for} \quad I_V=0, \quad \text{leads to} \begin{cases} g_{H1}(0), \qquad g_{H2}(0)=0, \qquad g'_A(0)=0, \qquad g_V(0)=\frac{\sigma_L L^*}{\mu_V}, \\ g'_{H1}(0)=\frac{p_H\beta_{VH}N_H}{[\mu_H+\gamma_H]}, \qquad g'_{H2}(0)=\frac{(1-p_H)(1-\varepsilon_H)\beta_{VH}N_H}{[\mu_H+\gamma_H]^2}, \\ g'_V(0)=-\mathscr{R}_0^2. \end{cases} \tag{5.131}$$

Furthermore;

$$\text{for} \quad I_V > 0, \quad \text{leads to} \begin{cases} g_{H1}(I_V) > 0, & g_{H2}(I_V) > 0, & g_A(I_V) > 0, & g_V(I_V) > 0, \\ g'_{H1}(I_V) > 0, & g'_{H2}(I_V) > 0, & g'_A(I_V) > 0, & g'_V(I_V) < 0, \end{cases} \tag{5.132}$$

From the above illustrations, note that $G'(0) = -\mu_V(1-\mathscr{R}_0^2)$. It implies that for $\mathscr{R}_0 = 1$, we have $G'(0) = 0$. For $\mathscr{R}_0 > 1$, then $G'(0) > 0$. Furthermore, it was noted that $G'(I_V) < 0, \forall I_V > 0$, implying that $G'(I_V)$ is a decreasing function on $[0;\infty)$ for $\mathscr{R}_0 > 1$. Therefore, it follows that for $\mathscr{R}_0 > 1$ system (3.5) admits a unique equilibrium point. □

Theorem 5.23

The DFE is globally asymptotically stable stable if $\mathscr{R}_0 < 1$, otherwise it is unstable.

Proof. The following Lyapunov functional was considered:

$$U_3(t) = U_{30}(t) + U_{31}(t), \tag{5.133}$$

with:

$$\left.\begin{aligned} U_{30} &= a_1[I_{H1}(t) + I_{H2}(t)] + a_2 I_A(t) + a_3 I_V(t), \\ U_{31} &= a_3 \int_{t-\tau}^{t} \Big[\beta_{HV}[I_{H1}(\theta) + (1-\varepsilon_H) I_{H2}(\theta)] S_V(\theta) + \beta_{AV} I_A(\theta) S_V(\theta)\Big] d\theta, \end{aligned}\right\} \tag{5.134}$$

where a_1, a_2, and a_3 are positive constants to be determined. Taking the derivative of $U_3(t)$ along the solutions of system (3.5) leads to:

$$\left.\begin{aligned} U'_3(t) &= a_1[I'_{H1}(t) + I'_{H2}(t)] + a_2 I'_A(t) + a_3 I'_V(t) \\ &\quad + a_3 \tfrac{d}{dt} \int_{t-\tau}^{t} \Big[\beta_{HV}[I_{H1}(\theta) + (1-\varepsilon_H) I_{H2}(\theta)] S_V(\theta) + \beta_{AV} I_A(\theta) S_V(\theta)\Big] d\theta \\ &= a_1[\beta_{VH} f(I_V) S_{H1} - (\mu_H + \gamma_H) I_{H1}] \\ &\quad + a_1[\beta_{VH}(1-\varepsilon_H) f(I_V) S_{H2} - (\mu_H + \gamma_H) I_{H2}] \\ &\quad + a_2[\beta_{VA} f(I_V) S_A - (\mu_A + \gamma_A) I_A] \\ &\quad + a_3[(\beta_{HV}(I_{H1}) + (1-\varepsilon_H) I_{H2}) + \beta_{AV} I_A) S_V e^{-\mu_V \tau} - \mu_V I_V]. \end{aligned}\right\} \tag{5.135}$$

Let a_1, a_2, and a_3 be

$$\left.\begin{aligned} a_1 &= \mu_V \beta_{HV}(\mu_A + \gamma_A) e^{\mu_V \tau}, \\ a_2 &= \mu_V \beta_{AV}(\mu_H + \gamma_H) e^{\mu_V \tau}, \\ a_3 &= \beta_{HV}\beta_{VH} N_H[(1-p_H)(1-\varepsilon_H)^2 + p_H][\mu_A + \gamma_A] + \beta_{VA}\beta_{AV} N_A[\mu_H + \gamma_H]. \end{aligned}\right\} \tag{5.136}$$

Simplifying $U_3'(t)$ leads to

$$\left.\begin{aligned} U_3'(t) &= -\mu_V[\mu_A+\gamma_A][\mu_H+\gamma_H][\beta_{HV}(I_{H1}+(1-\varepsilon_H)I_{H2})+\beta_{AV}I_A][1-\mathscr{R}_0^2]e^{\mu\tau} \\ &\quad -\mu_V\{\beta_{HV}\beta_{VH}N_H[(1-p_H)(1-\varepsilon_H)^2+p_H][\mu_A+\gamma_A] \\ &\quad +\beta_{VA}\beta_{AV}N_A[\mu_H+\gamma_H]\}\alpha f(I_V)I_V. \end{aligned}\right\} \tag{5.137}$$

Since all the parameters and variables in model (3.5) are non-negative, it follows that $U_3'(t) < 0$ holds if $\mathscr{R}_0 < 1$. On the other hand, $U_3'(t) = 0$ if and only if $I_{H1} = I_{H2} = I_A = I_A = 0$ and $\mathscr{R}_0 = 1$, leading to $S_{H1} = p_H N_H$, $S_{H2} = (1-p_H)N_H$, $S_A = N_A$, and $S_V = \frac{\sigma_L L^*}{\mu_V}$ for all $t \geq 0$. Hence it follows from , that the DFE of system (3.5) is globally asymptotically stable whenever $\mathscr{R}_0 \leq 1$. This completes the proof. □

Theorem 5.24

Whenever $\mathscr{R}_0 > 1$ system (3.5) admits a globally asymptotically stable equilibrium point.

Proof. The following Lyapunov functional was considered:

$$U_4(t) = U_{40}(t) + U_{41}(t), \tag{5.138}$$

with:

$$\left.\begin{aligned} U_{40}(t) &= \left(S_{H1}(t) - S_{H1}^* - S_{H1}^* \ln\tfrac{S_{H1}(t)}{S_{H1}^*}\right) + \left(I_{H1}(t) - I_{H1}^* - I_{H1}^* \ln\tfrac{I_{H1}(t)}{I_{H1}^*}\right) \\ &\quad + \left(S_{H2}(t) - S_{H2}^* - S_{H2}^* \ln\tfrac{S_{H2}(t)}{S_{H2}^*}\right) + \left(I_{H2}(t) - I_{H2}^* - I_{H2}^* \ln\tfrac{I_{H2}(t)}{I_{H2}^*}\right) \\ &\quad + \left(S_A(t) - S_A^* - S_A^* \ln\tfrac{S_A(t)}{S_A^*}\right) + \left(I_A(t) - I_A^* - I_A^* \ln\tfrac{I_A(t)}{I_A^*}\right) \\ &\quad + a_4\left(S_V(t) - S_V^* - S_V^* \ln\tfrac{S_V(t)}{S_V^*}\right) + a_4 e^{\mu_V\tau}\left(I_V(t) - I_V^* - I_V^* \ln\tfrac{I_V(t)}{I_V^*}\right), \end{aligned}\right\} \tag{5.139}$$

where a_4, is a positive constants to be determined. Furthermore:

$$\left.\begin{aligned} U_{41}(t) &= a_4\beta_{HV}\int_{t-\tau}^{t}\left(I_{H1}(\theta)S_V(\theta) - I_{H1}^*S_V^* - I_{H1}^*S_V^* \ln\tfrac{I_{H1}(\theta)S_V(\theta)}{I_{H1}^*S_V^*}\right)d\theta \\ &\quad + a_4(1-\varepsilon_H)\beta_{HV}\int_{t-\tau}^{t}\left(I_{H2}(\theta)S_V(\theta) - I_{H2}^*S_V^* - I_{H2}^*S_V^* \ln\tfrac{I_{H2}(\theta)S_V(\theta)}{I_{H2}^*S_V^*}\right)d\theta \\ &\quad + a_4\beta_{AV}\int_{t-\tau}^{t}\left(I_A(\theta)S_V(\theta) - I_A^*S_V^* - I_A^*S_V^* \ln\tfrac{I_A(\theta)S_V(\theta)}{I_A^*S_V^*}\right)d\theta. \end{aligned}\right\} \tag{5.140}$$

Taking the derivative of $U_{40}(t)$ along the solutions of system (3.5) leads to:

$$\left.\begin{aligned} U'_{40}(t) &= \left(1-\frac{S^*_{H1}}{S_{H1}}\right)\frac{dS_{H1}}{dt}+\left(1-\frac{I^*_{H1}}{I_{H1}}\right)\frac{dI_{H1}}{dt}+\left(1-\frac{S^*_{H2}}{S_{H2}}\right)\frac{dS_{H2}}{dt} \\ &+\left(1-\frac{I^*_{H2}}{I_{H2}}\right)\frac{dI_{H2}}{dt}+\left(1-\frac{S^*_{A}}{S_{A}}\right)\frac{dS_{A}}{dt}+\left(1-\frac{I^*_{A}}{I_{A}}\right)\frac{dI_{A}}{dt} \\ &+\left(1-\frac{S^*_{V}}{S_{V}}\right)\frac{dS_{V}}{dt}+\left(1-\frac{I^*_{V}}{I_{V}}\right)\frac{dI_{V}}{dt}. \end{aligned}\right\} \tag{5.141}$$

Furthermore, differentiating $U_{41}(t)$ along the solutions of system (3.5) gives:

$$\begin{aligned} U'_{41}(t) &= a_4\beta_{HV}\left(I_{H1}(t)S_V(t)-I_{H1}(t)S_V(t)+I^*_{H1}S^*_V\ln\frac{I_{H1}(t-\tau)S_V(t-\tau)}{I_{H1}(t)S_V(t)}\right) \\ &+a_4(1-\varepsilon_H)\beta_{HV}\left(I_{H2}(t)S_V(t)-I_{H2}(t)S_V(t)\right. \\ &\left.+I^*_{H2}S^*_V\ln\frac{I_{H2}(t-\tau)S_V(t-\tau)}{I_{H2}(t)S_V(t)}\right) \\ &+a_4\beta_{AV}\left(I_A(t)S_V(t)-I_A(t)S_V(t)\right. \\ &\left.+I^*_AS^*_V\ln\frac{I_A(t-\tau)S_V(t-\tau)}{I_A(t)S_V(t)}\right). \end{aligned} \tag{5.142}$$

Recall that at endemic equilibrium point the following identities holds:

$$\left.\begin{aligned} p_H\mu_HN_H &= \beta_{VH}f(I^*_V)S^*_{H1}+\mu_HS^*_{H1}, \\ (\mu_H+\gamma_H)I^*_{H1} &= \beta_{VH}f(I^*_V)S^*_{H1}, \\ (1-p_H)\mu_HN_H &= (1-\varepsilon_H)\beta_{VH}f(I^*_V)S^*_{H2}+\mu_HS^*_{H2}, \\ (\mu_h+\gamma_h)I^*_{h2} &= \beta_{vh}f(I^*_v)S^*_{h2}, \\ \mu_AN_A &= \beta_{VA}f(I^*_V)S^*_A+\mu_AS^*_A, \\ (\mu_A+\gamma_A)I^*_A &= \beta_{VA}f(I^*_V)S^*_A, \\ \sigma_LL^* &= (\beta_{HV}I^*_{H1}+(1-\varepsilon_H)\beta_{HV}I^*_{H2}+\beta_{AV}I^*_A)S^*_V+\mu_VS^*_V, \\ \mu_VI^*_Ve^{\mu_V\tau} &= (\beta_{HV}I^*_{H1}+(1-\varepsilon_H)\beta_{HV}I^*_{H2}+\beta_{AV}I^*_A)S^*_V. \end{aligned}\right\}. \tag{5.143}$$

Setting, $a_4 = \frac{\beta_{VH} f(I_V^*) S_{H1}^*}{\beta_{HV} I_{H1}^* S_V^*} + \frac{\beta_{VH} f(I_V^*) S_{H2}^*}{\beta_{HV} I_{H2}^* S_V^*} + \frac{\beta_{VA} f(I_V^*) S_A^*}{\beta_{AV} I_A^* S_V^*}$, and simplifying the Lyapunov gives:

$$\left.\begin{aligned} U_{41}'(t) &= \mu_H S_{H1}^* \left(2 - \frac{S_{H1}^*}{S_{H1}} - \frac{S_{H1}}{S_{H1}^*}\right) + \mu_H S_{H2}^* \left(2 - \frac{S_{H2}^*}{S_{H2}} - \frac{S_{H2}}{S_{H2}^*}\right) \\ &+ \left(\frac{\beta_{VH} f(I_V^*) S_{H1}^*}{\beta_{HV} I_{H1}^* S_V^*} + \frac{\beta_{VH} f(I_V^*) S_{H2}^*}{\beta_{HV} I_{H2}^* S_V^*} + \frac{\beta_{VA} f(I_V^*) S_A^*}{\beta_{AV} I_A^* S_V^*}\right)\left(2 - \frac{S_V^*}{S_V} - \frac{S_V}{S_V^*}\right) \\ &+ \beta_{VH} f(I_V^*) \left(\frac{S_{H2}^* I_{H1}^*}{I_{H2}^*} W_{H1}^1 + \frac{(1-\varepsilon_H) S_{H1}^* I_{H2}^*}{I_{H1}^*} W_{H2}^1\right) \\ &+ \frac{\beta_{HV} \beta_{VA} f(I_V^*) S_A^* I_{H1}^*}{\beta_{AV} I_A^*} W_{H1}^2 + \frac{\beta_{HV}(1-\varepsilon_H) \beta_{VA} f(I_V^*) S_A^* I_{H2}^*}{\beta_{AV} I_A^*} W_{H2}^2 \\ &+ \left(\frac{\beta_{VH} \beta_{AV} f(I_V^*) S_{H1}^* I_A^*}{\beta_{HV} I_{H1}^*} + \frac{\beta_{VH} \beta_{AV} f(I_V^*) S_{H2}^* I_A^*}{\beta_{HV} I_{H2}^*}\right) W_A^2 \\ &+ \beta_{VH} f(I_V^*) S_{H1}^* W_{H1}^3 + \beta_{VH}(1-\varepsilon_H) f(I_V^*) S_{H2}^* W_{H2}^3 + \beta_{VA} f(I_V^*) S_A^* W_A^3, \end{aligned}\right\}. \tag{5.144}$$

with:

$$\left.\begin{aligned} W_i^1 &= 1 - \frac{S_V^*}{S_V} + \frac{I_i}{I_i^*} - \frac{I_i(t-\tau) S_V(t-\tau) I_V^*}{I_i^* S_V^* I_V} + \ln \frac{I_i(t-\tau) S_V(t-\tau)}{I_i(t) S_V(t)}, \\ W_i^2 &= 2 - \frac{S_V^*}{S_V} + \frac{I_i}{I_i^*} - \frac{I_V}{I_V^*} - \frac{I_i(t-\tau) S_V(t-\tau) I_V^*}{I_i^* S_V^* I_V} + \ln \frac{I_i(t-\tau) S_V(t-\tau)}{I_i(t) S_V(t)}, \\ W_i^3 &= 4 - \frac{S_V^*}{S_V} - \frac{I_V}{I_V^*} + \frac{f(I_V)}{f(I_V^*)} - \frac{S_i^*}{S_i} - \frac{f(I_V) S_i I_i^*}{f(I_V^*) S_i^* I_i} - \frac{I_i(t-\tau) S_V(t-\tau) I_V^*}{I_i^* S_V^* I_V} \\ &\quad + \ln \frac{I_i(t-\tau) S_V(t-\tau)}{I_i(t) S_V(t)}, \end{aligned}\right\}. \tag{5.145}$$

for $i = H1, H2, A$.

Since the arithmetic mean is greater than or equal to the geometric mean. Furthermore, note that $G(x) = 1 - g(x) + \ln g(x)$ is always nonpositive for any function $g(x) > 0$, and $g(x) = 0$ if and only if $g(x) = 1$. Hence, it follows that $U_4'(t) \leq 0$. Therefore by the Lasalle Invariance principle (LaSalle, 1976) it follows that the endemic equilibrium point $\mathscr{E}^*$ is globally asymptotically stable if $\mathscr{R}_0 > 1$. This completes the proof. □

RESEARCH OUTPUTS

(i) Publications

Helikumi, M., Kgosimore, M., Kuznetsov, D., & Mushayabasa, S. (2019). Backward Bifurcation and optimal control analysis of a trypanosome brucei rhodesiense mod -el. *Mathematics,* 7(971) 1-16. https:// doi.org/10.3390/math7100971

Helikumi, M., Kgosimore, M., Kuznetsov, D., & Mushayabasa, S. (2020). Dynamical and optimal control analysis of a seasonal Trypanosoma brucei rho desiense model. *Mathematical Biosciences and Engineering,* MBE, 17(3): 2530–2556. https:// doi.org/10.3934/mbe2020139

Helikumi, M., Kgosimore, M., Kuznetsov, D., & Mushayabasa, S. (2020). A fractional-order Trypanosoma brucei rhodesiense model with vector saturation and temperature dependent parameters. *Advances in Difference Equations, 284 1-23*. https:// doi.org/10. 1186/s13662-020-02745-3

(ii) Poster Presentation

Backward Bifurcation and Optimal Control Analysis of a Trypanosoma brucei rhodesiense Model

Article · October 2019

DOI: 10.3390/math7100971

4 authors:

Mlyashimbi Helikumi
Mbeya University of Science and Technology .
5 PUBLICATIONS **8** CITATIONS
SEE PROFILE

Moatlhodi Kgosimore
Botswana University of Agriculture and Natural Resources
29 PUBLICATIONS **157** CITATIONS
SEE PROFILE

Dmitry Kuznetsov
The Nelson Mandela African Institute of Science and Technology
27 PUBLICATIONS **54** CITATIONS
SEE PROFILE

Steady Mushayabasa
University of Zimbabwe
107 PUBLICATIONS **742** CITATIONS
SEE PROFILE

mathematics

MDPI

Article

Backward Bifurcation and Optimal Control Analysis of a *Trypanosoma brucei rhodesiense* Model

Mlyashimbi Helikumi [1,2,*], Moatlhodi Kgosimore [3], Dmitry Kuznetsov [1] and Steady Mushayabasa [4,*]

[1] School of Computational and Communication Science and Engineering, The Nelson Mandela African Institution of Science and Technology, P.O. Box 447 Arusha, Tanzania; dmitry.kuznetsov@nm-aist.ac.tz
[2] Department of Natural Sciences, College of Science and Technical Education, Mbeya University of Science and Technology, P.O. Box 131 Mbeya, Tanzania
[3] Department of Basic Sciences, Botswana University of Agriculture and Natural Resources, Private Bag 0027, Gaborone, Botswana; mkgosi@buan.ac.bw
[4] Department of Mathematics, University of Zimbabwe, P.O. Box MP 167 Harare, Zimbabwe
* Correspondence: helikumim@nm-aist.ac.tz (M.H.); steadymushaya@gmail.com (S.M.)

Received: 9 September 2019; Accepted: 10 October 2019; Published: 14 October 2019

Abstract: In this paper, a mathematical model for the transmission dynamics of *Trypanosoma brucei rhodesiense* that incorporates three species—namely, human, animal and vector—is formulated and analyzed. Two controls representing awareness campaigns and insecticide use are investigated in order to minimize the number of infected hosts in the population and the cost of implementation. Qualitative analysis of the model showed that it exhibited backward bifurcation generated by awareness campaigns. From the optimal control analysis we observed that optimal awareness and insecticide use could lead to effective control of the disease even when they were implemented at low intensities. In addition, it was noted that insecticide control had a greater impact on minimizing the spread of the disease compared to awareness campaigns.

Keywords: human African trypanosomiasis; mathematical model; awareness programs; insecticide use; optimal control theory

MSC: 92B05; 93A30; 93C15

1. Introduction

Human African trypanosomiasis (HAT) is one of the neglected tropical diseases (NTDs) that affect humans and animals in sub-Saharan Africa [1]. More than 20 species of *Glossina* tsetse flies are responsible for the transmission of the two parasites associated with the disease: *Trypanosoma brucei rhodesiense*and *Trypanosoma brucei gambiense* [1]. Although these two parasites represent different pathological entities, they are both classified under the term HAT [2]. *T.b. gambiense* is found in West and Central Africa, while *T.b. rhodesiense* occurs only in the East and South of the African continent [1]. Global estimates report 70,000 HAT cases (range: 50,000–70,000) based on a total number of 17,500 new cases reported per year worldwide [3]. With more than 60 million in sub-Saharan Africa considered to be at risk of infection, how to prevent, control and possibly eradicate this disease remains one of the important topics from many points of view, including medical science and mathematics.

Since the pioneering work of Kermack and McKendrick [4] on compartment modeling, numerous mathematical models have been proposed to investigate the transmission dynamics of several infectious diseases (e.g., [5–11] and references therein). These studies and several other models have certainly produced many useful results and improved the existing knowledge on several infectious diseases, such that mathematical modeling has become an important tool in analyzing the spread and

control of infectious diseases. In particular, several mathematical models have already been proposed to investigate the complex epidemic and endemic behavior of human African trypanosomiasis [12–27]. For example, Hargrove et al. [12] modeled the control of trypanosomiasis caused by *Trypanosoma brucei rhodesiense* in multiple hosts. Their model predicted that treating cattle with insecticide would be generally more effective than treating cattle with drugs. In addition, Moore et al. [14] utilized a system of ordinary differential equations to explore the impact of climate change on *Trypanosoma brucei rhodesiense* dynamics. Results from their framework suggested that climate change could lead to 46–77 million additional people being at risk of exposure to HAT infection by 2090. These studies and those cited therein have undeniably produced many useful results and improved the existing knowledge on HAT dynamics.

Despite these efforts in the modeling and analysis of *Trypanosoma brucei rhodesiense* dynamics, several important questions regarding the transmission and control of the disease remain to be answered. For example, to what extent will awareness and insecticide use combined alter short- and long-term transmission and control of HAT? Thanks to Hargrove and co-workers [12], we are now aware that insecticide use has a greater impact on controlling the disease compared with the treatment of cattle with drugs. The key question is, if this intervention were to be combined with awareness campaigns, would this approach yield a significant change in *Trypanosoma brucei rhodesiense*? This is the key question that this study aimed to explore. There is no doubt that continuous advancement in information and communication technology (ICT) in recent years has greatly improved the level of information dissemination. In addition, media campaigns are known to be useful public health tools globally [28,29]. In particular, mass media campaigns have the potential to alter people's health behavior in the absence of multiple channels of communication [29,30]. Therefore, as suggested by Leak [31], understanding the impact of these intervention strategies on disease and vector population dynamics is a potential area for modeling and further development of existing models. Motivated by the discussion above, in this paper we seek to use optimal control theory to investigate the effects of awareness campaigns and insecticide use on the spread and control of *Trypanosoma brucei rhodesiense*. Stone and Chitnis' [16] model of HAT transmission, which does not incorporate an animal reservoir, does not effectively capture the dynamics of the disease. Hence, we propose a framework that demonstrates interplay between the vectors and multiple host species (human and animals). By incorporating the vectors and multiple hosts, our framework will be isomorphic to some of the earlier studies [12,14,16,23,27].

This paper is organized as follows. In Section 2, the methods and results of the study are presented. in particular, the *Trypanosoma brucei rhodesiense* model is formulated and analyzed. The analysis included the computation of the basic reproduction number and the existence of model steady states. The impact of two controls—awareness campaigns and insecticide use—as disease control measures against *Trypanosoma brucei rhodesiense* infection was also investigated. In addition, numerical simulations were conducted to support analytical findings. Finally, discussion and conclusions round up the paper.

2. Methods and Results

2.1. Model Formulation

The proposed model considers two hosts (i.e., animals and humans), subdivided into: susceptible $S_i(t)$, clinically infected $I_i(t)$ and removed $R_i(t)$, for $i = a$ and h - representing the animal and human, respectively. Thus the host population at time t is given by $N_i = S_i(t) + I_i(t) + R_i(t)$. Furthermore, the total tsetse vector population at time, denoted by $N_v(t)$, constitutes the susceptible $S_v(t)$ and infectious $I_v(t)$ populations. Once infected, vectors are assumed to remain infectious for their entire lifetime. Through mass media campaigns humans are assumed to become aware of the disease and those who become aware are assumed to have negligible chances of being infected. Hence, in our framework we introduced a constant rate θ_h to account for the transition of individuals from the susceptible compartment to the removed class. Thus, the removed compartment for humans comprises

individuals who were successfully treated and those who have become aware of the disease. With the passage of time these individuals may lose their awareness and become susceptible to infection again. In order to model disease transmission from the host to the vector and vice versa, we propose the following forces of infection:

$$\lambda_h(t) = \frac{\beta_{vh} I_v(t)}{N_v(t)}, \qquad \lambda_a(t) = \frac{\beta_{va} I_v(t)}{N_v(t)}, \qquad \lambda_v(t) = \frac{\beta_{hv} I_h(t)}{N_h(t)} + \frac{\beta_{av} I_a(t)}{N_a(t)},$$

where parameter β_{vi} $(i = a, h)$ denotes the transmission rate of HAT disease from an infected tsetse vector to a susceptible host i given that effective contact between the two occurs; β_{iv} represents disease transmission from infected host i to a susceptible vector given that effective contact between the two occurs. In addition, parameters μ_a, μ_h and μ_v represent the inflow of new individuals into the susceptible animal, human and vector populations, respectively, through birth, and are assumed to be equal to the natural mortality rates for each population. There is no vertical transmission of the disease in either the host or vector. Infected animals and humans recover at rates α_a and α_h, respectively, and they become susceptible to infection at rates γ_a and γ_h, respectively.

The proposed model is summarized by the following equations, where the prime $(')$ denotes the derivative of the component with respect to time:

$$\begin{cases} S_h'(t) &= \mu_h N_h(t) - \lambda_h(t) S_h(t) - (\mu_h + \theta_h) S_h(t) + \gamma_h R_h(t), \\ I_h'(t) &= \lambda_h(t) S_h(t) - (\mu_h + \alpha_h) I_h(t), \\ R_h'(t) &= \theta_h S_h(t) + \alpha_h I_h(t) - (\mu_h + \gamma_h) R_h(t), \\ S_a'(t) &= \mu_a N_a(t) - \lambda_a(t) S_a(t) - \mu_a S_a(t) + \gamma_a R_a(t), \\ I_a'(t) &= \lambda_a(t) S_a(t) - (\mu_a + \alpha_a) I_a(t), \\ R_a'(t) &= \alpha_a I_a(t) - (\mu_a + \gamma_a) R_a(t), \\ S_v'(t) &= \mu_v N_v(t) - \lambda_v(t) S_v(t) - \mu_v S_v(t), \\ I_v'(t) &= \lambda_v(t) S_v(t) - \mu_v I_v(t). \end{cases} \tag{1}$$

Table 1 presents the model parameters and their baseline values. The baseline values for these parameters were adopted from the work of Moore et al. [14] and Ndondo et al. [23]. In their studies, Moore et al. [14] and Ndondo et al. [23] proposed mathematical models with interplay between the vectors and multiple host species. In particular, the host species considered were humans and animals (cattle), hence the parameter values from these studies can also be used in this study.

Table 1. Description of parameters used in system (1). HAT: human African trypanosomiasis.

Symbol	Description	Value	Units	
β_{hv}	Transmission rate of HAT disease from infected human to susceptible vector	0.011715	day^{-1}	[14]
β_{av}	Transmission rate of HAT disease from infected animal to susceptible vector	0.011715	day^{-1}	[14]
β_{vh}	Transmission rate of HAT disease from infected vector to susceptible human	0.002739	day^{-1}	[14]
β_{va}	Transmission rate of HAT disease from infected vector to susceptible animal	0.002739	day^{-1}	[14]
γ_h	Progression rate of human population from recovered to susceptible class	$\frac{1}{90}$	day^{-1}	[23]
γ_a	Progression rate of animal population from recovered to susceptible class	$\frac{1}{75}$	day^{-1}	[23]
θ_h	Rate at which humans become aware of the disease	0.2	day^{-1}	
μ_h	Natural mortality rate of human population	$\frac{1}{365 \times 50}$	day^{-1}	[23]
μ_a	Natural mortality rate of animal population	$\frac{1}{365 \times 15}$	day^{-1}	[23]
μ_v	Natural mortality rate of vector population	$\frac{1}{33}$	day^{-1}	[23]
α_h	Recovery rate of infected human	$\frac{1}{30}$	day^{-1}	[23]
α_a	Recovery rate of infected animal	$\frac{1}{25}$	day^{-1}	[23]

From (1) we have $N_i'(t) = 0$ for $i = a, h, v$, hence without loss of generality we can use a dimensionless system to explore the dynamics of the disease. Now, to normalize the populations, let

$$\begin{aligned} s_h(t) &= \frac{S_h(t)}{N_h}, \quad i_h(t) = \frac{I_h(t)}{N_h}, \quad r_h(t) = \frac{R_h(t)}{N_h}, \quad s_a(t) = \frac{S_a(t)}{N_a}, \\ i_a(t) &= \frac{I_a(t)}{N_a}, \quad r_a(t) = \frac{R_a(t)}{N_a}, \quad s_v(t) = \frac{S_v(t)}{N_v}, \quad i_v(t) = \frac{I_v(t)}{N_v}. \end{aligned}$$

Therefore, the dimensionless system has the form:

$$\left\{ \begin{array}{rcl} s_h'(t) &=& \mu_h - \beta_{vh} i_v(t) s_h(t) - (\mu_h + \theta_h) s_h(t) + \gamma_h r_h(t), \\ i_h'(t) &=& \beta_{vh} i_v(t) s_h(t) - (\mu_h + \alpha_h) i_h(t), \\ r_h'(t) &=& \theta_h s_h(t) + \alpha_h i_h(t) - (\mu_h + \gamma_h) r_h(t), \\ s_a'(t) &=& \mu_a - \beta_{va} i_v(t) s_a(t) - \mu_a s_a(t) + \gamma_a r_a(t), \\ i_a'(t) &=& \beta_{va} i_v(t) s_a(t) - (\mu_a + \alpha_a) i_a(t), \\ r_a'(t) &=& \alpha_a i_a(t) - (\mu_a + \gamma_a) r_a(t), \\ s_v'(t) &=& \mu_v - (\beta_{hv} i_h(t) + \beta_{av} i_a(t)) s_v(t) - \mu_v s_v(t), \\ i_v'(t) &=& (\beta_{hv} i_h(t) + \beta_{av} i_a(t)) s_v(t) - \mu_v i_v(t). \end{array} \right. \tag{2}$$

Furthermore, by using the relations $r_h(t) = 1 - s_h(t) - i_h(t)$, $s_a = 1 - i_a(t) - r_a(t)$ and $s_v = 1 - i_v(t)$, system (2) reduces to

$$\left\{ \begin{array}{rl} s'(t) &= \mu_h - \beta_{vh} i_v(t) s_h(t) - (\mu_h + \theta_h) s_h(t) + \gamma_h (1 - s_h(t) - i_h(t)), \\ i_h'(t) &= \beta_{vh} i_v(t) s_h(t) - (\mu_h + \alpha_h) i_h(t), \\ i_a'(t) &= \beta_{va} i_v (1 - i_a(t) - r_a(t)) - (\mu_a + \alpha_a) i_a(t), \\ r_a'(t) &= \alpha_a i_a(t) - (\mu_a + \gamma_a) r_a(t), \\ i_v'(t) &= (\beta_{hv} i_h(t) + \beta_{av} i_a(t)) (1 - i_v(t)) - \mu_v i_v(t). \end{array} \right. \tag{3}$$

2.2. Positivity and Boundedness of Solutions

Model (3) is epidemiologically and mathematically well-posed in the domain:

$$\Omega = \left\{ \left(s_h, i_h, i_a, r_a, i_v \right) \in \mathbb{R}_+^5 \middle| s_h, i_h \geq 0,\ s_h + i_h \leq 1,\ i_a, r_a \geq 0,\ i_a + r_a \leq 1,\ 0 \leq i_v \leq 1 \right\}.$$

The domain, Ω, is valid epidemiologically as the normalized populations, s_h, i_h, i_a, r_a and i_v, are all non-negative and have sums over their species type that are less than or equal to unity.

Theorem 1. *Assuming that the initial conditions lie in Ω, the system of equations for the HAT model (3) has a unique solution that exists and remains in Ω for all time $t \geq 0$.*

Proof. The right-hand side of model (3) is continuous with continuous partial derivatives in Ω, so system (3) has a unique solution. In what follows we demonstrate that Ω is forward-invariant. It can easily be observed from (3) that if $s_h = 0$, then $s_h'(t) = \mu_h + \gamma_h(1 - i_h(t)) \geq 0$; if $i_h = 0$, then $i_h'(t) = \beta_{vh} i_v(t) s_h(t) \geq 0$; if $i_a = 0$, then $i_a'(t) = \beta_{va} i_v(t)(1 - r_a(t)) \geq 0$; if $r_a = 0$, then $r_a'(t) = \alpha_a i_a(t) \geq 0$; and if $i_v = 0$, then $i_v' = (\beta_{hv} i_h(t) + \beta_{av} i_a(t)) \geq 0$. It is also true that if $s_h(t) + i_h(t) = 1$ then $s_h'(t) + i_h'(t) < 0$, if $i_a(t) + r_a(t) = 1$ then $i_a'(t) + r_a'(t) < 0$ and if $i_v(t) = 1$ then $i_v'(t) < 0$. Therefore, none of the orbits can leave Ω and a unique solution exists for all time. □

2.3. The Basic Reproduction Number

In the absence of the disease in the community, model (3) admits a trivial equilibrium also known as the disease-free equilibrium (DFE), denoted by $\mathcal{E}^0$ and given by

$$\mathcal{E}^0 = \left(s_h^0, i_h^0, i_a^0, r_a^0, i_v^0\right) = \left(\frac{(\mu_h + \gamma_h)}{(\mu_h + \theta_h + \gamma_h)}, 0, 0, 0, 0\right).$$

Next, we determine the power of the disease to invade the population by computing the reproduction number $\mathcal{R}_0$. Here, the basic reproduction number $\mathcal{R}_0$ is defined as the expected number of secondary cases (vector, animal or humans) produced in a completely susceptible population, by one infectious individual (tsetse, animal or human, respectively) during its lifetime as infectious. To determine $\mathcal{R}_0$, we follow the next-generation matrix approach and notations in [32]. Thus, the non-negative matrix $\mathcal{F}$ that denotes the generation of new infection and the non-singular matrix $\mathcal{V}$ that denotes the disease transfer among compartments evaluated at $\mathcal{E}^0$ are respectively given by:

$$\mathcal{F} = \begin{pmatrix} 0 & 0 & \dfrac{\beta_{vh}(\mu_h + \gamma_h)}{(\mu_h + \gamma_h + \theta_h)} \\ 0 & 0 & \beta_{va} \\ \beta_{hv} & \beta_{av} & 0 \end{pmatrix} \quad \text{and} \quad \mathcal{V} = \begin{pmatrix} \mu_h + \alpha_h & 0 & 0 \\ 0 & \mu_a + \alpha_a & 0 \\ 0 & 0 & \mu_v \end{pmatrix}.$$

It follows that the basic reproductive number is the spectral radius of the next-generation matrix (i.e., $\rho(\mathcal{F}\mathcal{V}^{-1})$), and is given by

$$\begin{aligned} \mathcal{R}_0 &= \sqrt{\left(\frac{\beta_{vh}\beta_{vh}(\mu_h + \gamma_h)}{\mu_v(\mu_h + \alpha_h)(\mu_h + \gamma_h + \theta_h)}\right) + \left(\frac{\beta_{av}\beta_{va}}{\mu_v(\mu_a + \alpha_a)}\right)} \\ &= \sqrt{\mathcal{R}_{0h} + \mathcal{R}_{0a}}, \end{aligned}$$

where $\mathcal{R}_{0h}$ represents the basic reproduction number of the human–vector infection and $\mathcal{R}_{0a}$ is the basic reproduction number of animal–vector infection.

2.4. Existence and Uniqueness of the Endemic Equilibria

Let $\mathcal{E}^* = (s_h^*, i_h^*, i_a^*, r_a^*, i_v^*)$ be any endemic equilibrium of model (3). Solving the first four equations of system (3) in terms of i_v^* one gets the following results:

$$\begin{cases} s_h^* = \dfrac{m_2 m_3}{m_2(m_1 + \gamma_h) + \beta_{vh} i_v^*(m_2 + \gamma_h)}, & i_h^* = \dfrac{\beta_{vh} i_v^* m_3}{m_2(m_1 + \gamma_h) + \beta_{vh} i_v^*(m_2 + \gamma_h)}, \\ i_a^* = \dfrac{\beta_{va} i_v^* m_5}{m_4 m_5 + \beta_{va} i_v^*(\alpha_a + m_5)}, & r_a^* = \dfrac{\beta_{va} i_v^* \alpha_a}{m_4 m_5 + \beta_{va} i_v^*(\alpha_a + m_5)}, \end{cases}$$

with

$$\begin{aligned} m_1 &= (\mu_h + \theta_h), \quad m_2 = (\mu + \alpha_h), \quad m_3 = (\mu_h + \gamma_h), \\ m_4 &= (\mu_a + \alpha_a), \quad m_5 = (\mu_a + \gamma_a). \end{aligned}$$

Substituting i_h^* and i_a^* into the last equation of (3) yields

$$g(i_v^*) = A(i_v^*)^2 + Bi_v^* + C = 0, \tag{4}$$

where

$$\begin{aligned} A &= \beta_{vh}\beta_{va}[m_2(\alpha_a\mu_v + m_5(\mu_v + \beta_{av})) + \beta_{hv}m_3(\alpha_a + m_5) + \gamma_h(\alpha_a\mu_v + m_5(\mu_v + \beta_{av}))], \\ B &= \beta_{va}(m_1m_2(\mu_v\alpha_a + m_5(\mu_v + \beta_{av})) - \beta_{vh}\beta_{hv}m_3(\beta_{va}(\alpha_a + m_5) - m_4m_5) \\ &\quad -\beta_{vh}m_5\gamma_h(\beta_{av}\beta_{va} - m_4\mu_v) + m_2(m_4m_5\mu_v\beta_{vh} + \beta_{va}(\mu_v\alpha_a\gamma_h + m_5(\mu_v\gamma_h + \beta_{av}(\gamma_h - \beta_{vh})))), \\ &\quad -\beta_{vh}(\beta_{hv} + \beta_{av})))] + \alpha_h m_4\beta_{vh}(m_3(\mu_v + \delta_v) - \beta_{va}\beta_{av}), \\ C &= m_2m_4m_5\mu_v(m_1 + \gamma_h)(1 - \mathcal{R}_0^2). \end{aligned}$$

Based on the fact that all parameters in (3) are positive for $t \geq 0$, it follows from (4) that $A > 0$. Furthermore, $C > 0$ when $\mathcal{R}_0 < 1$. Therefore the number of possible positive real roots the polynomial (4) hinges on the signs of B and C. By applying the Descartes rule of signs on the quadratic equation $g(i_v^*) = 0$, given in (4), we list the various possibilities for the roots of $g(i_v^*)$ in Table 2.

Table 2. Number of possible positive real roots of $g(i_v^*)$ given in (4) for $\mathcal{R}_0 < 1$ and $\mathcal{R}_0 > 1$.

Case	*A*	*B*	*C*	Reproduction Number	No. of Sign Changes	No. of Possible Positive Real Roots
1	+	+	+	$\mathcal{R}_0 < 1$	0	0
2	+	+	-	$\mathcal{R}_0 > 1$	1	1
3	+	-	+	$\mathcal{R}_0 < 1$	2	0,2
4	+	-	-	$\mathcal{R}_0 > 1$	1	1

Based on the different possibilities presented in Table 2, we have the following results:

Theorem 2. *The model (3) admits:*

(i) A unique endemic equilibrium $\mathcal{E}^*$ if $\mathcal{R}_0 > 1$ and cases 2 and 4 are satisfied;

(ii) More than one endemic equilibrium if $\mathcal{R}_0 < 1$ and part of case 3 holds;

(iii) No endemic equilibrium if $\mathcal{R}_0 < 1$, and cases 1 and part of case 3 are satisfied.

The occurrence of a backward bifurcation, where a stable disease-free equilibrium coexists with a stable endemic equilibrium, is a common phenomenon in vector-borne disease models—more often for model that incorporates disease-related death for the host [33]. Since model (3) has disease-related death for both animals and humans, in what follows we check if the model does indeed have a backward bifurcation. To investigate the possibility of this phenomenon, the discriminant of Equation (4) is set to zero ($B^2 - 4AC = 0$) and solved to determine the critical value of $\mathcal{R}_0$, denoted by $\mathcal{R}_{0c}$, as follows:

$$\mathcal{R}_{0c} = \sqrt{1 - \frac{B^2}{4Am_2m_4m_5m_6(m_1 + \gamma_h)}}. \tag{5}$$

Numerical illustration in Figure 1 were performed using data in Table 1 in order to demonstrate that if $\mathcal{R}_0 < 1$ model (3) exhibits a backward bifurcation and for $\mathcal{R}_0 > 1$ the model admits a forward bifurcation. We have also noted that the switch occurs when $\theta_h = 0.764$, thus, $\mathcal{R}_{0c} = 0.139 < 1$. Overall, we conclude that the model has two endemic equilibria—one stable and the other unstable. As $\mathcal{R}_0$ approaches one, the unstable endemic equilibrium loses its nature and coalesces with the disease-free equilibrium at $\mathcal{R}_0 = 1$.

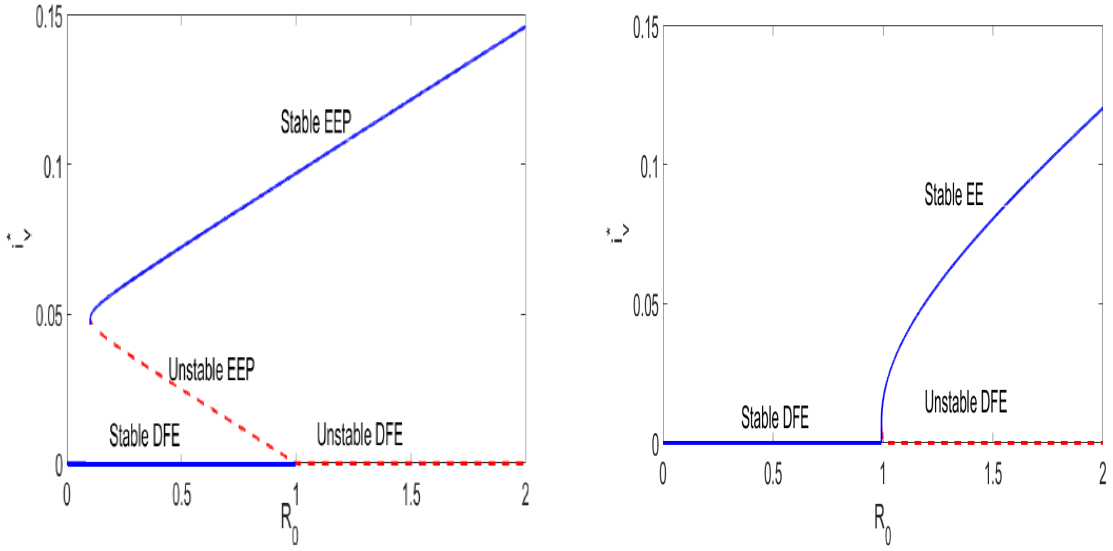

(**a**) (**b**)

Figure 1. Graphical results illustrating the possible bifurcations for model (3) for different values of awareness campaigns θ_h. The figures were generated with parameter values taken from Table 1. Parameters different from those listed in Table 1 are $\beta_{hv} = \beta_{av} = 0.65$, $\beta_{vh} = \beta_{va} = 0.4$. In (**a**) we set $\theta_h = 0.764$ and in (**b**) $\theta_h = 0.857$. For $\mathcal{R}_0 < 1$, the model has two endemic equilibria: one stable and the other unstable. As $\mathcal{R}_0$ approaches one the unstable endemic equilibrium loses its nature and coalesces with the disease-free equilibrium at $\mathcal{R}_0 = 1$. Therefore, we conclude that the model admits a backward bifurcation whenever $\mathcal{R}_0 < 1$ and a forward bifurcation for $\mathcal{R}_0 > 1$.

2.5. Optimal Control

Although there is no vaccine or drug for prophylaxis against African trypanosomiasis, there are other preventative and treatment options. HAT preventative strategies aim to minimize contact between the hosts and vectors. Humans can minimize contact with the tsetse vector by: using insect repellents, avoiding bushy areas, and wearing long-sleeved garments of medium-weight material in neutral colors that blend with the background environment. Spraying domesticated animals with insecticides also minimizes contact between the vector and the animals. Drugs can also be used to treat infected host species. Above all, the success of both preventative and corrective mechanisms revolves around the level of awareness of the human population. Through awareness, humans can effectively reduce contact between the vectors and multiple species. Thus, in this section we explore the impact of time-dependent awareness campaigns and time-dependent insecticides use on the dynamics of *Trypanosoma brucei rhodesiense*.

In order to investigate the effects of the aforementioned optimal control strategy, we reformulate system (3) to include time-dependent media campaigns $u_1(t)$ and insecticide use $u_2(t)$. The controls, $u_1(t)$ and $u_2(t)$, are functions of time and will be assigned reasonable upper and lower bounds. Furthermore, we also introduce an additional constant parameter δ to account for tsetse insecticide-induced mortality at the maximum possible rate. Using the same variable and parameter names as in (3), the system of differential equations describing our model with controls is:

$$\begin{cases} s_h'(t) &= \mu_h - \beta_{vh} i_v(t) s_h(t) - (\mu_h + u_1(t)\theta_h) s_h(t) + \gamma_h (1 - s_h(t) - i_h(t)), \\ i_h'(t) &= \beta_{vh} i_v(t) s_h(t) - (\mu_h + \alpha_h + d_h) i_h(t), \\ i_a'(t) &= \beta_{va} i_v(t)(1 - i_a(t) - r_a(t)) - (\mu_a + \alpha_a + d_a) i_a(t), \\ r_a'(t) &= \alpha_a(t) i_a(t) - (\mu_a + \gamma_a) r_a(t), \\ i_v'(t) &= (\beta_{hv} i_h(t) + \beta_{av} i_a(t))\,(1 - i_v(t)) - (\mu_v + u_2(t)\delta_v) i_v(t). \end{cases} \tag{6}$$

A successful control is one that minimizes the proportion of infected host (humans and animal), while minimizing the costs associated with these efforts. Thus, our goal is to find a control pair (u_1^*, u_2^*) that minimizes the proportion of infected host over a finite time interval $[0, t_f]$ at minimal cost. Mathematically, the objective functional is proposed as follows:

$$J(u_1(t), u_2(t)) = \int_0^{t_f} \left(c_1 i_h(t) + c_2 i_a(t) + \frac{w_1}{2} u_1^2(t) + \frac{w_2}{2} u_2^2(t) \right) dt, \tag{7}$$

subject to the constraints of the ODEs in system (6) and where c_1, c_2, w_1 and w_2 are positive constants also known as the balancing coefficients and their goal is to transfer the integral into monetary quantity over a finite time interval $[0, t_f]$. In (7) control efforts are assumed to be nonlinear-quadratic, since a quadratic structure in the control has mathematical advantages, such as: if the control set is compact and convex it follows that the Hamiltonian attains its minimum over the control set at a unique point [34]. The optimal control problem becomes seeking an optimal function, $(u_1^*(t), u_2^*(t))$, such that

$$J(u_1^*(t), u_2^*(t)) = \inf_{(u_1, u_2) \in U} J(u_1(t), u_2(t)) \tag{8}$$

for the admissible set $U = \{(u_1(t), u_2(t)) \in (L^\infty(0, t_f))^2 : 0 \leq u_i(t) \leq q_i; q_i \in \mathbb{R}^+, i = 1, 2\}$, where q_i denotes the upper bound of the controls.

2.5.1. Existence and Uniqueness Results

The following theorem proves the existence of the optimal controls.

Theorem 3. *There exists an optimal control pair $(u_1^*, u_2^*) \in U$ with corresponding non-negative states $(s_h^*, i_h^*, i_a^*, r_a^*, i_v^*)$ that minimizes the objective functional $J(u_1(t), u_2(t))$.*

Proof. The uniform boundedness and the positivity of the controls and state variables over the finite interval $[0, t_f]$ imply that there exists a minimizing sequence $(u_1^n(t), u_2^n(t))$ such that

$$\lim_{n \to \infty} J(u_1^n(t), u_2^n(t)) = \inf_{(u_1(t), u_2(t)) \in U} J(u_1(t), u_2(t)).$$

Let the corresponding sequence of state variables be denoted by $(s_h, i_h, i_a, r_a, i_v)$. Furthermore, the boundedness of all the state and control variables implies that all the derivatives of the state variables are also bounded. Hence, it follows that all state variables are Lipschitz continuous with the same Lipschitz constant. Thus, the sequence $(s_h, i_h, i_a, r_a, i_v)$ is uniformly equicontinuous in $[0, t_f]$. By the Arzela–Ascoli Theorem [35], it follows that the state sequence has a subsequence that converges uniformly to $(s_h, i_h, i_a, r_a, i_v)$ in $[0, t_f]$.

In addition, we can establish that the control sequence $u^n = (u_1^n(t), u_2^n(t))$ has a subsequence that converges weakly in $L^2(0, t_f)$. Let $(u_1^*, u_2^*) \in U$ be such that $u_i^n \rightharpoonup u_i^*$ weakly in $L^2(0, t_f)$ for $i = 1, 2$. Applying the lower semi-continuity of norms in weak L^2, one gets

$$\|u_i^*\|_{L^2}^2 \leq \lim_{n \to \infty} \inf \|u_i^n(t)\|_{L^2}^2, \qquad \text{for} \quad i = 1, 2.$$

Hence,

$$\begin{aligned} J(u_1^*, u_2^*) &\leq \lim_{n \to \infty} \int_0^{t_f} \left(c_1 i_h^n(t) + c_2 i_a^n(t) + \frac{w_1}{2} u_1^n(t) + \frac{w_2}{2} u_2^n(t) \right) dt \\ &= \lim_{n \to \infty} J(u_1^n, u_2^n). \end{aligned}$$

Therefore we conclude that there exists a pair of controls (u_1^*, u_2^*) that minimizes the objective functional $J(u_1(t), u_2(t))$. □

In what follows we characterize the optimal control pair by utilizing Pontryagin's Maximum Principle [36].

2.5.2. Characterization of an Optimal Control Pair

Since there exists an optimal control pair for minimizing the functional (7) subject to the constraints of the ODEs in system (6), we now apply Pontryagin's Maximum Principle [36] to derive the necessary conditions for this optimal control pair. Thus, system (6) is converted into an equivalent problem, namely, the problem of minimizing the Hamiltonian $H(t)$ given by:

$$\begin{aligned} H(t) &= c_1 i_h(t) + c_2 i_a(t) + \frac{w_1}{2}u_1^2(t) + \frac{w_2}{2}u_2^2(t) \\ &+\lambda_1(t)\Big[\mu_h - \beta_{vh} i_v(t) s_h(t) - (\mu_h + u_1(t)\theta_h) s_h(t) + \gamma_h(1 - s_h(t) - i_h(t))\Big] \\ &+\lambda_2(t)\Big[\beta_{vh} i_v(t) s_h(t) - (\mu_h + \alpha_h + d_h) i_h(t)\Big] \\ &+\lambda_3(t)\Big[\beta_{va} i_v(t)(1 - i_a(t) - r_a(t)) - (\mu_a + \alpha_a + d_a) i_a(t)\Big] \\ &+\lambda_4(t)\Big[\alpha_a i_a(t) - (\mu_a + \gamma_a) r_a(t)\Big] \\ &+\lambda_5(t)\Big[\left(\beta_{hv} i_h(t) + \beta_{av} i_a(t)\right)(1 - i_v(t)) - (\mu_v + u_2(t)\delta_v) i_v(t)\Big]. \end{aligned}$$

Given an optimal control pair (u_1^*, u_2^*) and solutions $(s_h, i_h, i_a, r_a, i_v)$, of the corresponding states system (6) there exist adjoint functions $\lambda_i(t)$, $(i = 1, 2, 3, 4, 5)$ [37], satisfying

$$\begin{aligned} \lambda_1'(t) &= \lambda_1(t)(\mu_h + u_1(t)\theta_h + \gamma_h + \beta_{vh} i_v(t)) - \lambda_2(t)\beta_{vh} i_v(t), \\ \lambda_2'(t) &= -c_1 + \lambda_1(t)\gamma_h + \lambda_2(t)(\mu_h + \alpha_h + d_h) - \lambda_5(t)\beta_{hv}(1 - i_h(t)), \\ \lambda_3'(t) &= -c_2 + \lambda_3(t)(\mu_a + \alpha_a + \beta_{va} i_v(t)) - \lambda_4(t)\alpha_a - \lambda_5(t)\beta_{av}(1 - i_v(t)), \\ \lambda_4'(t) &= \lambda_3(t)\beta_{va} i_v(t) + \lambda_4(t)(\mu_a + \gamma_a), \\ \lambda_5'(t) &= (\lambda_1(t) - \lambda_2(t))\beta_{vh} - \lambda_3(t)\beta_{va}(1 - i_a(t) - r_a(t)) + \lambda_5(t)(\mu_v + u_2(t)\delta + \beta_{hv} i_h(t) + \beta_{av} i_a(t)), \end{aligned}$$

with transversality conditions $\lambda_j(t_f) = 0$ for $j = 1, 2, 3, 4, 5$. Furthermore, the optimal solutions of the Hamiltonian are determined by taking the partial derivatives of the function $H(t)$ in (9) with respect to control functions u_1 and u_2, followed by setting the resultant equation to zero and then solving for u_1^* and u_2^*, as follows:

$$\frac{\partial H}{\partial u_1} = u_1^* w_1 - \lambda_1 \theta_h s_h, \qquad \text{and} \qquad \frac{\partial H}{\partial u_2} = u_2^* w_2 - \lambda_5 \delta_v i_v. \tag{9}$$

Setting (9) to zero and solving for u_1^* and u_2^*, one gets

$$u_1^* = \frac{\theta_h s_h \lambda_1}{w_1}, \qquad u_2^* = \frac{\delta_v i_v \lambda_5}{w_2}.$$

Using the standard arguments and the bounds for the controls, we obtain the characterization of this optimal pair as follows:

$$u_1(t) = \min\left\{q_1, \max\left(0, \frac{\theta_h s_h \lambda_1}{w_1}\right)\right\}, \qquad u_2(t) = \min\left\{q_2, \max\left(0, \frac{\delta_v i_v(t) \lambda_5}{w_2}\right)\right\}.$$

In what follows, we numerically investigate the impact of awareness campaigns and insecticide use using the forward–backward sweep algorithm as outlined in [37]. We set $c_1 = 2c_2$, implying that the minimization of the infected humans has more importance/weight compared to that of infected animals. Furthermore, we assumed that the intensity of implementation of awareness campaigns was

always higher than that of insecticide use since excessive insecticide use is associated with ecological side effects, hence their usage should always be kept as low as possible [38]. Thus, u_1 was assumed to be greater than u_2. It was also hypothetically assumed that the cost of insecticide use was higher than awareness campaign costs. The initial population levels were set as follows: $s_h = 0.99$, $i_h = 0.01$, $r_h = 0$, $i_a = 0.01$, $r_a = 0$, $i_v = 0.01$, that is, each species comprised 1% of the infected population and no recoveries for the hosts. Also, we assumed that $\delta_v = 1$ per day. The total number of new infections generated within the human population in the presence and absence of optimal control is:

$$T_h = \int_0^{t_f} \left(\beta_{vh} i_v(t) N_v s_v(t) N_h \right) dt.$$

Similarly, the total number of new infections generated within the animal population in the presence and absence of optimal control is:

$$T_a = \int_0^{t_f} \left(\beta_{va} i_v(t) N_v (1 - i_a(t) - r_a(t)) N_a \right) dt,$$

where N_h, N_a and N_v are constants and are equivalent to 100,000, 10,000 and 50,000, respectively. Figure 2 shows the dynamics of *Trypanosoma brucei rhodesiense* with $u_1 = 0.45$ and $u_2 = 0.3$. We can observe that in the presence of optimal intervention strategies, the proportion of infectious hosts and vectors would never exceed the initial assumed population levels (1%). In particular, in the presence of optimal awareness and insecticides use, the population levels for the hosts and vectors converged to the disease-free equilibrium suggesting that the aforementioned optimal control mechanisms could lead to disease eradication. Precisely, we noted that in the presence of optimal control, the total numbers of new infections for the human and animal populations generated over 300 days were 2.5635×10^5, 9.7×10^4, respectively, and the total cost was $J = 6.5028 \times 10^4$. However, in the absence of optimal controls (i.e., $u_1 = u_2 = 0$), one can observe that the disease persisted. In Figure 2d, we observe that the control profiles of u_1 and u_2 started at the maximum, and they remained there for approximately 200 and 250 days, respectively, suggesting that awareness campaigns could essentially be ceased after 200 days of implementation while insecticides use needed to be maintained at maximum strength for an additional 50 days.

Figure 3 shows the optimal control profiles for u_1 and u_2 when the upper bounds for these controls were less than unity (i.e., $q_1 = 0.5$ and $q_2 = 0.3$), with initial guesses of the controls set to $u_1 = 0.45$ and $u_2 = 0.3$. We again see that both u_1 and u_2 started from their maxima, and they stayed at the maximum strength for much longer periods of time than the previous case (compared to Figure 2), due to the reduced intensity bounds. When the upper bounds of the controls were reduced, the population levels for all the infected species would converge to zero within the defined time interval, $t_f = 300$ (the figures were omitted since their behavior was analogous to that of Figure 2). We also note that by reducing the bounds for the controls, the total cost $J(= 5.3582 \times 10^4)$ was reduced 17.6%, compared to that of Figure 2.

Numerical results in Figure 4 show the dynamics of *Trypanosoma brucei rhodesiense* disease when the population of infectious vectors was 3% and the hosts' infectious populations were 1% each, and the controls had the following bounds set to $q_1 = 0.5$, $q_2 = 0.3$ and the initial guesses of the controls were set to $u_1 = 0.45$ and $u_2 = 0.3$. Again, we can note that the population levels would converge to the disease-free equilibrium in the presence of optimal control, whereas in the absence of optimal control the disease persisted. The total numbers of new infections for the human and animal populations generated over 300 days were 3.7167×10^5 and 1.1232×10^4, respectively, and the total cost was $J = 5.4726 \times 10^4$. In Figure 4d, we note that the control profiles for u_1 and u_2 exhibited a similar behavior to the one illustrated in Figure 3. Comparing the results in Figure 2 and Figure 4, one

can observe that even if the total number of new infections for the hosts increased due to an increase in the infectious vector population, the total cost would still be lower by approximately 15.8%.

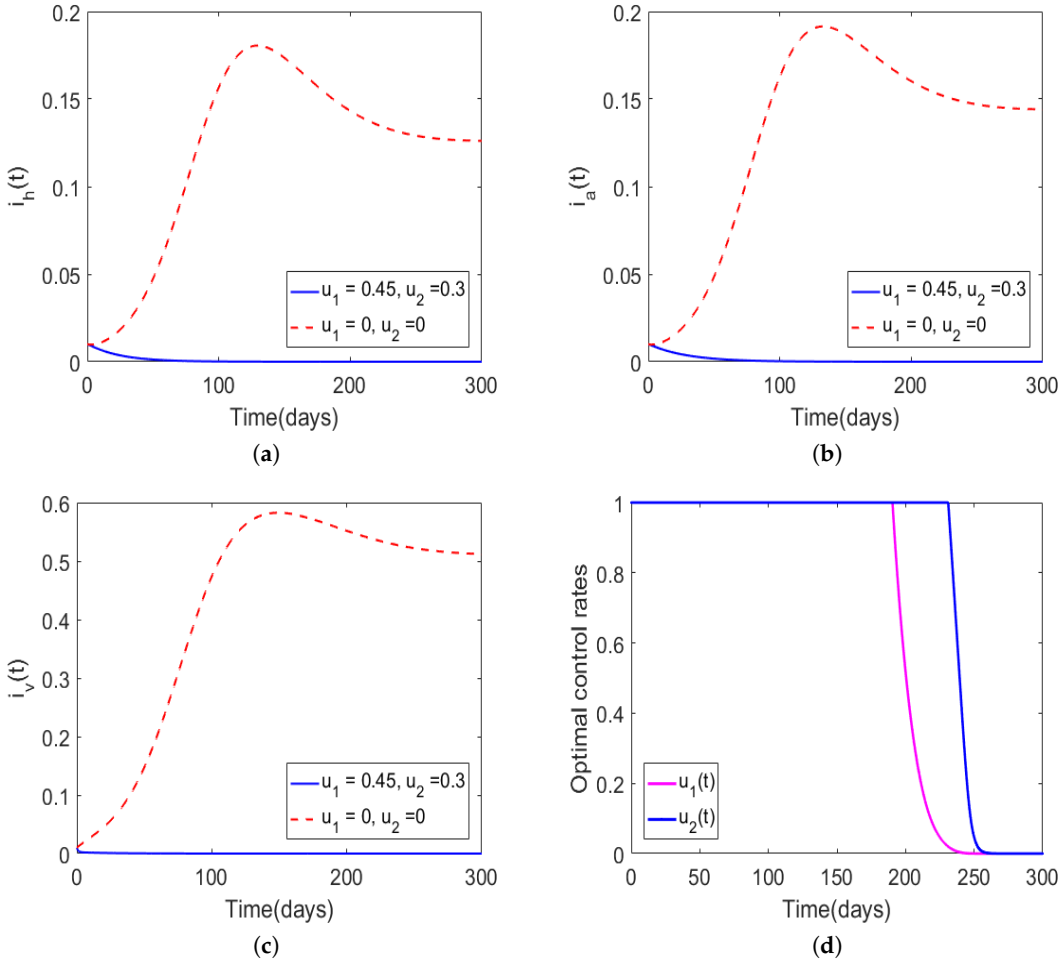

Figure 2. Simulations of model (6) with initial guess for the controls set to $u_1 = 0.45$, $u_2 = 0.3$ and the bounds of the controls were $q_1 = q_2 = 1$. The weight constants were set as $w_1 = 10$, $w_2 = 100$, and the model parameter values were adopted from Table 1. The solid curves in (**a**–**c**) represent the proportion of infectious humans, infectious animals, and infectious tsetse vectors, respectively, in the presence of time-dependent control, and the dotted lines denote the absence of optimal control. The optimal control rates are shown in (**d**).

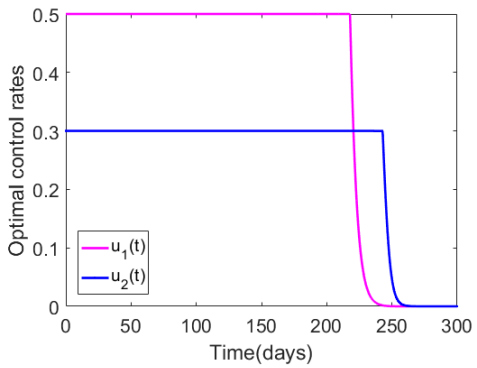

Figure 3. Numerical results illustrating the impact of the bounds for the control rates, with the initial guess for the controls set to $u_1 = 0.45$ and $u_2 = 0.3$, and the bounds for these controls fixed to $q_1 = 0.5$ and $q_2 = 0.3$. The remainder of the model parameter values are as in Table 1.

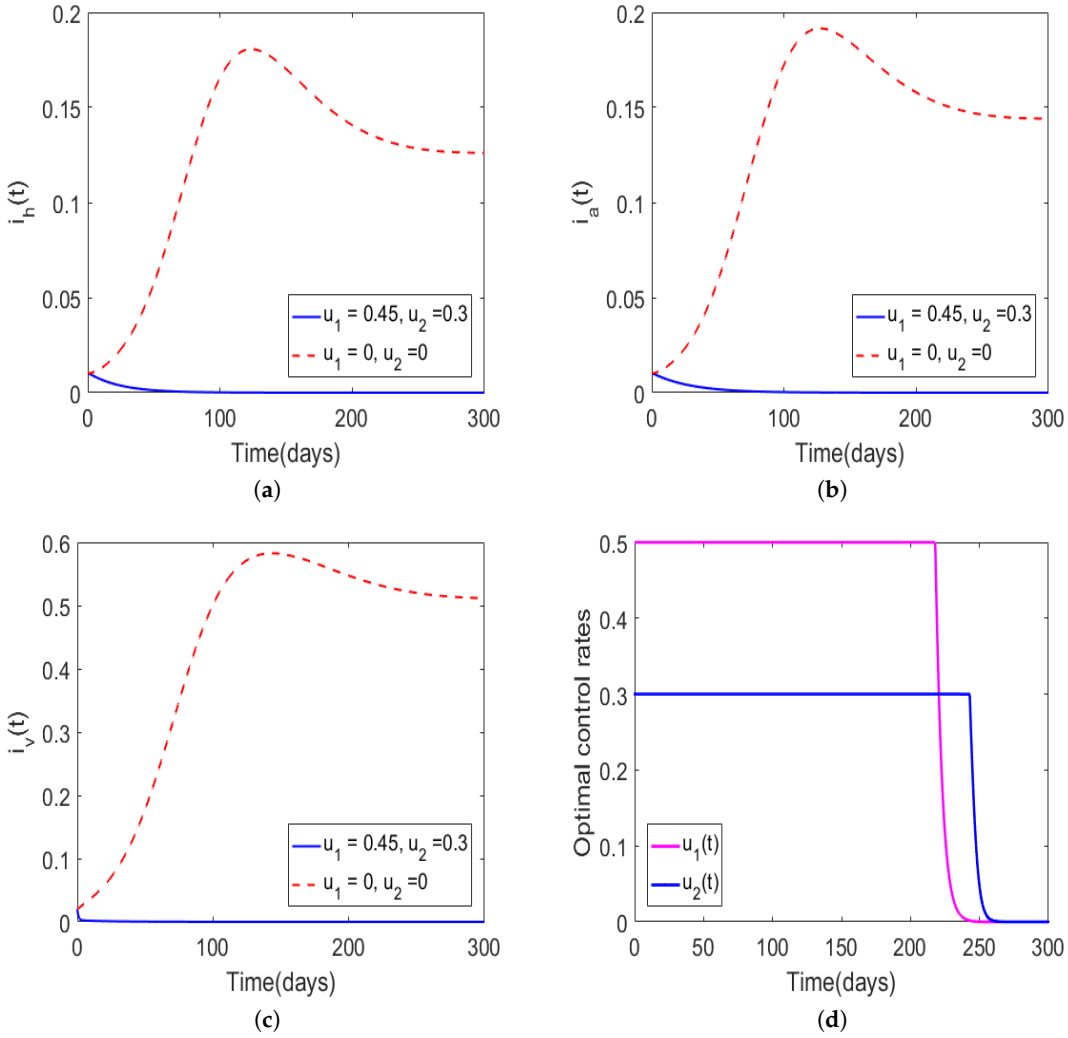

Figure 4. Simulations of model (6) with the initial guesses for the control set to $u_1 = 0.45$, $u_2 = 0.3$, and the bounds for the controls set to $q_1 = 0.5$ and $q_2 = 0.3$. The rest of the model parameter values were adopted from Table 1. The solid curves in (**a**–**c**) represent the proportion of infectious humans, infectious animals, and infectious tsetse vectors, respectively, in the presence of time-dependent control and the dotted lines denote the absence of optimal control. The optimal control rates are shown in (**d**).

Next, we determined the impact of extremely low-intensity controls on *Trypanosoma brucei rhodesiense* disease dynamics (Figure 5). We set the initial guess for the controls to $u_1 = 0.15$, $u_2 = 0.01$, and the upper bounds of the controls were set to $q_1 = 0.15$ and $q_2 = 0.01$. Furthermore, the we set the initial population levels and the weight constants to $i_h = i_a = 0.01$, $i_v = 0.03$, $r_h = r_a = 0$, $s_h = 1 - i_h - r_h$, $s_a = 1 - i_a - r_a$, $s_v = 1 - i_v$, $w_1 = 10$, and $w_2 = 100$. Although the Figures of the population level effects are not displayed, since their behavior was similar to that of Figure 4, we can report that in the presence of optimal control the infected population levels would converge to the disease-free equilibrium and the reverse would occur in the absence of optimal control. The total numbers of new infections for the human and animal populations generated over 300 days were 4.8695×10^5 and 1.2764×10^4, respectively, and the total cost was $J = 5.4519 \times 10^4$. From these simulation results, we see that for effective disease management the control profiles would have to be maintained at their maximum intensity for most of the implementation period. Despite the fact that we considered the insecticide control as more expensive than the awareness control, we note that this control had to be maintained at its maximum intensity for a slightly more time even after the awareness control was dropped.

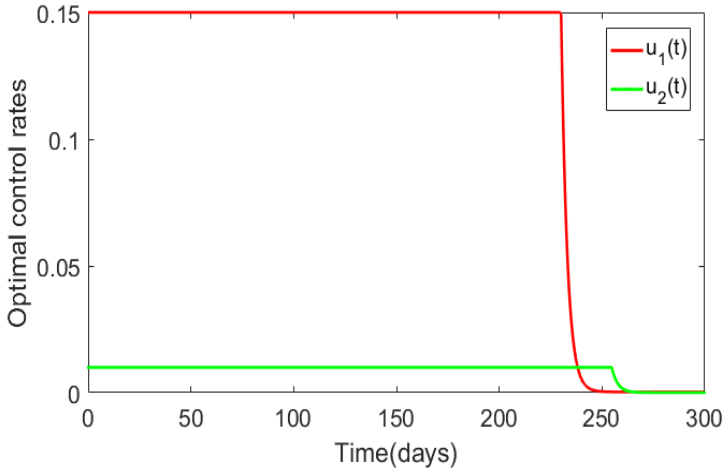

Figure 5. Numerical results illustrating the impact of the bounds for the control rates. The initial guess for the control were $u_1 = 0.15$ and $u_2 = 0.01$, the upper bounds of the controls were $q_1 = 0.15$ and $q_2 = 0.01$. The weights constants were set to $w_1 = 10$ and $w_2 = 100$ and the rest of the model parameter values were as in Table 1.

Next, we determined the number of new infections averted by the implementation of optimal control. This was determined by taking the difference between the total numbers of new infections observed in the absence of optimal control and those recorded when optimal control was implemented. The results are displayed in Table 3. The total numbers of new infections generated in the human and animal populations in the absence of optimal control were 1.0866×10^7 and 7.7237×10^7, respectively.

Table 3. Infection reduction due to the implementation of optimal control.

Case	Host	Total Number of New Infections Observed with Optimal Control	Infections Averted Due to Implementation of Optimal Control
Figure 2	Human population	2.5635×10^5	1.0097×10^7
	Animal population	9.7000×10^4	7.7141×10^7
Figure 4	Human population	3.7197×10^5	1.04943×10^7
	Animal population	1.1232×10^4	7.7226×10^7
Figure 5	Human population	4.8695×10^5	1.03791×10^7
	Animal population	1.2764×10^4	7.7224×10^7

From Table 3, we see that the number of infections averted was extremely high even when the intensity of the optimal controls was low, and this clearly shows the strength of optimal control strategies in minimizing the spread of the disease.

3. Concluding Remarks

In this paper, a mathematical model for *Trypanosoma brucei rhodesiense* transmission was proposed and analyzed. The framework incorporated three species: human, animal, and vector populations. In addition, the impact of optimal awareness campaigns and insecticides use to minimize the populations of infected humans and animals at minimal cost was investigated. The preliminary analysis of the proposed model revealed that the system always had a unique and positively bounded solution for all $t \geq 0$. Qualitative analysis of the model showed that it admitted a backward bifurcation generated by awareness campaigns. In particular, the backward bifurcation occurred whenever the reproduction number was less than unity and the awareness campaign rate, whereas for $\mathcal{R}_0 > 1$ the model exhibited a forward bifurcation.

Meanwhile, the basic *Trypanosoma brucei rhodesiense* model was extended to investigate the impact of optimal awareness and insecticide use to minimize the population of infected humans and animals at minimal cost. Analysis of the optimal model was done with the population levels for the hosts (humans and animals) fixed at 1% while the vector population was varied from 1% to 3%. In addition, in the entire analysis, the intensity of awareness campaigns was assumed to be higher than that of insecticide use since the excessive use of insecticides has some residual effects. Although the insecticide intensity was assumed to be low, the associated cost for this control was regarded to be higher than that of awareness campaigns. Furthermore, the minimization of the infected humans was considered to be more important than that of infected animals. Optimal control results indicate that optimal control awareness campaigns and insecticides use have the potential to eliminate the disease in the community, whereas in the absence of optimal control the disease may not be reduced to levels close to zero. We observed that when the bounds of the control were high the associated costs were also high, and the reverse was true. In particular, we observed that reducing the upper bound of u_1 from 1 to 0.5 and u_2 from 1 to 0.3 could lead to a reduction in costs by 17.6%. Overall, the study demonstrated that optimal awareness and insecticide use have the potential to reduce the population levels of infected species to levels close to zero, and for this to be attained the insecticide control has to be implemented for a slightly longer period compared to the awareness control. In addition, the results from this study suggest that the use of insecticides to control the spread of the disease could have more impact. The strength of using insecticides to control the transmission dynamics of the disease was also noted in the work of Hagrove et al. [12]. Utilizing a mathematical model, Hagrove et al. [12] demonstrated that using insecticides to treat cattle would have a greater impact on controlling the transmission of the disease compared treatment of cattle with drugs.

This work is not exhaustive. In future we hope to explore the dynamics of the disease by using a model with varying total populations for the species, since the constant population approach used in this study does not adequately capture the dynamics of the disease for long periods of time. We will also extend this work to explore the effects of climatic conditions on the long-term dynamics of the disease.

Author Contributions: Formal analysis and Methodology, M.H.; Supervision and writing—review, M.K., D.K. and S.M.

Funding: Mlyashimbi Helikumi acknowledges the financial support received from the Mbeya University of Science and Technology, Tanzania. The other authors are also grateful to their respective institutions for the support.

Acknowledgments: We would like to thank the three anonymous referees and the editors for their invaluable comments and suggestions.

Conflicts of Interest: The authors declare no conflict of interest.

Abbreviations

NTD	Neglected Tropical Disease
HAT	Human African Trypanosomiasis
ICT	Information and Communication Technology
ODE	Ordinary Differential Equation

References

1. World Health Organization. Human African trypanosomiasis (sleeping sickness): Epidemiological update. *Wkly. Epidemiol. Rec.* **2018**, *81*, 71–80.
2. Franco, J.R.; Simarro, P.P.; Diarra, A.; Jannin, J.G. Epidemiology of human African trypanosomiasis. *Clin. Epidemiol.* **2014**, *6*, 257–275.
3. Lutumba, P.; Makieya, E.; Shaw, A.; Meheus, F.; Boelaert, M. Human African Trypanosomiasis in a Rural Community, Democratic Republic of Congo. Emerging Infectious Diseases. Available online: www.cdc.gov/eid (accessed on 8 May 2012).

4. Kermack, W.O.; McKendrick, A.G. A contribution to the mathematical theory of epidemics. *Proc. Soc. Lond. Ser. Math. Phys. Eng. Sci.* **1927**, *115*, 700–721. [CrossRef]
5. Mushayabasa, S.; Posny, D.; Wang, J. Modeling the intrinsic dynamics of foot–and–mouth disease. *Math. Biosci. Eng.* **2016**, *13*, 425–442. [CrossRef] [PubMed]
6. Okosun, K.O.; Ouifki, R.; Marcus, N. Optimal control analysis of a malaria disease transmission model that includes treatment and vaccination with waning immunity. *BioSystems* **2011**, *106*, 136–145. [CrossRef] [PubMed]
7. Cai, L.; Li, X.; Tuncer, N.; Martcheva, M.; Lashari, A. Optimal control of a malaria model with asymptomatic class and superinfection. *Math. Biosci.* **2017**, *288*, 94–108. [CrossRef] [PubMed]
8. Kalinda, C.; Mushayabasa, S.; Chimbari, J.M.; Mukaratirwa, S. Optimal control applied to a temperature dependent schistosomiasis model. *Biosystems* **2017**, *175*, 47–56. [CrossRef]
9. Lolika, O.P.; Mushayabasa, S. On the role of short-term animal movements on the persistence of brucellosis. *Mathematics* **2018**, *6*, 154. [CrossRef]
10. Chitnis, N.; Hyman, J.M.; Cushing, J.M. Determining important parameters in the spread of malaria through the sensitivity analysis of a mathematical model. *Bull. Math. Biol.* **2018**, *70*, 1272–1296. [CrossRef]
11. Mushayabasa, S.; Bhunu, C.P. Modelling the impact of early therapy for latent tuberculosis patients and its optimal control analysis. *J. Biol. Phys.* **2013**, *39*, 723–747. [CrossRef]
12. Hargrove, J.W.; Ouifki, R.; Kajunguri, D.; Vale, G.A.; Torr, S.J. Modeling the control of trypanosomiasis using trypanocides or insecticide-treated livestock. *PLoS Negl. Trop. Dis.* **2012**, *6*, e1615. [CrossRef] [PubMed]
13. Kajunguri, D.; Hargrove, J.W.; Ouifki, R.; Mugisha, J.Y.T.; Coleman, P.G.; Welburn, S.C. Modelling the use of insecticide-treated cattle to control tsetse and Trypanosoma brucei rhodiense in a multi-host population. *Bull. Math. Biol.* **2014**, *76*, 673–696. [CrossRef] [PubMed]
14. Moore, S.; Shrestha, S.; Tomlinson, K.W.; Vuong, H. Predicting the effect of climate change on African trypanosomiasis: Integrating epidemiology with parasite and vector biology. *J. R. Soc. Interface* **2012**, *9*, 817–830 [CrossRef] [PubMed]
15. Peck, S.L.; Bouyer, J. Mathematical modeling, spatial complexity, and critical decisions in tsetse control. *J. Econ. Entomol.* **2012**, *105*, 1477–1486. [CrossRef]
16. Stone, C.M.; Chitnis, N. Implications of Heterogeneous Biting Exposure and Animal Hosts on Trypanosomiasis brucei gambiense Transmission and Control. *Plos Comput. Biol.* **2015**, *11*, e1004514. [CrossRef]
17. Artzrouni, M.; Gouteux, J.-P. Estimating tsetse population parameters: Application of a mathematical model with density-dependence. *Med. Vet. Entomol.* **2003**, *17*, 272–279. [CrossRef]
18. Artzrouni, M.; Gouteux, J.-P. A model of Gambian sleeping sickness with open vector populations. *Math. Med. Biol.* **2001**, *18*, 99–117. [CrossRef]
19. Artzrouni, M.; Gouteux, J.-P. Population dynamics of sleeping sickness: A microsimulation. *Simul. Gaming* **2001**, *32*, 215–227. [CrossRef]
20. Artzrouni, M.; Gouteux, J.-P. A compartmental model of sleeping sickness in Central Africa. *J. Biol. Syst.* **1996**, *4*, 459–477. [CrossRef]
21. Rogers, D.J. A general model for the African trypanosomiases. *Parasitology* **1998**, *97*, 193–212. [CrossRef]
22. Rock, K.S.; Ndeffo-Mbah, M.L.; Castaño, S. Assessing strategies against Gambiense sleeping sickness through mathematical modeling. *Clin. Infect. Dis.* **2018**, *66*, S286–S292. [CrossRef] [PubMed]
23. Ndondo, A.M.; Munganga, J.M.W.; Mwambakana, J.N.; Saad-Roy, M.C.; Van den Driessche, P.; Walo, O.R. Analysis of a model of gambiense sleeping sickness in human and cattle. *J. Biol. Dyn.* **2016**, *10*, 347–365. [CrossRef] [PubMed]
24. Gilbert, J.A.; Medlock, J.; Townsend, J.P.; Aksoy, S.; Mbah, M.N.; Galvani, A.P. Determinants of Human African Trypanosomiasis Elimination via Paratransgenesis. *PLoS Negl. Trop. Dis.* **2016**, *10*, e0004465. doi:10.1371/journal.pntd.0004465 [CrossRef] [PubMed]
25. Rock, K.S.; Torr, S.J.; Lumbala, C.; Keeling, M.J. Predicting the impact of intervention strategies for sleeping sickness in two high-endemicity health zones of the Democratic Republic of Congo. *PLoS Negl. Trop. Dis.* **2017**, *11*, e0005162. [CrossRef] [PubMed]
26. Rock, K.S.; Torr, S.J.; Lumbala, C.; Keeling, M.J. Quantitative evaluation of the strategy to eliminate human African trypanosomiasis in the Democratic Republic of Congo. *Parasit. Vectors* **2015**, *8*, 532. [CrossRef]

27. Rock, K.S.; Stone, C.M.; Hastings, I.M.; Keeling, M.J.; Torr, S.J.; Chitnis, N. Mathematical models of human African trypanosomiasis epidemiology. *Adv. Parasitol.* **2015**, *87*, 53–133.
28. Randolph, W.; Viswanath, K. Lessons learned from public health mass media campaigns: marketing health in a crowded media world. *Annu. Rev Public Health* **2004**, *25*, 419–437. [CrossRef]
29. Apollonio, D.E.; Malone, R.E. Turning negative into positive: Public health mass media campaigns and negative advertising. *Health Educ. Res.* **2009**, *24*, 483–495, [CrossRef]
30. Noar, S.M. A 10-year retrospective of research in health mass media campaigns: where do we go from here? *J. Health Commun.* **2006**, *11*, 21–42. [CrossRef]
31. Leak, S.G.A. Tsetse vector population dynamics: ILRAD's Requirements. In *Modelling Vector-Borne and Other Parasitic Diseases*; Hansen, J.W., Perry, B.D., Eds.; International Livestock Research Institute (ILRI): Nairobi, Kenya. 1994; p. 36. Available online: https://books.google.co.zw/books?isbn=9290552972 (accessed on 8 May 2012).
32. van den Driessche, P.; Watmough, J. Reproduction number and subthreshold endemic equilibria for compartment models of disease transmission. *Math. Biosci.* **2002**, *180*, 29–48. [CrossRef]
33. Gumel, A.B. Causes of backward bifurcation in some epidemiological models. *J. Math. Anal. Appl.* **2012**, *395*, 355–365. [CrossRef]
34. Silva, C.J.; Maurer, H.; Torres, D.F.M. Optimal control of a tuberculosis model with state and control delays. *Math. Biosci. Eng.* **2017**, *14*, 321–337. [CrossRef] [PubMed]
35. Lukes, D.L. *Differential Equations: Classical to Controlled, Mathematics in Science and Engineering*; Academic Press: New York, NY, USA, 1982, Volume 162
36. Pontryagin, L.S.; Boltyanskii, V.T.; Gamkrelidze, R.V.; Mishcheuko, E.F. *The Mathematical Theory of Optimal Processes*; Wiley: New York, NY, USA, 1962.
37. Lenhart, S.; Workman, J.T. *Optimal Control Applied to Biological Models*; Chapman and Hall/CRC: London, UK, 2007.
38. Chávez, J.P.; Götz, T.; Siegmund, S.; Wijaya, K.P. Wijaya An SIR-Dengue transmission model with seasonal effects and impulsive control. *Math. Biosci.* **2017**, *1*, 29–39. [CrossRef] [PubMed]

Dynamical and optimal control analysis of a seasonal Trypanosoma brucei rhodesiense model

Article · February 2020

CITATIONS
2

READS
118

4 authors, including:

Mlyashimbi Helikumi
Mbeya University of Science and Technology .
5 PUBLICATIONS **8** CITATIONS
SEE PROFILE

Moatlhodi Kgosimore
Botswana University of Agriculture and Natural Resources
29 PUBLICATIONS **157** CITATIONS
SEE PROFILE

Dmitry Kuznetsov
The Nelson Mandela African Institute of Science and Technology
27 PUBLICATIONS **54** CITATIONS
SEE PROFILE

Mathematical Biosciences and Engineering

http://www.aimspress.com/journal/MBE

MBE, 17(3): 2530–2556.
DOI: 10.3934/mbe.2020139
Received: 14 November 2019
Accepted: 07 February 2020
Published: 27 February 2020

Research article

Dynamical and optimal control analysis of a seasonal *Trypanosoma brucei rhodesiense* model

Mlyashimbi Helikumi1[1,2,*], Moatlhodi Kgosimore[3], Dmitry Kuznetsov[1] and Steady Mushayabasa[4,*]

[1] Institution of Science and Technology (NM-AIST), School of Computational and Communication Science and Engineering, The Nelson Mandela African, P. O. Box 447, Arusha, Tanzania
[2] Department of Mathematics and Statistics, Mbeya University of Science and Technology, College of Science and Technical Education, P.O. Box 131, Mbeya, Tanzania
[3] Department of Basic Sciences, Botswana University of Agriculture and Natural Resources Private Bag 0027, Gaborone, Botswana
[4] Department of Mathematics, University of Zimbabwe, P.O. Box MP 167, Harare, Zimbabwe

* **Correspondence:** Email: helikumim@nm-aist.ac.tz, steadymushaya@gmail.com.

Abstract: The effects of seasonal variations on the epidemiology of *Trypanosoma brucei rhodesiense* disease is well documented. In particular, seasonal variations alter vector development rates and behaviour, thereby influencing the transmission dynamics of the disease. In this paper, a mathematical model for *Trypanosoma brucei rhodesiense* disease that incorporates seasonal effects is presented. Owing to the importance of understanding the effective ways of managing the spread of the disease, the impact of time dependent intervention strategies has been investigated. Two controls representing human awareness campaigns and insecticides use have been incorporated into the model. The main goal of introducing these controls is to minimize the number of infected host population at low implementation costs. Although insecticides usage is associated with adverse effects to the environment, in this study we have observed that by totally neglecting insecticide use, effective disease management may present a formidable challenge. However, if human awareness is combined with low insecticide usage then the disease can be effectively managed.

Keywords: *Trypanosoma brucei rhodesiense*; seasonality; stability; optimal control

1. Introduction

Vector-borne diseases, such as dengue virus, Zika virus, malaria, yellow fever and human African trypanosomiais (HAT) are known to be highly sensitive to environmental changes, including

variations in climate and land-surface characteristics [1]. Seasonal variations in climatic factors, such as rainfall and temperature have a strong influence on the life cycle of vector thereby affecting the distribution and abundance of vectors seasonally [2]. For example, tsetse flies-vectors responsible for transmission of trypanosomiasis infection in humans and animals need a particular temperature (16–38 °C) and humidity (50–80% of relative humidity) to survive [3]. Therefore, they are linked to the presence of water that increases the local humidity, allowing for the growth of vegetation that protects them from direct sunlight and wind, and attracts the animals to where tsetse feed [3–5]. Therefore, as suggested by Leak [6] understanding the relationship between these factors and vector population dynamics is therefore a potential area for modelling and further development of existing models.

The main goal of this study is to understand the effects of seasonal variations on the transmission and control of *Trypanosoma brucei rhodesiense*. An analysis of *Trypanosoma brucei rhodesiense* datasets for Uganda demonstrated that the disease has seasonal variations with incidence higher during January, February, and March [7]. Another analysis of *Trypanosoma brucei rhodesiense* datasets for Maasai Steppe ecosystem of Tanzania also revealed marked seasonal variations on disease incidence [2, 8, 9]. *Trypanosoma brucei rhodesiense* is one of the two forms of Human African trypanosomiasis (HAT) a neglected disease that affects approximately 70 million people living in 1.55 million km^2 of sub-Saharan Africa [10, 11]. *Trypanosoma brucei rhodesiense* is prevalent in Eastern and Southern Africa while the other form *Trypanosoma brucei gambiense* is common in West and Central Africa [3]. According the World Health Organization (WHO), in 2015, 2804 cases of HAT were recorded, with 2733 attributed to *Trypanosoma brucei gambiense* (90% reduction since 1999) and 71 were attributed to *Trypanosoma brucei rhodesiense* (89% reduction since 1999); this number includes cases diagnosed in both endemic and non-endemic countries [12].

Despite an ambitious campaign led by WHO, many non-governmental organizations, and a public-private which managed to reduce HAT cases to less than 3000 in 2015 leading to the plans to eliminate HAT as a public health problem by 2020 [10], the disease is still endemic in some parts of sub-Saharan Africa, where it is a considerable burden on rural communities [12]. It is therefore essential to gain a better and more comprehensive understanding of effective ways to control disease in human and animal populations. In this study, we will evaluate the effects of optimal human awareness and insecticides use on controlling the spread of *Trypanosoma brucei rhodesiense* in a periodic environment. Effective management and control of *Trypanosoma brucei rhodesiense* has been regarded as complex, since disease transmission involves domestic animals, which serve as reservoirs for parasite transmission by the tsetse vector [10].

Mathematical models have proved to be an effective tool to investigate the long term dynamics of several infectious diseases. Several mathematical models have been proposed to qualitatively and quantitatively analyze the transmission and control of HAT [13–28]. Ackley et al. [16] developed a dynamic model with the goal to estimate tsetse fly mortality from ovarian dissection data in populations where age distribution is not essentially stable. One of the important results from their study was that mortality increases with temperature and this result is concurs with existing field and laboratory findings. Lord and co-workers [17] utilised a mathematical model to explore the effects of temperature on mortality, larviposition and emergence rates in tsetse vectors. Results from the work of Lord et al. [17] suggested that an increase in temperature maybe associated with the decline on tsetse abundance in Zimbabwe's Zambezi Valley. They also hypothesised that rising temperatures

may have made some higher, cooler, parts of Zimbabwe more suitable for tsetse leading to the emergence of new disease foci. Alderton et al. [18] proposed an agent-based model to assess the impact of seasonal climatic drivers on trypanosomiasis transmission rates. Simulation results from the work of Alderton et al. [18] demonstrated a perfect fit with observed HAT datasets thereby demonstrating that seasonality is key component on trypanosomiasis transmission rates. Stone and Chitnis [19] employed a system of ordinary differential equations (ODEs) to model to assess the implications of heterogeneous biting exposure and animal hosts on *Trypanosomiasis brucei gambiense* transmission and control. The work of Stone and Chitnis [19] had several outcomes, but overall, their study demonstrated that effective control of HAT hinges on understanding the ecological and environmental context of the disease, particularly for moderate and low transmission intensity settings.

Despite these efforts, none of the aforementioned works assessed the effects of optimal human awareness and insecticides use on long-term dynamics *Trypanosoma brucei rhodesiense* in a periodic environment. Thus in this study we will develop a periodic model for *Trypanosoma brucei rhodesiense* with an aim to evaluate the effects of optimal human awareness and insecticides use on long-term dynamics of the disease. As in [13, 19, 21, 22, 28], the proposed model assumes that both humans and animals are hosts for *Trypanosoma brucei rhodesiense*. Epidemiological stages of the disease that are sensitivity to seasonal variations have been modeled by periodic functions, such stages includes vector recruitment rate, natural mortality of vectors, vector biting rate and vector incubation period. Mathematical analysis and optimal control are applied to study the dynamical behavior of the model with and without optimal strategies. Overall, the results from the study demonstrated the strength of optimal control strategies on shaping long term dynamics of the disease. In particular, we have noted that effective control of the disease can be attained if optimal human awareness is coupled with insecticides use (even at extremely low intensity than when it is absent).

This paper is organized as follows. In section 2, we present the methods and results. In particular, we present periodic model for *Trypanosoma brucei rhodesiense* . The basic reproduction number of the model is computed and qualitatively used to show that it is an important threshold quantity that determines disease eradication or persistence in the community. We also extend the model to incorporate optimal human awareness and insecticide use. The main aim of introducing controls is to minimize the numbers of humans that are infected with disease over time at minimal costs. With the aid of optimal control theory, necessary conditions to achieve effective disease management in the presents of controls has been established. Finally, a brief discussion rounds up the paper in section 3.

2. Methods and results

2.1. Model formulation and boundedness of solutions

We consider a periodic ordinary differential equations model that incorporates the interplay between the vectors (tsetse flies) and two hosts (humans and animals). The compartments used for each population represents the epidemiological status of the species. Throughout this study, we will use the subscript a, h and v to denote variables or parameter associated with animals, humans and vector, respectively. Thus, each host population is subdivided into compartments of: Susceptible $S_i(t)$, exposed $E_i(t)$, infectious $I_i(t)$ and temporary immune $R_i(t)$, for $i = a, h$. Furthermore, the vector population is subdivided into compartments of: Susceptible $S_v(t)$, exposed $E_v(t)$ and infectious $I_v(t)$.

Thus, the total population of the hosts and vector at time t, denoted by $N_i(t)$ $(i = a, h)$ and $N_v(t)$, respectively is given by

$$N_i(t) = S_i(t) + E_i(t) + I_i(t) + R_i(t), \qquad N_v(t) = S_v(t) + E_v(t) + I_v(t).$$

The susceptible hosts (animals or humans) can acquire infection when they are bitten by an infectious tsetse vector. In this model, the following forces of infection describe vector-to-host disease transmission:

$$\lambda_h(t) = \frac{\sigma_v(t)N_v(t)\sigma_h}{\sigma_v(t)N_v(t) + \sigma_h N_h(t)}\beta_{vh}\frac{I_v(t)}{N_v(t)}, \qquad \text{and,} \quad \lambda_a(t) = \frac{\sigma_v(t)N_v(t)\sigma_a}{\sigma_v(t)N_v(t) + \sigma_a N_a(t)}\beta_{va}\frac{I_v(t)}{N_v(t)}. \quad (1)$$

The parameter β_{vi} is the probability of infection from an infectious vector to a susceptible host i given that a contact between the two occurs, σ_a and σ_h represents the maximum number of vector bites an animal host and human host can sustain per unit time, respectively. The parameter,

$$\sigma_v(t) = \sigma_{v0}\left\{1 - \sigma_{v1}\cos\left(\frac{2\pi}{365}(t + \tau)\right)\right\},$$

represents the frequency of feeding activity by the tsetse flies and is also known as the vector biting rate, σ_{v0} is the average vector biting rate, and σ_{v1} defines the amplitude of seasonal variations (degree of periodic forcing, $0 < \sigma_{v1} < 1$), τ is a phase-shifting parameter to capture the timing of seasonality. Also note that a one year cycle has been considered, that is, $\omega = \frac{2\pi}{365}$. Prior studies suggests that vector biting depends on seasonal variations. Precisely, the vector development rates and behaviour, depends on seasonal variations [13,29]. Furthermore, $\sigma_v(t)N_v(t)$ denotes the total number of bites that the tsetse vectors would like to achieve in unit time, $\sigma_a N_a(t)$ and $\sigma_h N_h(t)$ denotes the availability of hosts. The total number of tsetse-host contacts is half the harmonic mean of $\sigma_v(t)N_v(t)$ and $\sigma_i N_i(t)$ for $i = a, h$.

In addition, once infected, the susceptible host progresses to the exposed state, where they incubate the disease for $1/\kappa_i$ days, $(i = a, h)$ before they progress to the infectious stage. Infectious hosts recover from infection with temporary immunity through treatment at rate α_i, $(i = a, h)$, which is inversely proportional to the average duration of the infectious period. Infectious hosts that fail to recover from infection succumb to disease-related death at rate d_i. It is assumed that temporary immunity wanes out at rate γ_i $(i = a, h)$ and they become susceptible to infection again. Birth and natural mortality rates of the hosts are modelled by b_i and μ_i, $(i = a, h)$, respectively. We assume that there is no vertical transmission of the disease, hence all new recruits are assumed to be susceptible.

In this study, susceptible vectors are assumed to acquire infection when they bite an infectious host and the following force of infection accounts for disease transmission in this case:

$$\lambda_v(t) = \frac{\sigma_v(t)\sigma_h N_h(t)}{\sigma_v(t)N_v(t) + \sigma_h N_h(t)}\beta_{hv}\frac{I_h(t)}{N_h(t)} + \frac{\sigma_v(t)\sigma_a N_a(t)}{\sigma_v(t)N_v(t) + \sigma_a N_a(t)}\beta_{va}\frac{I_a(t)}{N_a(t)}. \quad (2)$$

The parameter β_{hv} represents the probability of infection from an infectious human to a susceptible vector given that a contact between the two occurs, β_{av} is the probability that disease transmission occurs whenever there is sufficient contact between a susceptible vector and an infectious animal. In the absence of seasonal forcing, the forces of infection considered in this study, that is, Eqs (1) and (2), are isomorphic to the ones proposed in [30, 31]. Upon infection, the vector moves to the exposed class and they progress to the infectious stage at rate

$$\kappa_v(t) = \kappa_{v0}[1 - \kappa_{v1}\cos(\omega t + \tau)],$$

κ_{v_0} denotes the average incubation rate in the absence of seasonal variations and κ_{v_1} $(0 < \kappa_{v_1} < 1)$ is the amplitude of the seasonal variation. In addition, vector recruitment rate $b_v(t)$ and natural mortality rate $\mu_v(t)$ have been assumed to follow seasonal variations with

$$b_v(t) = b_{v0}[1 - b_{v1}\cos(\omega t + \tau)], \qquad \text{and} \qquad \mu_v(t) = \mu_{v0}[1 - \mu_{v1}\cos(\omega t + \tau)],$$

where b_{v0}, μ_{v_0} denotes the average birth and natural mortality rates, respectively, and b_{v_1} $(0 < b_{v_1} < 1)$ μ_{v_1} $(0 < \mu_{v_1} < 1)$ is the amplitude of the seasonal variation. Infectious vectors are assumed to remain in that state for their entire lifespan.

Based on assumptions above, with all model variables and parameters assumed to be non-negative, the following system of nonlinear ordinary differential equations summaries the dynamics of *Trypanosoma brucei rhodesiense* disease:

$$\left.\begin{array}{rcl}
S_h'(t) &=& b_h N_h(t) - \lambda_h(t) S_h(t) - \mu_h S_h(t) + \gamma_h R_h(t), \\
E_h'(t) &=& \lambda_h(t) S_h(t) - (\mu_h + \kappa_h) E_h(t), \\
I_h'(t) &=& \kappa_h E_h(t) - (\mu_h + \alpha_h + d_h) I_h(t), \\
R_h'(t) &=& \alpha_h I_h(t) - (\mu_h + \gamma_h) R_h(t), \\
S_a'(t) &=& b_a N_a(t) - \lambda_a(t) S_a(t) - \mu_a S_a(t) + \gamma_a R_a(t), \\
E_a'(t) &=& \lambda_a(t) S_a(t) - (\mu_a + \kappa_a) E_a(t), \\
I_a'(t) &=& \kappa_a E_a(t) - (\mu_a + \alpha_a + d_a) I_a(t), \\
R_a'(t) &=& \alpha_a I_a(t) - (\mu_a + \gamma_a) R_a(t), \\
S_v'(t) &=& b_v(t) N_v(t) - \lambda_v(t) S_v(t) - \mu_v(t) S_v(t), \\
E_v'(t) &=& \lambda_v(t) S_v(t) - (\kappa_v(t) + \mu_v(t)) E_v(t), \\
I_v'(t) &=& \kappa_v(t) E_v(t) - \mu_v(t) I_v(t),
\end{array}\right\} \tag{3}$$

subject to the initial values:

$$\left\{\begin{array}{rcllll}
S_h(0) &=& S_{h0} \geq 0, & E_h(0) = E_{h0} \geq 0, & I_h(0) = I_{h0} \geq 0, & R_h(0) = R_{h0} \geq 0, \\
S_a(0) &=& S_{a0} \geq 0, & E_a(0) = E_{a0} \geq 0, & I_a(0) = I_{a0} \geq 0, & R_a(0) = R_{a0} \geq 0, \\
S_v(0) &=& S_{v0} \geq 0, & E_v(0) = E_{v0} \geq 0, & I_v(0) = I_{v0} \geq 0. &
\end{array}\right.$$

From the detailed computations in Appendix A, we conclude that the solutions $(S_h(t), E_h(t), I_h(t), R_h(t), S_a(t), E_a(t), I_a(t), R_a(t), S_v(t), E_v(t), I_v(t))$ of the model (3) are uniformly and ultimately bounded in

$$\Omega = \left\{ \begin{pmatrix} S_h(t) + E_h(t) + I_h(t) + R_h(t) \\ S_a(t) + E_a(t) + I_a(t) + R_a(t) \\ S_v(t) + E_v(t) + I_v(t) \end{pmatrix} \in \mathbb{R}_+^{11} \;\middle|\; \begin{array}{l} N_h(t) \leq N_{h0}, \\ N_a(t) \leq N_{a0}, \\ N_v(t) \leq N_{v0} \end{array} \right\},$$

with $N_h(0) = N_{h0}$, $N_a(0) = N_{a0}$ and $N_v(0) = N_{v0}$. Therefore we can conclude that model (3) is epidemiologically and mathematically well-posed in the region Ω for all $t \geq 0$.

2.2. Extinction and uniform persistence of the disease

In order to determine the extinction and uniform persistence of the disease we will begin by computing the reproduction number of system (3). Often denoted by $\mathcal{R}_0$, the reproduction number is an epidemiologically important threshold value which determines the ability of an infectious disease

invading a population. It can be determined by utilizing the next-generation matrix method [32]. Based on the computations in Appendix B, the basic reproduction number of the time-averaged autonomous system is

$$[\mathcal{R}_0] = \sqrt{\mathcal{R}_{0h} + \mathcal{R}_{0a}},$$

where

$$\begin{aligned}
\mathcal{R}_{0h} &= \left(\frac{\kappa_h \beta_{vh} N_{h0} \kappa_{v0} \beta_{hv} N_{v0}}{\mu_{v0}(\kappa_{v0} + \mu_{v0})(\kappa_h + \mu_h)(\mu_h + \alpha_h + d_h)}\right)\left(\frac{\sigma_h \sigma_{v0}}{\sigma_{v0} N_{v0} + \sigma_h N_{h0}}\right)^2, \\
\mathcal{R}_{0a} &= \left(\frac{\kappa_a \beta_{va} N_{a0} \kappa_{v0} \beta_{av} N_{v0}}{\mu_{v0}(\kappa_{v0} + \mu_{v0})(\kappa_a + \mu_a)(\mu_a + \alpha_a + d_a)}\right)\left(\frac{\sigma_a \sigma_{v0}}{\sigma_{v0} N_{v0} + \sigma_a N_{a0}}\right)^2.
\end{aligned}$$

The threshold quantities $\mathcal{R}_{0h}$ and $\mathcal{R}_{0a}$ represents the power of the disease to invade the human and animal host, respectively. Due to several time-dependent parameters in model (3), a detailed derivation of the seasonal reproduction number is presented in Appendix B. Furthermore, in Appendix B, we have also demonstrated that the reproduction number $\mathcal{R}_0$ is an important threshold parameter for disease extinction and persistence. In particular, the results show that when $\mathcal{R}_0 < 1$, model (3) admits a globally asymptotically stable disease-free equilibrium and if $\mathcal{R}_0 > 1$, the disease persists.

2.3. The optimal control problem

2.3.1. Model formulation

There are no vaccines for HAT but there exists a couple of preventative and treatment options. The main goal of the preventative strategies is to reduce contact between the hosts and vectors. Preventative strategies include use of trypanocides or insecticides. In addition, humans can also minimize vector contact by clothing on long-sleeved garments of medium-weight material with neutral colors that blend with the background environment. Prior studies have shown that insecticides or trypanocides use can be an effect strategy to control HAT [15]. However, it is worth noting that insecticides are expensive and individuals in many HAT endemic areas are may not be able to afford the cost. Moreover, excessive use of insecticides is associated with environmental adverse effects. Hence, there is need to investigate the effects of coupling insecticides use and other disease control mechanisms on long-term disease dynamics. In particular, a coupling in which low intensity use of insecticides would be more preferable. Thus, in this section, we seek to evaluate the impact of optimal and cost-effective media campaigns and insecticides use on long-term *Trypanosoma brucei rhodesiense* dynamics in a periodic environment. Once humans are aware of the disease they have the potential to minimize contact between the vectors and multiple species. In order to make this assessment, we extend model (3) to incorporate two controls $u_1(t)$ and $u_2(t)$, that represents time dependent media campaigns and insecticides use. These control will be assigned reasonable lower and upper bounds to reflect their limitations. Utilizing the same variables and parameter names as before (model (3)), the extended model with controls takes the form:

$$\left.\begin{array}{rcl} S_h'(t) &=& b_h N_h(t) - \lambda_h(t) S_h(t) - \mu_h S_h(t) - u_1(t) S_h(t) + \gamma_h R_h(t), \\ E_h'(t) &=& \lambda_h(t) S_h(t) - (\mu_h + \kappa_h) E_h(t), \\ I_h'(t) &=& \kappa_h E_h(t) - (\mu_h + \alpha_h + d_h) I_h(t), \\ R_h'(t) &=& u_1(t) S_h(t) + \alpha_h I_h(t) - (\mu_h + \gamma_h) R_h(t), \\ S_a'(t) &=& b_a N_a(t) - \lambda_a(t) S_a(t) - \mu_a S_a(t) + \gamma_a R_a(t), \\ E_a'(t) &=& \lambda_a(t) S_a(t) - (\mu_a + \kappa_a) E_a(t), \\ I_a'(t) &=& \kappa_a E_a(t) - (\mu_a + \alpha_a + d_a) I_a(t), \\ R_a'(t) &=& \alpha_a I_a(t) - (\mu_a + \gamma_a) R_a(t), \\ S_v'(t) &=& b_v(t) N_v(t) - \lambda_v(t) S_v(t) - (\mu_v(t) + u_2(t)) S_v(t), \\ E_v'(t) &=& \lambda_v(t) S_v(t) - (\kappa_v(t) + \mu_v(t) + u_2(t))) E_v(t), \\ I_v'(t) &=& \kappa_v(t) E_v(t) - (\mu_v(t) + u_2(t)) I_v(t), \end{array}\right\} \tag{4}$$

subject to the initial values:

$$\left\{\begin{array}{lllll} S_h(0) = S_{h0} \geq 0, & E_h(0) = E_{h0} \geq 0, & I_h(0) = I_{h0} \geq 0, & R_h(0) = R_{h0} \geq 0, \\ S_a(0) = S_{a0} \geq 0, & E_a(0) = E_{a0} \geq 0, & I_a(0) = I_{a0} \geq 0, & R_a(0) = R_{a0} \geq 0, \\ S_v(0) = S_{v0} \geq 0, & E_v(0) = E_{v0} \geq 0, & I_v(0) = I_{v0} \geq 0. & \end{array}\right.$$

Observe that in system (4), it is assumed that humans who become aware of the disease have negligible chances of acquiring the infection, and also insecticide use affects all the epidemiological classes of the vector populations. Further more, we assume that $u_i(t)$ ranges between 0 and q_i, that is $0 \leq u_i(t) \leq q_i < 1$, such that $u_i = 0$ reflects the absence of time dependent controls and q_i represents the upper bound of the control. The control set is

$$U = \left\{(u_1, u_2)| \in (L^\infty(0, t_f)) : 0 \leq u_i \leq q_i < 1, \quad q_i \in \mathbb{R}^+, \quad i = 1, 2.\right\}.$$

In developing response plans for effective management of diseases, policy makers seek optimal responses that can minimize the incidence and/or disease-related mortality rate while considering the cost of each mitigation strategy. Here, our goal is to minimize the number of infectious host(humans and animals) at minimal costs associated with strategy implementation. Thus the objective functional is given by

$$J(u_1(t), u_2(t)) = \int_0^{t_f} \left(C_1 I_h(t) + C_2 I_a(t) + \frac{W_1}{2} u_1^2(t) + \frac{W_2}{2} u_2^2(t)\right) dt, \tag{5}$$

subject to the constraints of the ODEs in system (4) and where C_1, C_2, W_1 and W_2 are positive constants also known as the balancing coefficients and their goal is to transfer the integral into monetary quantity over a finite time interval $[0, t_f]$. In (5) control efforts are assumed to be nonlinear-quadratic, since a quadratic structure in the control has mathematical advantages such as: If the control set is a compact and convex it follows that the Hamiltonian attains its minimum over the control set at a unique point. The basic framework of an optimal control problem is to prove the existence of an optimal control and then characterize it. Pontryagin's Maximum Principle is used to establish necessary conditions that must be satisfied by an optimal control solution [33]. Derivations on the existence of an optimal control pair as well as the necessary conditions that must be satisfied by optimal control solutions of system (4) are shown in Appendix C.

2.3.2. Numerical results and discussion

In this section, we present some numerical results of the proposed optimal control problem, (system(4)). The numerical solutions were obtained after solving the optimality system of eleven ordinary differential equations from the state and costate equations. The technique used is commonly known as the forward-backward sweep iterative method [34]. The first step of the forward-backward sweep method entails solving of the state equations with a guess for the controls over the simulated time using fourth-order Runge-Kutta scheme. "The controls are then updated by using a convex combination of the previous controls and the value from the characterizations of the controls. This process is repeated and iterations are ceased if the values of the unknowns at the previous iterations are very close to the ones at the present iterations" [34]. Table 1, below presents the essential steps carried out, for a detailed discussion we refer the reader to [34].

Table 1. Forward-backward sweep iterative method.

Algorithm
1. Subdivide the time interval $[t_0, t_f]$ into N equal subintervals. Set the state variable at different times as $x = x(t)$ and assume a piecewise-constant control $u_j^{(0)}(t)$, $t \in [t_k, t_{k+1}]$, where $k = 0, 1, 2, ..., N-1$ and $j = 1, 2$.
2. Apply the assumed control $u_j^{(0)}(t)$ to integrate the state system with an initial condition $x(t_0) = \mathbf{x}(0)$, forward in time $[t_0, t_f]$ using the fourth-order Runge-Kutta method, where $\mathbf{x}_0 = (S_h(0), E_h(0), I_h(0), R_h(0), S_a(0), E_a(0), I_a(0), R_a(0), S_v(0), E_v(0), I_v(0))$.
3. Apply the assumed control $u_j^{(0)}(t)$ to integrate the costate system with the transversality condition $\vec{\lambda}(t_f) = \lambda_i(t_f)$, $i = 1, 2, 3, ..., 11$, backward in time $[t_0, t_f]$ using the fourth-order Runge-Kutta method.
4. Update the control by entering the new state and costate solutions $\vec{x}(t)$ and $\vec{\lambda}(t_f)$, respectively, through the characterization Eq (16) (see, Appendix C).
5. STOP the algorithm if $\frac{\|\vec{x}^{i+1} - \vec{x}^{i}\|}{\|\vec{x}^{i+1}\|} < \xi$; otherwise update the control using a convex combination of the current and previous control and GO to step 2. Here, $\vec{x}^{i}$ is the i^{th} iterative solution of the state system and ξ is an arbitrarily small positive quantity (Tolerance level).

On simulating system (4) we assumed the following initial population levels: $S_h = 10000$, $E_h = 0$, $I_h = 500$, $R_h = 0$, $S_a = 5000$, $E_a = 0$, $I_a = 350$, $R_a = 0$, $S_v = 20000$, $E_v = 0$, $I_v = 1000$. Furthermore, the weight constants W_1 and W_2 are varied. In the simulations we assume that $C_2 = 2C_1$ (with C_1 fixed to unity), that is, minimization of the infected humans has more importance/weight compare to that of infected animals. Furthermore, the rest of the parameter values used were taken from Table 2, majority of parameters values were adopted from the work of Moore et al. [13] as well as Ndondo et al. [22], while a few were assumed within realistic ranges due to their unavailability.

The total number of new infections in human and cattle population were determined by the following formulas, respectively

$$T_h = \int^{t_f} \left(\frac{\sigma_v(t) N_v \sigma_h}{\sigma_v(t) N_v + \sigma_h N_h} \beta_{vh} \frac{I_v}{N_v} S_h \right) dt,$$

$$T_a = \int^{t_f} \left(\frac{\sigma_v(t) N_v \sigma_a}{\sigma_v(t) N_v + \sigma_a N_a} \beta_{va} \frac{I_v}{N_v} S_a \right) dt.$$

and the total cost associated with infected animals, infected humans and the controls J, which is given by (5).

Table 2. Description of model parameters of system (3), indicating baseline, ranges and references.

Symbol	Description			
b_a, b_h	Birth rate for the hosts	$\frac{1}{15\times365}, \frac{1}{50\times365}$	Day^{-1}	[22]
b_{v0}	Averaged birth rate of the vectors	$\frac{1}{33}$	Day^{-1}	[22]
μ_{v0}	Averaged mortality rate of the vectors	$\frac{1}{33}$	Day^{-1}	[22]
μ_a, μ_h	Natural mortality rate for the hosts	$\frac{1}{15\times365}, \frac{1}{50\times365}$	Day^{-1}	[22]
d_a, d_h	Disease-induced death rate for the hosts	$0.0008, \frac{1}{108}$	Day^{-1}	[13]
κ_{v0}	Average incubation rate for the vectors	$\frac{1}{25}(\frac{1}{25} - \frac{1}{30})$	Day^{-1}	[22]
κ_a, κ_h	Incubation rate for the hosts	$\frac{1}{12}(\frac{1}{10} - \frac{1}{14})$	Day^{-1}	[22]
σ_{v0}	Average vector biting rate	$\frac{1}{4}(\frac{1}{10} - \frac{1}{3})$	Day^{-1}	[22]
σ_{v1}	Amplitude of oscillations in $\sigma_v(t)$, respectively	0.8	Dimensionless	
b_{v1}	Amplitude of oscillations in $b_v(t)$, respectively	0.8	Dimensionless	
μ_{v1}	Amplitude of oscillations in $\mu_v(t)$, respectively	0.8	Dimensionless	
κ_{v1}	Amplitude of oscillations in $\kappa_v(t)$, respectively	0.8	Dimensionless	
τ	Phase-shifting parameter	50	Days	
σ_a, σ_h	The maximum number of vector bites the host can have per unit time. This is a function of the host's exposed surface area and any vector control interventions used by the host to reduce exposure to tsetse vectors.	0.62, 0.7	Day^{-1}	[22]
α_a, α_h	Recovery rate of the infectious host	$\frac{1}{25}, \frac{1}{30}$	Day^{-1}	[22]
γ_a, γ_h	Immunity waning rate for the recovered host	$\frac{1}{75}, \frac{1}{90}$	Day^{-1}	[22]
β_{va}, β_{vh}	Probability of infection from an infectious vector to a susceptible host given that a contact between the two occurs	0.62		[22]
β_{av}, β_{hv}	Probability that a vector becomes infected after biting an infectious animal, human	0.01		[22]

Simulation results in Figure 1 illustrates *Trypanosoma brucei rhodesiense* dynamics in the host and vector population, in the presence human awareness only, that is $0 \leq u_1(t) \leq 0.003$ and $u_2(t) = 0$. Overall, we can note that in the presence of optimal human awareness, the numbers of infected hosts and vectors is low compared to without optimal control. Furthermore, with optimal control, the numbers of infected host and vector converges to the disease-free equilibrium in a short time than when there is no optimal control. In addition, we noted that, the total number of infected human and

animal without control over a 2000 day period is $T_h = 4,535$ and $T_a = 2,471$, respectively, while in the presence of optimal human awareness campaigns only, the total number of infected human and animal population for the same period is $T_h = 2,985$ and $T_a = 1,9039$, respectively and the associated total costs of implementing the strategy is $J = 14,994$. Based on these results, one can conclude that the presence of optimal human awareness leads to reduction on cumulative infections for the human and animal host by $T_h = 1,550$ and $T_a = 567$, respectively. Comparing the infection reduction relative to the total number of infections recorded in without optimal control, it follows that, there is a 34.2% and 22.9% reduction in human and animal population, respectively. Figure 2 illustrates the control profile of $u_1(t)$, (note that $u_2(t) = 0$). We can see that, the control profile starts at its maxima and remains there for the entire time horizon. It gradually drops to its minima at the final horizon. This signifies that to attain the above results control $u_1(t)$ may need to be maintained at its maximum intensity for almost the entire time horizon.

Numerical results in Figure 3, illustrates the effects of combining optimal human awareness and insecticides use on long term *Trypanosoma brucei rhodesiense* dynamics in a periodic environment over 2000 days (we set $0 \leq u_1(t) \leq 0.003$ and $0 \leq u_1(t) \leq 0.001$, with $W_1 = 0.1$ and $W_2 = 100$). Once again we can observe that with optimal control strategies in place, few infections will be recorded compared to when there are no optimal control strategies. Precisely, with optimal control strategies in place, the total number of new infections over 2000 days is $T_h = 2,368$ and $T_a = 1,741$, for human and animal populations, respectively, and the associated costs of implementation is $J = 19,264$. We have also noted that without optimal control strategies, the total number of new infections for the human and animal host over 2000 days is $5,336$ and $2,703$ respectively. It follows that the optimal control strategies associated would have averted $2,368$ and 962 infections in human and animal populations. This represents approximately 44% and 36% reduction of infections in human and animal populations, in relation to when there are no controls. Comparing the results in Figures 1 and 3, we can note that combining optimal human awareness and insecticides use, leads to effective disease management in a short period (convergence of solutions to the disease-free equilibrium in Figure 3 takes less time than in Figure 1) compared to when there is optimal human awareness alone.

Simulation results in Figure 4 depicts the control profiles for $u_1(t)$ and $u_2(t)$ over 2000 days. We can observe that all the control profiles starts at their respective maximums and remain there for the greater part of the time horizon, in particular, the control profile for $u_1(t)$ drops on the final time while that of $u_2(t)$ drops just before the final time. These results suggests that for this scenario both controls can be maintained at their respective maximum intensities in order to effectively manage the spread of the disease.

In Figure 5, we varied the bounds of the controls; human awareness $u_1(t)$ and insecticides use $u_2(t)$. We set we set $0 \leq u_1(t) \leq 0.03$ and $0 \leq u_1(t) \leq 0.01$, with $W_1 = 0.1$ and $W_2 = 1000$. We assumed $u_2(t)$ will be significantly affected by changes on the bounds of the controls compared to $u_1(t)$, hence, we adjusted W_2 from 100 to 1000 while W_1 remains 0.1. Under this scenario, we noted that the total number of new infections generated in human and animal populations in the presence of controls over 2000 days will be $T_h = 482$ and $T_a = 544$, respectively, implying that optimal control strategies will be responsible for averting approximately $4,053$ and $1,927$ infections in human and animal populations, respectively. Thus, relative to the total number of infections in the absence of controls, the presence of controls will be associated with 89.4% and 78% reductions for human and animal

populations, respectively. Comparing with earlier scenarios (Figures 1 and 3), we can see that this scenario will have more impact on disease management. In addition, the control profiles associated with this scenario (Figure 6) suggests that for these results to be attained, control $u_1(t)$ will have to be maintained at its maximum intensity from the start to the final day, while control $u_2(t)$ can be maintained at maximum intensity from the start and can be ceased immediately after 500 $^{\text{th}}$ day of implementation. Thus at higher costs and intensity, control $u_2(t)$ cannot be maintained at its maximum intensity from the start till the final day. In addition, the total cost of implementation under this scenario will be $J = 32,559$.

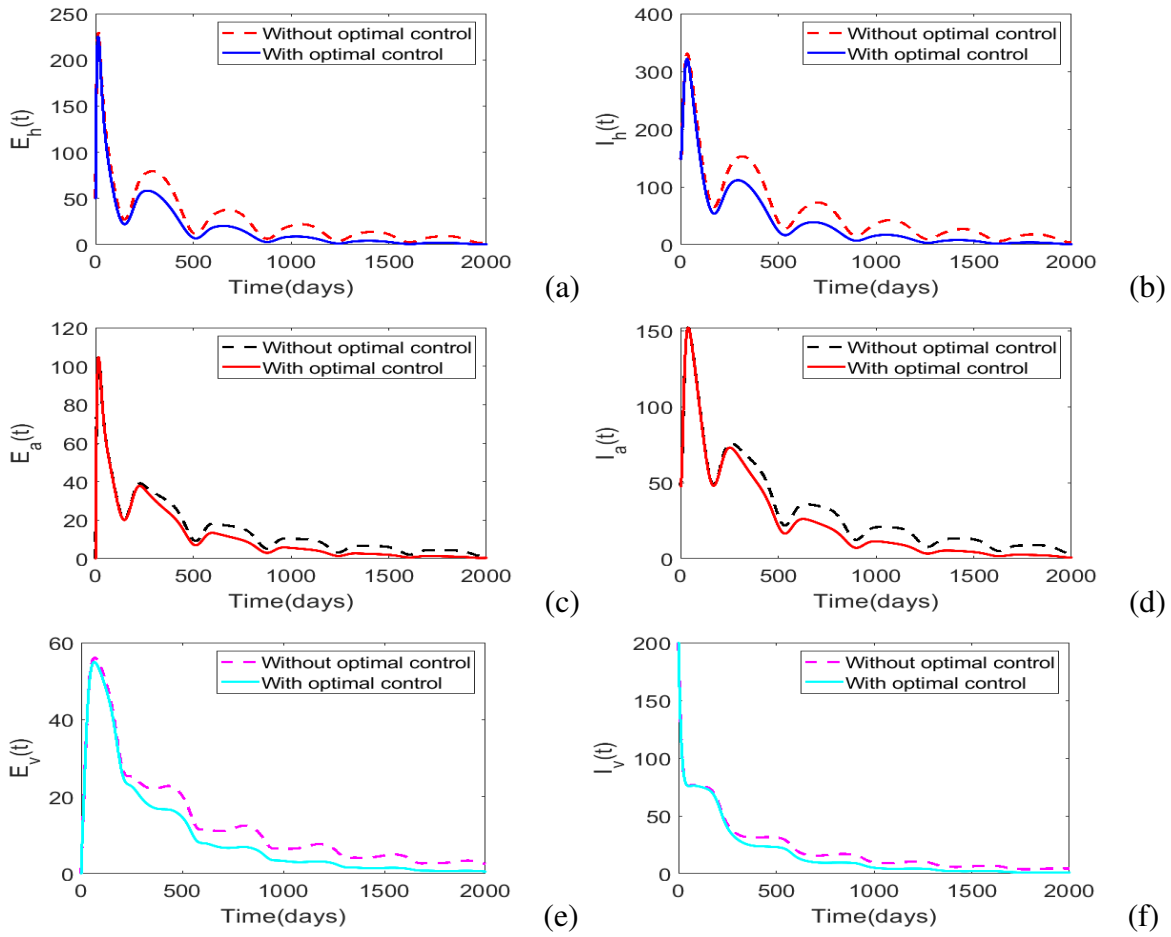

Figure 1. Simulations of model (4) with and without optimal control, with $0 \leq u_1(t) \leq 0.003$ and $u_2(t) = 0$, $W_1 = 0.1$ and $W_2 = 0$. The solid and dotted curves in (a)–(f) depicts the population levels in the host populations with and without optimal control, respectively. Overall, we can observe that with optimal control strategies, the total number of new infections for the hosts is low compared to when there are no optimal control strategies.

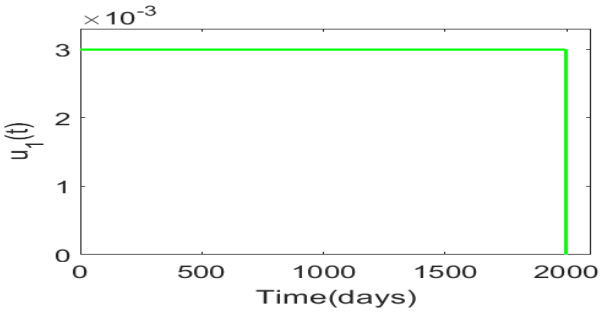

Figure 2. Control profile for $u_1(t)$, $(0 \leq u_1(t) \leq 0.03)$, $u_2(t) = 0$ and $w_1 = 0.1$. We can see that for effective disease management, control $u_1(t)$ will have to be maintained at its maxima for the entire time horizon.

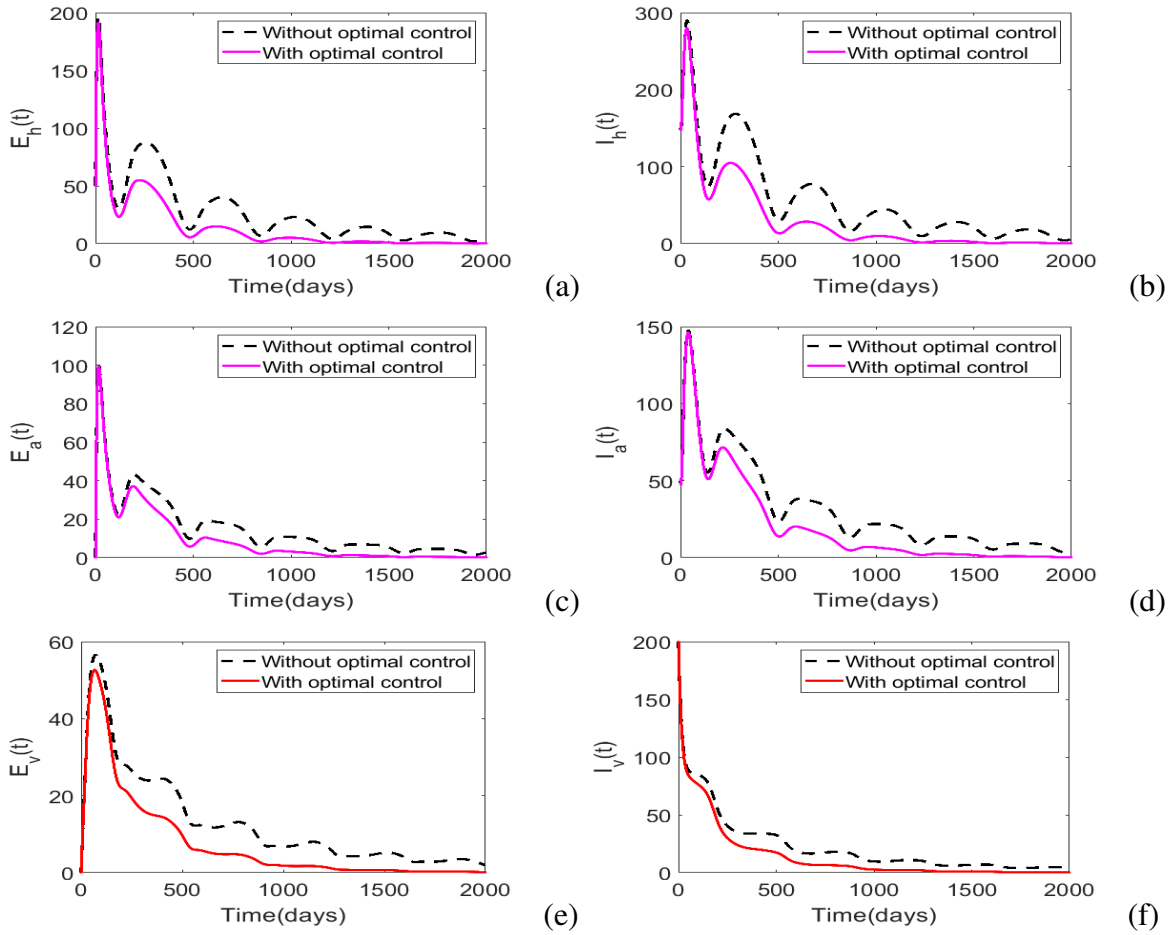

Figure 3. Simulations of model (4) with and without optimal human awareness and insecticides use over 2000 days. We set $0 \leq u_1(t) \leq 0.003$, $0 \leq u_2(t) \leq 0.001$, $W_1 = 0.1$ and $W_2 = 100$. We assume that insecticides use is more expensive relative to human awareness campaigns, hence $W_1 < W_2$. The solid and dotted curves in (a)–(f) represent the population levels in the host populations with and without optimal control, respectively.

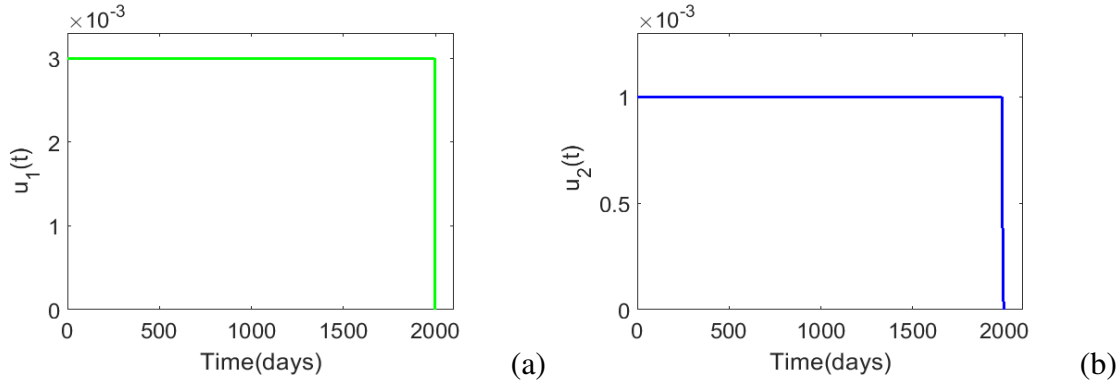

Figure 4. Numerical results illustrating the control profiles for $u_1(t)$, $(0 \leq u_1(t) \leq 0.003)$ and $u_2(t)$ $(0 \leq u_2(t) \leq 0.001)$, with $W_1 = 0.1$ and $W_2 = 100$. The results suggests that for effective disease management both controls need to be maintained at their respective maxima for the entire time horizon.

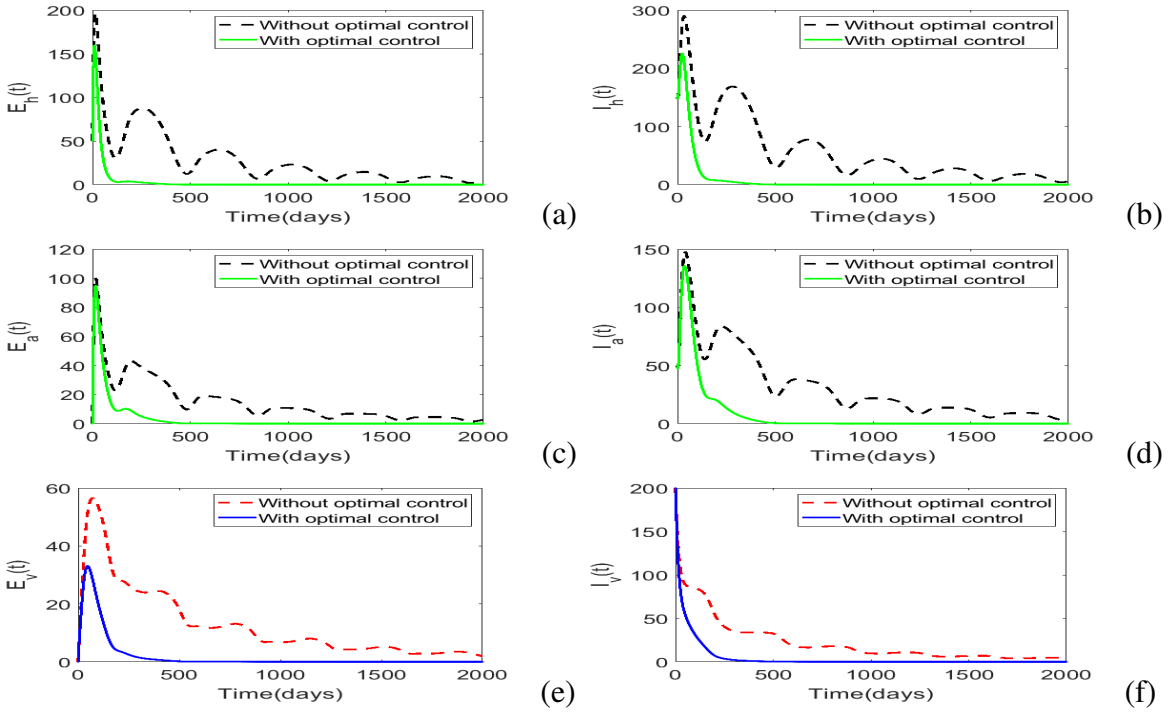

Figure 5. Simulations of model (4) with and without optimal human awareness and insecticides use over 2000 days. We set $0 \leq u_1(t) \leq 0.03$, $0 \leq u_2(t) \leq 0.01$, $W_1 = 0.1$ and $W_2 = 1000$. Once again, we assume that insecticides use is more expensive compared to human awareness campaigns, hence $W_1 < W_2$. The solid and dotted curves in (a)–(f) represent the population levels in the host populations with and without optimal control, respectively.

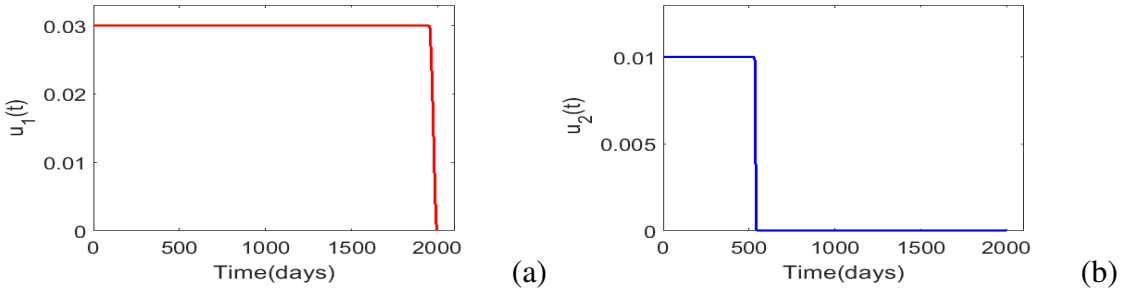

Figure 6. Numerical results illustrating the control profiles for $u_1(t)$, $(0 \leq u_1(t) \leq 0.03)$ and $u_2(t)$ $(0 \leq u_2(t) \leq 0.01)$, with $W_1 = 0.1$ and $W_2 = 10^3$. The results suggests that for these weight constants, the human awareness control $u_1(t)$ will have to maintained at its maxima from the start till the end and the insecticide control, $u_2(t)$ need to be implemented at its maxima from the start and can be ceased immediately after 500 days.

3. Discussion and concluding remarks

In this study, a periodic model consisting of two hosts (animals and humans) and the tsetse vector has been proposed and comprehensively analysed with a view to explore the impact of optimal human awareness and insecticides use on transimission and control of *Trypanosoma brucei rhodesiense* in a periodic environment. We computed the basic reproduction number and demonstrated that it is an important threshold quantity for disease persistence and extinction. In particular, we have demonstrated that whenever the basic reproduction number is less than unity then the disease dies out and the reverse occurs whenever it is greater than unity. The main goal of introducing the two controls in the proposed model was necessitated by the desire to identify effective ways of minimizing the number of infected human over time at minimal costs. Hence utilizing optimal control theory several possible outcomes of effectively managing the disease were explored. One of the important outcome from this study was that effective control of the disease can be managed if optimal human awareness campaigns are combined with optimal insecticides use. This result was attained after comparing the strength of optimal human awareness alone and when it is combined with optimal insecticides use. We also made this comparison based on the fact that insecticides use is known to be associated with some adverse effects to the environment. Therefore, this study suggests that by totally eliminating insecticides use from a whole matrix of other *Trypanosoma brucei rhodesiense* intervention strategies may present a formidable challenge on effective disease management. We have also noted that at certain implementation costs, effective management can be attained with low intensity use of insecticides for a shorter period of time.

The proposed model is not exhaustive. In future, we will incorporate the effects of host movement, which is one of the integral factors in transmission and control of *Trypanosoma brucei rhodesiense*.

Acknowledgements

Mlyashimbi Helikumi acknowledges the financial support received from the Mbeya University of Science and Technology, Tanzania. The other authors are also grateful to their respective institutions

for the support.

We would like to thank the three anonymous referees and the editors for their invaluable comments and suggestions.

Conflict of interest

The authors declare that they have no competing interests.

References

1. R. Lowe, The impact of global environmental change on vector-borne disease risk: A modelling study, *Lancet Planet. Health*., **2** (2018), S1.
2. H. J. Nnko, A. Ngonyoka, L. Salekwa, A. B. Estes, P. J. Hudson, P. S. Gwakisa, et al. Seasonal variation of tsetse fly species abundance and prevalence of trypanosomes in the Maasai steppe, Tanzania, *J. Vector Ecol*., **42** (2017), 24–33.
3. J. R. Franco, P. P. Simarro, A. Diarra, J. G. Jannin. Epidemiology of human African trypanosomiasis, *Clin. Epidemiol*., **6** (2014), 257–275.
4. World Health Organization Report, Control and Surveillance of Human African Trypanosomiasis, 2013. Available from: https://apps.who.int/iris/handle/10665/95732.
5. World Health Organization, Human African trypanosomiasis (sleeping sickness): Epidemiological update, *Wkly Epidemiol. Rec*., **81** (2018), 71–80.
6. S. G. A. Leak, Tsetse vector population dynamics, in *Modelling Vector-Borne and Other Parasitic Diseases* (eds. J. W. Hansen and B.D. Perry), International Livestock research Institute, (1994), 36.
7. F. L. Berrang, C. Wamboga, A. Kakembo, Trypanosoma brucei rhodesiense sleeping sickness, Uganda, *Emerg. Infect. Dis*., **18** (2012), 1686–1687.
8. K. Ngongolo, A. B. Estes, P. J. Hudson, P. S. Gwakisa, Influence of seasonal cattle movement on prevalence of trypanosome infections in cattle in the Maasai Steppe, Tanzania, *J. Infect. Dis. Epidemiol*., **5** (2019), 079.
9. E. G. Kimaro, J. L. Toribio, P. Gwakisa, S. M. Mor, Occurrence of trypanosome infections in cattle in relation to season, livestock movement and management practices of Maasai pastoralists in Northern Tanzania, *Vet. Parasitol. Reg. Stud. Reports*., **12** (2018), 91–98.
10. S. Aksoy, P. Buscher, M. Lehane, P. Solano, J. Van Den Abbeele, Human African trypanosomiasis control: Achievements and challenges, *PLoS Negl. Trop. Dis*., **11** (2017), e0005454.
11. P. P. Simarro, G. Cecchi, J. R. Franco, M. Paone, A. Diarra, J. A. Ruiz-Postigo, et al., Estimating and mapping the population at risk of sleeping sickness, *PLoS Negl. Trop. Dis*., **6** (2012), e1859.
12. P. Büscher, G. Cecchi, V. Jamonneau, G. Priotto, Human African trypanosomiasis, *Lancet*., **390** (2017), 2397–2409.
13. S. Moore, S. Shrestha, K. W. Tomlinson, H. Vuong, Predicting the effect of climate change on African trypanosomiasis: Integrating epidemiology with parasite and vector biology, *J. R. Soc. Interface*., **9** (2012), 817–830.

14. S. L. Peck, J. Bouyer, Mathematical modeling, spatial complexity, and critical decisions in tsetse control, *J. Econ. Entomol*., **105** (2012), 1477–1486.
15. J. W. Hargrove, R. Ouifki, D. Kajunguri, G. A. Vale, S. J. Torr, Modeling the control of trypanosomiasis using trypanocides or insecticide-treated livestock, *PLoS Negl. Trop. Dis*., **6** (2012), e1615.
16. S. F. Ackley, J. W. Hargrove, A dynamic model for estimating adult female mortality from ovarian dissection data for the tsetse fly Glossina pallidipes Austen sampled in Zimbabwe, *PLoS Negl. Trop. Dis*., **11** (2017), e0005813.
17. J. S. Lord, J.W. Hargrove JW, S. J. Torr, G. A. Vale, Climate change and African trypanosomiasis vector populations in Zimbabwes Zambezi Valley: A mathematical modelling study, *PLoS Med*., 15 (2018), e1002675.
18. S. Alderton, E. T. Macleod, N. E. Anderson, G. Palmer, N. Machila, M. Simuunza, et al., An agent-based model of tsetse fly response to seasonal climatic drivers: Assessing the impact on sleeping sickness transmission rates, *PLoS Negl. Trop. Dis*., **12** (2018), e0006188.
19. C. M. Stone, N. Chitnis N, Implications of heterogeneous biting exposure and animal hosts on trypanosomiasis *Brucei Gambiense* transmission and control, *PLoS Comput. Biol*., **11** (2015): e1004514.
20. D. J. Rogers, A general model for the African trypanosomiases, *Parasitology*., **97** (1988), 193–212.
21. K. S. Rock, M. L. Ndeffo-Mbah, S. Castaño, C. Palmer, A. Pandey, K. E. Atkins, et al. Assessing strategies against Gambiense sleeping sickness through mathematical modeling, *Clin. Infect. Dis*., **66** (2018), S286–S292.
22. A. M. Ndondo, J. M. W. Munganga, J. N. Mwambakana, M. C. Saad-Roy, P. van den Driessche, O. R. Walo. Analysis of a model of Gambiense sleeping sickness in human and cattle, *J. Biol. Dyn*., **10** (2016), 347–365.
23. J. A. Gilbert, J. Medlock, J. P. Townsend, S. Aksoy, M. L. Ndeffo-Mbah, A. P. Galvani, Determinants of human African trypanosomiasis elimination via paratransgenesis, *PLoS Negl. Trop. Dis*., **10** (2016), e0004465.
24. K. S. Rock, S, J. Torr, C. Lumbala, M. J. Keeling, Predicting the impact of intervention strategies for sleeping sickness in two high-endemicity health zones of the Democratic Republic of Congo, *PLoS Negl. Trop. Dis*., **11** (2017), e0005162.
25. K. S. Rock, S, J. Torr, C. Lumbala, M. J Keeling, Quantitative evaluation of the strategy to eliminate human African trypanosomiasis in the Democratic Republic of Congo, *Parasit. Vectors*., **8** (2015), 532.
26. K. S. Rock, C. M. Stone, I. M. Hastings, M. J. Keeling, S. J. Torr, N. Chitnis, Mathematical models of human African trypanosomiasis epidemiology, *Adv. Parasitol*., **87** (2015), 53–133.
27. T. Madsen, D. I. Wallace, N. Zupan, Seasonal fluctuations in tsetse fly populations and human African trypanosomiasis: A mathematical model, in *BiIOMAT 2012: International Symposium on Mathematical and Computational Biology* (ed. R. P. Mondaini), World Scientific Publishing Company, Singapore, (2013), 56–69.

28. H. Helikumi, M. Kgosimore, D. Kuznetsov, S. Mushayabasa S, Backward bifurcation and optimal control analysis of a *Trypanosoma Brucei Rhodesiense* model, *Mathematics*., **7** (2019), 971.

29. A. R. Cossins, K. Blower, *Temperature biology of animals*, New York, Chapman and Hall, 1987.

30. N. Chitnis, J. M. Cushing, J. M. Hyman, Bifurcation analysis of a mathematical model for malaria transmission, *SIAM J. Appl. Math*., **67** (2006), 24–45.

31. N. Chitnis, J. M. Hyman, J. M. Cushing, Determining important parameters in the spread of malaria through the sensitivity analysis of a mathematical model, *Bull. Math. Biol*., **70** (2008), 1272–1296.

32. P. van den Driessche, J. Watmough, Reproduction numbers and sub-threshold endemic equilibria for compartmental models of disease transmission, *Math. Biosci*., **180** (2002), 29–48.

33. L. S. Pontryagin, V. T. Boltyanskii, R. V. Gamkrelidze, E. F. Mishcheuko, *The mathematical theory of optimal processes*, Wiley, New Jersey, 1962.

34. S. Lenhart, J. T. Workman, *Optimal Control Applied to Biological Models*, Chapman and Hall/CRC, London, 2007.

35. W. Wang, X. Q Zhao, Threshold dynamics for compartment epidemic models in periodic environments, *J. Dyn. Differ. Equ*., **20** (2008), 699–717.

36. D. Posny, J. Wang, Computing basic reproductive numbers for epidemiological models in non-homogeneous environments, *Appl. Math. Comput*., **242** (2014), 473–490.

37. W. D. Wang, X. Q. Zhao, An epidemic model in a patchy environment, *Math. Biosci*., **190** (2004), 97–112.

38. X. Q. Zhao, *Dynamical System in Population Biology*, Springer-Verlag, New York, 2003.

39. X. Q. Zhao, *Dynamical Systems in Population Biology*, Springer: New York, 2003.

40. W. H. Fleming, R. W. Rishel, *Deterministic and Stochastic Optimal Control*, Springer-Verag, New York, 1975.

Supplementary

Appendix A. Positivity and boundedness of solutions

Theorem 1. *The solutions* $(S_h(t), E_h(t), I_h(t), R_h(t),\ S_a(t), E_a(t), I_a(t), R_a(t),\ S_v(t), E_v(t), I_v(t))$ *of the model (3) are uniformly and ultimately bounded in*

$$\Omega = \left\{ \begin{pmatrix} S_h(t) + E_h(t) + I_h(t) + R_h(t) \\ S_a(t) + E_a(t) + I_a(t) + R_a(t) \\ S_v(t) + E_v(t) + I_v(t) \end{pmatrix} \in \mathbb{R}^{11}_{+} \middle| \begin{array}{l} N_h(t) \le N_{h0}, \\ N_a(t) \le N_{a0}, \\ N_v(t) \le N_{v0} \end{array} \right\},$$

with $N_h(0) = N_{h0}$, $N_a(0) = N_{a0}$ *and* $N_v(0) = N_{v0}$.

Proof. For the *Trypanosoma brucei rhodesiense* model (3) to be epidemiologically meaningful, it is important to demonstrate that all its state variables are non-negative for all $t \ge 0$. In other words, one needs to show that solutions of system (3) with non-negative initial data will remain non-negative for

all $t \geq 0$. Let the initial data $S_i(0) \geq 0$, $E_i(0) \geq 0$, $I_i(0) \geq 0$, $R_i(0) \geq 0$, for $i = a, h$, and $S_v(0) \geq 0$, $E_v(0) \geq 0$, and $I_v(0) \geq 0$, such that from the second equation of model (3) we have

$$E_h(t) = e^{-(\mu_h+\kappa_h)t}\left(E_h(0) + \int_0^t \lambda_h(s)S_h(s)ds\right), \qquad t \geq 0.$$

Thus, $E_h(t) \geq 0$ for all $t \geq 0$. A similar approach can be utilised to show that all the other variables of model (3) are positive for all $t \geq 0$. In what follows, we now determine the feasible region of model (3). One can easily verify the that rate of change of the total host populations N_i, $(i = a, h)$ is

$$N_i'(t) = (b_i - \mu_i)N_i(t) - d_iI_i(t) \leq (b_i - \mu_i)N_i(t), \qquad \text{where} \qquad \mu_i \leq b_i.$$

As suggested in [13] we set $b_i = \mu_i$, otherwise the population will grow without bound or become extinct. Therefore, $N_i(t) \leq N_i(0)$. Similarly, by adding all the last three equations of model (3), and setting $b_v(t) = \mu_v(t)$ as in [13], one gets $N(t) \leq N_{v0}$. Thus, model (3) is epidemiologically and mathematically well-posed in the domain:

$$\Omega = \left\{ \begin{pmatrix} S_h(t) + E_h(t) + I_h(t) + R_h(t) \\ S_a(t) + E_a(t) + I_a(t) + R_a(t) \\ S_v(t) + E_v(t) + I_v(t) \end{pmatrix} \in \mathbb{R}_+^{11} \middle| \begin{array}{l} N_h(t) \leq N_{h0}, \\ N_a(t) \leq N_{a0}, \\ N_v(t) \leq N_{v0} \end{array} \right\},$$

with $N_h(0) = N_{h0}$, $N_a(0) = N_{a0}$ and $N_v(0) = N_{v0}$. This completes the proof of theorem. □

Appendix B. Extinction and uniform persistence of the disease

Before we investigate the extinction and persistence of the disease, we need to determine the basic reproduction number of the model. Commonly denoted by $\mathcal{R}_0$, the basic reproduction number is an epidemiologically important threshold value which determines the ability of an infectious disease invading a population. To determine the reproduction number of model (3), the next-generation matrix method [32] will be utilized. One can easily verify that model (3) has a disease-free equilibrium $\mathcal{E}^0 : (S_h^0, E_h^0, I_h^0, R_h^0, S_a^0, E_a^0, I_a^0, R_a^0, S_v^0, E_v^0, I_v^0) = (N_{h0}, 0, 0, 0, 0, N_{a0}, 0, 0, 0, N_{v0}, 0, 0)$.

The infected compartments of model (3) is comprised of $(E_j(t), I_j(t))$ classes, for $j = h, a, v$. Following the next-generation matrix approach, the nonnegative matrix $F(t)$ of the infection terms and the non-singular matrix, $V(t)$ of the transition terms evaluated at $\mathcal{E}^0$ are,

$$F(t) = \begin{bmatrix} 0 & 0 & 0 & 0 & 0 & \dfrac{\sigma_v(t)\sigma_h\beta_{vh}N_{h0}}{\sigma_v(t)N_v(t) + \sigma_hN_{h0}} \\ 0 & 0 & 0 & 0 & 0 & 0 \\ 0 & 0 & 0 & 0 & 0 & \dfrac{\sigma_v(t)\sigma_a\beta_{va}N_{a0}}{\sigma_v(t)N_v(t) + \sigma_aN_{a0}} \\ 0 & 0 & 0 & 0 & 0 & 0 \\ 0 & \dfrac{\sigma_h\sigma_v(t)\beta_{hv}N_v(t)}{\sigma_v(t)N_v(t) + \sigma_hN_{h0}} & 0 & \dfrac{\sigma_a\sigma_v(t)\beta_{va}N_v(t)}{\sigma_v(t)N_v(t) + \sigma_aN_{a0}} & 0 & 0 \\ 0 & 0 & 0 & 0 & 0 & 0 \end{bmatrix},$$

and

$$V(t) = \begin{bmatrix} \kappa_h + \mu_h & 0 & 0 & 0 & 0 & 0 \\ -\kappa_h & \mu_h + \alpha_h + d_h & 0 & 0 & 0 & 0 \\ 0 & 0 & \kappa_a + \mu_a & 0 & 0 & 0 \\ 0 & 0 & -\kappa_a & \mu_a + \alpha_a + d_a & 0 & 0 \\ 0 & 0 & 0 & 0 & \kappa_v(t) + \mu_v(t) & 0 \\ 0 & 0 & 0 & 0 & -\kappa_v(t) & \mu_v(t) \end{bmatrix}. \quad (6)$$

Therefore, the basic reproduction number of the time-averaged autonomous system is

$$[\mathcal{R}_0] = \sqrt{\mathcal{R}_{0h} + \mathcal{R}_{0a}},$$

where

$$\mathcal{R}_{0h} = \left(\frac{\kappa_h \beta_{vh} N_{h0} \kappa_{v0} \beta_{hv} N_{v0}}{\mu_{v0}(\kappa_{v0} + \mu_{v0})(\kappa_h + \mu_h)(\mu_h + \alpha_h + d_h)}\right)\left(\frac{\sigma_h \sigma_{v0}}{\sigma_{v0} N_{v0} + \sigma_h N_{h0}}\right)^2,$$
$$\mathcal{R}_{0a} = \left(\frac{\kappa_a \beta_{va} N_{a0} \kappa_{v0} \beta_{av} N_{v0}}{\mu_{v0}(\kappa_{v0} + \mu_{v0})(\kappa_a + \mu_a)(\mu_a + \alpha_a + d_a)}\right)\left(\frac{\sigma_a \sigma_{v0}}{\sigma_{v0} N_{v0} + \sigma_a N_{a0}}\right)^2.$$

In order to define the basic reproduction number of this non-autonomous model, we follow the work of Wang and Zhao [35]. They introduced the next-infection operator L for a model in periodic environments by

$$(L\phi)(t) = \int_0^\infty Y(t, t-s) F(t-s) \phi(t-s) ds\,,$$

where $Y(t, s)$, $t \geq s$, is the evolution operator of the linear ω-periodic system $\frac{dy}{dt} = -V(t)y$ and $\phi(t)$, the initial distribution of infectious animals, is ω-periodic and always positive. The effective reproductive number for a periodic model is then determined by calculating the spectral radius of the next infection operator,

$$\mathcal{R}_0 = \rho(L). \quad (7)$$

For model (3), the evolution operator can be determined by solving the system of differential equations $\frac{dy}{dt} = -V(t)y$ with the initial condition $Y(s, s) = I_{6\times 6}$; thus, one gets

$$Y(t, s) = \begin{bmatrix} y_{11}(t, s) & 0 & 0 & 0 & 0 & 0 \\ y_{21}(t, s) & y_{22}(t, s) & 0 & 0 & 0 & 0 \\ 0 & 0 & y_{33}(t, s) & 0 & 0 & 0 \\ 0 & 0 & y_{43}(t, s) & y_{44}(t, s) & 0 & 0 \\ 0 & 0 & 0 & 0 & y_{55}(t, s) & 0 \\ 0 & 0 & 0 & 0 & y_{65}(t, s) & e^{-\mu_v(t-s)} \end{bmatrix}.$$

where

$$y_{11}(t, s) = e^{-(\mu_h + \kappa_h)(t-s)},$$

$$
\begin{aligned}
y_{21}(t,s) &= \frac{\kappa_h}{d_h+\alpha_h-\kappa_h}\left(e^{-(\mu_h+\kappa_h)(t-s)} - e^{-(\mu_h+d_h+\alpha_h)(t-s)}\right),\\
y_{22}(t,s) &= e^{-(\mu_h+d_h+\alpha_h)(t-s)},\\
y_{33}(t,s) &= e^{-(\mu_a+\gamma_a)(t-s)},\\
y_{43}(t,s) &= \frac{\kappa_a}{d_a+\alpha_a-\kappa_a}\left(e^{-(\mu_a+\gamma_a)(t-s)} - e^{-(\mu_a+d_a+\alpha_a)(t-s)}\right),\\
y_{44}(t,s) &= e^{-(\mu_a+d_a+\alpha_a)(t-s)},\\
y_{55}(t,s) &= \exp-\left\{\kappa_{vo}(t-s)+\frac{2\kappa_{v0}\kappa_{v1}}{\omega}\cos\left(\frac{\omega}{2}(t+\tau+s)\right)\sin\left(\frac{\omega}{2}(t+\tau-s)\right)\right.\\
&\quad \left.+\mu_{vo}(t-s)+\frac{2\mu_{v0}\mu_{v1}}{\omega}\cos\left(\frac{\omega}{2}(t+\tau+s)\right)\sin\left(\frac{\omega}{2}(t-s)\right)\right\},\\
y_{65}(t,s) &= \left(e^{-\int\mu_v(t)dt}\right)\int_s^t e^{\mu_v(x)}\kappa_v(x)y_{55}(x,s)dx,\\
y_{66}(t,s) &= \exp-\left\{\mu_{vo}(t-s)+\frac{2\mu_{v0}\mu_{v1}}{\omega}\cos\left(\frac{\omega}{2}(t+\tau+s)\right)\sin\left(\frac{\omega}{2}(t+\tau-s)\right)\right\}.
\end{aligned}
$$

Utilising the techniques described in [36] one can numerically analyse the basic reproduction number defined in Eq (7). The following lemma shows that the basic reproduction number $\mathcal{R}_0$ is the threshold parameter for local stability of the disease-free equilibrium $\mathcal{E}^0$.

Lemma 1. *(Theorem 2.2 in Wang and Zhao [35]). Let $x(t) = (E_i(t), I_i(t))$, $i = a, h, v$, denote the vector of all infected class variables system (3), such that the linearization of system (3) at disease-free equilibrium $\mathcal{E}^0$ is*

$$\dot{x}(t) = (F(t) - V(t))x(t), \tag{8}$$

where $F(t)$ and $V(t)$ are defined earlier on Eq (6). Furthermore, let $\Phi_{F-V(t)}$ and $\rho(\Phi_{F-V(\omega)}$ be the monodromy matrix of system (8) and the spectral radius of $\Phi_{F-V(t)}(\omega)$, respectively, then the following statements are valid:

(i) $\mathcal{R}_0 = 1$, *if and only if* $\rho(\Phi_{F-V}(\omega)) = 1$;

(ii) $\mathcal{R}_0 > 1$, *if and only if* $\rho(\Phi_{F-V}(\omega)) > 1$;

(iii) $\mathcal{R}_0 < 1$, *if and only if* $\rho(\Phi_{F-V}(\omega)) < 1$.

Thus, the disease-free equilibrium $\mathcal{E}^0$ of system (3) is locally asymptotically stable if $\mathcal{R}_0 < 1$ and unstable if $\mathcal{R}_0 > 1$.

In what follows, we now demonstrate that the reproduction number $\mathcal{R}_0$ is an important threshold parameter for disease extinction and persistence. Precisely, we will show that when $\mathcal{R}_0 < 1$, model (3) admits a globally asymptotically stable disease-free equilibrium $\mathcal{E}^0$, and if $\mathcal{R}_0 > 1$, the disease persists. The mathematical analysis follows the approach in [37].

Theorem 2. *If $\mathcal{R}_0 < 1$, then the disease-free equilibrium $\mathcal{E}^0$ of system (3) is globally asymptotically stable in Ω.*

Proof. According to Lemma 1, if $\mathcal{R}_0 < 1$, then the disease-free equilibrium $\mathcal{E}^0$ of system (3) is locally asymptotically stable. Hence, it is sufficient to demonstrate that for $\mathcal{R}_0 < 1$, the disease-free equilibrium is the global attractor. Assume that $\mathcal{R}_0 < 1$, again from Lemma 1, we have, we have $\rho(\Phi_{F-V}(\omega)) < 1$. From the second, third, sixth, seventh, tenth and eleventh equations of model (3) we have:

$$\begin{cases} \dot{E}_h(t) &\leq \left(\dfrac{\sigma_v(t)\sigma_h\beta_{vh}I_v}{\sigma_v(t)N_v(t)+\sigma_hN_h}\right)S_h^0 - (\mu_h+\kappa_h)E_h, \\ \dot{I}_h(t) &= \kappa_hE_h - (\mu_h+d_h+\alpha_h)I_h, \\ \dot{E}_a(t) &\leq \left(\dfrac{\sigma_v(t)\sigma_a\beta_{va}I_v}{\sigma_v(t)N_v(t)+\sigma_aN_a}\right)S_a^0 - (\mu_a+\kappa_a)E_a, \\ \dot{I}_a(t) &= \kappa_aE_a - (\mu_a+d_a+\alpha_a)I_a, \\ \dot{E}_v(t) &\leq \left(\dfrac{\sigma_v(t)\sigma_h\beta_{hv}I_h}{\sigma_v(t)N_v(t)+\sigma_hN_h} + \dfrac{\sigma_v(t)\sigma_a\beta_{va}I_a}{\sigma_v(t)N_v(t)+\sigma_aN_a}\right)S_v^0 - (\kappa_v(t)+\mu_v(t))E_v, \\ \dot{I}_v(t) &= \kappa_v(t)E_v - \mu_v(t)I_v, \end{cases}$$

for $t \geq 0$. Consider the following auxiliary system:

$$\begin{cases} \dot{\widetilde{E}}_h(t) &= \left(\dfrac{\sigma_v(t)\sigma_h\beta_{vh}\widetilde{I}_v}{\sigma_v(t)\widetilde{N}_v+\sigma_h\widetilde{N}_h}\right)S_h^0 - (\mu_h+\kappa_h)\widetilde{E}_h, \\ \dot{\widetilde{I}}_h(t) &= \kappa_h\widetilde{E}_h - (\mu_h+d_h+\alpha_h)\widetilde{I}_h, \\ \dot{\widetilde{E}}_a(t) &= \left(\dfrac{\sigma_v(t)\sigma_a\beta_{va}\widetilde{I}_v}{\sigma_v\widetilde{N}_v+\sigma_a\widetilde{N}_a}\right)S_a^0 - (\mu_a+\kappa_a)\widetilde{E}_a, \\ \dot{\widetilde{I}}_a(t) &= \kappa_a\widetilde{E}_a(t) - (\mu_a+d_a+\alpha_a)\widetilde{I}_a(t), \\ \dot{\widetilde{E}}_v(t) &= \left(\dfrac{\sigma_v(t)\sigma_h\beta_{hv}\widetilde{I}_h}{\sigma_v(t)\widetilde{N}_v(t)+\sigma_h\widetilde{N}_h} + \dfrac{\sigma_v(t)\sigma_a\beta_{va}\widetilde{I}_a}{\sigma_v(t)\widetilde{N}_v(t)+\sigma_a\widetilde{N}_a}\right)S_v^0 - (\kappa_v(t)+\mu_v(t))\widetilde{E}_v, \\ \dot{\widetilde{I}}_v(t) &= \kappa_v(t)\widetilde{E}_v - \mu_v(t)\widetilde{I}_v. \end{cases}$$

By Lemma 1 and the standard comparison principle, there exist a positive $\omega-$periodic function $\widetilde{x}(t)$ such that $x(t) \leq \widetilde{x}(t)e^{pt}$, where $\widetilde{x}(t) = (\widetilde{E}_i(t), \widetilde{I}_i(t))^{\mathrm{T}}$, for $i = a, h, v$, and $p = \frac{1}{\omega}\ln\rho(\Phi_{(F-V)(\cdot)}(\omega)) < 0$. Thus we conclude that $x(t) \to 0$ as $t \to \infty$, that is,

$$\lim_{t\to\infty} E_i(t) = 0, \quad \lim_{t\to\infty} I_i(t) = 0, \quad \lim_{t\to\infty} R_a(t) = 0, \quad \text{and} \quad \lim_{t\to\infty} R_h(t) = 0, \qquad i = a, h, v.$$

Hence it follows that

$$\lim_{t\to\infty} S_i(t) = S_i^0, \qquad \text{and} \qquad \lim_{t\to\infty} N_h(t) = N_i^0, \qquad i = a, h, v.$$

Therefore, the disease-free equilibrium $\mathcal{E}^0$ of system (3) is globally asymptotically stable. □

Theorem 3. *If $R_0 > 1$, then system (3) is uniformly persistent, i.e., there exists a positive constant η, such that for all initial values of $(S_i(0), E_i(0), I_i(0), R_k(0))\mathbb{R}_+^5 \times Int(\mathbb{R}_+)^6$, $(i = a, h, v,\ k = a, h)$ the solution of model (3) satisfies:*

$$\liminf_{t\to\infty} S_i(t) \geq \eta, \quad \liminf_{t\to\infty} E_i(t) \geq \eta, \quad \liminf_{t\to\infty} I_i(t) \geq \eta, \quad \liminf_{t\to\infty} R_k(t) \geq \eta.$$

Proof. Let us define

$$X = \mathbb{R}_+^{11}; \qquad X_0 = \mathbb{R}_+^5 \times \text{Int}(\mathbb{R}_+)^6; \qquad \partial X_0 = X \backslash X_0.$$

Let $P : X \longrightarrow X$ be the Poincaré map associated with our model (3) such that $P(x_0) = u(\omega, x_0)\ \forall x_0 \in X$, where $u(t, x_0)$ denotes the unique solution of the system with $u(0, x_0) = x_0$.

We begin by demonstrating that P is uniformly persistent with respect to $(X_0, \partial X_0)$. One can easily deduce that from model (3), X and X_0 are positively invariant. Moreover, ∂X_0 is a relatively closed set in X. It follows from Theorem 1 that solutions of model (3) uniformly and ultimately bounded. Thus the semiflow P is point dissipative on $\mathbb{R}_+^{11}$, and $P : \mathbb{R}_+^{11} \to \mathbb{R}_+^{11}$ is compact. By Theorem 3.4.8 in [38], it then follows that P admits a global attractor, which attracts every bounded set in $\mathbb{R}_+^{11}$.
Define

$$M_\partial = \{(S_i(0), E_i(0), I_i(0), R_k(0)) \in \partial X_0 : \ P^m(S_i(0), E_i(0), I_i(0), R_k(0)) \in \partial X_0, \ \forall m \geq 0\},$$

for $i = a, h, v, \quad k = a, h$.
Next, we claim that $M_\partial = \{(S_h(0), 0, 0, R_h(0), S_a(0), 0, 0, R_a(0), S_v(0), 0, 0) : S_i \geq 0, R_k \geq 0\}$. Clearly, $\widetilde{M} = \{(S_h(0), 0, 0, R_h(0), S_a(0), 0, 0, R_a(0), S_v(0), 0, 0) : S_i \geq 0, R_k \geq 0\} \subseteq M_\partial$.
Now, for any $(S_i(0), E_i(0), I_i(0), R_k(0)) \in \partial X_0 \backslash M$; if $E_h(0) = I_h(0) = 0$, it follows that $S_i(0) > 0$, $R_h(0) > 0$, $E_a(0) > 0$, $I_a(0) > 0$, $R_a(0) > 0$, $E_v(0) > 0$, $I_v(0) > 0$, $\dot{E}_h(0) = \lambda_h(0) S_h(0) > 0$, and $\dot{I}_h(0) = 0$. If $E_a(0) = I_a(0) = 0$, it follows that $S_i(0) > 0$, $E_h(0) > 0$, $I_h(0) > 0$, $R_h(0) > 0$, $R_a(0) = 0$, $E_v(0) > 0$, $I_v(0) > 0$, $\dot{E}_a(0) = \lambda_a(0) S_a(0) > 0$, and $\dot{I}_a(0) = 0$. If $E_v(0) = I_v(0) = 0$, it follows that $S_i(0) > 0$, $E_h(0) = 0$, $I_h(0) = 0$, $R_h(0) > 0$, $E_a(0) = 0$, $I_a(0) = 0$, $R_a(0) = 0$, $\dot{E}_v(0) = 0$, and $\dot{I}_a(0) = 0$. Thus, we have $(S_i(0), E_i(0), I_i(0), R_k(0)) \notin \partial X_0$ for $0 < t \ll 1$. By the positive invariance of X_0, we know that $P^m(S_i(0), E_i(0), I_i(0), R_k(0)) \notin \partial X_0$ for $m \geq 1$, hence $(S_i(0), E_i(0), I_i(0), R_k(0)) \notin M_\partial$, and thus $M_\partial = \{(S_h(0), 0, 0, R_h(0), S_a(0), 0, 0, R_a(0), S_v(0), 0, 0) : S_i \geq 0, R_k \geq 0\}$.

Now consider the fixed point $M_0 = (S_h^0, 0, 0, R_h^0, S_a^0, 0, 0, 0, S_v^0, 0, 0)$ of the Poincaré map P, where and define $W^S(M_0) = \{x_0 : P^m(x_0) \to M_0, m \to \infty\}$. We show that

$$W^S(M_0) \cap X_0 = \emptyset. \tag{9}$$

Based on the continuity of solutions with respect to the initial conditions, for any $\epsilon > 0$, there exists $\delta > 0$ small enough such that for all $(S_i(0), E_i(0), I_i(0), R_k(0)) \in X_0$ with $\|(S_i(0), E_i(0), I_i(0), R_k(0)) - M_0\| \leq \delta$, we have

$$\|u(t, (S_i(0), E_i(0), I_i(0), R_k(0)) - u(t, M_0)\| < \epsilon, \quad \forall t \in [0, \omega].$$

To obtain (9), we claim that

$$\limsup_{m\to\infty} \|P^m(S_i(0), E_i(0), I_i(0), R_k(0)) - M_0\| \geq \delta, \quad \forall (S_i(0), E_i(0), I_i(0), R_k(0)) \in X_0.$$

We prove this claim by contradiction; that is, we suppose $\limsup_{m\to\infty} \|P^m(S_i(0), E_i(0), I_i(0), R_k(0)) - M_0\| < \delta$ for some $(S_i(0), E_i(0), I_i(0), R_k(0)) \in X_0$. Without loss of generality, we assume that $\|P^m(S_i(0), E_i(0), I_i(0), R_k(0)) - M_0\| < \delta, \ \forall m \geq 0$. Thus,

$$\|u(t, P^m(S_i(0), E_i(0), I_i(0), R_k(0)) - u(t, M_0)\| < \epsilon, \quad \forall t \in [0, \omega] \text{ and } m \geq 0.$$

Moreover, for any $t \geq 0$, we write $t = t_0 + q\omega$ with $t_0 \in [0, \omega)$ and $q = [\frac{t}{\omega}]$, the greatest integer less than or equal to $\frac{t}{\omega}$. Then we obtain

$$\|u(t, (S_i(0), E_i(0), I_i(0), R_k(0)) - u(t, M_0)\| = \|u(t_0, P^m(S_i(0), E_i(0), I_i(0), R_k(0)) - u(t_0, M_0)\| < \epsilon$$

for any $t \geq 0$. Let $(S_i(t), E_i(t), I_i(t), R_k(t)) = u(t, (S_i(0), E_i(0), I_i(0), R_k(0))$. It follows that $N_{i0} - \epsilon < S_i(t) < N_{i0} + \epsilon$, $0 < E_i(t) < \epsilon$, $0 < I_i(t) < \epsilon$, and $0 < R_k(t) < \epsilon$. Then from the second equation of system (3) we have

$$\begin{aligned}
\frac{dE_h}{dt} &= \frac{\sigma_v(t)\sigma_h\beta_{vh}I_vS_h}{\sigma_v(t)N_v + \sigma_hN_h} - (\mu_h + \kappa_h)E_h, \\
&\geq \frac{\sigma_v(t)\sigma_h\beta_{vh}I_v(N_{h0} - \epsilon)}{\sigma_v(t)(N_{v0} + \epsilon) + \sigma_h(N_{h0} + \epsilon)} - (\mu_h + \kappa_h)E_h, \\
&= \left(\frac{\sigma_v(t)\sigma_h\beta_{vh}N_{h0}}{\sigma_v(t)N_{v0} + \sigma_hN_{h0}}\right)\left(1 - \frac{2\epsilon\sigma_h\left(1 + \frac{\sigma_v(t)}{2\sigma_h} + \frac{\sigma_v(t)N_{v0}}{2\sigma_hN_{h0}}\right)}{\sigma_v(t)\,(N_{v0} + \epsilon) + \sigma_h\,(N_{h0} + \epsilon)}\right)I_v - (\mu_h + \kappa_h)E_h,
\end{aligned}$$

Recall that the third equation of system (3) has the form

$$\dot{I}_h(t) = \kappa_hE_h(t) - (\mu_h + \alpha_h + d_h)I_h.$$

From the sixth equation of system (3) we have

$$\begin{aligned}
\frac{dE_a}{dt} &\geq \frac{\sigma_v(t)\sigma_a\beta_{va}I_v(N_{a0} - \epsilon)}{\sigma_v(t)(N_{v0} + \epsilon) + \sigma_h(N_{a0} + \epsilon)} - (\mu_a + \kappa_a)E_a, \\
&= \left(\frac{\sigma_v(t)\sigma_a\beta_{va}N_{a0}}{\sigma_vN_{v0} + \sigma_aN_{a0}}\right)\left(1 - \frac{2\epsilon\sigma_a\left(1 + \frac{\sigma_v(t)}{2\sigma_a} + \frac{\sigma_v(t)N_{v0}}{2\sigma_aN_{a0}}\right)}{\sigma_v(t)\,(N_{v0} + \epsilon) + \sigma_a\,(N_{a0} + \epsilon)}\right)I_v - (\mu_a + \kappa_a)E_a,
\end{aligned}$$

The seventh equation of system (3) has the form

$$\dot{I}_a(t) = \kappa_aE_a - (\mu_a + \alpha_a + d_a)I_a.$$

The ninth equation of system (3) satisfies

$$\begin{aligned}
\frac{dE_v}{dt} &\geq \frac{\sigma_v(t)\sigma_h\beta_{hv}I_h(N_{v0} - \epsilon)}{\sigma_v(t)(N_{v0} + \epsilon) + \sigma_h(N_{h0} + \epsilon)} + \frac{\sigma_v(t)\sigma_a\beta_{av}I_a(N_{v0} - \epsilon)}{\sigma_v(t)(N_{v0} + \epsilon) + \sigma_a(N_{a0} + \epsilon)} - (\mu_v(t) + \kappa_v(t))E_v, \\
&= +\left(\frac{\sigma_v(t)\sigma_h\beta_{hv}N_{v0}}{\sigma_v(t)N_{v0} + \sigma_hN_{h0}}\right)\left(1 - \frac{2\epsilon\sigma_v(t)\left(1 + \frac{\sigma_h}{2\sigma_v(t)} + \frac{\sigma_hN_{h0}}{2\sigma_v(t)N_{v0}}\right)}{\sigma_v(t)\,(N_{v0} + \epsilon) + \sigma_h\,(N_{h0} + \epsilon)}\right)I_h \\
&\quad +\left(\frac{\sigma_v(t)\sigma_a\beta_{av}N_{v0}}{\sigma_v(t)N_{v0} + \sigma_aN_{a0}}\right)\left(1 - \frac{2\epsilon\sigma_v(t)\left(1 + \frac{\sigma_a}{2\sigma_v(t)} + \frac{\sigma_aN_{a0}}{2\sigma_v(t)N_{v0}}\right)}{\sigma_v(t)\left(\frac{\Lambda_v}{\mu_v(t)} + \epsilon\right) + \sigma_a\,(N_{a0} + \epsilon)}\right)I_a - (\mu_v(t) + \kappa_v(t))E_v(t).
\end{aligned}$$

Recall that the tenth equation of system (3) has the form

$$\dot{I}_v(t) = \kappa_v(t)E_v - \mu_v(t)I_v.$$

Let

$$M_\epsilon = \begin{bmatrix} 0 & 0 & 0 & 0 & 0 & \frac{2\epsilon\sigma_h\left(1+\frac{\sigma_v(t)}{2\sigma_h}+\frac{\sigma_v(t)N_{v0}}{2\sigma_h N_{h0}}\right)}{\sigma_v(t)(N_{v0}+\epsilon)+\sigma_h(N_{h0}+\epsilon)} \\ 0 & 0 & 0 & 0 & 0 & 0 \\ 0 & 0 & 0 & 0 & 0 & \frac{2\epsilon\sigma_a\left(1+\frac{\sigma_v(t)}{2\sigma_a}+\frac{\sigma_v(t)N_{v0}}{2\sigma_a N_{a0}}\right)}{\sigma_v(t)(N_{v0}+\epsilon)+\sigma_a(N_{a0}+\epsilon)} \\ 0 & 0 & 0 & 0 & 0 & 0 \\ 0 & \frac{2\epsilon\sigma_v(t)\left(1+\frac{\sigma_h}{2\sigma_v(t)}+\frac{\sigma_h N_{h0}}{2\sigma_v(t)N_{v0}}\right)}{\sigma_v(t)(N_{v0}+\epsilon)+\sigma_h(N_{h0}+\epsilon)} & 0 & \frac{2\epsilon\sigma_v(t)\left(1+\frac{\sigma_a}{2\sigma_v(t)}+\frac{\sigma_a N_{a0}}{2\sigma_v(t)N_{v0}}\right)}{\sigma_v(t)\left(\frac{\Lambda_v}{\mu_v(t)}+\epsilon\right)+\sigma_a(N_{a0}+\epsilon)} & 0 & 0 \\ 0 & 0 & 0 & 0 & 0 & 0 \end{bmatrix},$$

such that

$$[\dot{E}_h, \quad \dot{I}_h, \quad \dot{E}_a, \quad \dot{I}_a, \quad \dot{E}_v, \quad \dot{I}_v]^{\mathrm{T}} \geq [F - V - M_\epsilon][E_h, \quad I_h, \quad E_a, \quad I_a, \quad E_v, \quad I_v]^{\mathrm{T}}.$$

Again based on ([35], Theorem 2.2) , we know that if $\rho(\Phi_{F-V}(\omega)) > 1$, then we can choose ϵ small enough such that $\rho(\Phi_{F-V-M_\epsilon}(\omega)) > 1$. Again by ([35], Theorem 2.2) and and the standard comparison principle, there exists a positive $\omega-$ periodic function $v(t)$ such that $x(t) \geq \widetilde{x}_1(t)e^{p_1 t}$, where $\widetilde{x}_1(t) = (\widetilde{E}_i(t), \widetilde{I}_i(t))^{\mathrm{T}}$, for $i = a, h, v$, and $p_1 = \frac{1}{\omega}\ln\rho(\Phi_{(F-V-M_\epsilon)}(\omega)) > 0$ which implies that

$$\lim_{t\to\infty} E_i(t) = \infty, \qquad \text{and} \qquad \lim_{t\to\infty} I_i(t) = \infty, \quad i = a, h, v.$$

which is a contradiction in M_∂ since M_∂ converges to M_0. and M_0 is acyclic in M_∂. By ([39], Theorem 1.3.1), for a stronger repelling property of ∂X_0, we conclude that P is uniformly persistent with respect to $(X_0, \partial X_0)$, which implies the uniform persistence of the solutions of system (3) with respect to $(X_0, \partial X_0)$ ([39], Theorem 3.1.1). It follows from Theorem 3.1.1 in [39] that the solution of (3) is uniformly persistent. □

Appendix C. Optimal control framework

In this section, an optimal control problem for a seasonal *Trypanosoma brucei rhodesiense* model (4) is formulated and analysed. The main goal being to minimize the population of infected humans at minimal cost of implementation. We define our objective functional as follows

$$J(u_1(t), u_2(t)) = \int_0^{t_f} \left(C_1 I_h(t) + C_2 I_a(t) + \frac{W_1}{2}u_1^2(t) + \frac{W_2}{2}u_2^2(t)\right) dt. \tag{10}$$

The optimal control problem becomes seeking an optimal functions, $U^* = (u_1^*(t), u_2^*(t))$, such that

$$J(u_1^*(t), u_2^*(t)) = \inf_{(u_1,u_2)\in U} J(u_1(t), u_2(t)),$$

for the admissible set $U = \{(u_1(t), u_2(t)) \in (L^\infty(0, t_f))^2 : 0 \leq u_i(t) \leq q_i; q_i \in \mathbb{R}^+, i = 1, 2\}$, where q_i denotes the upper bound of the controls.

In what follows, we investigate the existence of an optimal control pair basing our analysis on the work of Fleming and Rishel (1975) [40]. Based on Theorem 1 we are now aware that all the variables of system (4) have a lower and upper bounds.

Theorem 4. *There exists an optimal control U^* to the problem (4).*

Proof. Suppose that $\mathbf{f}(t, \mathbf{x}, \mathbf{u})$ be the right-hand side of the (4) where by $\mathbf{x} = (S_h, E_h, I_h, R_h, S_a, E_a, I_a, R_a, S_v, E_v, I_v$ and $\mathbf{u} = (u_1(t), u_2(t))$ represent the vector of state variables and control functions respectively. We list the requirements for the existence of optimal control as presented in Fleming and Rishel (1975) [40]:

1. The function $\mathbf{f}$ is of class C^1 and there exists a constant C such that $|\mathbf{f}(t, 0, 0)| \leq C, |\mathbf{f}_{\mathbf{x}}(t, \mathbf{x}, \mathbf{u})| \leq C(1 + |\mathbf{u}|), |\mathbf{f}_{\mathbf{u}}(t, \mathbf{x}, \mathbf{u})| \leq C$;
2. the admissible set of all solutions to system (4) with corresponding control in Ω is nonempty;
3. $\mathbf{f}(t, \mathbf{x}, \mathbf{u}) = \mathbf{a}(t, \mathbf{x}) + \mathbf{b}(t, \mathbf{x})\mathbf{u}$;
4. the control set $U = [0, u_{1\max}] \times [0, u_{2\max}]$ is closed, convex and compact;
5. the integrand of the objective functional is convex in U.

In order to verify these conditions we write

$$\mathbf{f}(t, \mathbf{x}, \mathbf{u}) = \begin{bmatrix} b_h N_h(t) - \lambda_h(t) S_h(t) - \mu_h S_h(t) - u_1(t) S_h(t) + \gamma_h R_h(t) \\ \lambda_h(t) S_h(t) - (\mu_h + \kappa_h) E_h(t) \\ \kappa_h E_h(t) - (\mu_h + \alpha_h + d_h) I_h(t) \\ u_1(t) S_h(t) + \alpha_h I_h(t) - (\mu_h + \gamma_h) R_h(t) \\ b_a N_a(t) - \lambda_a(t) S_a(t) - \mu_a S_a(t) + \gamma_a R_a(t) \\ \lambda_a(t) S_a(t) - (\mu_a + \kappa_a) E_a(t) \\ \kappa_a E_a(t) - (\mu_a + \alpha_a + d_a) I_a(t) \\ \alpha_a I_a(t) - (\mu_a + \gamma_a) R_a(t) \\ b_v(t) N_v(t) - \lambda_v(t) S_v(t) - (\mu_v(t) + u_2(t)) S_v(t) \\ \lambda_v(t) S_v(t) - (\kappa_v(t) + \mu_v(t) + u_2(t))) E_v(t) \\ \kappa_v(t) E_v(t) - (\mu_v(t) + u_2(t)) I_v(t) \end{bmatrix}. \tag{11}$$

From (11), it is clear that $\mathbf{f}(t, \mathbf{x}, \mathbf{u})$ is of class C^1 and $|\mathbf{f}(t, \mathbf{0}, \mathbf{0})| = 0$. In addition, we have one can easily compute $|\mathbf{f}_{\mathbf{x}}(t, \mathbf{x}, \mathbf{u})|$ and $|\mathbf{f}_{\mathbf{u}}(t, \mathbf{x}, \mathbf{u})|$ and demonstrate that

$$|\mathbf{f}(t, \mathbf{0}, \mathbf{0})| \leq C, \quad |\mathbf{f}_{\mathbf{x}}(t, \mathbf{x}, \mathbf{u})|, \leq C(1 + |\mathbf{u}|) \quad |\mathbf{f}_{\mathbf{u}}(t, \mathbf{x}, \mathbf{u})| \leq C.$$

Due to the condition 1, the existence of the unique solution for condition 2 for bounded control is satisfied. On the other hand, the quantity $\mathbf{f}(t, \mathbf{x}, \mathbf{u})$ is expressed as linear function of control variables which satisfy the condition 3. □

After demonstrating the existence of optimal controls, in what follows, we characterize the optimal control functions by utilizing the Pontryagin's Maximum Principle [33]. Pontryagin's Maximum Principle introduces adjoint functions that allow the state system (4) to be attached to the objective functional, that is, it converts the system (4) into the problem of minimizing the Hamiltonian $H(t)$ given by:

$$\begin{aligned} H(t) \;=\; & C_1 I_h(t) + C_2 I_a(t) + \frac{W_1}{2} u_1^2(t) + \frac{W_2}{2} u_2^2(t) + \lambda_1(t)[b_h N_h(t) - \lambda_h(t) S_h(t) - (u_1(t) + \mu_h) S_h + \gamma_h R_h(t)] \\ & + \lambda_2(t)[\lambda_h(t) S_h(t) - (\mu_h + \kappa_h) E_h(t)] + \lambda_3(t)[\kappa_h E_h(t) - (\mu_h + d_h + \alpha_h) I_h(t)] \\ & + \lambda_4(t)[u_1(t) S_h(t) + \alpha_h I_h(t) - (\mu_h + \gamma_h) R_h(t)] + \lambda_5(t)[\Lambda_a - \lambda_a(t) S_a(t) - \mu_a S_a(t) + \gamma_a R_a(t)] \end{aligned}$$

$$+\lambda_6(t)[b_aN_a(t) - \lambda_a(t)S_a - (\mu_a + \kappa_a)E_a(t)] + \lambda_7(t)[\kappa_aE_a(t) - (\mu_a + d_a + \alpha_a)I_a(t)]$$
$$+\lambda_8(t)[\alpha_aI_a(t) - (\mu_a + \gamma_a)R_a(t)] + \lambda_9(t)[b_v(t)N_v(t) - \lambda_v(t)S_v(t) - (\mu_v(t) + u_2(t))S_v(t)]$$
$$+\lambda_{10}(t)[\lambda_v(t)S_v - (\mu_v(t) + \kappa_v(t) + u_2(t))E_v(t)] + \lambda_{11}(t)[\kappa_v(t)E_v - (\mu_v(t) + u_2(t))I_v(t)]. \quad (12)$$

Note that the first part of the terms in $H(t)$ came from the integrand of the objective functional. Given an optimal control solution (u^*) and the corresponding state solutions $(S_h, E_h, I_h, R_h, S_a, E_a, I_a, R_a, S_v, E_v, I_v)$ there exist adjoint functions $\lambda_i(t)$, $(i = 1, 2, 3, \cdots, 11)$ [34] satisfying

$$\frac{\partial \lambda_i}{dt} = -\frac{\partial H}{\partial \mathbf{x}},$$

with transversality condition $\lambda(t_f) = 0$. Thus the adjoint system is:

$$\begin{aligned}
\frac{d\lambda_1}{dt} &= \lambda_1\mu_h + u_1(t)(\lambda_1 - \lambda_4) + (\lambda_1 - \lambda_2)\frac{\sigma_v(t)\sigma_h\beta_{vh}I_v}{\sigma_v(t)N_v + \sigma_hN_h} + (\lambda_2 - \lambda_1)\frac{\sigma_v(t)\sigma_h^2\beta_{vh}I_vS_h}{(\sigma_v(t)N_v + \sigma_hN_h)^2} \\
&\quad +(\lambda_{10} - \lambda_9)\frac{\sigma_v(t)\sigma_h^2\beta_{hv}I_hS_v}{(\sigma_v(t)N_v + \sigma_hN_h)^2}, \\
\frac{d\lambda_2}{dt} &= \lambda_2\mu_h + (\lambda_2 - \lambda_3)\kappa_h + (\lambda_2 - \lambda_1)\frac{\sigma_v(t)\sigma_h^2\beta_{vh}I_vS_h}{(\sigma_v(t)N_v + \sigma_hN_h)^2} + (\lambda_{10} - \lambda_9)\frac{\sigma_v(t)\sigma_h^2\beta_{hv}I_hS_v}{(\sigma_v(t)N_v + \sigma_hN_h)^2}, \\
\frac{d\lambda_3}{dt} &= -C_1 + \lambda_3(\mu_h + d_h) + \alpha_h(\lambda_3 - \lambda_4) + (\lambda_2 - \lambda_1)\frac{\sigma_v(t)\sigma_h^2\beta_{vh}I_vS_h}{(\sigma_v(t)N_v + \sigma_hN_h)^2} + (\lambda_9 - \lambda_{10})\frac{\sigma_v(t)\sigma_h\beta_{hv}S_v}{\sigma_v(t)N_v + \sigma_hN_h} \\
&\quad +(\lambda_{10} - \lambda_9)\frac{\sigma_v(t)\sigma_h^2\beta_{hv}I_hS_v}{(\sigma_v(t)N_v + \sigma_hN_h)^2}, \\
\frac{d\lambda_4}{dt} &= \lambda_4\mu_h + (\lambda_4 - \lambda_1)\gamma_h + (\lambda_2 - \lambda_1)\frac{\sigma_v(t)\sigma_h^2\beta_{vh}I_vS_h}{(\sigma_v(t)N_v + \sigma_hN_h)^2} + (\lambda_{10} - \lambda_9)\frac{\sigma_v(t)\sigma_h^2\beta_{hv}I_hS_v}{(\sigma_v(t)N_v + \sigma_hN_h)^2}, \\
\frac{d\lambda_5}{dt} &= \lambda_5\mu_a + (\lambda_5 - \lambda_6)\frac{\sigma_v(t)\sigma_a\beta_{va}I_v}{\sigma_v(t)N_v + \sigma_aN_a} + (\lambda_6 - \lambda_5)\frac{\sigma_v(t)\sigma_a^2\beta_{va}I_vS_a}{(\sigma_v(t)N_v + \sigma_aN_a)^2} + (\lambda_{10} - \lambda_9)\frac{\sigma_v(t)\sigma_a^2\beta_{av}I_aS_v}{(\sigma_v(t)N_v + \sigma_aN_a)^2}, \\
\frac{d\lambda_6}{dt} &= \lambda_6\mu_a + (\lambda_6 - \lambda_7)\kappa_a + (\lambda_6 - \lambda_5)\frac{\sigma_v(t)\sigma_a^2\beta_{va}I_vS_a}{(\sigma_v(t)N_v + \sigma_aN_a)^2} + (\lambda_{10} - \lambda_9)\frac{\sigma_v(t)\sigma_a^2\beta_{av}I_aS_v}{(\sigma_v(t)N_v + \sigma_aN_a)^2}, \\
\frac{d\lambda_7}{dt} &= -C_2 + \lambda_7(\mu_a + d_a) + \alpha_a(\lambda_7 - \lambda_8) + (\lambda_6 - \lambda_5)\frac{\sigma_v(t)\sigma_a^2\beta_{va}I_vS_a}{(\sigma_v(t)N_v + \sigma_aN_a)^2} + (\lambda_9 - \lambda_{10})\frac{\sigma_v(t)\sigma_a\beta_{av}S_v}{\sigma_v(t)N_v + \sigma_aN_a} \\
&\quad +(\lambda_{10} - \lambda_9)\frac{\sigma_v(t)\sigma_a^2\beta_{av}I_aS_v}{(\sigma_v(t)N_v + \sigma_aN_a)^2}, \\
\frac{d\lambda_8}{dt} &= \lambda_8\mu_a + (\lambda_8 - \lambda_5)\gamma_a + (\lambda_6 - \lambda_5)\frac{\sigma_v(t)\sigma_a^2\beta_{va}I_vS_a}{(\sigma_v(t)N_v + \sigma_aN_a)^2} + (\lambda_{10} - \lambda_9)\frac{\sigma_v(t)\sigma_a^2\beta_{av}I_aS_v}{(\sigma_v(t)N_v + \sigma_aN_a)^2}, \\
\frac{d\lambda_9}{dt} &= \lambda_9(\mu_v(t) + u_2(t)) + (\lambda_2 - \lambda_1)\frac{\sigma_v^2(t)\sigma_h\beta_{vh}I_vS_h}{(\sigma_v(t)N_v + \sigma_hN_h)^2} + (\lambda_6 - \lambda_5)\frac{\sigma_v^2(t)\sigma_a\beta_{va}I_vS_a}{(\sigma_v(t)N_v + \sigma_aN_a)^2} \\
&\quad +(\lambda_9 - \lambda_{10})\frac{\sigma_v(t)\sigma_h\beta_{hv}I_h}{\sigma_v(t)N_v + \sigma_hN_h} + (\lambda_9 - \lambda_{10})\frac{\sigma_v(t)\sigma_a\beta_{av}I_a}{\sigma_v(t)N_v + \sigma_aN_a} \\
&\quad +(\lambda_{10} - \lambda_9)\frac{\sigma_v^2\sigma_a\beta_{av}I_aS_v}{(\sigma_vN_v + \sigma_aN_a)^2} + (\lambda_{10} - \lambda_9)\frac{\sigma_v^2(t)\sigma_h\beta_{hv}I_hS_v}{(\sigma_v(t)N_v + \sigma_hN_h)^2},
\end{aligned}$$

$$\begin{aligned}
\frac{d\lambda_{10}}{dt} &= \lambda_{10}(\mu_v(t)+u_2(t))+\kappa_v(t)(\lambda_{10}-\lambda_{11})+(\lambda_2-\lambda_1)\frac{\sigma_v^2(t)\sigma_h\beta_{vh}I_vS_h}{(\sigma_v(t)N_v+\sigma_hN_h)^2}+(\lambda_6-\lambda_5)\frac{\sigma_v^2(t)\sigma_a\beta_{va}I_vS_a}{(\sigma_v(t)N_v+\sigma_aN_a)^2}\\
&\quad+(\lambda_{10}-\lambda_9)\frac{\sigma_v^2(t)\sigma_a\beta_{av}I_aS_v}{(\sigma_v(t)N_v+\sigma_aN_a)^2}+(\lambda_{10}-\lambda_9)\frac{\sigma_v^2(t)\sigma_h\beta_{hv}I_hS_v}{(\sigma_v(t)N_v+\sigma_hN_h)^2},\\
\frac{d\lambda_{11}}{dt} &= \lambda_{11}(\mu_v(t)+u_2(t))+(\lambda_1-\lambda_2)\frac{\sigma_v(t)\sigma_h\beta_{vh}S_h}{\sigma_v(t)N_v+\sigma_hN_h}+(\lambda_2-\lambda_1)\frac{\sigma_v^2(t)\sigma_h\beta_{vh}I_vS_h}{(\sigma_v(t)N_v+\sigma_hN_h)^2}\\
&\quad+(\lambda_5-\lambda_6)\frac{\sigma_v(t)\sigma_a\beta_{va}S_a}{\sigma_v(t)N_v+\sigma_aN_a}+(\lambda_6-\lambda_5)\frac{\sigma_v^2(t)\sigma_a\beta_{va}I_vS_a}{(\sigma_v(t)N_v+\sigma_aN_a)^2}+(\lambda_{10}-\lambda_9)\frac{\sigma_v^2(t)\sigma_a\beta_{av}I_aS_v}{(\sigma_v(t)N_v+\sigma_aN_a)^2}\\
&\quad+(\lambda_{10}-\lambda_9)\frac{\sigma_v^2(t)\sigma_h\beta_{hv}I_hS_v}{(\sigma_v(t)N_v+\sigma_hN_h)^2}. \qquad (13)
\end{aligned}$$

In addition, the optimal solution of the Hamiltonian are determined by taking the partial derivatives of the function $H(t)$ in (12) with respect to control functions u_i, followed by setting the resultant equation to zero and then solve for u_i^*, $i = 1, 2$ follows:

$$\frac{\partial H}{\partial u_1} = u_1^*W_1-(\lambda_1-\lambda_4)S_h. \qquad (14)$$

$$\frac{\partial H}{\partial u_2} = u_2^*W_2-(\lambda_9S_v+\lambda_{10}E_v+\lambda_{11}I_v). \qquad (15)$$

Observe that $\frac{\partial^2 H}{\partial u^i} = W_i > 0$ and this demonstrates that the optimal control problem has minimum value at the optimal solution $U^*(t)$. Furthermore by setting (15) to zero and solve for u_i^* gives

$$u_1^* = \frac{(\lambda_1-\lambda_4)S_h}{W_1}, \qquad u_2^* = \frac{(S_v\lambda_9+E_v\lambda_{10}+I_v\lambda_{11})}{W_2}.$$

By applying the the standard arguments and the bounds for the controls, we obtain the characterization of the optimal controls as follows:

$$u_i = \min\left\{q_i, \max\left(0, u_i^*\right)\right\}. \qquad (16)$$

Advances in Difference Equations
a SpringerOpen Journal

RESEARCH Open Access

A fractional-order *Trypanosoma brucei rhodesiense* model with vector saturation and temperature dependent parameters

Mlyashimbi Helikumi[1,2*], Moatlhodi Kgosimore[3], Dmitry Kuznetsov[1] and Steady Mushayabasa[4*]

*Correspondence:
helikumim@nm-aist.ac.tz;
steadymushaya@gmail.com
[1]School of Computational and Communication Science and Engineering, The Nelson Mandela African Institution of Science and Technology (NM-AIST), Arusha, Tanzania
[4]Department of Mathematics, University of Zimbabwe, Harare, Zimbabwe
Full list of author information is available at the end of the article

Abstract

Temperature is one of the integral environmental drivers that strongly affect the distribution and density of tsetse fly population. Precisely, ectotherm performance measures, such as development rate, survival probability and reproductive rate, increase from low values (even zero) at critical minimum temperature, peak at an optimum temperature and then decline to low levels (even zero) at a critical maximum temperature. In this study, a fractional-order *Trypanosoma brucei rhodesiense* model incorporating vector saturation and temperature dependent parameters is considered. The proposed model incorporates the interplay between vectors and two hosts, humans and animals. We computed the basic reproduction number and established results on the threshold dynamics. Meanwhile, we explored the effects of vector control and screening of infected host on long-term disease dynamics. We determine threshold levels essential to reducing the basic reproduction number to level below unity at various temperature levels. Our findings indicate that vector control and host screening could significantly control spread of the disease at different temperature levels.

MSC: 92B05; 93A30; 93C15

Keywords: *Trypanosoma brucei rhodesiense*; Temperature; Mathematical model; Caputo fractional derivative; Vector saturation

1 Introduction

Human African trypanosomiasis (HAT), also known as sleeping sickness, is a neglected tropical disease that continues to affect people living in world's poorest communities. In particular, it is more prevalent in nations or communities with weak health infrastructure, scanty health information and low food security. Two forms of the disease exist depending on the parasite involved: *Trypanosoma brucei gambiense*, which is a chronic form of the disease present in western and central Africa, and *Trypanosoma brucei rhodesiense*, which is an acute disease located in eastern and southern Africa [1]. Of the HAT cases recorded in the last decade, approximately 98% are attributed to the gambiense form and the remainder to rhodesiense [1]. With such statistics, several researchers believe that the

rhodesiense form is a zoonotic disease that affects mainly animals (livestock and wildlife), with humans being only accidentally infected [1].

Although the signs and symptoms of HAT are generally similar for both forms, their frequency, severity and kinetic appearance differ. The rhodesiense form is an acute disease that usually progresses to death within six months, whereas the gambiense form is usually a chronic progressive infection with an average duration of almost three years [1]. Furthermore, clinical signs and symptoms are unspecific in both forms of the disease, and their appearance varies between individuals and foci. Some of the main signs and symptoms of the first stage of infection are intermittent fever, headache, lymphadenopathies, weakness, asthenia, anemia, cardiac disorders, endocrine disturbances, musculoskeletal pains and hepatosplenomegaly [1]. Neuropsychiatric signs and symptoms, including sleep disturbances, are often presented by patients in the second stage of infection. It is worth noting that most of the symptoms of both stages overlap, rendering the distinction between the stages unclear [1].

HAT is transmitted by more than 20 species of *Glossina* tsetse flies. Prior studies have shown that all metabolic processes that occur in tsetse flies strongly depend on temperature. In particular, it was observed that the interlarval period, pupal period, adult lifespan and the period between successive feeds are reduced as temperature increases [2]. Phelps and Lovemore [3] noted that temperature does not only alter the different developmental periods of the vector but it also plays a huge role in the fly's flight activity. Furthermore, for temperature below 17°C it was noted that tsetse flies will rest in direct sunlight and when temperatures are above 32°C the vectors will be inactive and they will seek artificial refuges, and in most cases these are cool shaded places [4].

According to Phelps and Burrow [5], temperatures above 40°C are fatal to both small and large flies and pupae. Bursell [6] opines that temperature and the size of the fly affect the amount of fat reservation in the fly. Precisely, smaller flies have less fat than larger ones. This is one of the reasons why temperatures below 16°C are known not to be suitable for the development of smaller flies, since the fat which would have been reserved during the larval periods will get exhausted before the pupa is fully matured. Thus fat reservation is integral for the development of the fly from pupa to adult as well as the survival of the fly till it gets its first blood-meal [6]. Phelps and Clarke [7] demonstrated that extreme temperature is associated with higher mortality among young flies, particularly in small male flies.

The above discussion clearly demonstrates that temperature has an integral role on tsetse population dynamics and can be one of the strongest abiotic determinants of tsetse distributions [8]. Hence, as opined by Leak [9], understanding the relationship between these factors and vector population dynamics is therefore a potential area for modelling and further development of the existing models. Mathematical modelling, as a powerful tool in quantifying the complex and numerous factors, has been widely used to understand the transmission and control of HAT [8, 10–32]. The aforementioned studies improved the existing knowledge on HAT dynamics. For example, the study of Hagrove et al. [10] demonstrated that treating cattle with insecticides could be useful on HAT management. Pandey et al. [11], Funk et al. [12], Ndondo et al. [13] and Rock et al. [14] among others explored the role of animals as reservoirs on HAT dynamics. Their studies demonstrated that animals play an integral role of HAT dynamics hence they need to be incorporated in the frameworks that seek to explore the intrinsic dynamics of HAT. Stone and Chitnis

[15] utilised a mathematical model to explore the effects of heterogeneous biting exposure and animal hosts on *Trypanosoma brucei gambiense* transmission and control. Outcomes from their study highlighted that heterogeneity biting rates as well as ecological and environmental factors play a crucial role on *Trypanosoma brucei gambiense* transmission and control.

Recently, Lord et al. [16], Alderton et al. [17] and Ackley and Hagrove [18] explored the role of temperature on HAT dynamics. Alderton et al. [17] utilised an agent based model to explore the effects of temperature on seasonal HAT transmission. Among several other outcomes, their work suggested that mathematical models could strongly mirror the transmission dynamics of HAT. In particular, they found out that their model solutions were in agreement with reality. Lord et al. [16] developed a mathematical model for HAT that incorporated the effects of temperature on mortality, larviposition and emergence rates. Making use of the epidemiological data for infection in cattle they validated their framework, and findings from their work highlighted that temperature variations are key to tsetse distribution and abundance. Ackley and Hagrove [18] developed a dynamical model to simulate female tsetse populations and the associated changes in their age distribution. One of the key findings from their work is that for temperatures greater than 25°C mortality among immature classes of the vector increases substantially.

As concerted efforts to "eliminate" HAT continue to increase, with the current set target being "the reduction of gambiense HAT incidence to less than 1 new case per 10,000 population at risk in at least 90% of foci with fewer than 2000 cases reportedly globally by 2020" and "to target zero incidence of the disease by 2030" [19], different modelling approaches need to be utilised to continue the characterisation of the relationship between temperature and HAT. In this paper, we utilise fractional calculus to explore the effects of temperature on *Trypanosoma brucei rhodesiense*.

Although the aforementioned studies improved our quantitative and qualitative knowledge on the relationship between temperature and HAT, most of the mathematical models of infectious diseases have been described by the ordinary differential equations (ODEs) in which the order of derivative is an integer. However, recent studies suggest that models that use integer-order differentiation do not adequately capture memory effects, long-rage interactions and hereditary properties, which govern many real world problems [33]. In contrast, it has been proved that models that utilise fractional differentiation provide "more reasonable" outcomes compared to those that use integer-order differentiation [33] since they can capture memory effects. Moreover, several researchers concur that many real world problems are influenced by history, suggesting that memory has a strong impact on the underlying dynamics. Based on this notion, fractional-order calculus has been widely and extensively used in many fields such as engineering, biochemistry, finance, chemistry, medicine, biology and so on, compared to the classical order [34, 35].

Prior studies suggest that evolution and control of epidemic processes in human societies cannot be considered without any memory effect [33–36]. In particular, they argue that whenever a disease spreads within a community, individuals gain knowledge or experience, which greatly influences their response [33]. Thus once people are aware of a certain disease and its impact they use suitable mitigation strategies to minimise contact between themselves and vectors, thereby minimising chances of being infected. Evidently, this results in some endogenous controlled suppression of the spreading, although other factors can help [33]. Based on this assertion, fractional-order derivative is more suited

for modelling problems involving memory, which is the case in most biological systems [36]. Another advantage of using fractional-order derivative is that it enlarges the stability region of the dynamical systems [36]. Motivated by this discussion we believe that the memory has an effect on HAT dynamics. The framework proposed in this study includes the life cycle of tsetse flies, humans and animals. Furthermore, the model incorporates the formulae proposed by Artzrouni and Gouteux [25] to explore the role of human detection and vector control on short and long term dynamics of the disease at different temperature levels.

The rest of the paper is organised as follows. In Sect. 2, we present preliminaries on the Caputo fractional calculus. The proposed model and analytical results are presented in Sect. 3. In Sect. 4, the dynamical behaviour of the proposed model is investigated. Precisely, we compute the basic reproduction number and investigate the stability of the model's steady states. In Sect. 5, numerical experiments are done in order to verify theoretical results presented in the study. Finally, a brief discussion rounds up the paper.

2 Preliminaries on the Caputo fractional calculus

We begin by introducing the definition of Caputo fractional derivative and stating related theorems (see [37–41]) that we will utilise to derive important results in this work.

Definition 2.1 Suppose that $\alpha > 0$, $t > a$, $\alpha, a, t \in \mathbb{R}$. The Caputo fractional derivative is given by

$$ {}_a^c D_t^\alpha f(t) = \frac{1}{\Gamma(n-\alpha)} \int_a^t \frac{f^n(\xi)}{(t-\xi)^{\alpha+1-n}}\, d\xi, \quad n-1 < \alpha, n \in \mathbb{N}. $$

Definition 2.2 (Linearity property [37]) Let $f(t), g(t) : [a, b] \to \mathbb{R}$ be such that ${}_a^c D_t^\alpha f(t)$ and ${}_a^c D_t^\alpha g(t)$ exist almost everywhere, and let $c_1, c_2 \in \mathbb{R}$. Then ${}_a^c D_t^\alpha (c_1 f(t)) + {}_a^c D_t^\alpha (c_2 g(t))$ exists everywhere, and

$$ {}_a^c D_t^\alpha \big(c_1 f(t) + c_2 g(t)\big) = c_1 {}_a^c D_t^\alpha f(t) + c_2 {}_a^c D_t^\alpha g(t). $$

Definition 2.3 (Caputo derivative of a constant [40]) The fractional derivative for a constant function $f(t) = c$ is zero, that is,

$$ {}_a^c D_t^\alpha c = 0. $$

Let us consider the following general type of fractional differential equations involving Caputo derivative:

$$ {}_{t_0}^c D_t^\alpha x(t) = f\big(t, x(t)\big), \quad \alpha \in (0, 1) \tag{1} $$

with initial condition $x_0 = x(t_0)$.

Definition 2.4 (see [37]) The constant x^* is an equilibrium point of the Caputo fractional dynamic system (1) if and only if $f(t, x^*) = 0$.

Definition 2.5 (see [41]) For the system described by (1):

(i) The trivial solution is said to be stable if, for any $t_0 \in \mathbb{R}$ and any $\epsilon > 0$, there exists $\delta = \delta(t_0, \epsilon)$ such that $\|x(t_0)\| < \delta$ implies $\|x(t)\| < \epsilon$ for all $t > t_0$.

(ii) The trivial solution is said to be asymptotically stable if it is stable and, for any $t_0 \in \mathbb{R}$ and any $\epsilon > 0$, there exists $\delta_a = \delta_a(t_0, \epsilon) > 0$ such that $\|x(t)\| < \delta_a$ implies $\lim_{t\to\infty} \|x(t)\| = 0$.

(iii) The trivial solution is said to be uniformly stable if it is stable and $\delta = \delta(\epsilon) > 0$ can be chosen independently of t_0.

(iv) The trivial solution is uniformly asymptotically stable if it is uniformly stable and there exists $\delta_a.0$, independent of t_0, such that if $\|x(t_0)\| < \delta_a$, then $\lim_{t\to\infty} \|x(t)\| = 0$.

(v) The trivial solution is globally (uniformly) asymptotically stable if it is (uniformly) asymptotically stable and δ_a can be an arbitrary large finite number.

Theorem 2.1 (Uniform asymptotic stability [37, 42]) *Let x^* be an equilibrium point for the nonautonomous fractional-order system (1) and $\Omega \subset \mathbb{R}^n$ be a domain containing x^*. Let $L : [0, \infty) \times \Omega \to \mathbb{R}$ be a continuously differentiable function such that*

$$W_1(x) \le L\big(t, x(t)\big) \le W_2(x)$$

and

$${}_a^c D_t^\alpha L\big(t, x(t)\big) \le -W_3(x)$$

for all $\alpha \in (0, 1)$ and all $x \in \Omega$, where $W_1(x)$, $W_2(x)$ and $W_3(x)$ are continuous positive definite functions on Ω. Then the equilibrium point of system (1) is uniformly asymptotically stable.

The following theorem summarises a lemma proved in [37], where a Volterra-type Lyapunov function is obtained for fractional-order epidemic systems.

Theorem 2.2 (see [37]) *Let $x(\cdot)$ be a continuous and differentiable function with $x(t) \in \mathbb{R}_+$. Then, for any time instant $t \ge t_0$, one has*

$${}_{t_0}^c D_t^\alpha \left(x(t) - x^* - x^* \ln \frac{x(t)}{x^*} \right) \le \left(1 - \frac{x^*}{x(t)} \right) {}_{t_0}^c D_t^\alpha x(t), \quad x^* \in \mathbb{R}^+, \forall \alpha \in (0, 1).$$

Theorem 2.3 (see [43]) *Let $\alpha > 0$, $n - 1 < \alpha < n - \mathbb{N}$. Suppose that $f(t), f'(t), \dots, f^{(n-1)}(t)$ are continuous on $[t_0, \infty)$ and the exponential order and that ${}_{t_0}^c D_t^\alpha f(t)$ is piecewise continuous on $[t_0, \infty)$. Then*

$$\mathcal{L}\big\{ {}_{t_0}^c D_t^\alpha f(t) \big\} = s^\alpha \mathcal{F}(s) - \sum_{k=0}^{n-1} s^{\alpha-k-1} f^{(k)}(t_0),$$

where $\mathcal{F}(s) = \mathcal{L}\{f(t)\}$.

Theorem 2.4 (see [44]) *Let $\mathbb{C}$ be a complex plane. For any $\alpha > 0$ $\beta > 0$ and $A \in \mathbb{C}^{n\times n}$, we have*

$$\mathcal{L}\big\{ t^{\beta-1} E_{\alpha,\beta}\big(At^\alpha\big) \big\} = s^{\alpha-\beta} \big(s^\alpha - A\big)^{-1}$$

for $\mathcal{R}s > \|A\|^{\frac{1}{\alpha}}$, where $\mathcal{R}s$ represents the real part of the complex number s, and $E_{\alpha,\beta}$ is the Mittag-Leffler function [45].

3 Mathematical model

In this section, the Caputo fractional calculus has been used to formulate and explore the role of temperature on the transmission and control of *Trypanosoma brucei rhodesiense*. The proposed mathematical model demonstrates the interplay between the tsetse and two hosts, humans and animals. Furthermore, the proposed framework consists of two parts (i) the life cycle of the tsetse flies and (ii) the full model that governs HAT transmission dynamics when the tsetse fly population growth persists. Comprehensive details on the modelling of the early stages of the tsetse flies can be found in [13]. As proposed in [13], let the following system summarise the dynamical growth of the tsetse fly:

$$\left.\begin{aligned} {}^{c}_{t_0}D^{\alpha}_{t}L(t) &= b^{\alpha}_{l}WN_{v}\left(1-\tfrac{L}{K^{\alpha}_{l}}\right)-(\sigma^{\alpha}_{l}+\mu^{\alpha}_{p})L,\\ {}^{c}_{t_0}D^{\alpha}_{t}N_{v}(t) &= \sigma^{\alpha}_{l}L-\mu^{\alpha}_{v}N_{v}. \end{aligned}\right\} \tag{2}$$

The variable $L(t)$ represent the pupal stage of the tsetse, and $N_v(t)$ denotes the total adult vector population at time t, which is comprised of susceptible $S_v(t)$ and infectious $I_v(t)$. Thus, $N_v = S_v + I_v$. In addition, all model parameters and variables in system (2) are considered to be positive, and the parameters are defined as follows: b_l represents the rate at which female flies give birth to larvae; W denotes a fraction of female flies in the population of adult flies; K_l is the pupal carrying capacity of the nesting site; σ_l is the transition from pupal stage into an adult fly, thus $1/\sigma_l$ represents the average time a fly spends as a pupa; μ_p and μ_v account for mortality rate of pupae and adult flies, respectively.

Assuming that the growth of the tsetse fly persists, we now present the full model that governs disease transmission. Thus, we subdivide the two host populations (humans and animals) into compartments of: the susceptible $S_i(t)$, the infectious $I_i(t)$ and the recovered $R_i(t)$, $i = a, h$. The subscripts a and h represent the animal and human populations, respectively. It follows that the total population of each host at time t is given by $N_i(t) = S_i(t) + I_i(t) + R_i(t)$. The proposed fractional-order model has the form

$$\left.\begin{aligned} {}^{c}_{t_0}D^{\alpha}_{t}S_{v}(t) &= \sigma^{\alpha}_{l}L-(\beta^{\alpha}_{hv}I_{h}+\beta^{\alpha}_{av}I_{a})S_{v}-\mu^{\alpha}_{v}S_{v},\\ {}^{c}_{t_0}D^{\alpha}_{t}I_{v}(t) &= (\beta^{\alpha}_{hv}I_{h}+\beta^{\alpha}_{av}I_{a})S_{v}-\mu^{\alpha}_{v}I_{v},\\ {}^{c}_{t_0}D^{\alpha}_{t}S_{h}(t) &= \Lambda^{\alpha}_{h}-\beta^{\alpha}_{vh}f(I_{v})S_{h}-\mu^{\alpha}_{h}S_{h},\\ {}^{c}_{t_0}D^{\alpha}_{t}I_{h}(t) &= \beta^{\alpha}_{vh}f(I_{v})S_{h}-(\mu^{\alpha}_{h}+\gamma^{\alpha}_{h})I_{h},\\ {}^{c}_{t_0}D^{\alpha}_{t}S_{a}(t) &= \Lambda^{\alpha}_{a}-\beta^{\alpha}_{va}f(I_{v})S_{a}-\mu^{\alpha}_{a}S_{a},\\ {}^{c}_{t_0}D^{\alpha}_{t}I_{a}(t) &= \beta^{\alpha}_{va}f(I_{v})S_{a}-(\mu^{\alpha}_{a}+\gamma^{\alpha}_{a})I_{a},\\ {}^{c}_{t_0}D^{\alpha}_{t}R_{h}(t) &= \gamma^{\alpha}_{h}I_{h}-\mu^{\alpha}_{h}R_{h},\\ {}^{c}_{t_0}D^{\alpha}_{t}R_{a}(t) &= \gamma^{\alpha}_{a}I_{a}-\mu^{\alpha}_{a}R_{a}. \end{aligned}\right\} \tag{3}$$

All model parameters and variables in system (3) are considered to be positive, and the parameters are defined as follows: parameter Λ_j, $j = a, h$, represents the constant recruitment rate of the host population through birth and they are assumed to be susceptible, μ_i, $i = a, h, v$, denotes natural mortality rate, β_{vk} represents the transmission rate of infection from an infected tsetse vector to a susceptible host k given that effective contact between the two species occurs, β_{kv} represents disease transmission from an infected host k to a susceptible vector given that effective contact between the two occurs, γ_k is the recovery rate for the host population. Furthermore, disease transmission from infectious vectors to susceptible hosts is modelled by a nonlinear incidence rate, and the function $f(I_v)$ is

equivalent to

$$f(I_v) = \frac{I_v}{1 + \theta I_v},$$

where θ is a positive constant.

As highlighted earlier, temperature plays a crucial role on *Trypanosoma brucei rhodesiense* transmission dynamics. To account for this effect, we now remodel parameters of system (2) and (3): b_l is the rate at which female flies give birth to larvae; σ_l denotes pupal development rate; μ_p denotes pupal mortality rate and μ_v is adult tsetse mortality rate; and functions of temperature. In particular, we adopted the following function [16, 46] to model the rate at which female flies give birth to larvae:

$$b_l = d_1 + d_2(T - T_0), \tag{4}$$

where T_0 was set to 20°C [16]. Function (4) was derived by Hargrove [46] when the author used ovarian dissection data from marked and released *G. m. morsitans* and *G. pallidipes* at Rekomitjie. Precisely, Hargrove's work suggested that the larviposition rate per day increases linearly between 20°C and 30°C. Adult fly mortality rate μ_v is now modelled by

$$\mu_v = \begin{cases} a_1 & \text{for } T \leq 25, \\ a_1 e^{a_2(T-25)} & \text{for } T > 25, \end{cases}$$

where T is the temperature in °C, a_2 parameterises the increase at higher temperatures. Based on the laboratory experiments performed by Phelps [2], pupal survival to adulthood depends on temperature variations and is highest for temperatures between about 20°C and 30°C. As temperatures move from this range, the mortality rises sharply, leading to a U-shaped curve, and a suitable function to represent this relation is

$$\mu_p = b_1 + b_2 \exp\big(-b_3(T - T_2)\big) + b_4 \exp\big(b_5(T - T_3)\big),$$

where T is the temperature in °C, T_2 and T_3 are not parameters but are constants selected to ensure that the coefficients b_3 and b_5 are in a convenient range, and in our simulation these will be set to 16°C and 32°C as in [16].

Additional important result from Phelps' work was the quantification of the daily rate of pupal development σ_L in *G. m. morsitans* as a function of constant temperature. The following function was considered to be the best representation of pupal emergence and temperature variations:

$$\sigma_l = \frac{c_1}{1 + \exp(c_2 + c_3 T)},$$

where T represents the mean daily temperature and c_1, c_2 and c_3 parametrise pupal hatching rate [16].

Remark 3.1 Note that, in order to avoid flaws regarding the time dimension, we introduced α in the model parameters (right-hand side) of both systems (2) and (3), so that the dimensions of these parameters become $(\text{time})^{-\alpha}$, which is in agreement with the left-hand side of the model.

It is worth noting that there is need to derive the threshold quantity that determines the growth of the tsetse fly population. Thus, the analysis of the proposed model will begin with system (2). Once this threshold condition has been determined, one can then proceed to investigating the dynamical behaviour of system (3).

4 Analytical results of the proposed framework

4.1 The dynamical behaviour of system (2)

In this section, the dynamical behaviour of system (2) is investigated. The basic properties of the model and other fundamental results will be established.

4.1.1 Basic properties of the model

Theorem 4.1 *Let $\mathcal{X}(t) = (L(t), N_v(t))$ be the unique of model (2) for $t \geq 0$. Then the solution $\mathcal{X}(t)$ remains in $\mathbb{R}^2_+$.*

Proof To demonstrate that the solution $\mathcal{X}(t)$ of model (2) is nonnegative, there is need to investigate the direction of the vector field given by the right-hand side of (2) on each space and determine whether the vector field points to the interior of $\mathbb{R}^2_+$ or is tangent to the coordinate space. Since

$$
\begin{aligned}
&{}^{c}_{t_0}D^{\alpha}_{t} L(t)|_{L=0} = b^{\alpha}_{l} W N_v \geq 0,\\
&{}^{c}_{t_0}D^{\alpha}_{t} N_v(t)|_{N_v=0} = \sigma^{\alpha}_{l} L \geq 0.
\end{aligned}
$$

The results presented imply that the vector field given by the right-hand side of (2) on each coordinate plane is either tangent to the coordinate plane or points to the interior of $\mathbb{R}^2_+$. Hence, the domain $\mathbb{R}^2_+$ is a positively invariant region. Moreover, if the initial conditions of system (2) are nonnegative, then it follows that the corresponding solutions of model (2) are nonnegative. □

Theorem 4.2 *Let $\mathcal{X}(t) = (L(t), N_v(t))$ be the unique of model (2) for $t \geq 0$. Then the solution $\mathcal{X}(t)$ is bounded above, that is, $\mathcal{X}(t) \in \Omega$ where Ω denotes the feasible region and is given by*

$$
\Omega = \left\{(L, N_v) \in \mathbb{R}^2_+ | 0 \leq L \leq K^{\alpha}_{l}, 0 \leq N_v \leq C\right\}.
$$

Proof For model (2) to be biologically meaningful, all model solutions need to be positive. Hence, from the first equation of model (2), one can easily note that for all solutions of this equation to remain positive the following condition must hold $0 \leq L(t) \leq K^{\alpha}_{l}$; otherwise, the solutions will be negative and biologically irrelevant. From the bounds of $L(t)$, it follows that

$$
\begin{aligned}
{}^{c}_{t_0}D^{\alpha}_{t} N_v(t) &= \sigma^{\alpha}_{l} L - \mu^{\alpha}_{v} N_v\\
&\leq \sigma^{\alpha}_{l} K^{\alpha}_{l} - \mu^{\alpha}_{v} N_v.
\end{aligned}
$$

By closely following Theorems 2.3 and 2.4, applying the Laplace transform leads to

$$
s^{\alpha}\mathcal{L}\big(N_V(t)\big) - s^{\alpha-1}N_v(0) \leq \frac{\sigma^{\alpha}_{l} K^{\alpha}_{l}}{s} - \mu^{\alpha}_{v}\mathcal{L}\big(N_v(t)\big).
$$

Combining the like terms, one gets

$$\begin{aligned}\mathcal{L}\big(N_v(t)\big) &\leq \sigma_l^\alpha K_l^\alpha \frac{s^{-1}}{s^\alpha + \mu_v^\alpha} + N_v(0)\frac{s^{\alpha-1}}{s^\alpha + \mu_v^\alpha} \\ &= \sigma_l^\alpha K_l^\alpha \frac{s^{\alpha-(1+\alpha)}}{s^\alpha + \mu_v^\alpha} + N_v(0)\frac{s^{\alpha-1}}{s^\alpha + \mu_v^\alpha}.\end{aligned}$$

Applying the inverse Laplace transform leads to

$$\begin{aligned}N_v(t) &\leq \mathcal{L}^{-1}\left\{\sigma_l^\alpha K_l^\alpha \frac{s^{\alpha-(1+\alpha)}}{s^\alpha + \mu_v^\alpha}\right\} + \mathcal{L}^{-1}\left\{N_v(0)\frac{s^{\alpha-1}}{s^\alpha + \mu_v^\alpha}\right\} \\ &\leq \sigma_l^\alpha K_l^\alpha t^\alpha E_{\alpha,\alpha+1}\big(-\mu_v t^\alpha\big) + N_V(0)E_{\alpha,1}\big(-\mu_v t^\alpha\big) \\ &\leq \frac{\sigma_l^\alpha K_l^\alpha}{\mu_v^\alpha}\mu_v^\alpha t^\alpha E_{\alpha,\alpha+1}\big(-\mu_v t^\alpha\big) + N_V(0)E_{\alpha,1}\big(-\mu_v t^\alpha\big) \\ &\leq \max\left\{\frac{\sigma_l^\alpha K_l^\alpha}{\mu_v^\alpha}, N_v(0)\right\}\big(\mu_v^\alpha t^\alpha E_{\alpha,\alpha+1}\big(-\mu_v t^\alpha\big) + E_{\alpha,1}\big(-\mu_v t^\alpha\big)\big) \\ &= \frac{C}{\Gamma(1)} = C, \end{aligned} \tag{5}$$

where $C = \max\{\frac{\sigma_l^\alpha K_l^\alpha}{\mu_v^\alpha}, N_v(0)\}$. Thus, $N_V(t)$ is bounded from above. Hence, one can conclude that the solution $X_1(t)$ is bounded above. □

4.1.2 Equilibrium points and their stability

In what follows, we derive the fundamental results for model (2). Through direct calculations, one can note that model (2) has two equilibrium points, trivial $(L, N_v) = (0, 0)$ and nontrivial

$$\{L^*, N_v^*\} = \left\{\left(1 - \frac{1}{r}\right)K_l^\alpha, \frac{\sigma_l^\alpha}{\mu_v^\alpha}\left(1 - \frac{1}{r}\right)K_l^\alpha\right\},$$

where

$$r = \frac{\sigma_l^\alpha}{\sigma_l^\alpha + \mu_p^\alpha}\frac{b_l^\alpha}{\mu_v^\alpha}W,$$

r is a threshold quantity that determines growth of the tsetse fly population. It is defined as the likelihood of the fly to survive the pupal stage multiplied by the surviving population of female flies [13].

Theorem 4.3

(i) *If* $r \leq 1$, *then the equilibrium point* $(0, 0)$ *is the sole equilibrium point of system* (2) *and it is globally* (*uniformly*) *asymptotically stable in* Ω.

(ii) *If* $r > 1$, *then the equilibrium* (L^*, N_v^*) *is globally* (*uniformly*) *asymptotically stable in* $\text{int}(\Omega)$.

Proof We will use Lyapunov functionals to demonstrate that Theorem 4.3 holds.

(i) To investigate the first part of Theorem 4.3, we consider the following Lyapunov function:

$$U_1(t) = \frac{\mu_v^\alpha}{b_l^\alpha W} L(t) + N_v(t).$$

Observe that the function $U(t)$ is defined, continuous and positive definite for all $L(t)$ and $N_v(t)$. It follows from Definition (2.2) that

$$\begin{aligned} {}_{t_0}^{c}D_t^\alpha U_1(t) &= \frac{\mu_v^\alpha}{b_l^\alpha W} {}_{t_0}^{c}D_t^\alpha L(t) + {}_{t_0}^{c}D_t^\alpha N_v(t) \\ &= \frac{\mu_v^\alpha}{b_l^\alpha W}\left[b_l^\alpha W N_v\left(1 - \frac{L}{K_l^\alpha}\right) - \left(\sigma_l^\alpha + \mu_p^\alpha\right)L\right] + \sigma_l^\alpha L - \mu_v^\alpha N_v \\ &= -\frac{\mu_v^\alpha N_v L}{K_l^\alpha} - \frac{\sigma_l^\alpha}{r}(1-r). \end{aligned}$$

Since ${}_{t_0}^{c}D_t^\alpha U(t) < 0$, for $r < 1$, we can conclude that the equilibrium point $(0,0)$ is globally (uniformly) asymptotically stable in Ω. Now, we proceed to demonstrating item (ii).

(ii) Consider the following Lyapunov function:

$$U_2(t) = a_1\left[L(t) - L^* - L^* \ln\left(\frac{L(t)}{L^*}\right)\right] + a_2\left[N_v(t) - N_v^* - N_v^* \ln\left(\frac{N_v(t)}{N_v^*}\right)\right],$$

where a_1 and a_2 are positive constants to be determined. Applying Lemma 2.2 leads to

$$\begin{aligned} {}_{t_0}^{c}D_t^\alpha U_2(t) &\le a_1\left(1 - \frac{L^*}{L(t)}\right) {}_{t_0}^{c}D_t^\alpha L(t) + a_2\left(1 - \frac{N_v^*}{N_v(t)}\right) {}_{t_0}^{c}D_t^\alpha N_v(t) \\ &= a_1\left(1 - \frac{L^*}{L(t)}\right)\left(g(N_v, L) - \left(\sigma_l^\alpha + \mu_p^\alpha\right)L\right) \\ &\quad + a_2\left(1 - \frac{N_v^*}{N_v(t)}\right)\left(\sigma_l^\alpha L - \mu_v^\alpha N_v\right), \end{aligned}$$

with $g(N_v, L) = b_l^\alpha W N_v(1 - \frac{L}{K_l^\alpha})$.

Setting $a_1 = 1$ and $a_2 = g(N_v^*, L^*) > 0$, with $g(N_v^*, L^*) = b_l^\alpha W N_v(1 - \frac{L^*}{K_l^\alpha})$. Furthermore, by utilising the identities $g(N_v^*, L^*) = (\sigma_l^\alpha + \mu_p^\alpha)L^*$ and $\sigma_l^\alpha L^* = \mu_v^\alpha N_v^*$, one gets

$${}_{t_0}^{c}D_t^\alpha U_2(t) \le g\left(N_v^*, L^*\right)\left(2 - \frac{N_v}{N_v^*} - \frac{LN_v^*}{L^*N_v} - \frac{L^*}{L}\frac{g(N_v, L)}{g(N_v^*, L^*)} + \frac{g(N_v, L)}{g(N_v^*, L^*)}\right).$$

Let $\Phi(x) = 1 - x + \ln x$ for $x > 0$. It follows that $\Phi(x) \le 0$, with the equality satisfied if and only if $x = 1$. Using this relation, we have

$$\begin{aligned} &2 - \frac{N_v}{N_v^*} - \frac{LN_V^*}{L^*N_V} - \frac{L^*}{L}\frac{g(N_V, L)}{g(N_V^*, L^*)} + \frac{g(N_V, L)}{g(N_V^*, L^*)} \\ &\quad = \Phi\left(\frac{LN_V^*}{L^*N_V}\right) + \Phi\left(\frac{L^*}{L}\frac{g(N_V, L)}{g(N_V^*, L^*)}\right) - \frac{N_v}{N_v^*} + \frac{g(N_V, L)}{g(N_V^*, L^*)} \end{aligned}$$

$$
\begin{aligned}
&- \ln\left(\frac{N^* g(N_V, L)}{N g(N_V^*, L^*)}\right) \\
&\leq \ln\left(\frac{N_v}{N_v^*}\right) - \frac{N_v}{N_v^*} + \frac{g(N_V, L)}{g(N_V^*, L^*)} - \ln\left(\frac{g(N_V, L)}{g(N_V^*, L^*)}\right) \\
&\leq 0.
\end{aligned}
$$

Hence, we can conclude that if $r > 1$, then the equilibrium (L^*, N_v^*) is globally (uniformly) asymptotically stable in $\text{int}(\Omega)$. From the above analytical results we can also deduce that if $r < 1$, then the tsetse vector population will go into extinction and for $r > 1$ it will persist. Thus, as we proceed to perform the analysis of (2), we will consider $r > 1$ implying the tsetse flies are at the equilibrium (L^*, N_v^*). □

4.2 Analysis of the full model

We have noted that the tsetse population grows if $r > 1$ and the equilibrium (L^*, N_V^*) will be globally (uniformly) asymptotically stable. Therefore, in this section, we explore the dynamics of the full model, and we will consider $L = L^*$. Furthermore, as we can observe, the last two equations in system (3) do not influence the dynamics of the disease since all the other six equations do not depend on these equations. Hence, without loss of generality one can explore the dynamics of the disease based on a reduced system:

$$
\left.
\begin{aligned}
{}_{t_0}^{c}D_t^{\alpha} S_v(t) &= \sigma_l^{\alpha} L^* - (\beta_{hv}^{\alpha} I_h + \beta_{av}^{\alpha} I_a) S_v - \mu_v^{\alpha} S_v, \\
{}_{t_0}^{c}D_t^{\alpha} I_v(t) &= (\beta_{hv}^{\alpha} I_h + \beta_{av}^{\alpha} I_a) S_v - \mu_v^{\alpha} I_v, \\
{}_{t_0}^{c}D_t^{\alpha} S_h(t) &= \Lambda_h^{\alpha} - \beta_{vh}^{\alpha} f(I_v) S_h - \mu_h^{\alpha} S_h, \\
{}_{t_0}^{c}D_t^{\alpha} I_h(t) &= \beta_{vh}^{\alpha} f(I_v) S_h - (\mu_h^{\alpha} + \gamma_h^{\alpha}) I_h, \\
{}_{t_0}^{c}D_t^{\alpha} S_a(t) &= \Lambda_a^{\alpha} - \beta_{va}^{\alpha} f(I_v) S_a - \mu_a^{\alpha} S_a, \\
{}_{t_0}^{c}D_t^{\alpha} I_a(t) &= \beta_{va}^{\alpha} f(I_v) S_a - (\mu_a^{\alpha} + \gamma_a^{\alpha}) I_a.
\end{aligned}
\right\} \tag{6}
$$

4.2.1 Basic properties of the model

By closely following the approach in Sect. 4.1.1 one can easily verify the positivity and boundedness of solutions for system (6). For instance, we can note that all the solutions of system (6) are unique and positive since

$$
\left.
\begin{aligned}
{}_{t_0}^{c}D_t^{\alpha} S_v(t) &= \sigma_l^{\alpha} L^* \geq 0, \\
{}_{t_0}^{c}D_t^{\alpha} I_v(t) &= (\beta_{hv}^{\alpha} I_h + \beta_{av}^{\alpha} I_a) S_v \geq 0, \\
{}_{t_0}^{c}D_t^{\alpha} S_h(t) &= \Lambda_h^{\alpha} \geq 0, \\
{}_{t_0}^{c}D_t^{\alpha} I_h(t) &= \beta_{vh}^{\alpha} f(I_v) S_h \geq 0, \\
{}_{t_0}^{c}D_t^{\alpha} S_a(t) &= \Lambda_a^{\alpha} \geq 0, \\
{}_{t_0}^{c}D_t^{\alpha} I_a(t) &= \beta_{va}^{\alpha} f(I_v) S_a \geq 0.
\end{aligned}
\right\} \tag{7}
$$

Moreover, by following the approach used earlier, it can determined that $0 \leq N_i(t) \leq \max\{\frac{\Lambda_i^{\alpha}}{\mu_i^{\alpha}}, N_i(0)\}$ for $i = a, h$ implying that all the solutions of system (6) are bounded above.

4.2.2 Equilibrium points and their stability

In the absence of the disease in the community, system (6) admits a trivial equilibrium point also known as the disease-free equilibrium (DFE) and given by

$$
\mathcal{E}^0 : \left(S_h^0, I_h^0, S_a^0, I_a^0, S_v^0, I_v^0\right) = \left(\frac{\Lambda_h^{\alpha}}{\mu_h^{\alpha}}, 0, \frac{\Lambda_a^{\alpha}}{\mu_a^{\alpha}}, 0, \frac{\sigma_l^{\alpha}}{\mu_v^{\alpha}}\left(1 - \frac{1}{r}\right) K_l^{\alpha}, 0\right).
$$

Following the next generation matrix approach [47, 48], it can easily be verified that the basic reproduction number of system (6) is

$$\mathcal{R}_0 = \sqrt{K_l^\alpha \frac{\sigma_l^\alpha}{\mu_v^\alpha}\left(1-\frac{1}{r}\right)\left(\frac{\beta_{vh}^\alpha \beta_{hv}^\alpha \Lambda_h^\alpha}{\mu_v^\alpha \mu_h^\alpha(\mu_h^\alpha+\gamma_h^\alpha)}+\frac{\beta_{av}^\alpha \beta_{va}^\alpha \Lambda_a^\alpha}{\mu_v^\alpha \mu_a^\alpha(\mu_a^\alpha+\gamma_a^\alpha)}\right)}. \tag{8}$$

The basic reproduction number $\mathcal{R}_0$ is defined to be the expected number of secondary cases (vector or host) produced in a completely susceptible population by one infectious individual (vector or host, respectively) during its lifetime as infectious. The basic reproduction number is an integral epidemiological metric for understanding *Trypanosoma brucei rhodesiense* persistence and extinction. As we can observe, this metric depends on disease transmission parameters β_{ij} for $i \neq j = a, h, v$, the average infectious period of the vector (host) $\frac{1}{(\mu_i^\alpha+\gamma_i^\alpha)}$, vector competence and survival $\frac{\sigma_l^\alpha}{\mu_v^{2\alpha}}(1-\frac{1}{r})K_l^\alpha$.

Remark 4.1 From the expression of the basic reproduction number (8), one can observe that if $r = 1$, $\mathcal{R}_0 = 0$, and for $r < 1$, we have $\mathcal{R}_0 \leq 1$. This implies that whenever $r \leq 1$ the disease will not persist in the community since the tsetse fly population would naturally become extinct.

Next, we investigate the stability of the steady states of system (6). We will begin with the disease-free equilibrium (DFE).

Theorem 4.4 *For $\alpha \in (0,1)$, the disease-free equilibrium of system (6) is globally (uniformly) asymptotically stable for $\mathcal{R}_0 < 1$.*

Proof Consider the following Lyapunov functional:

$$\begin{aligned}\mathcal{L}_0(t) = {} & c_1\left\{S_h(t) - S_h^0 - S_h^0 \ln\frac{S_h(t)}{S_h^0}\right\} + c_1 I_h(t) + c_2\left\{S_a(t) - S_a^0 - S_a^0 \ln\frac{S_a(t)}{S_a^0}\right\} \\ & + c_2 I_a(t) + c_3\left\{S_v(t) - S_v^0 - S_v^0 \ln\frac{S_v(t)}{S_v^0} + I_v(t)\right\},\end{aligned}$$

where c_1, c_2 and c_3 are positive constants to be determined. Now, it follows from Definition 2.2 and Lemma 4.3 that

$$\begin{aligned}{}_{t_0}^{c}D_t^\alpha \mathcal{L}_0(t) \leq {} & c_1\left(1-\frac{S_h^0}{S_h}\right){}_{t_0}^{c}D_t^\alpha S_h + c_1 {}_{t_0}^{c}D_t^\alpha I_h + c_2\left(1-\frac{S_a^0}{S_a}\right){}_{t_0}^{c}D_t^\alpha S_a \\ & + c_2 {}_{t_0}^{c}D_t^\alpha I_a + c_3\left(1-\frac{S_v^0}{S_v}\right){}_{t_0}^{c}D_t^\alpha S_v + c_3 {}_{t_0}^{c}D_t^\alpha I_v.\end{aligned}$$

Setting

$$\begin{aligned}& c_1 = \mu_v^\alpha \beta_{hv}^\alpha\left(\mu_a^\alpha+\gamma_a^\alpha\right), \qquad c_2 = \mu_v^\alpha \beta_{av}^\alpha\left(\mu_h^\alpha+\gamma_h^\alpha\right), \\ & c_3 = \left(\frac{\beta_{hv}^\alpha \beta_{vh}^\alpha \Lambda_h^\alpha(\mu_a^\alpha+\gamma_a^\alpha)}{\mu_h^\alpha}+\frac{\beta_{va}^\alpha \beta_{av}^\alpha \Lambda_a^\alpha(\mu_h^\alpha+\gamma_h^\alpha)}{\mu_a^\alpha}\right)\end{aligned}$$

and simplifying one gets:

$$
\begin{aligned}
{}_{t_0}^{c}D_t^{\alpha}\mathcal{L}_0(t) \leq{}& -\mu_v^{\alpha}\mu_h^{\alpha}\beta_{hv}^{\alpha}\left(\mu_a^{\alpha}+\gamma_a^{\alpha}\right)\frac{(S_h-S_h^0)^2}{S_h}-\mu_v^{\alpha}\mu_a^{\alpha}\beta_{av}^{\alpha}\left(\mu_h^{\alpha}+\gamma_h^{\alpha}\right)\frac{(S_a-S_a^0)^2}{S_a}\\
&-\left(\frac{\beta_{hv}^{\alpha}\beta_{vh}^{\alpha}\Lambda_h^{\alpha}(\mu_a^{\alpha}+\gamma_a^{\alpha})\mu_v^{\alpha}}{\mu_h^{\alpha}}+\frac{\beta_{va}^{\alpha}\beta_{av}^{\alpha}\Lambda_a^{\alpha}(\mu_h^{\alpha}+\gamma_h^{\alpha})\mu_v^{\alpha}}{\mu_a^{\alpha}}\right)\frac{(S_v-S_v^0)^2}{S_v}\\
&-\left(\frac{\beta_{hv}^{\alpha}\beta_{vh}^{\alpha}\Lambda_h^{\alpha}(\mu_a^{\alpha}+\gamma_a^{\alpha})\mu_v^{\alpha}}{\mu_h^{\alpha}}+\frac{\beta_{va}^{\alpha}\beta_{av}^{\alpha}\Lambda_a^{\alpha}(\mu_h^{\alpha}+\gamma_h^{\alpha})\mu_v^{\alpha}}{\mu_a^{\alpha}}\right)\theta f(I_v)I_v\\
&-\mu_v^{\alpha}\left(\mu_a^{\alpha}+\gamma_a^{\alpha}\right)\left(\mu_h^{\alpha}+\gamma_h^{\alpha}\right)\left(\beta_{hv}^{\alpha}I_h+\beta_{av}^{\alpha}Ia\right)\left(1-\mathcal{R}_0^2\right).
\end{aligned}
$$

Since all the parameters and variables in system (6) are nonnegative, it follows that ${}_{t_0}^{c}D_t^{\alpha}\mathcal{L}_0(t)<0$ holds if $\mathcal{R}_0<1$. Therefore, by the LaSalle invariance principle [49], we conclude that the DFE of system (6) is globally (uniformly) asymptotically stable whenever $\mathcal{R}_0<1$. This completes the proof. Biologically, this implies that whenever $\mathcal{R}_0<1$ then the disease dies out in the community. □

Theorem 4.5 *Let $\mathcal{E}^*=(S_i^*,I_i^*)$ for $i=a,h,v$ be the endemic equilibrium point of system (6). Then, for $\alpha\in(0,1)$ and $\mathcal{R}_0>1$, the endemic equilibrium point $\mathcal{E}^*$ is globally (uniformly) asymptotically stable.*

Proof Consider the following Lyapunov functional:

$$
\begin{aligned}
\mathcal{L}_1(t) ={}& b_1\left(S_h(t)-S_h^*-S_h^*\ln\frac{S_h(t)}{S_h^*}\right)+b_2\left(I_h(t)-I_h^*-I_h^*\ln\frac{I_h(t)}{I_h^*}\right)\\
&+b_3\left(S_a(t)-S_a^*-S_a^*\ln\frac{S_a(t)}{S_a^*}\right)+b_4\left(I_a(t)-I_a^*-I_a^*\ln\frac{I_a(t)}{I_a^*}\right)\\
&+b5\left(S_v(t)-S_v^*-S_v^*\ln\frac{S_v(t)}{S_v^*}\right)+b_6\left(I_v(t)-I_v^*-I_v^*\ln\frac{I_v(t)}{I_v^*}\right),
\end{aligned}
$$

where $b_i=$, $i=1,2,3,\ldots,6$, are positive constants to be determined. Applying Lemma 4.3 leads to

$$
\begin{aligned}
{}_{t_0}^{c}D_t^{\alpha}\mathcal{L}_1(t) \leq{}& b_1\left(1-\frac{S_h^*}{S_h}\right){}_{t_0}^{c}D_t^{\alpha}S_h+b_2\left(1-\frac{I_h^*}{I_h}\right){}_{t_0}^{c}D_t^{\alpha}I_h+b_3\left(1-\frac{S_a^*}{S_a}\right){}_{t_0}^{c}D_t^{\alpha}S_a\\
&+b_4\left(1-\frac{I_a^*}{I_a}\right){}_{t_0}^{c}D_t^{\alpha}I_a+b_5\left(1-\frac{S_v^*}{S_v}\right){}_{t_0}^{c}D_t^{\alpha}S_v+b_6\left(1-\frac{I_v^*}{I_v}\right){}_{t_0}^{c}D_t^{\alpha}I_v.
\end{aligned}
$$

Setting $b_i=1$ for $i=1,2,3,4$ and $b_5=b_6=\frac{\beta_{vh}^{\alpha}f(I_v^*)S_h^*}{\beta_{hv}^{\alpha}I_h^*S_v^*}+\frac{\beta_{va}^{\alpha}f(I_v^*)S_a^*}{\beta_{av}^{\alpha}I_a^*S_v^*}$ and utilising the following identities (which exist at the endemic point)

$$
\begin{cases}
\Lambda_h^{\alpha}=\beta_{vh}^{\alpha}f(I_v^*)S_h^*+\mu_h^{\alpha}S_h^*, & (\mu_h^{\alpha}+\gamma_h^{\alpha})I_h^*=\beta_{vh}^{\alpha}f(I_v^*)S_h^*,\\
\Lambda_a^{\alpha}=\beta_{va}^{\alpha}f(I_v^*)S_a^*+\mu_a^{\alpha}S_a^*, & (\mu_a^{\alpha}+\gamma_a^{\alpha})I_a^*=\beta_{va}^{\alpha}f(I_v^*)S_a^*,\\
\sigma_l^{\alpha}L^*=(\beta_{hv}^{\alpha}I_h^*+\beta_{av}^{\alpha}I_a^*)S_v^*+\mu_v^{\alpha}S_v^*, & \mu_v^{\alpha}I_v^*=(\beta_{hv}^{\alpha}I_h^*+\beta_{av}^{\alpha}I_a^*(t))S_v^*,
\end{cases}
$$

one gets

$$
\begin{aligned}
D^{\alpha}\mathcal{L}_1(t) \leq{}& \mu_h^{\alpha}S_h^*\underbrace{\left(2-\frac{S_h}{S_h^*}-\frac{S_h^*}{S_h}\right)}_{(1)}+\beta_{va}^{\alpha}f\left(I_v^*\right)S_a^*\frac{\beta_{hv}^{\alpha}I_h^*}{\beta_{av}^{\alpha}I_a^*}\underbrace{\left(2-\frac{S_v^*}{S_v}-\frac{I_v}{I_v^*}-\frac{S_vI_v^*I_h}{S_v^*I_vI_h^*}+\frac{I_h}{I_h^*}\right)}_{(2)}\\
&+\beta_{vh}^{\alpha}f\left(I_v^*\right)S_h^*\underbrace{\left(4-\frac{S_h^*}{S_h}-\frac{S_hI_h^*f(I_v)}{S_h^*I_hf(I_v^*)}-\frac{S_v^*}{S_v}-\frac{I_v}{I_v^*}-\frac{S_vI_v^*I_h}{S_v^*I_vI_h^*}+\frac{f(I_v)}{f(I_v^*)}\right)}_{(3)}\\
&+\mu_a^{\alpha}S_a^*\underbrace{\left(2-\frac{S_a}{S_a^*}-\frac{S_a^*}{S_a}\right)}_{(4)}+\beta_{vh}^{\alpha}f\left(I_v^*\right)S_h^*\frac{\beta_{av}^{\alpha}I_a^*}{\beta_{hv}^{\alpha}I_h^*}\underbrace{\left(2-\frac{S_v^*}{S_v}-\frac{I_v}{I_v^*}-\frac{S_vI_v^*I_a}{S_v^*I_vI_a^*}+\frac{I_a}{I_a^*}\right)}_{(5)}\\
&+\beta_{va}^{\alpha}f\left(I_v^*\right)S_a^*\underbrace{\left(4-\frac{S_a^*}{S_a}-\frac{S_aI_a^*f(I_v)}{S_a^*I_af(I_v^*)}-\frac{S_v^*}{S_v}-\frac{I_v}{I_v^*}-\frac{S_vI_v^*I_a}{S_v^*I_vI_a^*}+\frac{f(I_v)}{f(I_v^*)}\right)}_{(6)}\\
&+\mu_v^{\alpha}S_v^*\left(\frac{\beta_{vh}^{\alpha}f(I_v^*)S_h^*}{\beta_{hv}^{\alpha}I_h^*S_v^*}+\frac{\beta_{va}^{\alpha}f(I_v^*)S_a^*}{\beta_{av}^{\alpha}I_a^*S_v^*}\right)\underbrace{\left(2-\frac{S_v}{S_v^*}-\frac{S_v^*}{S_v}\right)}_{(7)}.
\end{aligned}
$$

Since the arithmetic mean is greater than or equal to the geometric mean, it follows that for (1), (4) and (7) the following is satisfied:

$$
\left(2-\frac{S_i}{S_i^*}-\frac{S_i^*}{S_i}\right)\leq 0. \tag{9}
$$

Furthermore, let $\Phi(x)=1-x+\ln x$ for $x>0$. It follows that $\Phi(x)\leq 0$ with equality if and only if $x=1$. Utilising the aforementioned properties of $\Phi(x)$, we can demonstrate that the terms in the brackets are less or equal to zero. Let $k=a,h$, so that from (2) and (5) we can write

$$
\begin{aligned}
&2-\frac{S_v^*}{S_v}+\frac{I_k}{I_k^*}-\frac{I_v}{I_v^*}-\frac{S_vI_v^*I_k}{S_v^*I_vI_k^*},\\
&\quad=\Phi\left(\frac{S_v^*}{S_v}\right)+\Phi\left(\frac{S_vI_v^*I_k}{S_v^*I_vI_k^*}\right)-\ln\left(\frac{I_v^*I_k}{I_vI_k^*}\right)+\frac{I_k}{I_k^*}-\frac{I_v}{I_v^*}\\
&\quad\leq\frac{I_k}{I_k^*}-\ln\left(\frac{I_k}{I_k^*}\right)-\frac{I_v}{I_v^*}+\ln\left(\frac{I_v}{I_v^*}\right)\\
&\quad\leq 0.
\end{aligned} \tag{10}
$$

In addition, from (3) and (6) we have

$$
\begin{aligned}
&4-\frac{S_k^*}{S_k}-\frac{S_kI_k^*f(I_v)}{S_k^*I_kf(I_v^*)}-\frac{S_v^*}{S_v}-\frac{I_v}{I_v^*}-\frac{S_vI_v^*I_k}{S_v^*I_vI_k^*}+\frac{f(I_v)}{f(I_v^*)},\\
&\quad=\Phi\left(\frac{S_k^*}{S_k}\right)+\Phi\left(\frac{S_v^*}{S_v}\right)+\Phi\left(\frac{S_kI_k^*f(I_v)}{S_k^*I_kf(I_v^*)}\right)+\Phi\left(\frac{S_vI_v^*I_k}{S_v^*I_vI_k^*}\right)\\
&\qquad-\frac{I_v}{I_v^*}+\frac{f(I_v)}{f(I_v^*)}-\ln\left(\frac{f(I_v)I_v^*}{f(I_v^*)I_v}\right)
\end{aligned}
$$

$$\leq \ln\left(\frac{I_v}{I_v^*}\right) - \frac{I_v}{I_v^*} + \frac{f(I_v)}{f(I_v^*)} - \ln\left(\frac{f(I_v)}{f(I_v^*)}\right)$$

$$\leq 0. \tag{11}$$

From (9), (10) and (11), it follows that $D^\alpha \mathcal{L}_1(t) \leq 0$ whenever $\mathcal{R}_0 > 1$. Therefore, by the invariant principle of LaSalle [49], system (6) admits a globally (uniformly) asymptotically stable endemic equilibrium for $\mathcal{R}_0 > 1$. In a nutshell, the result implies that whenever $\mathcal{R}_0 > 1$ the disease will persist unless intervention strategies that are capable of reducing $\mathcal{R}_0$ to value less than unity are implemented. □

5 Numerical results and discussion

In this section, numerical experiments are conducted using MATLAB software in order to support analytical findings presented in the previous section. For the numerical implementation of fractional derivatives, we have utilised the Adam–Bashforth–Moulton (ABM) scheme, which has been implemented in the Matlab code fde12 by Garrappa [50]. This code implements a predictor-corrector PECE method of ABM type, as described in [51]. For aspects on convergence and accuracy of the numerical technique utilised, we refer readers to [52]. Furthermore, comprehensive details on stability of predictor-corrector algorithms for fractional differential equations are found in [53].

The baseline values for temperature dependent parameters are given in Table 1, and the remaining model parameters which are not temperature are given in Table 2. We have redefined some of the parameters as follows: $\Lambda_h = \mu_h N_h$, $\Lambda_a = \mu_a N_a$, implying that the host birth rate is now regarded to be equivalent to natural mortality rate. In addition, we set $\beta_{av} = p\xi\psi$, $\beta_{hv} = (1-p)\xi\omega$, $\beta_{va} = p\xi u$ and $\beta_{vh} = (1-p)\xi b$, where p is the proportion of tsetse fly bite on animals, ξ^α is the fly biting rate, ψ is the probability that a susceptible fly gets infected upon contact with an infectious animals, ω is the probability that a susceptible fly gets infected upon contact with an infectious human, u and b represent the probability that an infectious fly infects an animal and a human, respectively, upon contact. In all the simulation results we set $\omega = \psi = 3.55 \times 10^{-4}$ and $b = u = 8.3 \times 10^{-4}$. These baseline values were based upon consultation of several published frameworks.

On simulating system (6) we assumed the following initial population levels: $L = 1300$, $N_v = 1500$, $S_v = 1000$, $I_v = 500$, $S_h = 900$, $I_h = 100$, $S_a = 380$, $I_a = 120$ and $\theta = 0.8$. Without loss of generality, we set the values of the fractional order to be $\alpha = 0.5$, $\alpha = 0.7$, $\alpha = 0.9$, $\alpha = 1.0$. Model parameters that are considered to be independent of temperature are in Table 2. All the baseline values for these parameters were adopted from the work of Ndondo et al. [13]. Note that K will be varied in order to obtain different values of $\mathcal{R}_0$. Additional model parameters dependent on temperature are presented in Table 1, and all the baseline values were adopted from the work of Lord et al. [16].

Numerical results in Fig. 1 demonstrate the relationship between the basic reproduction number $\mathcal{R}_0$ and temperature in °C. We can observe that as temperature increases from the critical minimum $T = 16°$ C, the basic reproduction number $\mathcal{R}_0$ gradually increases till the highest value is attained at optimum temperature $T = 25$°C, thereafter $\mathcal{R}_0$ sharply declines. Furthermore, we can also note that when $T < 16$°C then $\mathcal{R}_0 < 1$.

Numerical results in Fig. 2 illustrate the dynamics of the infected population when for $\mathcal{R}_0 \leq 1$. As we can note, all the populations converged to the disease-free equilibrium,

Table 1 Description of temperature dependent model parameters used in system (6). All the parameter values were adopted from the work of Lord et al. [16]

Function	Definition	Parameter	Baseline value	Range
b_l (day^{-1})	Larviposition rate	d_1	0.1050	0.1046 ± 0.0004
	Larviposition rate	d_2	0.0053	0.0052 ± 0.0001
μ_v (day^{-1})	Adult mortality rate	a_1	0.027	0.027 ± 0.001
	Adult mortality rate	a_2	0.153	0.153 ± 0.020
μ_p (day^{-1})	Pupal mortality rate	b_1	0.0019	0.0019 ± 0.0004
	Pupal mortality rate	b_2	0.006	0.006 ± 0.001
	Pupal mortality rate	b_3	1.4881	1.481 ± 0.681
	Pupal mortality rate	b_4	0.003	0.003 ± 0.001
	Pupal mortality rate	b_5	1.094	1.211 ± 0.117
σ_l (day^{-1})	Pupal emergence rate	c_1	0.05884	0.05884 ± 0.00289
	Pupal emergence rate	c_2	4.8829	4.8829 ± 0.0993
	Pupal emergence rate	c_3	−0.2159	-0.2159 ± 0.0050

Table 2 Description of non-temperature dependent model parameters used in system (6). All the parameter values were adopted from the work of Ndondo et al. [13]

Symbol	Description	Value	Units
W	Proportion of female flies	0.6	Dimensionless
μ_h	Human population birth/natural death rate	$\frac{1}{50\times365}$	Day^{-1}
μ_a	Animal population birth/death rate	$\frac{1}{15\times365}$	Day^{-1}
γ_h	Human recovery rate	$\frac{1}{30}$	Day^{-1}
γ_a	Animal recovery rate	$\frac{1}{25}$	Day^{-1}
ξ	Tsetse fly biting rate	$\frac{1}{4}$	Day^{-1}
p	Proportion of tsetse fly bite on animal	0.7	Dimensionless

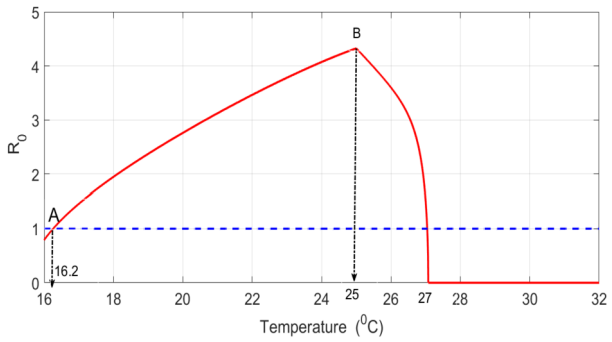

Figure 1 The relationship between the basic reproduction number $\mathcal{R}_0$ and temperature T. Parameter values used are given in Tables 2 and 1. Furthermore, we set $K_l = 1500$, $N_h = 1000$, $N_a = 500$, $N_v = 1500$ and varied the temperature from 16–27°C

despite the chosen value of α. These results concur with analytical findings presented in Theorem 4.4 that whenever $\mathcal{R}_0 \leq 1$ the proposed model is stable and the disease dies out in the community.

Simulation results in Fig. 3 show the solutions of model (6) at different levels of $\alpha = (0.5, 0.7, 0.9, 1.0)$ for $\mathcal{R}_0 = 3.7 > 1$. We set $T = 25°C$ and $K_l = 3300$. As we can note, solution profiles converge to a nonzero equilibrium point, implying that whenever $\mathcal{R}_0 > 1$ the model is stable and admits a unique endemic equilibrium point. Biologically, this means

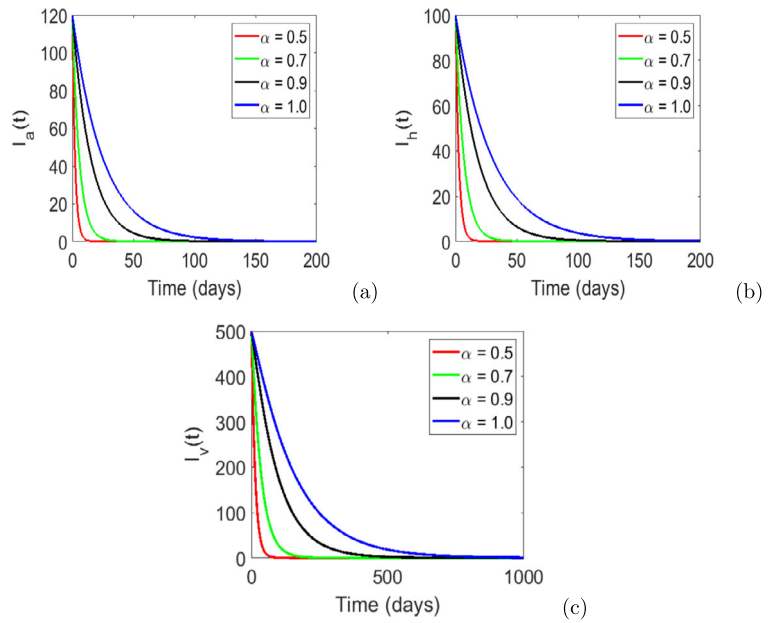

Figure 2 Numerical results of system (6) demonstrating the convergence of infected population to the disease-free equilibrium for $\mathcal{R}_0 \leq 1$. On construction of the simulations, we considered initial population levels discussed earlier, while baseline values for the model parameters are as in Tables 2 and 1. In addition, we also set $T = 16.5°C$ and $K = 3300$, giving $\mathcal{R}_0 = 1.0$. As we can observe, the results concur with analytical findings presented in Theorem 4.4 that whenever $\mathcal{R}_0 \leq 1$ the disease dies out in the community

that $\mathcal{R}_0 > 1$ the disease will persist in the community. These simulation results support analytical findings presented in Theorem 4.5.

Figure 4 shows the numbers of infected vectors, humans and animals, at different temperature values over a period of 500 days. As we can observe, low temperature values ($T < 25°\text{C}$) are associated with low infection levels and as the temperature increased to the optimum value $T = 25°\text{C}$, the number of infections increases over time. We can also observe that for $t < 100$ days the impact of different temperature values on population levels will not be extremely distinct. However, thereafter there is a significant distinction.

Next, we investigate the effects of screening infected hosts and vector control on disease dynamics. Detection and treatment of humans has been a primary control strategy for HAT. Cases detection can be carried out either periodically (usually large-scale screening) or on continuous basis (usually small scale) at health care centres [29]. In this study, we explore the potential effects of continuous detection and treatment and we follow the approach in Artzrouni and Gouteux [25]. Artzrouni and Gouteux proposed a model for HAT that had a new parameter C_h, which was meant to account for the month percent detections of infected individuals. Furthermore, Artzrouni and Gouteux proposed that the rate of exit of infected host to the recovery stage can be presented as a composite of the intrinsic underlying disease progression (say, γ_{int} and the removal rate by treatment (extrinsic, say γ_{ext}) such that

$$\gamma_h = \gamma_{\text{int}} + \gamma_{\text{ext}}, \tag{12}$$

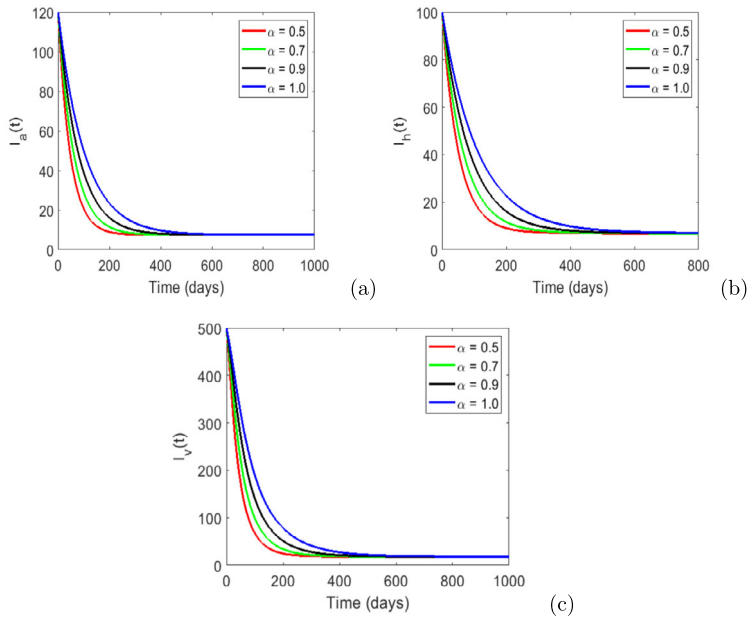

Figure 3 Numerical results of system (6) demonstrating the convergence of infected population to the endemic equilibrium for $\mathcal{R}_0 > 1$. On simulating the model, we considered initial population levels discussed earlier, while baseline values for the model parameters are as in Tables 2 and 1. In addition, we also set $T = 25°C$ and $K = 3300$, giving $\mathcal{R}_0 = 3.7$. As we can observe, the results concur with analytical findings presented in Theorem 4.5 that whenever $\mathcal{R}_0 > 1$ the system is stable and the infection persists in the community

then the monthly percent detection is given by

$$C_h = 100\big[1 - \exp(-30\gamma_{\text{ext}})\big]. \tag{13}$$

Consequently, the exit rate from the infected class for human host is given by

$$\gamma_h = \gamma_{\text{int}} - \frac{1}{30}\ln\left(1 - \frac{C_h}{100}\right). \tag{14}$$

From (14) we can observe that linear detection of infected individual does not result in linear changes in γ_h. Rock et al. [29] opine that this representation of the recovery rate leads to a meaningful way in which the influence of the parameter on the basic reproduction number can be extensively explored.

Despite the fact that there are several methods to control the density of the tsetse, such as aerial spraying and the deployment of natural or artificial baits, essentially altering the total population parameter N_v, birth rate and natural mortality rate μ_v^α will alter the density of the tsetse population. Cognisant of these fundamental parameters, Artzrouni and Gouteux [25] hypothesised that tsetse controls will affect mortality rate but not the population size. Hence in an analogous approach to modelling detection and treatment of human, they model 'natural' mortality rate of the vectors a follows:

$$\mu_v = \mu_{v,\text{int}} + \mu_{v,\text{ext}}, \tag{15}$$

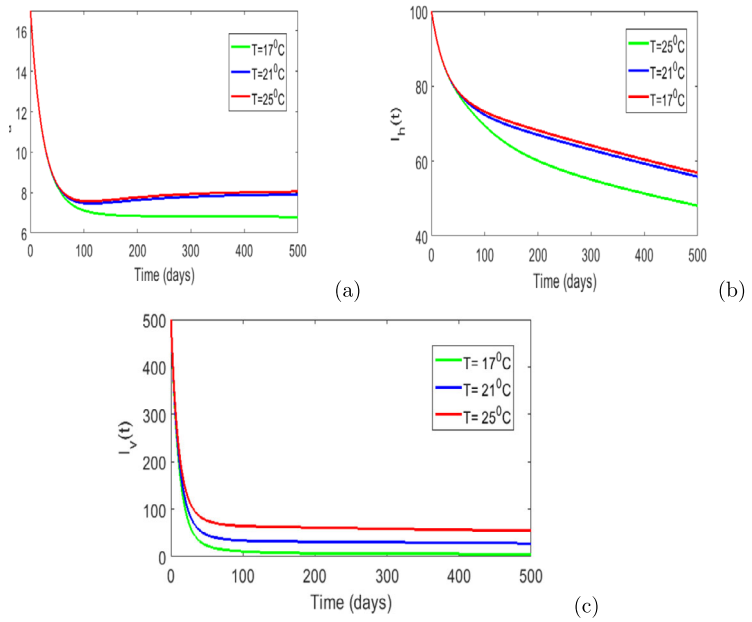

Figure 4 Numerical results depicting the effects of temperature variation on the dynamics of infected hosts and vectors. We set $\boldsymbol{\alpha} = 0.7$, $K_l = 3300$, $N_h = 1000$, $N_a = 500$, $L = 1300$, $N_v = 1500$, $S_v = 1000$, $I_v = 500$, $I_h = 100$, $S_a = 380$ and $I_a = 17$. The rest of the model parameters were adopted as in Tables 2 and 1

where $\mu_{v,\text{int}}$ accounts for the mortality experienced by flies in their environment and $\mu_{v,\text{ext}}$ describes an additional death rate which occurs as result of control strategies. Furthermore, they suggested that this death rate μ_v^{α} is related to the daily percentage of flies killed and denoted here by C_v:

$$C_v = 100\big[1 - \exp(-30\mu_{v,\text{ext}})\big]. \tag{16}$$

Thus, the total mortality rate of vectors due to 'natural' and control measures is given by

$$\mu_v = \mu_{v,\text{int}} - \ln\left(1 - \frac{C_v}{100}\right). \tag{17}$$

Note that in the work of Artzrouni and Gouteux they used rates with three days as the unit of time on equation (17).

In what follows, we numerically explore the effectiveness of case detection and vector on the spread of the disease. Precisely, we will use contour plot to determine the influence of c_h and c_v on the basic reproduction number, since it an integral epidemiological metric for understanding the power of *Trypanosoma brucei rhodesiense* to invade the community. A contour plot in Fig. 5 illustrates the impact of human case detection and vector control on *Trypanosoma brucei rhodesiense* dynamics at $T = 20°\text{C}$. As we can observe, an increase in both case detection and vector control percentages will lead to a decrease in the magnitude of $\mathcal{R}_0$. We can also note that vector control has a strong influence on minimising the magnitude of $\mathcal{R}_0$ compared to human detection. In particular, whenever $C_v > 30$, then $\mathcal{R}_0 < 1$ despite any value of C_h.

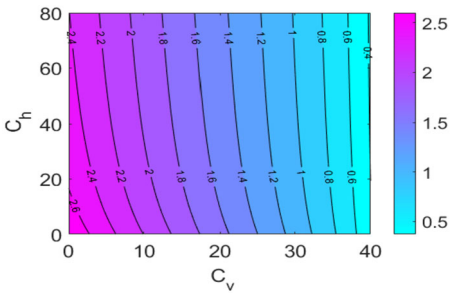

Figure 5 A contour plot illustrating the effects of human detection and vector control on *Trypanosoma brucei rhodesiense* dynamics. We set $T = 20°C$, $K_l = 3300$, $\beta_{hv} = \beta_{av} = 3.55 \times 10^{-4}$, $\beta_{vh} = \beta_{va} = 8.3 \times 10^{-4}$, $N_h = 1000$, $N_a = 500$, $\gamma_{\text{int}} = 0.009$ and $\mu_{v,\text{int}} = 0.027$

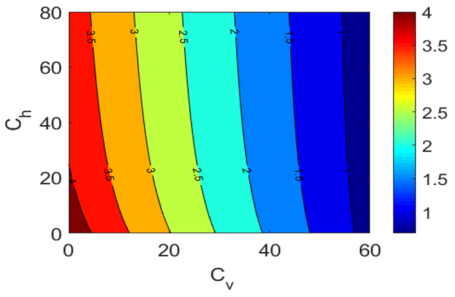

Figure 6 A contour plot illustrating the effects of human detection and vector control on *Trypanosoma brucei rhodesiense* dynamics. We set $T = 25°C$, $K_l = 1500$, $N_h = 1000$, $N_a = 500$, $\gamma_{\text{int}} = 0.009$ and $\mu_{v,\text{int}} = 0.027$

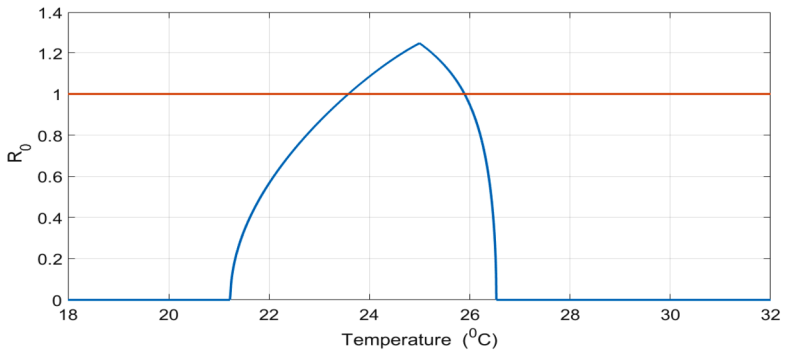

Figure 7 Simulation results showing the effects of temperature on $\mathcal{R}_0$ in the presence of human screening and vector control. We set $C_h = C_v = 50$, $K_l = 1500$, $N_h = 1000$, $N_a = 500$, $L = 1300$, $N_v = 1500$, $S_v = 1000$, $I_v = 500$, $I_h = 100$, $S_a = 380$ and $I_a = 17$. The rest of the parameter values are as in Tables 2 and 1

A contour plot in Fig. 6 demonstrates the impact of C_h and C_v on the transmission dynamics of *Trypanosoma brucei rhodesiense* at $T = 25°C$. Comparing the results in Fig. 5 and Fig. 6, we can observe that at optimum temperature $T = 25°C$, vector control needs to be greater that 50 ($C_v > 50$) in order to reduce the magnitude of the basic reproduction number to values less than unity, whereas in Fig. 5, $C_v > 30$ is sufficient to obtain $\mathcal{R}_0 < 1$. Therefore, we can conclude that if the average temperature in the community is very close to the optimum temperature, then intensity of vector control needs to be at least 50%.

In Fig. 7 we explore the relationship between temperature and $\mathcal{R}_0$ in the presence of human screening and vector control. Wet set $C_h = C_v = 50$. As we can observe, $\mathcal{R}_0 > 1$ for $23 < T < 26°C$. This implies that at 50% human detection and 50% killing of vectors, the disease can only persist in the community when the average temperature is between 23

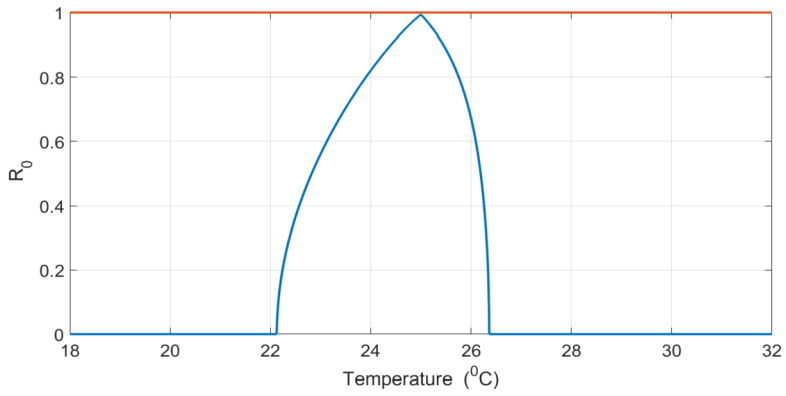

Figure 8 Simulation results showing the effects of temperature on $\mathcal{R}_0$ in the presence of human screening and vector control. We set $C_h = 50$, $C_v = 55$, $k_l = 1500$, $N_h = 1000$, $N_a = 500$, $L = 1300$, $N_v = 1500$, $S_v = 1000$, $I_v = 500$, $I_h = 100$, $S_a = 380$ and $I_a = 17$. The rest of the parameter values are as in Tables 2 and 1

and 26°C; otherwise, the disease dies out. However, if we set $C_h = 50$ and $C_v = 55$ (Fig. 8), the disease will not persist even at optimum temperature $T = 25°$C.

6 Concluding remarks

In this work, a fractional-order model with long run memory has been used to explore the effects of temperature on *Trypanosoma brucei rhodesiense* transmission and control. The memory effects are represented by the Caputo derivative. The proposed model incorporates the interplay between the tsetse flies and two hosts, humans and animals. The model incorporates all the necessary and relevant biological information concerning transmission and control of *Trypanosoma brucei rhodesiense*, hence in the framework we incorporated the early stages of the vector. Key stages of the vector population that strongly depend on temperature were modelled as functions of temperature. We computed the basic reproduction number and established results on the threshold dynamics. Furthermore, we utilised the formulae proposed by Artzrouni and Gouteux [25] to explore the effects of daily human detection and vector control on long term disease dynamics. Among other several outcomes, we have established that vector control has strong influence on minimising the spread of the disease. In particular, we note that when daily averaged temperature is around $T = 20°C$, destruction of 30% or more vectors in three days will reduce the basic reproduction number to levels below unity despite any level of human detection. In addition, we also observed that if human detection is around 50% and vector control is 55% or more, then the disease will die out in the community even at optimum temperature $T = 25°C$. Overall, findings from this study have demonstrated the impact of temperature and control strategies on long term dynamics of *Trypanosoma brucei rhodesiense*, and the outcomes enhance our understanding on effective management of the disease.

Like other modelling studies, the proposed study could be extended by validating the model using data obtained from specific countries and associated laboratory experiments conducted in those countries. Aspects of heterogeneity (high and low risk populations) can also be included. Instead of average daily temperatures, seasonal variation in temperature can also be factored into the framework.

Acknowledgements
Mlyashimbi Helikumi acknowledges the financial support received from the Simons Foundation and Mbeya University of Science and Technology, Tanzania. Other authors are also grateful to their respective institutions for the support. In addition, the authors are grateful to the anonymous referees and the handling editor for their invaluable comments and suggestions, which have helped to improve the presentation of this work significantly.

Funding
Not applicable.

Availability of data and materials
All the datasets used as well as generated in this study are included in the manuscript.

Competing interests
The authors declare that they have no competing interests.

Authors' contributions
Formal analysis and Methodology, MH; Supervision and writing-review, MK, DK and SM. All the authors read and approved the final manuscript.

Author details
[1]School of Computational and Communication Science and Engineering, The Nelson Mandela African Institution of Science and Technology (NM-AIST), Arusha, Tanzania. [2]Department of Mathematics and Statistics, College of Science and Technical Education, Mbeya University of Science and Technology, Mbeya, Tanzania. [3]Department of Basic Sciences, Botswana University of Agriculture and Natural Resources, Gaborone, Botswana. [4]Department of Mathematics, University of Zimbabwe, Harare, Zimbabwe.

Publisher's Note

Received: 27 January 2020 Accepted: 1 June 2020 Published online: 11 June 2020

References

1. Franco, J.R., Simarro, P.P., Diarra, A., Jannin, J.G.: Epidemiology of human African trypanosomiasis. J. Clin. Epidemiol. **6**, 257–275 (2014)
2. Phelps, R.: The effect of temperature on fat consumption during the puparial stages of Glossina morsitans morsitans Westw. (Dipt., Glossinidae) under laboratory conditions, and its implication in the field. Bull. Entomol. Res. **62**, 423 (1973)
3. Phelps, R.J., Lovemore, D.F.: Vectors: tsetse flies. In: Coetzer, J.A., Thomson, G.R., Tustin, R.C. (eds.) Infectious Disease of Livestock, pp. 25–52. Oxford University Press, Cape Town (1994)
4. Vale, G.A.: Artificial refuges for tsetse flies (Glossina spp.). Bull. Entomol. Res. **61**, 331–350 (1971)
5. Phelps, R.J., Burrows, P.M.: Puparial duration in Glossina morsitans orientalis under conditions of constant temperature. Entomol. Exp. Appl. **12**, 33–43 (1969)
6. Bursell, E.: The effect of temperature on the consumption of fat during pupal development in Glossina. Bull. Entomol. Res. **51**, 583–598 (1960)
7. Phelps, R.J., Clarke, G.P.Y.: Seasonal elimination of some size classes in males of Glossina morsitans Westw. (Diptera, Glossinidae). Bull. Entomol. Res. **64**, 313–324 (1974)
8. Moore, S., Shrestha, S., Tomlinson, K.W., Vuong, H.: Predicting the effect of climate change on African trypanosomiasis: integrating epidemiology with parasite and vector biology. J. R. Soc. Interface **9**, 817–830 (2012)
9. Leak, S.G.A.: Tsetse vector population dynamics: ILRAD's requirements. In: Hansen, J.W., Perry, B.D. (eds.) Modelling Vector-Borne and Other Parasitic Diseases, p. 36. International Livestock Research Institute (ILRI), Nairobi (1994) Available online: https://books.google.co.zw/books?isbn=9290552972 (accessed on 8 May 2018)
10. Hargrove, J.W., Ouifki, R., Kajunguri, D., Vale, G.A., Torr, S.J.: Modeling the control of trypanosomiasis using trypanocides or insecticide-treated livestock. PLoS Negl. Trop. Dis. **6**, e1615 (2012)
11. Pandey, A., Atkins, K.E., Bucheton, B., Camara, M., Aksoy, S., Galvani, A.P., Ndeffo-Mbah, M.L.: Evaluating long-term effectiveness of sleeping sickness control measures in Guinea. Parasites Vectors **8**, 550 (2015)
12. Funk, S., Nishiura, H., Heesterbeek, H., John, E.W., Checchi, F.: Identifying transmission cycles at the human-animal interface: the role of animal reservoirs in maintaining gambiense human African trypanosomiasis. PLoS Comput. Biol. **9**, e1002855 (2013)
13. Ndondo, A.M., Munganga, J.M.W., Mwambakana, J.N., Saad-Roy, M.C., Van den Driessche, P., Walo, O.R.: Analysis of a model of gambiense sleeping sickness in human and cattle. J. Biol. Dyn. **10**, 347–365 (2016)
14. Rock, K.S., Torr, S.J., Lumbala, C., Keeling, M.J.: Predicting the impact of intervention strategies for sleeping sickness in two high-endemicity health zones of the Democratic Republic of Congo. PLoS Negl. Trop. Dis. **11**, e0005162 (2017)
15. Stone, C.M., Chitnis, N.: Implications of heterogeneous biting exposure and animal hosts on Trypanosomiasis brucei gambiense transmission and control. PLoS Comput. Biol. **11**, e1004514 (2015)
16. Lord, J.S., Hargrove, J.W., Torr, S.J., Vale, G.A.: Climate change and African trypanosomiasis vector populations in Zimbabwe's Zambezi Valley: a mathematical modelling study. PLoS Med. **15**, e1002675 (2018)
17. Alderton, S., Macleod, E.T., Anderson, N.E., Palmer, G., Machila, N., Simuunza, M., Welburn, S.C., Atkinson, P.M.: An agent-based model of tsetse fly response to seasonal climatic drivers: assessing the impact on sleeping sickness transmission rates. PLoS Negl. Trop. Dis. **12**, e0006188 (2018)
18. Ackley, S.F., Hargrove, J.W.: A dynamic model for estimating adult female mortality from ovarian dissection data for the tsetse fly Glossina pallidipes Austen sampled in Zimbabwe. PLoS Negl. Trop. Dis. **11**, e0005813 (2017)

19. Rock, K.S., Torr, S.J., Lumbala, C., Keeling, M.J.: Quantitative evaluation of the strategy to eliminate human African trypanosomiasis in the Democratic Republic of Congo. Parasites Vectors **8**, 532 (2015)
20. Peck, S.L., Bouyer, J.: Mathematical modeling, spatial complexity, and critical decisions in tsetse control. J. Econ. Entomol. **105**, 1477–1486 (2012)
21. Artzrouni, M., Gouteux, J.-P.: Estimating tsetse population parameters: application of a mathematical model with density-dependence. Med. Vet. Entomol. **17**, 272–279 (2003)
22. Artzrouni, M., Gouteux, J.-P.: A model of Gambian sleeping sickness with open vector populations. Math. Med. Biol. **18**, 99–117 (2001)
23. Artzrouni, M., Gouteux, J.-P.: Population dynamics of sleeping sickness: a microsimulation. Simul. Gaming **32**, 215–227 (2001)
24. Artzrouni, M., Gouteux, J.-P.: A compartmental model of sleeping sickness in Central Africa. J. Biol. Syst. **4**, 459–477 (1996)
25. Artzrouni, M., Gouteux, J.-P.: Control strategies for sleeping sickness in Central Africa: a model-based approach. Trop. Med. Int. Health **1**, 753–764 (1996)
26. Rogers, D.J.: A general model for the African trypanosomiases. Parasitology **97**, 193–212 (1988)
27. Gilbert, J.A., Medlock, J., Townsend, J.P., Aksoy, S., Mbah, M.N., Galvani, A.P.: Determinants of human African trypanosomiasis elimination via paratransgenesis. PLoS Negl. Trop. Dis. **10**, e0004465 (2016)
28. Rock, K.S., Ndeffo-Mbah, M.L., Castaño, S., Palmer, C., Pandey, A., Atkins, E.K., Ndung'u, M.J., Hollingsworth, D.T., Galvani, A., Bever, C., Chitnis, N., Keeling, M.J.: Assessing strategies against Gambiense sleeping sickness through mathematical modeling. Clin. Infect. Dis. **66**, S286–S292 (2018)
29. Rock, K.S., Stone, C.M., Hastings, I.M., Keeling, M.J., Torr, S.J., Chitnis, N.: Mathematical models of human African trypanosomiasis epidemiology. Adv. Parasitol. **87**, 53–133 (2015)
30. Meisner, J., Barnabas, R.V., Rabinowitz, P.M.: A mathematical model for evaluating the role of trypanocide treatment of cattle in the epidemiology and control of Trypanosoma brucei rhodesiense and T. b. gambiense sleeping sickness in Uganda. Parasite Epidemiol. Control **3**, e00106 (2019)
31. Helikumi, M., Kgosimore, M., Kuznetsov, D., Mushayabasa, S.: Backward bifurcation and optimal control analysis of a Trypanosoma brucei rhodesiense model. Mathematics **7**, 971 (2019)
32. Helikumi, M., Kgosimore, M., Kuznetsov, D., Mushayabasa, S.: Dynamical and optimal control analysis of a seasonal Trypanosoma brucei rhodesiense model. Math. Biosci. Eng. **17**, 2530–2556 (2020)
33. Saeedian, M., Khalighi, M., Azimi-Tafreshi, N., Jafari, G.R., Ausloos, M.: Memory effects on epidemic evolution: the susceptible-infected-recovered epidemic model. Phys. Rev. E **95**, 022409 (2017)
34. Rihan, A.F., Al-Mdallal, M.Q., AlSakaji, J.H., Hashish, A.: A fractional-order epidemic model with time-delay and nonlinear incidence rate. Chaos Solitons Fractals **126**, 97–105 (2019)
35. Hamdan, N.I., Kılıçman, A.: Analysis of the fractional order dengue transmission model: a case study in Malaysia. Adv. Differ. Equ. **2019**, 3 (2019)
36. Mouaouine, A., Boukhouima, A., Hattaf, K., Yousfi, N.: A fractional order SIR epidemic model with nonlinear incidence rate. Adv. Differ. Equ. **2018**, 160 (2018)
37. Vargas-De-León, C.: Volterra-type Lyapunov functions for fractional-order epidemic systems. Commun. Nonlinear Sci. Numer. Simul. **24**, 75–85 (2015)
38. Caputo, M.: Linear models of dissipation whose Q is almost frequency independent, Part II. Geophys. J. R. Astron. Soc. **13**, 529–539 (1967) Reprinted in Fract. Calc. Appl. Anal. 11, 4–14 (2008)
39. Diethelm, K.: The Analysis of Fractional Differential Equations: An Application-Oriented Exposition Using Differential Operators of Caputo Type. Springer, Berlin (2010). p. 247
40. Podlubny, I.: Fractional Differential Equations. Academic Pres, San Diego (1999)
41. Supajaidee, N., Moonchai, S.: Stability analysis of a fractional-order two-species facultative mutualism model with harvesting. Adv. Differ. Equ. **2017**, 372 (2017). https://doi.org/10.1186/s13662-017-1430-9
42. Delavari, H., Baleanu, D., Sadati, J.: Stability analysis of Caputo fractional-order nonlinear systems revisited. Nonlinear Dyn. **67**, 2433–2439 (2012)
43. Liang, S., Wu, R., Chen, L.: Laplace transform of fractional order differential equations. Electron. J. Differ. Equ. **2015**, 139 (2015)
44. Kexue, L., Jigen, P.: Laplace transform and fractional differential equations. Appl. Math. Lett. **24**(12), 2019–2023 (2011)
45. Igor, P.: Fractional Differential Equations. Mathematics in Science and Engineering, vol. 198. Academic Press, New York (1999)
46. Hargrove, J.W.: Reproductive rates of tsetse flies in the field in Zimbabwe. Physiol. Entomol. **19**, 307–318 (1994)
47. van-den Driessche, P., Watmough, J.: Reproduction number and sub-threshold endemic equilibria for compartment models of disease transmission. Math. Biosci. **180**, 29–48 (2002)
48. Diekmann, O., Heesterbeek, J.A.P., Metz, J.A.J.: On the definition and the computation of the basic reproduction ratio $\mathcal{R}_0$ in models for infectious diseases in heterogeneous populations. J. Math. Biol. **28**, 365–382 (1990)
49. LaSalle, J.P.: The Stability of Dynamical Systems. SIAM, Philadelphia (1976)
50. Garrappa, R.: Predictor-corrector PECE method for fractional differential equations. MATLAB Central File Exchange (2011) File ID: 32918
51. Diethelm, K., Freed, D.A.: The FracPECE subroutine for the numerical solution of differential equations of fractional order. In: Heinzel, S., Plesser, T. (eds.) Forschung und wissenschaftliches Rechnen 1998. GWDG-Berichte, vol. 52, pp. 57–71. Gesellschaft für wissenschaftliche Datenverarbeitung, Göttingen (1999)
52. Diethelm, K., Ford, J.N., Freed, D.A.: Detailed error analysis for a fractional Adams method. Numer. Algorithms **36**, 31–52 (2004)
53. Garrappa, R.: On linear stability of predictor-corrector algorithms for fractional differential equations. Int. J. Comput. Math. **87**, 2281–2290 (2010)

Terms and Conditions

Springer Nature journal content, brought to you courtesy of Springer Nature Customer Service Center GmbH ("Springer Nature").

Springer Nature supports a reasonable amount of sharing of research papers by authors, subscribers and authorised users ("Users"), for small-scale personal, non-commercial use provided that all copyright, trade and service marks and other proprietary notices are maintained. By accessing, sharing, receiving or otherwise using the Springer Nature journal content you agree to these terms of use ("Terms"). For these purposes, Springer Nature considers academic use (by researchers and students) to be non-commercial.

These Terms are supplementary and will apply in addition to any applicable website terms and conditions, a relevant site licence or a personal subscription. These Terms will prevail over any conflict or ambiguity with regards to the relevant terms, a site licence or a personal subscription (to the extent of the conflict or ambiguity only). For Creative Commons-licensed articles, the terms of the Creative Commons license used will apply.

We collect and use personal data to provide access to the Springer Nature journal content. We may also use these personal data internally within ResearchGate and Springer Nature and as agreed share it, in an anonymised way, for purposes of tracking, analysis and reporting. We will not otherwise disclose your personal data outside the ResearchGate or the Springer Nature group of companies unless we have your permission as detailed in the Privacy Policy.

While Users may use the Springer Nature journal content for small scale, personal non-commercial use, it is important to note that Users may not:

1. use such content for the purpose of providing other users with access on a regular or large scale basis or as a means to circumvent access control;
2. use such content where to do so would be considered a criminal or statutory offence in any jurisdiction, or gives rise to civil liability, or is otherwise unlawful;
3. falsely or misleadingly imply or suggest endorsement, approval , sponsorship, or association unless explicitly agreed to by Springer Nature in writing;
4. use bots or other automated methods to access the content or redirect messages
5. override any security feature or exclusionary protocol; or
6. share the content in order to create substitute for Springer Nature products or services or a systematic database of Springer Nature journal content.

In line with the restriction against commercial use, Springer Nature does not permit the creation of a product or service that creates revenue, royalties, rent or income from our content or its inclusion as part of a paid for service or for other commercial gain. Springer Nature journal content cannot be used for inter-library loans and librarians may not upload Springer Nature journal content on a large scale into their, or any other, institutional repository.

These terms of use are reviewed regularly and may be amended at any time. Springer Nature is not obligated to publish any information or content on this website and may remove it or features or functionality at our sole discretion, at any time with or without notice. Springer Nature may revoke this licence to you at any time and remove access to any copies of the Springer Nature journal content which have been saved.

To the fullest extent permitted by law, Springer Nature makes no warranties, representations or guarantees to Users, either express or implied with respect to the Springer nature journal content and all parties disclaim and waive any implied warranties or warranties imposed by law, including merchantability or fitness for any particular purpose.

Please note that these rights do not automatically extend to content, data or other material published by Springer Nature that may be licensed from third parties.

If you would like to use or distribute our Springer Nature journal content to a wider audience or on a regular basis or in any other manner not expressly permitted by these Terms, please contact Springer Nature at

onlineservice@springernature.com

A fractional-order Trypanosoma brucei rhodesiense model with vector saturation and temperature dependent parameters

Mlyashimbi Helikumi[1,2], Moatlhodi Kgosimore[3], Dmitry Kuznetsov[1] Steady Mushayabasa[4]
[1]Institution of Science and Technology (NM-AIST), School of Computational and Communication Science and Engineering, The Nelson Mandela African, P. O. Box 447, Arusha, Tanzania [2]Department of Mathematics and Statistics, Mbeya University of Science and Technology, College of Science and Technical Education, P.O. Box 131, Mbeya, Tanzania, [3]Department of Basic Sciences, Botswana University of Agriculture and Natural Resources Private Bag 0027, Gaborone, Botswana, Department of Basic Sciences, [4] Department of Mathematics, University of Zimbabwe, P.O. Box MP 167, Harare, Zimbabwe.

1. Introduction

- Human African trypanosomiasis (HAT), also known as sleeping sickness, is a neglected tropical disease (NTD) caused by parasites of the genus Trypanosoma, which are transmitted by tsetse flies.
- The disease has two forms, *T. brucei gambiense* in West and Central Africa and *T. brucei rhodesiense* in East Africa.
- The HAT can be transmitted to humans and animals (both livestock and wildlife) by over 20 species of *Glossina* tsetse flies.
- The symptoms of HAT disease include fever, headache, sleeping sickness, enlarged lymph nodes, fatigue, change of behavior and endocrine disorders.

2. Materials and Methods

- In this study we proposed a fractional-order model for *T. brucei rhodesiense* disease with three species namely; the humans, animals and vectors.
- To capture the memory effects, mathematical model for *T. brucei rhodesiense* disease was formulated using fractional-order derivatives.
- To capture the effects of temperature in the dynamics of *T. brucei rhodesiense*, I incorporated the temperature in four parameter of the vectors that is birth rate, incubation period, biting rate and mortality rate.

3. Results

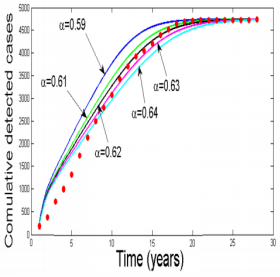

Figure 2: Model system (3.31) fitted to r-HAT cases in Tanzania at α = 0.59, 0.61, 0.62, 0.63, and 0.64. The results showed that the rhodesiense HAT cases in Tanzania fit well with the formulated model.

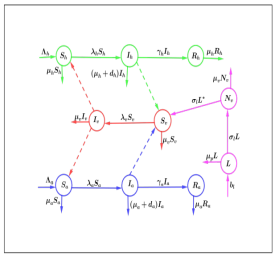

Figure 1: Compartmental model for *T. brucei rhodesiense* disease transmission.

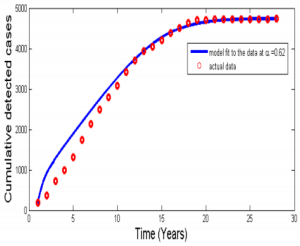

Figure 3: Model fitted to r-HAT cases in Tanzania at α = 0.62.and the results show the best fit of the model.

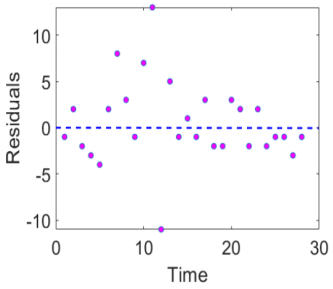

Figure 4:A time series plot of residuals against time. The results here showed that, residuals did not appear to follow a particular path. Precisely the plot showed that residuals have no pattern and this imply that model was really a good fit.

$$
\begin{aligned}
{}_{t_0}^{c}D_t^{\alpha}L(t) &= b_l^{\alpha}WN_v\left(1-\frac{L}{K_l^{\alpha}}\right)-(\sigma_l^{\alpha}+\mu_p^{\alpha})L,\\
{}_{t_0}^{c}D_t^{\alpha}N_v(t) &= \sigma_l^{\alpha}L-\mu_v^{\alpha}N_v,\\
{}_{t_0}^{c}D_t^{\alpha}S_v(t) &= \sigma_l^{\alpha}L-(\beta_{hv}^{\alpha}I_h+\beta_{av}^{\alpha}I_a)S_v-\mu_v^{\alpha}S_v,\\
{}_{t_0}^{c}D_t^{\alpha}I_v(t) &= (\beta_{hv}^{\alpha}I_h+\beta_{av}^{\alpha}I_a)S_v-\mu_v^{\alpha}I_v,\\
{}_{t_0}^{c}D_t^{\alpha}S_h(t) &= \Lambda_h^{\alpha}-\beta_{vh}^{\alpha}f(I_v)S_h-\mu_h^{\alpha}S_h,\\
{}_{t_0}^{c}D_t^{\alpha}I_h(t) &= \beta_{vh}^{\alpha}f(I_v)S_h-(\mu_h^{\alpha}+\gamma_h^{\alpha})I_h,\\
{}_{t_0}^{c}D_t^{\alpha}S_a(t) &= \Lambda_a^{\alpha}-\beta_{va}^{\alpha}f(I_v)S_a-\mu_a^{\alpha}S_a,\\
{}_{t_0}^{c}D_t^{\alpha}I_a(t) &= \beta_{va}^{\alpha}f(I_v)S_a-(\mu_a^{\alpha}+\gamma_a^{\alpha})I_a,\\
{}_{t_0}^{c}D_t^{\alpha}R_h(t) &= \gamma_h^{\alpha}I_h-\mu_h^{\alpha}R_h,\\
{}_{t_0}^{c}D_t^{\alpha}R_a(t) &= \gamma_a^{\alpha}I_a-\mu_a^{\alpha}R_a.
\end{aligned}
$$

4. Conclusion

- In this work, a fractional-order model with long run memory has been used to explore the effects of temperature on *Trypanosoma brucei rhodesiense* transmission and control.
- The memory effects are represented by the Caputo derivative.
- Among other several outcomes, we have established that vector control has strong influence on minimizing the spread of the disease. In particular, we note that when daily averaged temperature is around T = 20 Centigrade, destruction of 30% or more vectors in three days will reduce the basic reproduction number to levels below unity despite any level of human detection.

5. Recommendations

- Sleeping sickness or HAT is a neglected disease that impacts 70 million people living in 1.55 million km2 in sub- Saharan Africa. Several modelling studies have been undertaken to assess the feasibility of the WHO's goal of eliminating the disease by 2030.
- However, this study overlooked the effects of temperature, use of insecticides, case detection for infected humans and memory effects.
- In this study, analyzed to assmathematical model was shaping the short-and long-term dynamics of the disease

6. Funding

This study was supported by Mbeya University of Science and Technology, P.O. Box 131, Mbeya, Tanzania,

7. References

Rock, K. S., Stone, C. M., Hastings, I. M., Keeling, M. J., Torr, S. J. and Chitnis, N. (2015b). Mathematical models of human african trypanosomiasis epidemiology. Advances in parasitology. 87: 53–133.

Email: mhelikumi@yahoo.co.uk
Mob: +255(0)756615739